Electronic Supplementary Material (ESI) for Organic Chemistry Frontiers.

Supporting Information

Controlling Rotary Motion of Molecular Motors Based on Oxindole

Daisy R. S. Pooler, Daniel Doellerer, Stefano Crespi and Ben L. Feringa*

Stratingh Institute for Chemistry, University of Groningen

Nijenborgh 4, 9746 AG Groningen, The Netherlands

Email: b.l.feringa@rug.nl

Table of Contents

1. General procedures

All reactions involving air sensitive reagents were performed under an N_2 atmosphere. Solvents were degassed by purging with N_2 for a minimum of 30 min or by three freeze-pump-thaw cycles. Reagents were purchased from Sigma Aldrich, Fluorochem or TCI Europe and were used without further purification. Solvents were reagent grade and used without prior water removal unless otherwise indicated. Anhydrous solvents were obtained from a solvent purification system (MBraun SPS-800). Flash column chromatography was performed on silica gel (Merck, type 9385, 230–400 mesh) or on a Büchi Reveleris purification system using Büchi silica cartridges. Thin layer chromatography (TLC) was carried out on aluminium sheets coated with silica gel 60 F254 (Merck). Compounds were visualised with a UV lamp (254 nm) and/or by staining with $KMnO_4$ or CAM.

^1H and ^{13}C NMR spectra were recorded on a Varian Mercury-Plus 400 or a Bruker Avance 600 NMR spectrometer at 298 K unless otherwise indicated. PSS studies were performed on a Varian Unity Plus 500 NMR spectrometer. Chemical shifts are given in parts per million (ppm) relative to the residual solvent signal ($CDCl_3$ = δ 7.26 for ^1H, δ 77.2 for ^{13}C; CD_2Cl_2 = δ 5.32 for ^1H, δ 53.8 for ^{13}C; d_4-methanol = δ 3.31 for ^1H; d_8-THF = δ 5.02 for ^1H, δ 67.2 for ^{13}C). Multiplets in 1H NMR spectra are designated as follows: s (singlet), d (doublet), t (triplet), q (quartet), p (pentet), m (multiplet), br (broad). High resolution mass spectrometry (HRMS, ESI+) was performed on an LTQ Orbitrap XL spectrometer. Semi-prep high-performance liquid chromatography was performed on a Shimadzu Prominence HPLC system, using a Phenomenex Luna 10 µm PREP Silica(3) column (250 x 10.0 mm, particle size 100 Å). UV-Vis absorption spectra were recorded on an Agilent 8453 UV-Vis Diode Array System, equipped with a Quantum Northwest Peltier controller, in 10 mm quartz cuvettes. Irradiation experiments were performed using LEDs obtained from Thorlabs Incorporated.

2. Preparation and characterisation of compounds

2.1 Upper halves

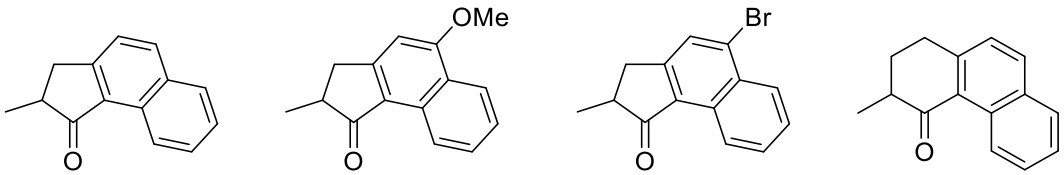

S1 **S2** **S3** **S4**

Ketones **S1**,[1] **S2**,[2] **S3**[2] and **S4**[3] were synthesised according to literature procedures.

2.2 Lower halves

1-phenylindolin-2-one (S5)

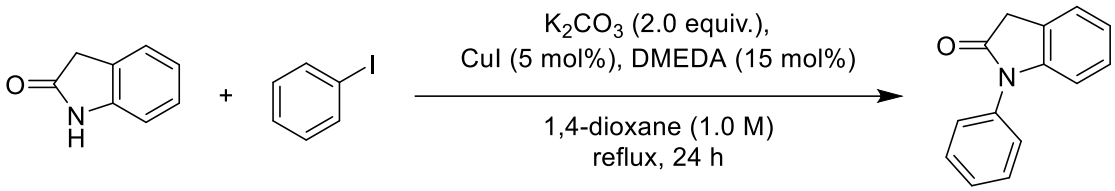

S5

Oxindole **S5** was synthesised according to a modified literature procedure.[4] An oven-dried N_2 filled Schlenk tube was charged with CuI (190 mg, 0.10 mmol, 10 mol%), K_2CO_3 (5.53 g, 40.0 mmol, 2.0 equiv.) and oxindole (3.15 g, 24.0 mmol, 1.2 equiv.). The Schlenk tube was fitted with a rubber septum, and then was added dry 1,4-dioxane (20 mL, 1.0 M). Iodobenzene (2.24 mL, 20.0 mmol, 1.0 equiv.) and *N*,*N'*-dimethylethylenediamine (DMEDA) (0.32 mL, 0.15 mmol, 15 mol%) were added successively. The rubber septum was removed and the Schlenk tube was quickly sealed with a glass stopper fitted with a Glindemann® PTFE sealing ring, and the tap of the Schlenk tube was then closed to N_2. The Schlenk tube was immersed in an oil bath pre-heated to 110 °C and stirred vigorously for 24 h. The reaction mixture was cooled to room temperature, diluted with EtOAc (15 mL) and filtered through a plug of celite, eluting with EtOAc (50 mL). The volatiles were evaporated *in vacuo* and the resulting residue was purified by flash column chromatography (SiO_2, pentane:EtOAc 9:1) to provide **S5** as a white solid (2.54 g, 61%). **^{1}H NMR** (400 MHz, $CDCl_3$) δ 7.53 (t, J = 7.8 Hz, 2H), 7.45 – 7.38 (m, 3H), 7.35 – 7.28 (m, 1H), 7.21 (td, J = 7.8, 1.3 Hz, 1H), 7.08 (td, J = 7.5, 1.1 Hz, 1H), 6.79 (d, J = 7.9 Hz, 1H), 3.72 (s, 2H); **^{13}C NMR** (101 MHz, $CDCl_3$) δ 174.6, 145.4, 134.7, 129.8, 128.2, 127.9, 126.8, 124.8, 124.5, 122.9, 109.5, 36.2.

1-(4-methoxyphenyl)indolin-2-one (S6)

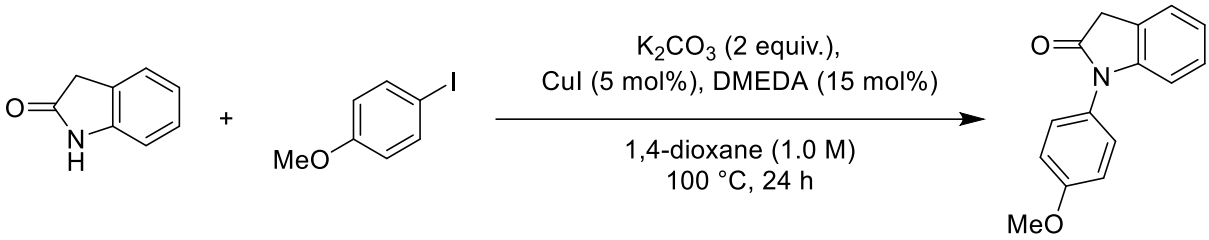

S6

Oxindole **S6** was synthesised according to a modified literature procedure.[5] An oven-dried N_2 filled 5 mL crimp-top vial was charged with CuI (9.50 mg, 0.05 mmol, 5 mol%), K_2CO_3 (276 mg, 2.00 mmol, 2.0 equiv.), oxindole (160 mg, 1.2 mmol, 1.2 equiv.) and 4-iodoanisole (234 mg, 1.0 mmol, 1.0 equiv.). Subsequently, dry 1,4-dioxane (1 mL, 1.0 M) and DMEDA (16.0 µL, 0.15 mmol, 15 mol%) were added. The vial was placed inside an aluminium heating block pre-heated to 100 °C and stirred for 24 h. The reaction mixture was cooled to room temperature, diluted with EtOAc (15 mL) and filtered through a plug of celite, eluting with EtOAc (50 mL). The volatiles were evaporated *in vacuo* and the resulting residue was purified by flash column chromatography (SiO_2, pentane:EtOAc 4:1) to provide **S6** as a pale pink solid (212 mg, 89%). **^{1}H NMR** (300 MHz, $CDCl_3$) δ 7.35 – 7.25 (m, 3H), 7.25 – 7.14 (m, 1H), 7.12 – 6.97 (m, 3H), 6.73 (d, J = 7.9 Hz, 1H), 3.85 (s, 3H), 3.70 (s, 2H); **^{13}C NMR** (101 MHz, $CDCl_3$) δ 174.9, 159.3, 146.0, 128.1, 127.9, 127.0, 124.7, 124.4, 122.8, 115.1, 109.4, 55.7, 36.1.

1-(4-bromophenyl)indolin-2-one (S7)

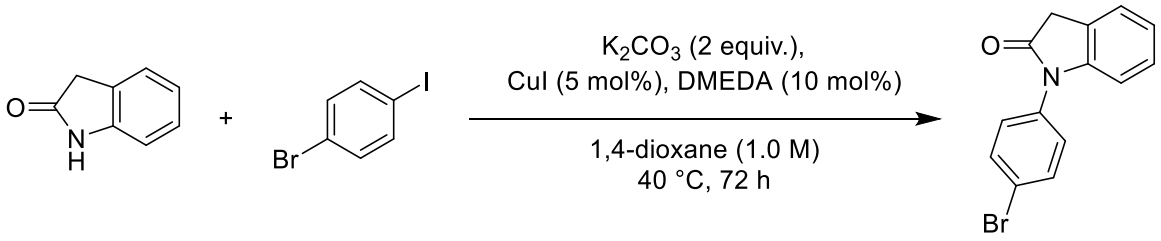

S7

Oxindole **S7** was synthesised according to a modified literature procedure.[5] An oven-dried N_2 filled 10 mL crimp-top vial was charged with CuI (35.8 mg, 0.19 mmol, 5 mol%), K_2CO_3 (1.04 g, 7.51 mmol, 2.0 equiv.), oxindole (500 mg, 3.75 mmol, 1.2 equiv.) and 1-bromo-4-iodobenzene (1.28 g, 4.51 mmol, 1.2 equiv.). Subsequently, dry 1,4-dioxane (3.80 mL, 1.0 M) and DMEDA (40.0 µL, 0.38 mmol, 10 mol%) were added. The vial was placed inside an aluminium heating block pre-heated to 40 °C and stirred for 72 h. The reaction mixture was cooled to room temperature, diluted with EtOAc (30 mL) and filtered through a plug of celite, eluting with EtOAc (100 mL). The volatiles were evaporated *in vacuo* and the resulting residue was purified by flash column chromatography (SiO_2, pentane:EtOAc 4:1) to provide **S7** as a pale pink solid

(700 mg, 65%). **^{1}H NMR** (300 MHz, $CDCl_3$) δ 7.67 – 7.61 (m, 2H), 7.35 – 7.27 (m, 3H), 7.25 – 7.15 (m, 1H), 7.09 (td, *J* = 7.5, 1.1 Hz, 1H), 6.79 (d, *J* = 7.9 Hz, 1H), 3.70 (d, *J* = 1.8 Hz, 2H); **^{13}C NMR** (101 MHz, $CDCl_3$) δ 174.4, 144.8, 139.0, 133.0, 128.3, 128.0, 128.0, 124.9, 124.4, 123.2, 121.8, 109.4, 36.1.

2.3 Motors

General procedure for the synthesis of oxindole-based motors

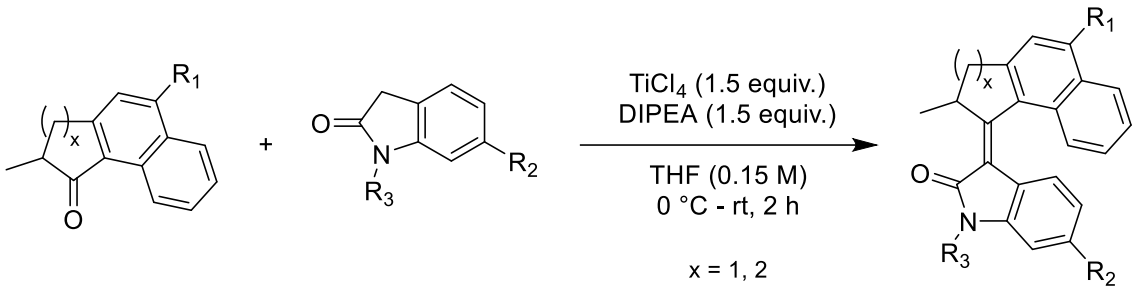

upper half ***lower half*** ***motor***

An oven-dried Schlenk tube under N_2 atmosphere was charged with the appropriate ketone (**S1** – **S4**) (0.50 mmol, 1.0 equiv.) in dry THF (2 mL, 0.25 M), and cooled to 0 °C in an ice bath. $TiCl_4$ (0.08 mL, 0.75 mmol, 1.5 equiv.) was added dropwise and the resulting suspension was stirred for 5 min at this temperature. To this mixture was added a solution of the appropriate oxindole derivative (oxindole, 6-bromooxindole, or **S5**–**S7**) (0.75 mmol, 1.5 equiv.) in dry THF (1 mL, 0.75 M) *via* syringe. Subsequently, DIPEA (0.10 mL, 0.75 mmol, 1.5 equiv.) was added dropwise, and the resulting mixture was allowed to warm to room temperature and stirred for 2 h. The reaction was quenched with aqueous HCl solution (1 M, 5 mL) and extracted with EtOAc (3 x 10 mL). The combined organic layers were washed with brine and dried over $MgSO_4$, and the volatiles removed *in vacuo* to yield a yellow oil. The crude was subsequently purified by flash column chromatography (SiO_2, pentane:EtOAc 4:1), and subsequently recrystallised *via* slow evaporation of MeOH into a concentrated solution of the product in $CHCl_3$ to yield the corresponding motor exclusively as the stable *E* isomer.

(*E*)-3-(2-methyl-2,3-dihydro-1H-cyclopenta[a]naphthalen-1-ylidene)indolin-2-one (*E*$_S$-1)

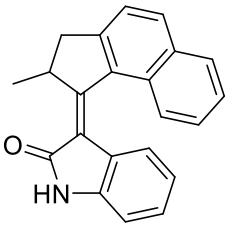

***E*$_S$-1**

Motor ***E*$_S$-1** was synthesised according to the general procedure to yield orange needles (56.0 mg, 36%). **^{1}H NMR** (600 MHz, $CDCl_3$) δ 8.40 (br s, 1H), 8.00 (d, *J* = 8.2 Hz, 1H), 7.99 – 7.95 (m, 1H), 7.64 (dd, *J* = 8.4, 1.2 Hz, 1H), 7.59 (d, *J* = 8.2 Hz, 1H), 7.53 (ddd, *J* = 8.2, 6.8, 1.2 Hz, 1H), 7.43 (ddd, *J* = 8.2, 6.8, 1.2 Hz, 1H), 7.11 (td, *J* = 7.6, 1.2 Hz, 1H), 6.90 (ddd, *J* = 7.8, 1.1, 0.6 Hz, 1H), 6.63 (td, *J* = 7.6, 1.1 Hz, 1H), 6.41 – 6.34 (m, 1H), 4.69 – 4.62 (m, 1H), 3.53 (dd, *J* = 15.6, 5.9 Hz, 1H), 2.78 (d, *J* = 15.6 Hz, 1H), 1.30 (d,

J = 6.8 Hz, 3H); **^{13}C NMR** (151 MHz, $CDCl_3$) *δ* 170.5, 162.7, 150.8, 140.1, 134.9, 133.0, 132.9, 129.3, 129.0, 127.8, 127.6, 127.0, 125.8, 125.6, 124.2, 123.2, 120.6, 120.1, 109.0, 43.7, 41.7, 19.6; **HRMS** (ESI+, *m*/*z*) calcd for $C_{22}H_{18}NO$ $[M+H]^+$ = 312.1383, found 312.1382.

(*Z*)-3-(2-methyl-2,3-dihydro-1H-cyclopenta[a]naphthalen-1-ylidene)indolin-2-one (*Z*$_S$-1)

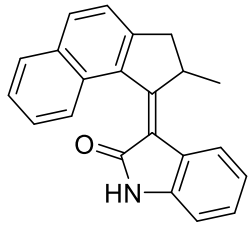

***Z*$_S$-1**

An oven-dried N_2 filled crimp-top vial was charged with motor ***E*$_S$-1** (20.0 mg), dissolved in degassed (freeze-pump-thaw, three cycles) EtOAc (40 mL) and irradiated with a 365 nm LED for 16 h while stirring. The volatiles were removed *in vacuo* to give an orange oil, which was subsequently purified by flash column chromatography (SiO_2, pentane:EtOAc 100:0 – 90:10, gradient over 1 h) to yield ***Z*$_S$-1** (5.00 mg, 25%). **^{1}H NMR** (600 MHz, $CDCl_3$) δ 8.12 (br s, 1H), 7.94 (d, *J* = 8.2 Hz, 1H), 7.91 – 7.88 (m, 1H), 7.87 – 7.84 (m, 1H), 7.64 (d, *J* = 7.6 Hz, 1H), 7.54 – 7.48 (m, 3H), 7.23 (td, *J* = 7.7, 1.1 Hz, 1H), 7.10 (d, *J* = 1.1 Hz, 1H), 6.80 (ddd, *J* = 7.7, 1.1, 0.5 Hz, 1H), 4.08 (p, *J* = 6.9, 1H), 3.55 (dd, *J* = 15.4, 5.8 Hz, 1H), 2.77 (d, *J* = 15.4 Hz, 1H), 1.37 (d, *J* = 6.9 Hz, 3H); **^{13}C NMR** (151 MHz, $CDCl_3$) δ 167.0, 161.6, 148.9, 140.3, 134.6, 133.3, 132.7, 131.0, 128.4, 128.3, 127.9, 126.0, 125.5, 125.3, 123.5, 123.2, 121.7, 120.2, 109.7, 44.3, 41.4, 19.5.

(*E*)-3-(5-methoxy-2-methyl-2,3-dihydro-1H-cyclopenta[a]naphthalen-1-ylidene)indolin-2-one (*E*$_S$-2)

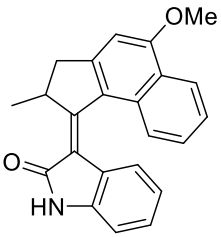

***E*$_S$-2**

Motor ***E*$_S$-2** was synthesised according to the general procedure, with some modifications. An oven-dried Schlenk tube under N_2 atmosphere was charged with ketone **S2** (113 mg, 0.50 mmol, 1.0 equiv.) in dry THF (2 mL, 0.25 M), and cooled to 0 °C in an ice bath. $TiCl_4$ (0.08 mL, 0.7 mmol, 1.5 equiv.) was added dropwise and the resulting suspension was stirred for 5 min at this temperature. To this mixture was added a solution of oxindole (100 mg, 0.75 mmol, 1.5 equiv.) in dry THF (1 mL, 0.75 M) *via* syringe. Subsequently, DIPEA (0.10 mL, 0.75 mmol, 1.5 equiv.) was added dropwise, and the resulting mixture was allowed to warm to room temperature and stirred for 2 h. The reaction was quenched with sat. aqueous NH_4Cl solution (5 mL) which caused the formation of an orange precipitate. The precipitate was filtered off and washed with pentane followed by cold CH_2Cl_2 to yield motor ***E*$_S$-2** as an orange precipitate (124 mg, 73%). **^{1}H NMR** (600 MHz, d_8-THF) δ 9.43 (br s, 1H), 8.38 – 8.26 (m, 1H), 7.55 (d, *J* = 8.3 Hz, 1H), 7.46 (ddd, *J* = 8.3, 6.8, 1.3 Hz, 1H), 7.39 (ddd, *J* = 8.3, 6.8, 1.4 Hz, 1H), 7.11 (s, 1H), 6.98 (td, *J* = 7.6, 1.2 Hz, 1H), 6.79 – 6.74 (m, 1H), 6.49 (td, *J* = 7.6, 1.1 Hz, 1H), 6.28 (d, *J* = 7.7 Hz, 1H), 4.56 (p, *J* = 6.7 Hz, 1H), 4.11 (s, 3H), 3.52 – 3.39 (m, 1H), 2.71 (d, *J* = 15.6 Hz, 1H), 1.21 (d, *J* = 6.7 Hz 3H); **^{13}C NMR** (151 MHz, d_8-THF) δ 170.5, 161.3, 160.5, 153.5, 142.5, 131.0, 128.5, 128.2, 128.1, 127.9, 126.1, 125.9, 125.7,

124.5, 123.8, 120.3, 119.6, 109.2, 103.6, 56.5, 44.1, 42.8, 20.2; **HRMS** (ESI+, *m*/*z*) calcd for $C_{23}H_{19}NO$ $[M+H]^+$ = 342.1489, found 342.1490.

(*E*)-3-(5-bromo-2-methyl-2,3-dihydro-1H-cyclopenta[a]naphthalen-1-ylidene)indolin-2-one (S8)

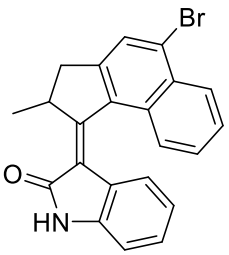

S8

Motor **S8** was synthesised according to the general procedure to yield orange crystals (67.0 mg, 34%). **^{1}H NMR** (300 MHz, $CDCl_3$) δ 8.39 (d, *J* = 8.5 Hz, 1H), 7.93 (br s, 1H), 7.85 (s, 1H), 7.64 (dd, *J* = 12.9, 8.0 Hz, 2H), 7.47 (t, *J* = 7.7 Hz, 1H), 7.12 (t, *J* = 7.7 Hz, 1H), 6.87 (d, *J* = 7.8 Hz, 1H), 6.61 (t, *J* = 7.7 Hz, 1H), 6.31 (d, *J* = 7.8 Hz, 1H), 4.63 (p, *J* = 6.6 Hz, 1H), 3.50 (dd, *J* = 15.9, 5.9 Hz, 1H), 2.74 (d, *J* = 15.8 Hz, 1H), 1.27 (d, *J* = 6.7 Hz, 3H); **^{13}C NMR** (101 MHz, $CDCl_3$) δ 170.0, 161.2, 150.5, 140.1, 135.1, 131.2, 130.0, 128.5, 128.3, 128.2, 128.0, 127.9, 127.8, 127.2, 125.5, 123.0, 120.7, 120.6, 109.1, 43.6, 41.4, 19.5; **HRMS** (ESI+, *m*/*z*) calcd for $C_{22}H_{16}BrNO$ $[M+H]^+$ = 390.0488, found 390.0485.

(*E*)-2-methyl-1-(2-oxoindolin-3-ylidene)-2,3-dihydro-1H-cyclopenta[a]naphthalene-5-carbonitrile (*E*$_S$-3)

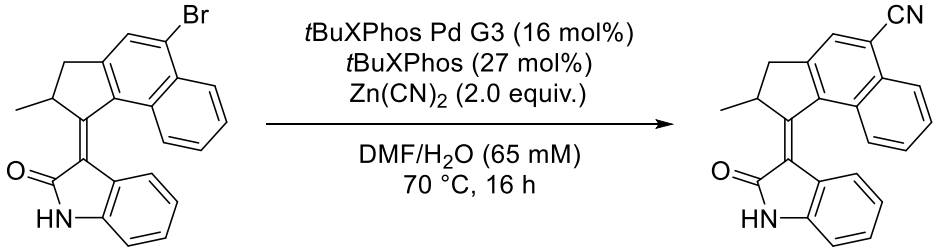

S8 **3**

An oven-dried Schlenk tube under N_2 atmosphere was charged with motor **S8** (44.0 mg, 113 µmol, 1.0 equiv.) tBuXPhos G3 (16.0 mg, 18.0 µmol, 16 mol%), *t*BuXPhos (12.9 mg, 30.4 µmol, 27 mol%) and $Zn(CN)_2$ (26.5 mg, 22.5 mmol, 2.0 equiv.). A degassed (3x freeze-pump-thaw) mixture of DMF/H_2O (99:1, 1.70 mL, 65.0 mM) was added and the resulting solution was heated to 70 °C and stirred for 16 h. After cooling to room temperature, the mixture was diluted with EtOAc, washed with brine, dried over $MgSO_4$, and the volatiles were removed *in vacuo*. The crude product was purified by flash column chromatography (SiO_2, pentane:EtOAc 9:1), and subsequently recrystallised *via* slow evaporation of MeOH into a concentrated solution of the product in $CHCl_3$ to yield motor ***E*$_S$-3** as deep red crystals (37.0 mg, 98%).

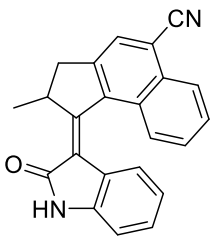

***E*S-3**

^{1}H NMR (400 MHz, $CDCl_3$) δ 8.39 (d, *J* = 8.4 Hz, 1H), 8.01 (s, 1H), 7.92 (br s, 1H), 7.77 (d, *J* = 8.5 Hz, 1H), 7.73 (ddd, *J* = 8.3, 6.9, 1.2 Hz, 1H), 7.54 (ddd, *J* = 8.3, 6.9, 1.2 Hz, 1H), 7.14 (td, *J* = 7.7, 1.1 Hz, 1H), 6.87 (d, *J* = 7.8 Hz, 1H), 6.62 (td, *J* = 7.7, 1.1 Hz, 1H), 6.29 (d, *J* = 7.8 Hz, 1H), 4.69 (p, *J* = 6.6 Hz, 1H), 3.53 (dd, *J* = 15.9, 6.0 Hz, 1H), 2.80 (d, *J* = 15.8 Hz, 1H), 1.26 (d, *J* = 6.8 Hz, 3H); **^{13}C NMR** (101 MHz, $CDCl_3$) δ 169.7, 159.4, 148.2, 140.6, 140.4, 132.0, 130.3, 129.1, 128.8, 128.4, 128.4, 128.1, 126.3, 125.7, 122.8, 122.5, 120.9, 117.9, 113.3, 109.4, 43.5, 41.2, 19.2; **HRMS** (ESI+, *m*/*z*) calcd for $C_{23}H_{16}N_2O$ $[M+H]^+$ = 337.1335, found 337.1332.

(*Z*)-2-methyl-1-(2-oxoindolin-3-ylidene)-2,3-dihydro-1H-cyclopenta[a]naphthalene-5-carbonitrile (*Z*S-3)

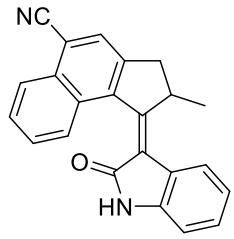

***Z*S-3**

An oven-dried N_2 filled crimp-top vial was charged with motor ***E*S-3** (10.0 mg) was dissolved in degassed (freeze-pump-thaw, three cycles) EtOAc (20 mL) and irradiated with a 365 nm LED for 16 h while stirring. The volatiles were removed *in vacuo* to give a red oil, was subsequently purified by semi-prep high performance liquid chromatography (SiO_2, heptane/propan-2-ol 99:1, 4.0 mL min^{-1}, 60 min, see section 4 for details) to yield ***Z*S-3** (3.00 mg, 30%). **^{1}H NMR** (600 MHz, $CDCl_3$) δ 8.32 (d, *J* = 8.2 Hz, 1H), 7.96 (d, *J* = 8.5 Hz, 1H), 7.94 (s, 1H), 7.74 – 7.69 (m, 2H), 7.66 (d, *J* = 7.7 Hz, 1H), 7.63 (t, J = 7.4 Hz, 1H), 7.31 (t, *J* = 7.4 Hz, 1H), 7.15 (t, *J* = 7.4 Hz, 1H), 6.91 (d, *J* = 7.7 Hz, 1H), 4.12 (p, *J* = 7.0 Hz, 1H), 3.58 (dd, *J* = 15.5, 7.0 Hz, 1H), 2.83 (d, *J* = 15.5 Hz, 1H), 1.39 (d, *J* = 7.0 Hz, 3H); **^{13}C NMR** (151 MHz, $CDCl_3$) δ 169.2, 161.2, 148.5, 139.5, 138.6, 131.9, 130.1, 128.5, 128.5, 128.4, 127.6, 126.4, 126.2, 125.7, 123.6, 121.5, 120.9, 117.6, 113.8, 110.0, 43.4, 41.1, 19.1.

(*E*)-3-(3-methyl-2,3-dihydrophenanthren-4(1H)-ylidene)indolin-2-one (*E*S-4)

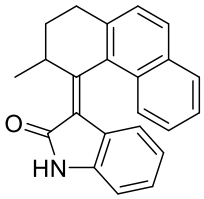

***E*S-4**

Motor ***E*S-4** was synthesised according to the general procedure to yield pale yellow crystals (102 mg, 62%). **^{1}H NMR** (600 MHz, $CDCl_3$) δ 7.90 (dd, *J* = 8.3, 2.2 Hz, 2H), 7.78 (d, *J* = 8.5 Hz, 1H), 7.63 (br s, 1H), 7.47 – 7.38 (m, 2H), 7.31 (ddd, *J* = 8.3, 6.9, 1.4 Hz, 1H), 6.96 (td, *J* = 7.6, 1.3 Hz, 1H), 6.75 (d, *J* = 7.7 Hz, 1H), 6.31 (td, *J* = 7.7, 1.2 Hz, 1H), 5.67 (d, *J* = 7.9 Hz, 1H), 4.89 (h, *J* = 7.0 Hz, 1H), 2.78 (ddd, *J* = 14.6, 4.6, 3.1 Hz, 1H), 2.60 (ddd, *J* = 14.4, 12.5, 5.3 Hz, 1H), 2.37 (ddq, *J* = 12.8, 5.3, 3.1 Hz, 1H), 1.19 – 1.11 (m, 4H); **^{13}C NMR** (151 MHz, $CDCl_3$) δ 169.2, 156.7, 141.1, 139.5, 132.1, 131.6, 130.4, 129.7, 128.7, 128.1, 127.3, 126.1, 125.4, 125.0, 124.0, 123.1, 122.7, 121.2, 108.8, 32.5, 29.7, 29.4, 20.9; **HRMS** (ESI+, *m*/*z*) calcd for $C_{23}H_{19}NO$ $[M+H]^+$ = 348.1359, found 348.1357.

(*Z*)-3-(3-methyl-2,3-dihydrophenanthren-4(1H)-ylidene)indolin-2-one (*Z*$_S$-4)

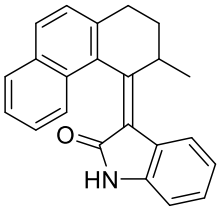

***Z*$_S$-4**

An oven-dried N_2 filled crimp-top vial was charged with motor ***E*$_S$-4** (10.0 mg) was dissolved in degassed (freeze-pump-thaw, three cycles) EtOAc (20 mL) and irradiated with a 365 nm LED for 16 h while stirring. The colour change of the solution during irradiation from yellow to orange indicated the generation of the ***Z*$_M$-4** isomer. The mixture was then heated to reflux in the dark for 2 h, and the solution had turned yellow once again. After being left to cool to room temperature, the volatiles were removed *in vacuo* to give a yellow oil. This was subsequently purified by flash column chromatography (SiO_2, pentane:EtOAc 100:0 – 90:10, gradient over 1 h) to yield ***Z*$_S$-4** (5.00 mg, 50%). **^{1}H NMR** (400 MHz, $CDCl_3$) δ 8.00 (d, *J* = 8.2 Hz, 1H), 7.88 – 7.80 (m, 2H), 7.78 (br s, 1H), 7.74 (d, *J* = 7.8 Hz, 1H), 7.42 (dd, *J* = 6.9, 1.3 Hz, 1H), 7.39 – 7.33 (m, 2H), 7.24 (d, *J* = 7.7 Hz, 1H), 7.10 (t, *J* = 7.7 Hz, 1H), 6.72 (d, *J* = 7.7 Hz, 1H), 3.95 (h, *J* = 7.2 Hz, 1H), 2.75 (dt, *J* = 14.2, 3.6 Hz, 1H), 2.57 (td, *J* = 13.7, 4.7 Hz, 1H), 2.39 (dddd, *J* = 12.6, 7.7, 4.7, 2.8 Hz, 1H), 1.28 (d, *J* = 6.9 Hz, 3H), 1.13 (tdd, *J* = 12.5, 7.5, 4.2 Hz, 1H); **^{13}C NMR** (151 MHz, $CDCl_3$) δ 167.1, 154.1, 141.0, 139.6, 133.0, 131.9, 131.8, 129.6, 128.5, 128.4, 126.5, 125.6, 124.9, 124.6, 124.4, 123.7, 123.5, 121.8, 109.8, 35.3, 29.9, 29.7, 20.3.

(*E*)-6-bromo-3-(3-methyl-2,3-dihydrophenanthren-4(1H)-ylidene)indolin-2-one (S9)

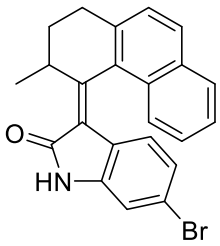

S9

Motor **S9** was synthesised according to the general procedure to yield yellow crystals (121 mg, 60%). **^{1}H NMR** (600 MHz, $CDCl_3$) δ 8.18 (s, 1H), 7.94 – 7.88 (m, 2H), 7.73 (dd, *J* = 8.5, 1.0 Hz, 1H), 7.45 – 7.41 (m, 3H), 7.33 (ddd, *J* = 8.3, 6.7, 1.3 Hz, 1H), 6.95 (d, *J* = 1.8 Hz, 1H), 6.44 (dd, *J* = 8.4, 1.8 Hz, 1H), 5.49 (d, *J* = 8.4 Hz, 1H), 4.86 (dt, *J* = 7.8, 6.8 Hz, 1H), 2.60 (ddd, *J* = 14.6, 12.4, 5.3 Hz, 1H), 2.38 (dddd, *J* = 13.1, 8.2, 5.3, 3.1 Hz, 1H), 1.21 – 1.10 (m, 4H); **^{13}C NMR** (151 MHz, $CDCl_3$) δ 169.3, 157.8, 141.3, 140.7, 132.1, 131.3, 130.2, 130.0, 128.8, 127.5, 126.1, 125.5, 125.0, 124.8, 124.2, 122.0, 122.0, 121.6, 112.3, 32.8, 29.7, 29.2, 20.8; **HRMS** (ESI+, *m*/*z*) calcd for $C_{23}H_{18}BrNO$ $[M+H]^+$ = 404.0645, found 404.0641.

(*E*)-6-methoxy-3-(3-methyl-2,3-dihydrophenanthren-4(1H)-ylidene)indolin-2-one (*E*$_S$-5)

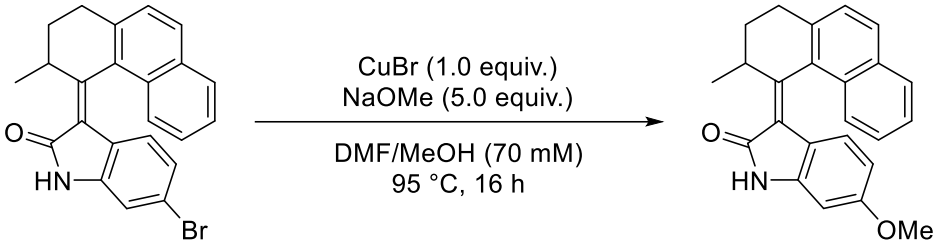

S9 **5**

An oven-dried Schlenk tube under N_2 atmosphere was charged with motor **S9** (20.0 mg, 50.0 µmol, 1.0 equiv.) and CuBr (7.10 mg, 50.0 µmol, 1.0 equiv.). A degassed (sparged with N_2 for 30 min) mixture of MeOH/DMF (5:2, 0.7 mL, 70.0 mM) was added, followed by NaOMe (54.0 µL, 25 wt. % in MeOH, 5.0 equiv.) and the resulting solution was heated to 95 °C for 16 h. After cooling to room temperature, the mixture was extracted with CH_2Cl_2, washed with brine, dried over $MgSO_4$, and the volatiles were removed *in vacuo*. The crude product was purified by flash column chromatography (SiO_2, pentane:EtOAc 4:1), and subsequently recrystallised *via* slow evaporation of MeOH into a concentrated solution of the product in $CHCl_3$ to yield motor ***E*$_S$-5** as yellow needles (15.0 mg, 85%).

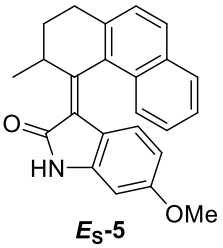

***E*$_S$-5**

^{1}H NMR (600 MHz, $CDCl_3$) δ 8.29 (s, 1H), 7.95 – 7.84 (m, 2H), 7.80 (dd, *J* = 8.5, 1.3 Hz, 1H), 7.42 (t, *J* = 7.5 Hz, 2H), 7.32 (ddd, *J* = 8.3, 6.8, 1.3 Hz, 1H), 6.37 (d, *J* = 2.4 Hz, 1H), 5.86 (dd, *J* = 8.7, 2.4 Hz, 1H), 5.57 (d, *J* = 8.7 Hz, 1H), 4.86 (h, *J* = 7.0 Hz, 1H), 3.66 (s, 3H), 2.77 (ddd, *J* = 14.5, 4.5, 3.0 Hz, 1H), 2.60 (ddd, *J* = 14.4, 12.5, 5.3 Hz, 1H), 2.37 (dddd, *J* = 13.0, 8.2, 5.2, 3.0 Hz, 1H), 1.19 – 1.08 (m, 4H); **^{13}C NMR** (151 MHz, $CDCl_3$) δ 170.3, 160.0, 153.5, 141.2, 141.1, 132.1, 131.9, 130.4, 129.4, 128.7, 127.2, 126.1, 125.3, 125.2, 125.0, 122.6, 116.2, 106.2, 96.0, 55.4, 32.3, 29.8, 29.6, 21.0; **HRMS** (ESI+, *m*/*z*) calcd for $C_{24}H_{21}NO_2$ $[M+H]^+$ = 356.1645, found 356.1642.

(*Z*)-6-methoxy-3-(3-methyl-2,3-dihydrophenanthren-4(1H)-ylidene)indolin-2-one (*Z*$_S$-5)

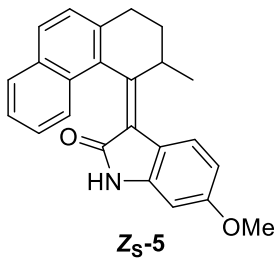

***Z*$_S$-5**

An oven-dried N_2 filled crimp-top vial was charged with motor ***E*$_S$-5** (5.00 mg) was dissolved in degassed (freeze-pump-thaw, three cycles) EtOAc (10 mL) and irradiated with a 365 nm LED for 16 h while stirring. The colour change of the solution during irradiation from yellow to orange indicated the generation of the ***Z*$_M$-5** isomer. The mixture was then heated to reflux in the dark for 2 h, and the solution had turned yellow once again. After being left to cool to room temperature, the volatiles were removed *in vacuo* to give a yellow oil. This was subsequently purified by semi-prep high performance

liquid chromatography (SiO_2, heptane:EtOAc 80:20, 3.5 mL min^{-1}, 40 min, see section 4 for details) to yield ***Z*S-5** (2.00 mg, 40%). **^{1}H NMR** (500 MHz, $CDCl_3$) δ 8.03 – 7.91 (m, 1H), 7.87 – 7.78 (m, 3H), 7.71 (s, 1H), 7.44 – 7.31 (m, 4H), 6.45 (s, 1H), 3.94 (s, 3H), 3.84 – 3.75 (m, 1H), 2.81 – 2.69 (m, 1H), 2.56 (td, *J* = 13.7, 4.7 Hz, 1H), 2.41 (dd, *J* = 7.9, 4.8 Hz, 1H), 1.30 – 1.24 (d, 3H), 1.13 (tdd, *J* = 12.6, 7.6, 4.3 Hz, 1H); **^{13}C NMR** (151 MHz, $CDCl_3$) δ 169.9, 160.0, 153.5, 141.1, 141.0, 132.1, 131.8, 130.4, 129.4, 128.7, 127.2, 126.1, 125.3, 125.2, 125.0, 122.3, 116.2, 106.2, 95.8, 55.4, 32.3, 29.8, 29.6, 21.0.

(*E*)-3-(3-methyl-2,3-dihydrophenanthren-4(1H)-ylidene)-2-oxoindoline-6-carbonitrile (*E*S-6)

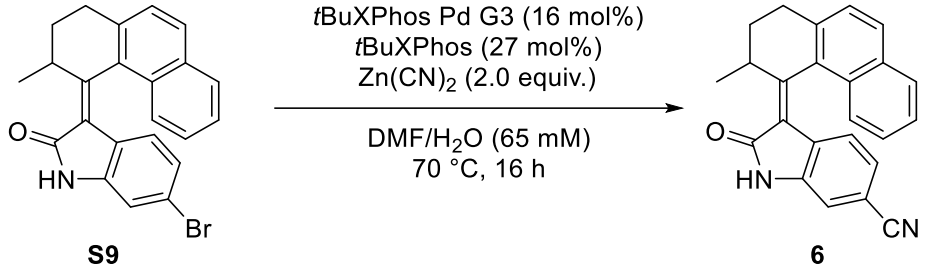

An oven-dried Schlenk tube under N_2 atmosphere was charged with motor **S8** (50.0 mg, 124 µmol, 1.0 equiv.) tBuXPhos G3 (17.6 mg, 20.0 µmol, 16 mol%), *t*BuXPhos (14.1 mg, 33.0 µmol, 27 mol%) and $Zn(CN)_2$ (29.0 mg, 24.7 mmol, 2.0 equiv.). A degassed (3x freeze-pump-thaw) mixture of DMF/H_2O (99:1, 1.9 mL, 65 mM) was added and the resulting solution was heated to 70 °C for 16 h. After cooling to room temperature, the mixture was diluted with EtOAc, washed with brine, dried over $MgSO_4$, and the volatiles were removed *in vacuo*. The crude product was purified by flash column chromatography (SiO_2, pentane:EtOAc 9:1), and subsequently recrystallised *via* slow evaporation of MeOH into a concentrated solution of the product in $CHCl_3$ to yield motor ***E*S-6** exclusively as yellow crystals of the *E* isomer (38.0 mg, 88%).

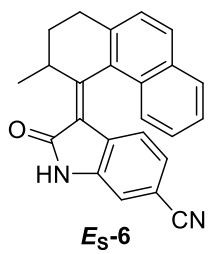

***E*S-6**

^{1}H NMR (600 MHz, $CDCl_3$) δ 8.69 (s, 1H), 7.95 (d, *J* = 8.3 Hz, 1H), 7.93 – 7.90 (m, 1H), 7.69 (d, *J* = 8.5 Hz, 1H), 7.51 – 7.39 (m, 2H), 7.32 (ddd, *J* = 8.4, 6.8, 1.3 Hz, 1H), 7.05 (d, *J* = 1.5 Hz, 1H), 6.62 (dd, *J* = 8.1, 1.5 Hz, 1H), 5.71 (d, *J* = 8.2 Hz, 1H), 4.89 (h, *J* = 7.0 Hz, 1H), 2.84 (ddd, *J* = 14.8, 4.6, 3.1 Hz, 1H), 2.61 (ddd, *J* = 14.7, 12.4, 5.4 Hz, 1H), 2.40 (dddd, *J* = 13.1, 8.2, 5.4, 3.1 Hz, 1H), 1.25 – 1.15 (m, 4H); **^{13}C NMR** (151 MHz, $CDCl_3$) δ 169.0, 162.0, 141.6, 139.8, 132.2, 130.7, 130.7, 130.1, 129.0, 127.8, 127.2, 126.2, 125.7, 125.6, 124.4, 123.9, 121.6, 119.1, 111.7, 110.6, 33.3, 29.6, 28.9, 20.7; **HRMS** (ESI+, *m*/*z*) calcd for $C_{24}H_{18}N_2O$ $[M+H]^+$ = 351.1492, found 351.1493.

(*Z*)-3-(3-methyl-2,3-dihydrophenanthren-4(1H)-ylidene)-2-oxoindoline-6-carbonitrile (*Z*$_S$-6)

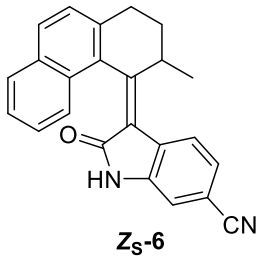

***Z*$_S$-6**

An oven-dried N_2 filled crimp-top vial was charged with motor ***E*$_S$-6** (5.00 mg) was dissolved in degassed (freeze-pump-thaw, three cycles) EtOAc (10 mL) and irradiated with a 365 nm LED for 16 h while stirring. The colour change of the solution during irradiation from yellow to orange indicated the generation of the ***Z*$_M$-6** isomer. The mixture was then heated to reflux in the dark for 2 h, and the solution had turned yellow once again. After being left to cool to room temperature, the volatiles were removed *in vacuo* to give an orange oil. This was subsequently purified by semi-prep high performance liquid chromatography (SiO_2, heptane:EtOAc 80:20, 3.5 mL min^{-1}, 30 min, see section 4 for details) to yield ***Z*$_S$-6** (2 mg, 40%). **^{1}H NMR** (600 MHz, $CDCl_3$) δ 8.05 (s, 1H), 7.92 (d, *J* = 8.6 Hz, 2H), 7.89 (t, *J* = 8.8 Hz, 1H), 7.79 (d, *J* = 8.0 Hz, 1H), 7.47 (t, *J* = 7.4 Hz, 1H), 7.38 (m, 4H), 6.88 (d, *J* = 1.5 Hz, 1H), 3.90 (h, *J* = 7.3 Hz, 1H), 2.79 (dt, *J* = 14.4, 3.7 Hz, 1H), 2.57 (td, *J* = 13.8, 4.8 Hz, 1H), 2.41 (ddq, *J* = 12.4, 7.8, 3.5 Hz, 1H), 1.30 (d, *J* = 6.9 Hz, 3H), 1.18 (tdd, *J* = 12.5, 7.4, 4.2 Hz, 1H); **^{13}C NMR** (151 MHz, $CDCl_3$) δ 166.4, 159.2, 141.0, 140.2, 132.7, 131.9, 131.1, 130.7, 128.7, 127.8, 126.9, 126.1, 125.6, 125.2, 124.5, 124.2, 122.3, 119.1, 112.2, 111.0, 35.8, 29.7, 29.2, 20.4.

(*E*)-3-(3-methyl-2,3-dihydrophenanthren-4(1H)-ylidene)-1-phenylindolin-2-one (*E*$_S$-7)

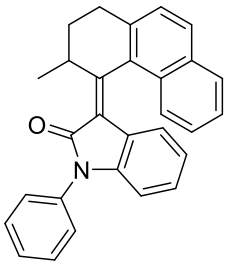

***E*$_S$-7**

Motor ***E*$_S$-7** was synthesised according to the general procedure to yield yellow crystals (123 mg, 61%). **^{1}H NMR** (600 MHz, $CDCl_3$) δ 7.94 – 7.91 (m, 2H), 7.89 (d, *J* = 8.5 Hz, 1H), 7.58 – 7.51 (m, 4H), 7.48 – 7.40 (m, 3H), 7.37 (ddd, *J* = 8.2, 6.7, 1.3 Hz, 1H), 6.95 (td, *J* = 7.7, 1.2 Hz, 1H), 6.78 – 6.73 (m, 1H), 6.37 (td, *J* = 7.7, 1.1 Hz, 1H), 5.77 (dd, *J* = 7.9, 1.1 Hz, 1H), 4.99 – 4.90 (m, 1H), 2.81 (ddd, *J* = 14.5, 4.5, 2.9 Hz, 1H), 2.63 (ddd, *J* = 14.4, 12.7, 5.2 Hz, 1H), 2.39 (dddd, *J* = 13.0, 8.1, 5.2, 2.9 Hz, 1H), 1.21 – 1.10 (m, 4H); **^{13}C NMR** (151 MHz, $CDCl_3$) δ 167.3, 157.1, 142.3, 141.2, 135.0, 132.2, 131.7, 130.5, 129.8, 129.6, 128.7, 127.9, 127.9, 127.4, 127.2, 126.1, 125.4, 125.0, 123.7, 122.5, 122.3, 121.7, 108.7, 32.9, 29.8, 29.5, 20.9; **HRMS** (ESI+, *m*/*z*) calcd for $C_{29}H_{23}NO$ $[M+H]^+$ = 424.1672, found 424.1673.

(*Z*)-3-(3-methyl-2,3-dihydrophenanthren-4(1H)-ylidene)-1-phenylindolin-2-one (*Z*$_S$-7)

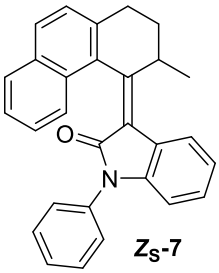

***Z*$_S$-7**

An oven-dried N_2 filled crimp-top vial was charged with motor ***E*$_S$-7** (10.0 mg) was dissolved in degassed (freeze-pump-thaw, three cycles) EtOAc (20 mL) and irradiated with a 365 nm LED for 16 h while stirring. The volatiles were removed *in vacuo* to give an orange oil, which was subsequently purified by flash column chromatography (SiO_2, pentane:EtOAc 100:0 – 90:10, gradient over 1 h) to yield ***Z*$_S$-7** (5.00 mg, 50%). **^{1}H NMR** (600 MHz, $CDCl_3$) δ 8.13 – 8.03 (m, 1H), 7.87 (d, *J* = 7.7 Hz, 1H), 7.83 – 7.78 (m, 2H), 7.42 – 7.36 (m, 4H), 7.35 (d, *J* = 8.2 Hz, 1H), 7.30 – 7.24 (m, 5H), 7.18 (td, *J* = 7.7, 1.1 Hz, 1H), 6.89 (d, *J* = 7.9 Hz, 1H), 4.06 (h, *J* = 7.2 Hz, 1H), 2.77 (dt, *J* = 14.2, 3.6 Hz, 1H), 2.63 (td, *J* = 13.7, 4.8 Hz, 1H), 2.43 (dddd, *J* = 12.6, 7.8, 4.8, 2.9 Hz, 1H), 1.34 (d, *J* = 6.9 Hz, 3H), 1.17 (tdd, *J* = 12.5, 7.4, 4.2 Hz, 1H); **^{13}C NMR** (151 MHz, $CDCl_3$) δ 165.0, 154.7, 143.6, 139.5, 134.8, 132.9, 132.0, 131.9, 129.6, 129.4, 128.5, 128.4, 127.6, 127.2, 126.6, 125.5, 125.0, 124.5, 124.3, 123.2, 122.9, 122.2, 109.3, 35.4, 29.9, 29.7, 20.5.

(*E*)-1-(4-methoxyphenyl)-3-(3-methyl-2,3-dihydrophenanthren-4(1H)-ylidene)indolin-2-one (*E*$_S$-8)

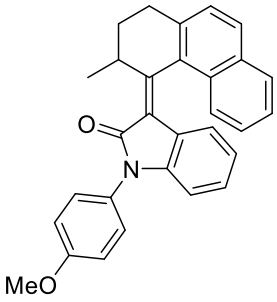

***E*$_S$-8**

Motor **8** was synthesised according to the general procedure to yield bright yellow crystals (120 mg, 59%). **^{1}H NMR** (400 MHz, $CDCl_3$) δ 7.94 – 7.90 (m, 2H), 7.88 (d, *J* = 8.6 Hz, 1H), 7.43 (ddt, *J* = 12.3, 7.6, 3.4 Hz, 4H), 7.36 (ddd, *J* = 8.2, 6.7, 1.3 Hz, 1H), 7.11 – 7.03 (m, 2H), 6.94 (t, *J* = 7.7 Hz, 1H), 6.68 (d, *J* = 7.8 Hz, 1H), 6.35 (t, *J* = 7.7 Hz, 1H), 5.75 (d, *J* = 7.8 Hz, 1H), 4.93 (h, *J* = 7.0 Hz, 1H), 3.88 (s, 3H), 2.80 (dt, *J* = 14.5, 3.8 Hz, 1H), 2.62 (td, *J* = 13.5, 5.2 Hz, 1H), 2.38 (dddd, *J* = 12.9, 8.0, 5.1, 2.9 Hz, 1H), 1.18 – 1.08 (m, 4H); **^{13}C NMR** (101 MHz, $CDCl_3$) δ 167.5, 159.1, 157.0, 142.7, 141.2, 132.1, 131.7, 130.5, 129.8, 128.7, 128.5, 127.9, 127.6, 127.4, 126.1, 125.4, 125.1, 123.7, 122.5, 122.2, 121.6, 114.9, 108.6, 55.7, 32.9, 29.8, 29.5, 20.9; **HRMS** (ESI+, *m*/*z*) calcd for $C_{30}H_{25}NO_2$ $[M+H]^+$ = 432.1958, found 432.1956.

(*E*)-1-(4-bromophenyl)-3-(3-methyl-2,3-dihydrophenanthren-4(1H)-ylidene)indolin-2-one (S10)

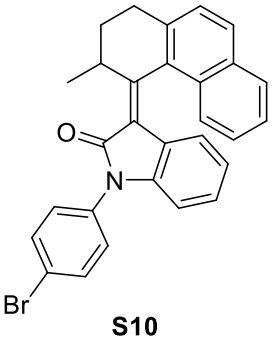

S10

Motor **S10** was synthesised according to the general procedure to yield yellow crystals (145 mg, 60%). **^{1}H NMR** (600 MHz, $CDCl_3$) δ 7.96 – 7.91 (m, 2H), 7.90 – 7.84 (m, 1H), 7.72 – 7.65 (m, 2H), 7.48 – 7.41 (m, 4H), 7.36 (ddd, *J* = 8.3, 6.7, 1.3 Hz, 1H), 6.96 (td, *J* = 7.7, 1.2 Hz, 1H), 6.77 – 6.71 (m, 1H), 6.39 (td, *J* = 7.7, 1.1 Hz, 1H), 5.78 (dd, *J* = 8.0, 1.2 Hz, 1H), 4.96 – 4.85 (m, 1H), 2.81 (ddd, *J* = 14.5, 4.5, 2.9 Hz, 1H), 2.62 (ddd, *J* = 14.5, 12.7, 5.2 Hz, 1H), 2.39 (dddd, *J* = 13.0, 8.2, 5.2, 3.0 Hz, 1H), 1.22 – 1.11 (m, 4H); **^{13}C NMR** (151 MHz, $CDCl_3$) δ 167.0, 157.6, 141.7, 141.3, 138.7, 134.0, 132.8, 132.2, 131.6, 130.4, 129.9, 128.9, 128.8, 128.7, 128.0, 127.4, 126.1, 125.4, 124.9, 123.8, 122.4, 122.2, 122.0, 121.3, 108.6, 33.0, 29.8, 29.4, 20.8; **HRMS** (ESI+, *m*/*z*) calcd for $C_{29}H_{22}BrNO$ $[M+H]^+$ = 480.0958, found 480.0952.

(*E*)-4-(3-(3-methyl-2,3-dihydrophenanthren-4(1H)-ylidene)-2-oxoindolin-1-yl)benzonitrile (*E*$_S$-9)

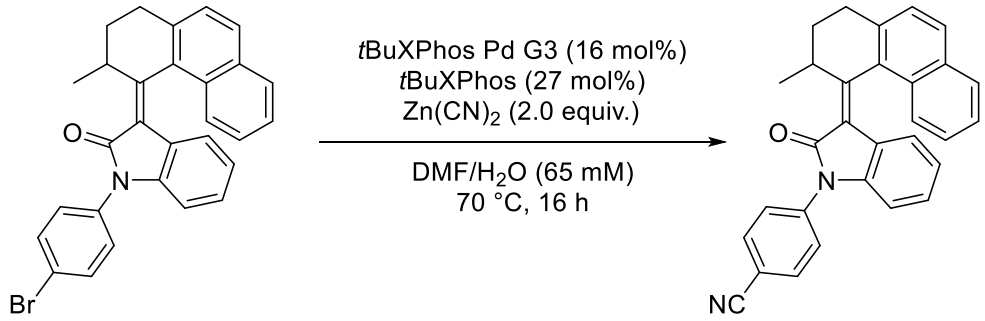

S10 **E_S-9**

An oven-dried Schlenk tube under N_2 atmosphere was charged with motor **S10** (30 mg, 62.0 µmol, 1.0 equiv.) tBuXPhos G3 (9.00 mg, 10.0 µmol, 16 mol%), *t*BuXPhos (7.00 mg, 17.0 µmol, 27 mol%) and $Zn(CN)_2$ (14.1 mg, 12.0 mmol, 2.0 equiv.). A degassed (3x freeze-pump-thaw) mixture of DMF/H_2O (99:1, 96 µL, 65 mM) was added and the resulting solution was heated to 70 °C for 16 h. After cooling to room temperature, the mixture was diluted with EtOAc, washed with brine, dried over $MgSO_4$, and the volatiles were removed *in vacuo*. The crude product was purified by flash column chromatography (SiO_2, pentane:EtOAc 9:1), and subsequently recrystallised *via* slow evaporation of MeOH into a concentrated solution of the product in $CHCl_3$ to yield motor ***E*$_S$-9** as deep yellow crystals (47.0 mg, 75%).

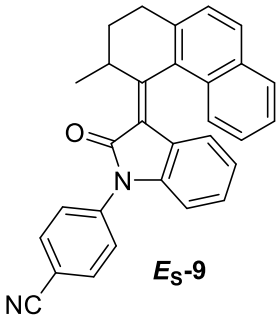

***E*S-9**

^{1}H NMR (600 MHz, $CDCl_3$) δ 7.93 (t, *J* = 8.6 Hz, 2H), 7.85 (d, *J* = 8.3 Hz, 2H), 7.83 (d, *J* = 8.8 Hz, 1H), 7.73 (d, *J* = 8.4 Hz, 2H), 7.46 (d, *J* = 8.4 Hz, 1H), 7.43 (d, *J* = 7.6 Hz), 7.35 (ddt, *J* = 8.1, 6.8, 1.2 Hz, 1H), 6.98 (t, *J* = 7.6 Hz, 1H), 6.83 (d, *J* = 7.9 Hz, 1H), 6.42 (t, *J* = 7.9 Hz) 5.79 (d, *J* = 7.9 Hz, 1H), 4.87 (s, 1H), 2.82 (dt, *J* = 14.6, 3.8 Hz, 1H), 2.61 (td, *J* = 13.6, 5.2 Hz, 1H), 2.39 (dddd, *J* = 11.0, 8.2, 5.2, 2.9 Hz, 1H), 1.20 – 1.11 (m, 4H); **^{13}C NMR** (151 MHz, $CDCl_3$) δ 166.6, 158.4, 141.3, 140.5, 139.1, 133.3, 132.1, 131.2, 130.2, 130.0, 129.2, 129.1, 128.9, 128.7, 128.2, 127.9, 127.4, 127.1, 126.0, 125.4, 125.3, 124.7, 123.9, 122.5, 122.5, 121.7, 118.5, 110.8, 108.5, 33.1, 29.7, 29.2, 20.7; **HRMS** (ESI+, *m*/*z*) calcd for $C_{30}H_{22}N_2O$ $[M+H]^+$ = 427.1805, found 427.1806.

(*Z*)-4-(3-(3-methyl-2,3-dihydrophenanthren-4(1H)-ylidene)-2-oxoindolin-1-yl)benzonitrile (*Z*S-9)

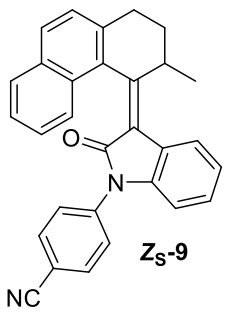

***Z*S-9**

An oven-dried N_2 filled crimp-top vial was charged with motor ***E*S-9** (10.0 mg) was dissolved in degassed (freeze-pump-thaw, three cycles) EtOAc (20 mL) and irradiated with a 365 nm LED for 16 h while stirring. The colour change of the solution during irradiation from yellow to orange indicated the generation of the ***Z*M-9** isomer. The mixture was then heated to reflux in the dark for 2 h, and the solution had turned yellow once again. After being left to cool to room temperature, the volatiles were removed *in vacuo* to give an orange oil. This was subsequently purified by semi-prep high performance liquid chromatography (SiO_2, heptane:EtOAc 97:3, 3.5 mL min^{-1}, 30 min, see section 4 for details) to yield ***Z*S-9** (2.00 mg, 40%). **^{1}H NMR** (600 MHz, CDCl3) δ 8.08 – 8.00 (m, 1H), 7.85 (d, J = 7.7 Hz, 1H), 7.83 – 7.77 (m, 2H), 7.51 – 7.47 (m, 2H), 7.40 – 7.31 (m, 3H), 7.28 – 7.25 (m, overlaps $CDCl_3$, 1H), 7.22 – 7.15 (m, 3H), 6.86 (dd, *J* = 7.9, 1.1 Hz, 1H), 4.03 (h, *J* = 7.2 Hz, 1H), 2.76 (dt, *J* = 14.3, 3.7 Hz, 1H), 2.60 (td, *J* = 13.7, 4.8 Hz, 1H), 2.42 (dddd, *J* = 12.7, 7.8, 4.8, 2.9 Hz, 1H), 1.32 (d, *J* = 6.9 Hz, 3H), 1.20 – 1.11 (m, 1H); **^{13}C NMR** (151 MHz, $CDCl_3$) δ 164.8, 155.3, 143.0, 139.6, 133.9, 132.9, 132.6, 131.9, 131.9, 129.8, 128.7, 128.5, 128.4, 126.6, 125.5, 125.0, 124.4, 124.4, 123.0, 122.6, 121.1, 109.2, 35.5, 29.9, 29.7, 20.5.

3. NMR spectra

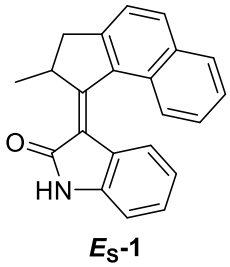

E_S-1

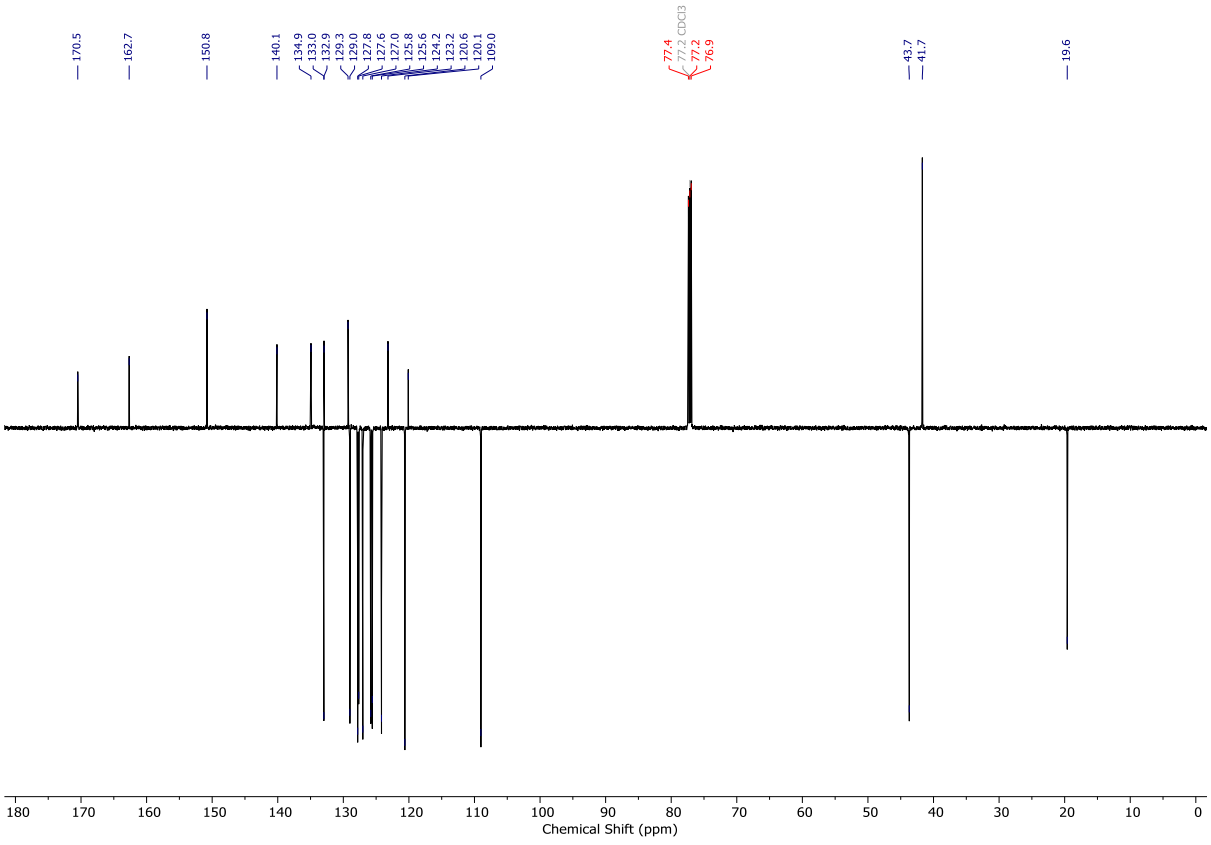

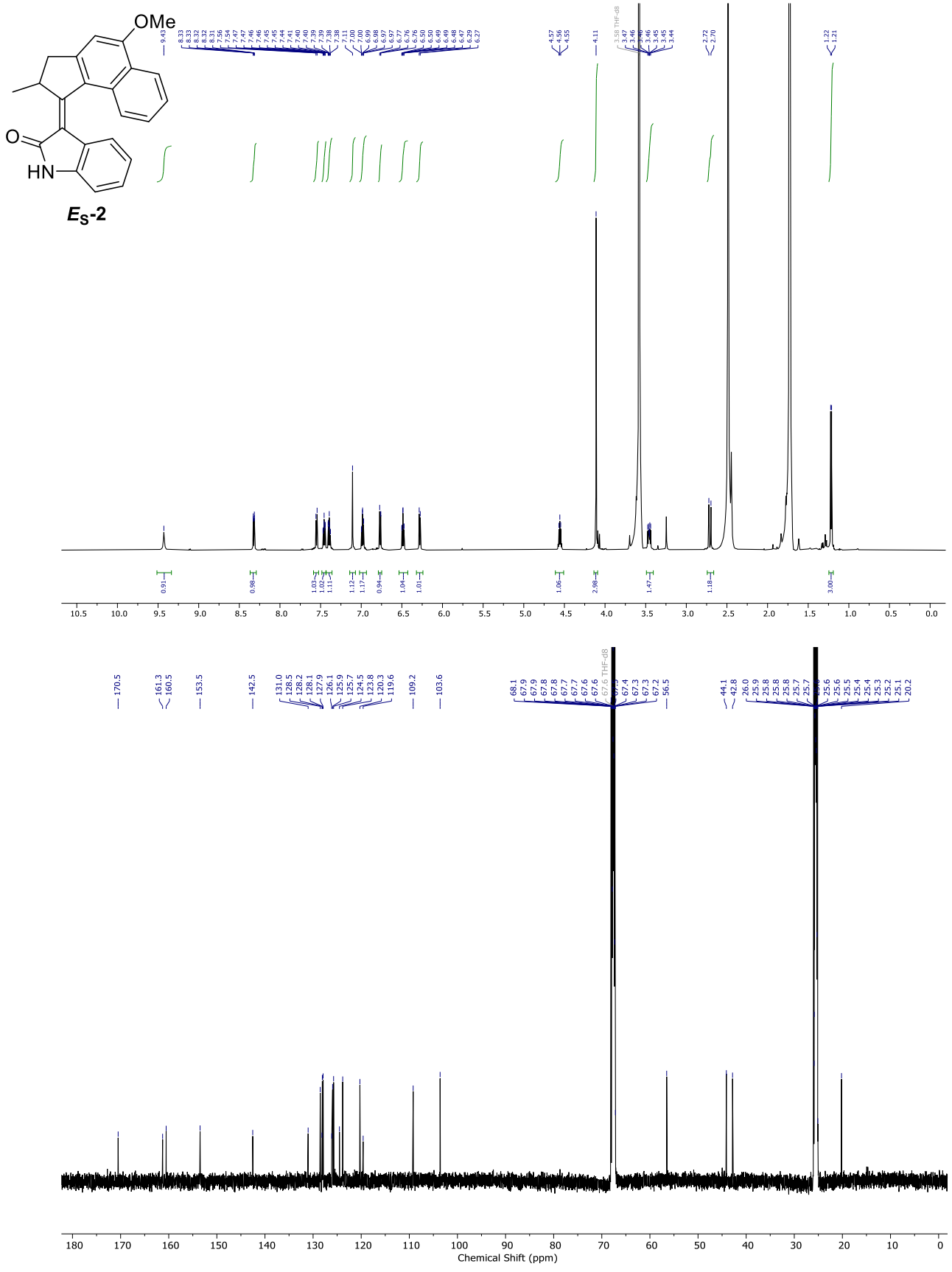
OMe
O
HN
E_S-2
Chemical Shift (ppm)

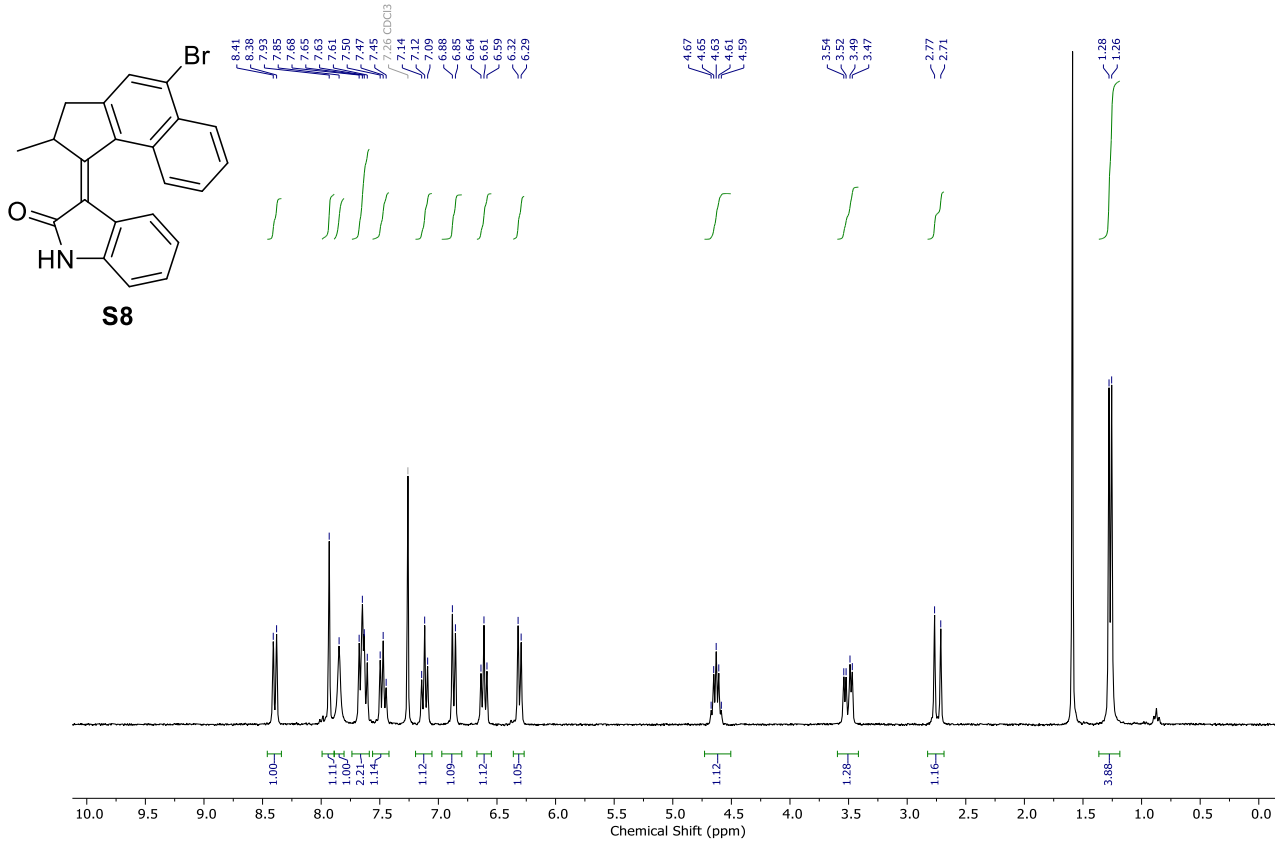
Br
O
HN
S8
8.41
8.38
7.93
7.85
7.68
7.65
7.63
7.61
7.50
7.47
7.45
7.26 CDCl3
7.14
7.12
7.09
6.88
6.85
6.64
6.61
6.59
6.32
6.29
4.67
4.65
4.63
4.61
4.59
3.54
3.52
3.49
3.47
2.77
2.71
1.28
1.26
1.00
1.11
1.00
2.21
1.14
1.12
1.09
1.12
1.05
1.12
1.28
1.16
3.88
Chemical Shift (ppm)

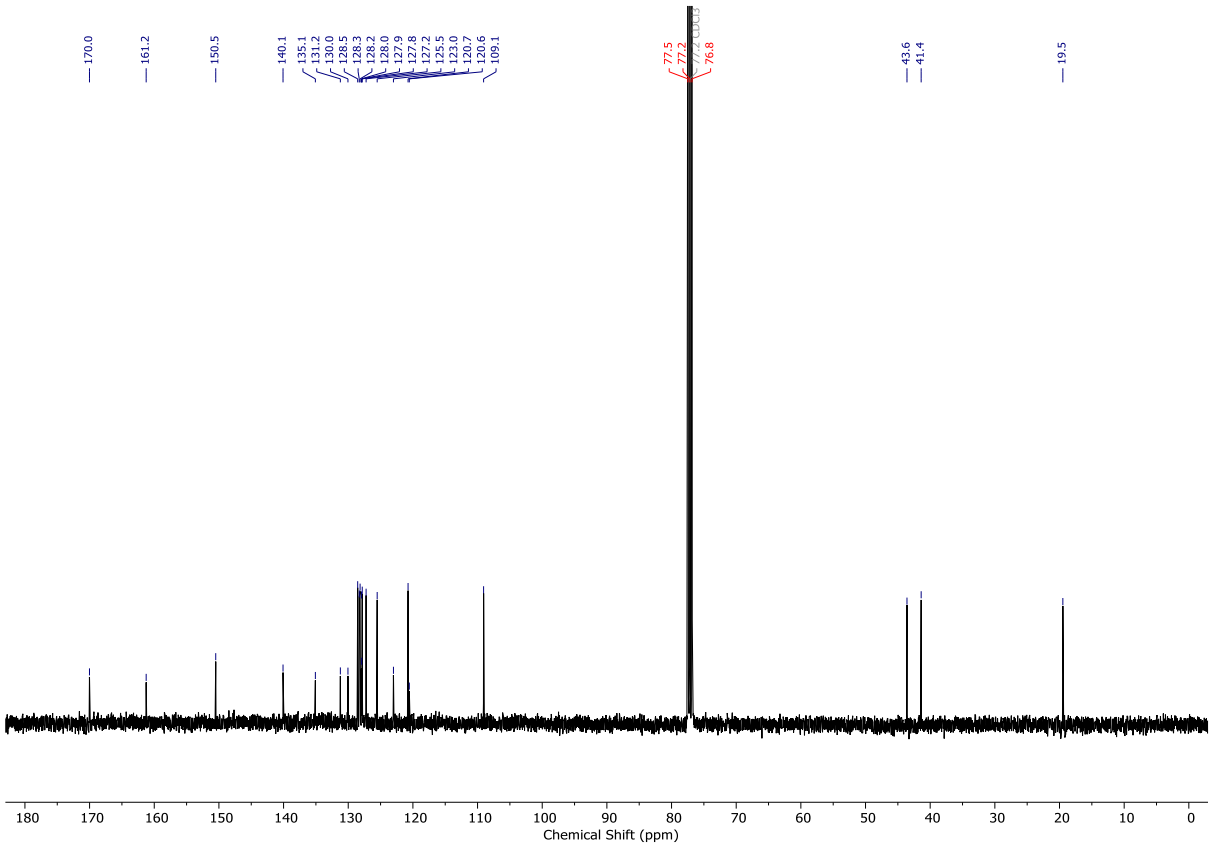
170.0
161.2
150.5
140.1
135.1
131.2
130.0
128.5
128.3
128.2
128.0
127.9
127.8
127.2
125.5
123.0
120.7
120.6
109.1
77.5
77.2
76.8 CDCl3
43.6
41.4
19.5
Chemical Shift (ppm)

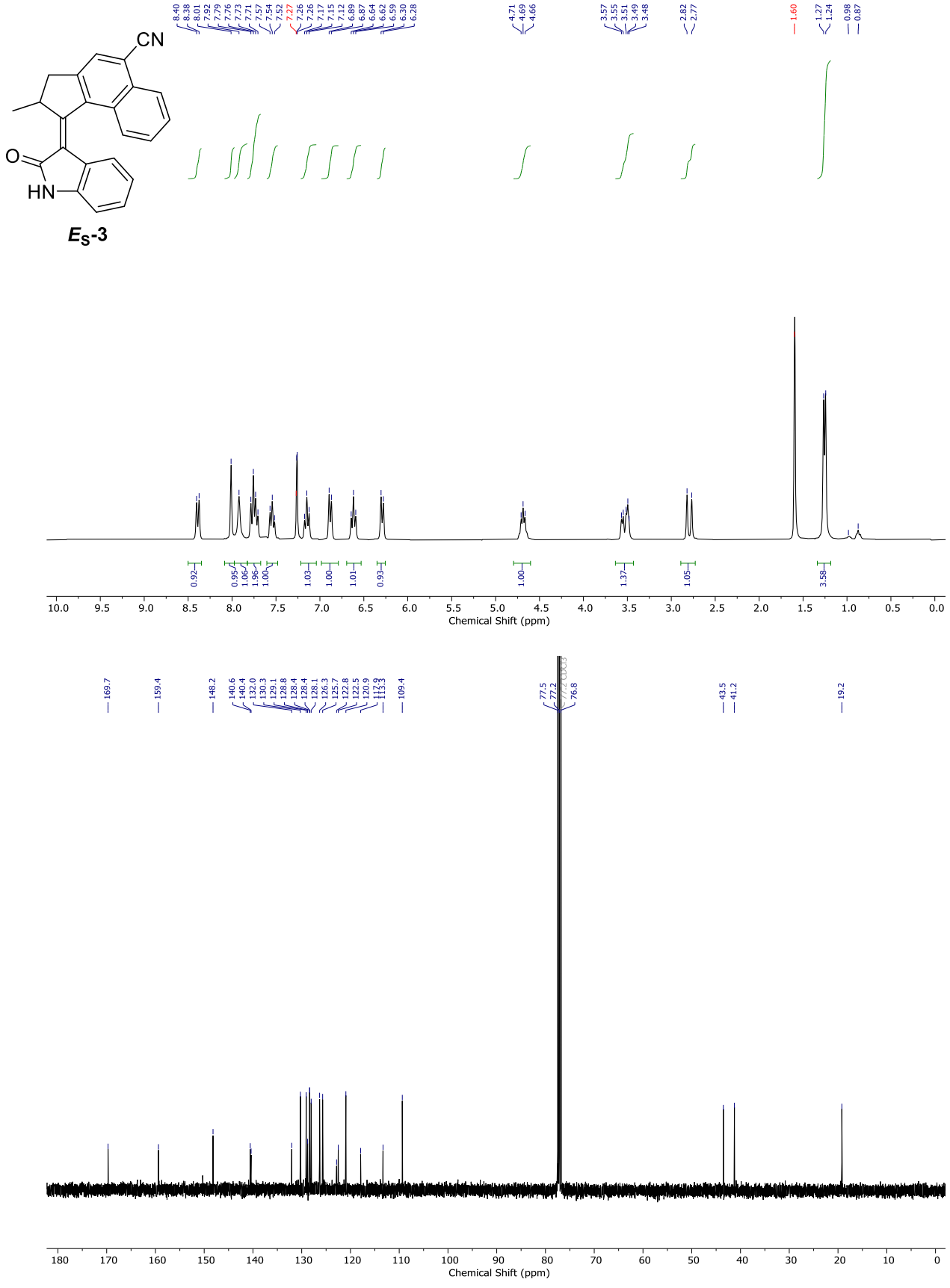
CN
O
HN
E_S-3
Chemical Shift (ppm)
Chemical Shift (ppm)

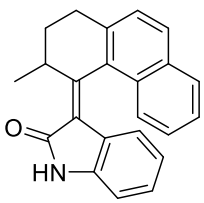
O
HN

***E*S-4**

7.90
7.89
7.79
7.77
7.50
7.44
7.43
7.42
7.40
7.32
7.31
7.30
7.26
7.26 CDCl3
6.97
6.96
6.95
6.74
6.73
6.33
6.31
6.30
5.67
5.66
4.91
4.89
4.88
4.87
2.80
2.79
2.79
2.78
2.77
2.76
2.62
2.61
2.60
2.60
2.59
2.58
2.57
2.38
2.37
2.37
2.36
1.17
1.16
1.15
1.14
1.13
1.11
1.95
0.98
0.92
2.14
1.17
1.01
0.99
1.03
0.99
1.06
1.05
1.06
1.09
4.36
10.0
9.5
9.0
8.5
8.0
7.5
7.0
6.5
6.0
5.5
5.0
4.5
4.0
3.5
3.0
2.5
2.0
1.5
1.0
0.5
0.0
Chemical Shift (ppm)

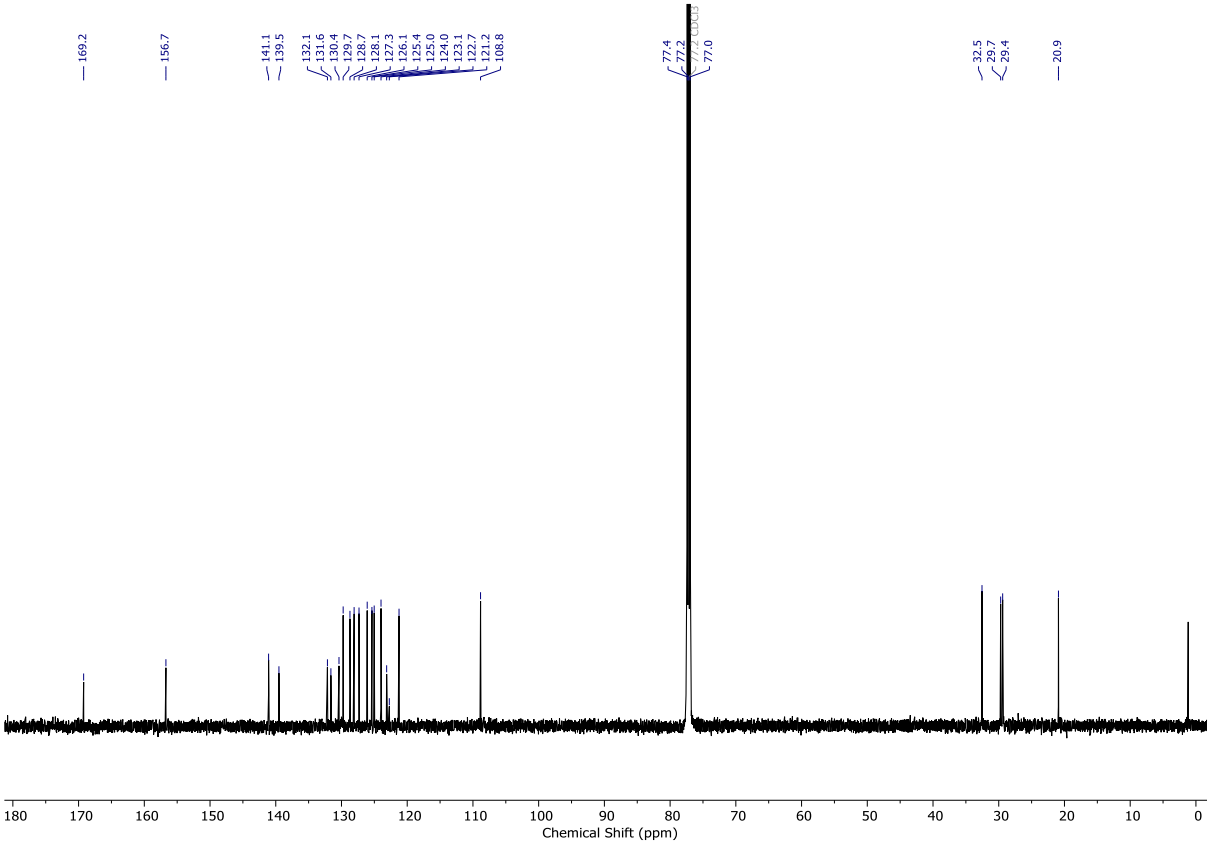
169.2
156.7
141.1
139.5
132.1
131.6
130.4
129.7
128.7
128.1
127.3
126.1
125.4
125.0
124.0
123.1
122.7
121.2
108.8
77.4
77.2
77.0
77.2 CDCl3
32.5
29.7
29.4
20.9
180
170
160
150
140
130
120
110
100
90
80
70
60
50
40
30
20
10
0
Chemical Shift (ppm)

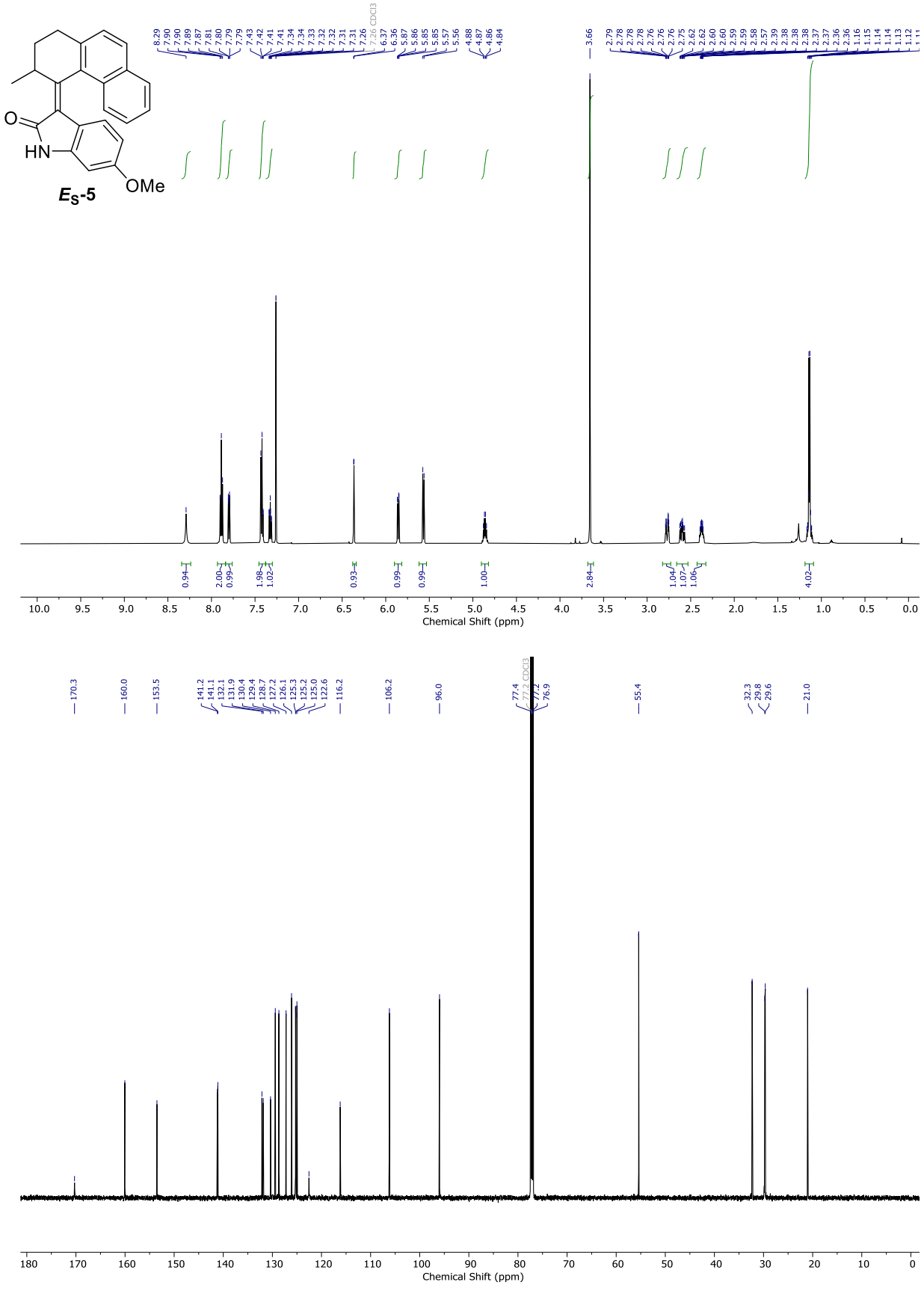
O
HN
OMe
E_S-5
Chemical Shift (ppm)
Chemical Shift (ppm)

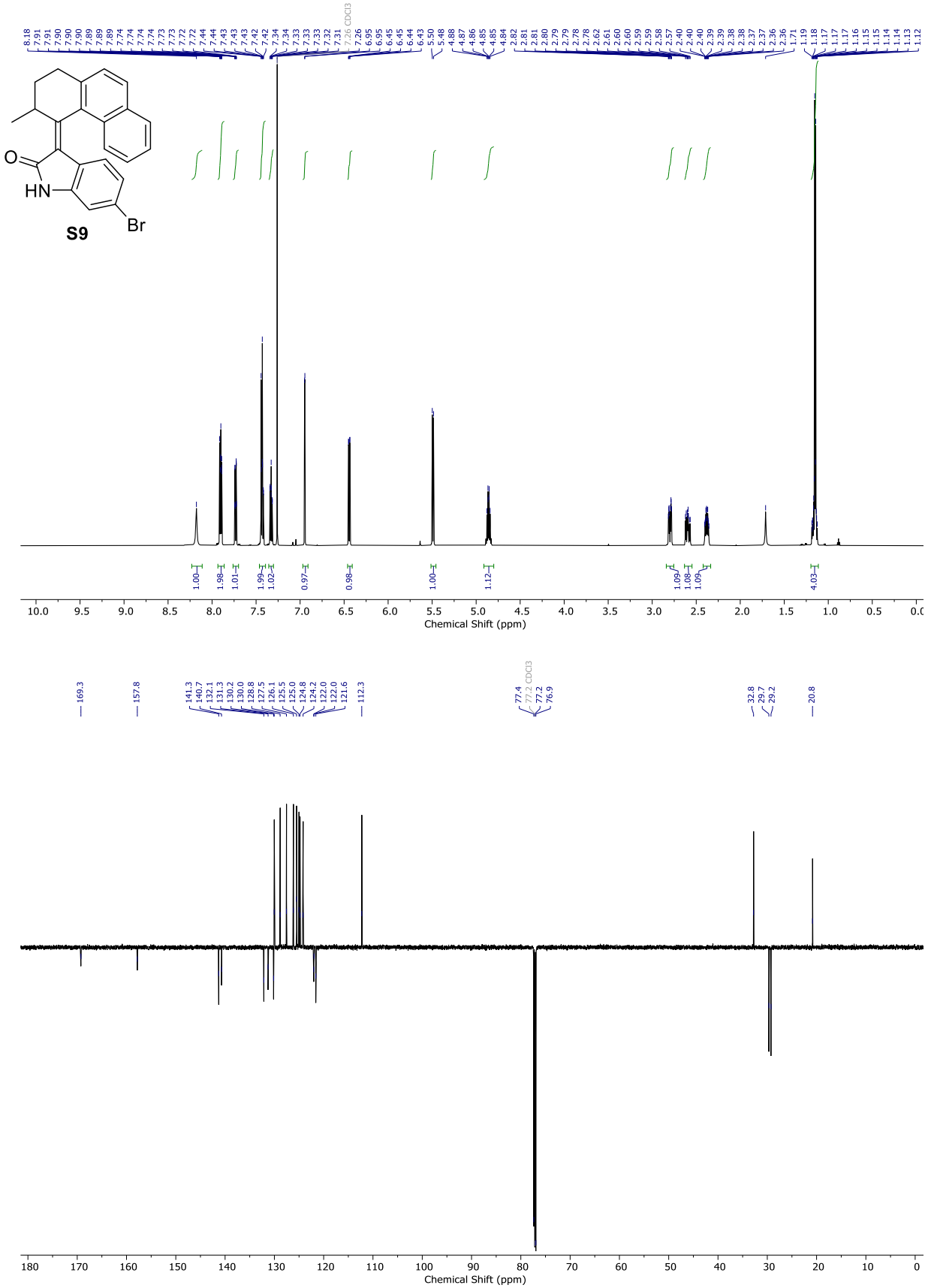
O
HN
Br
S9
Chemical Shift (ppm)
Chemical Shift (ppm)

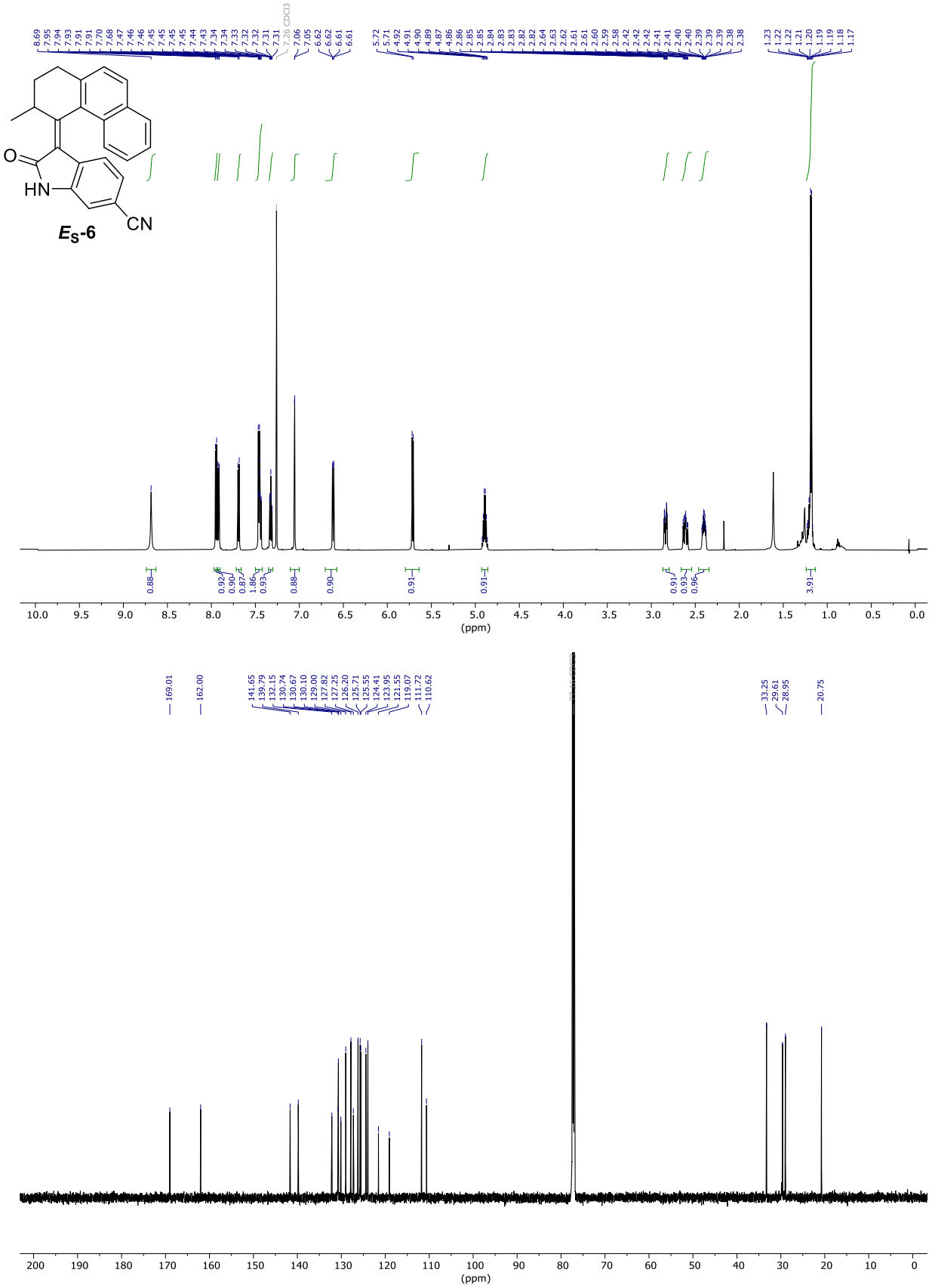
O
HN
CN
E_S-6
(ppm)
(ppm)

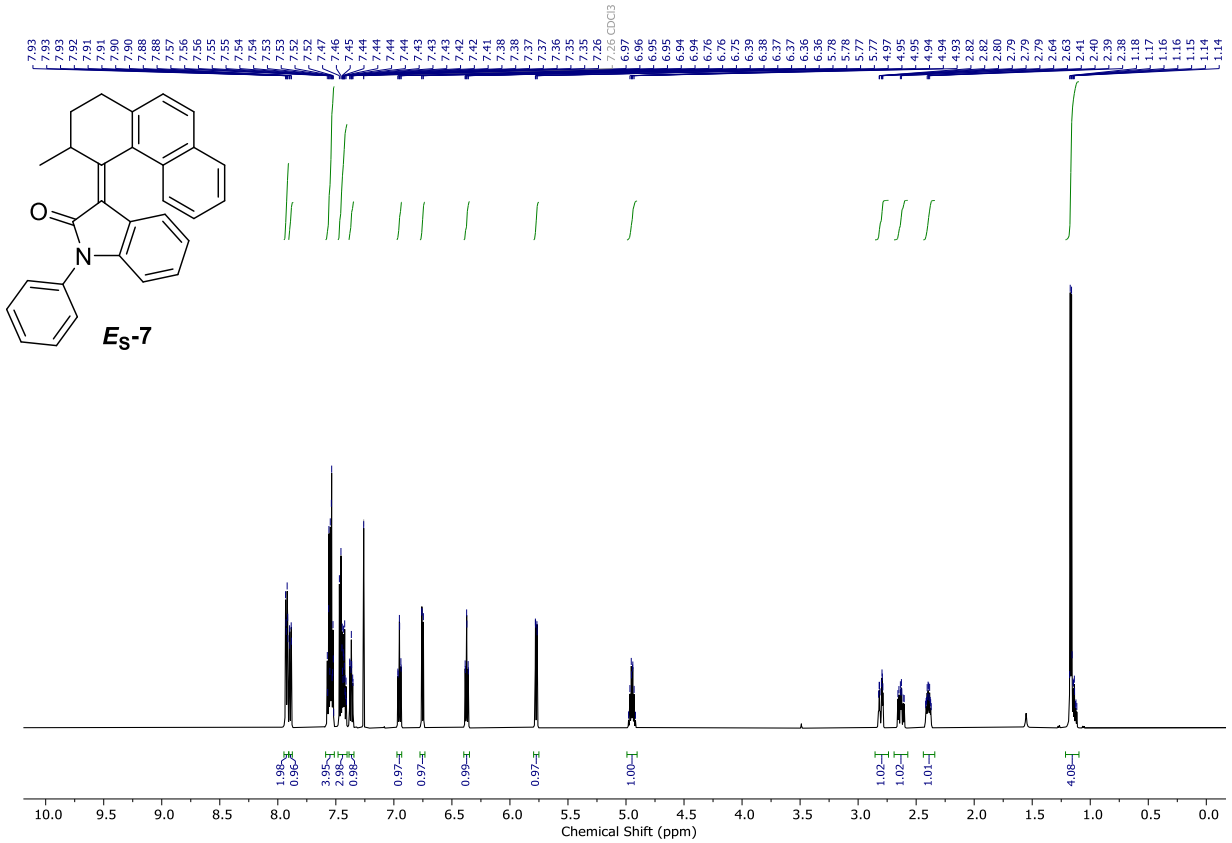
O
N
E_S-7
Chemical Shift (ppm)

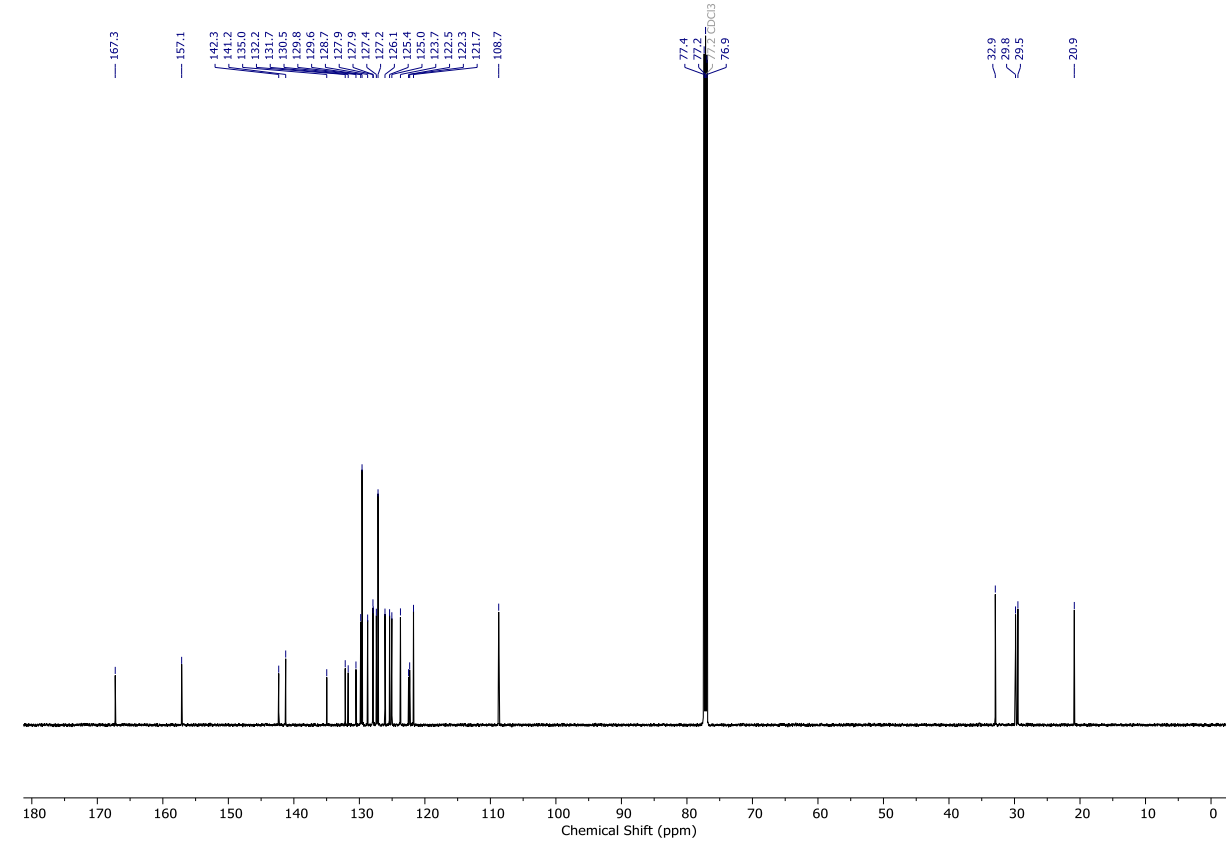
Chemical Shift (ppm)

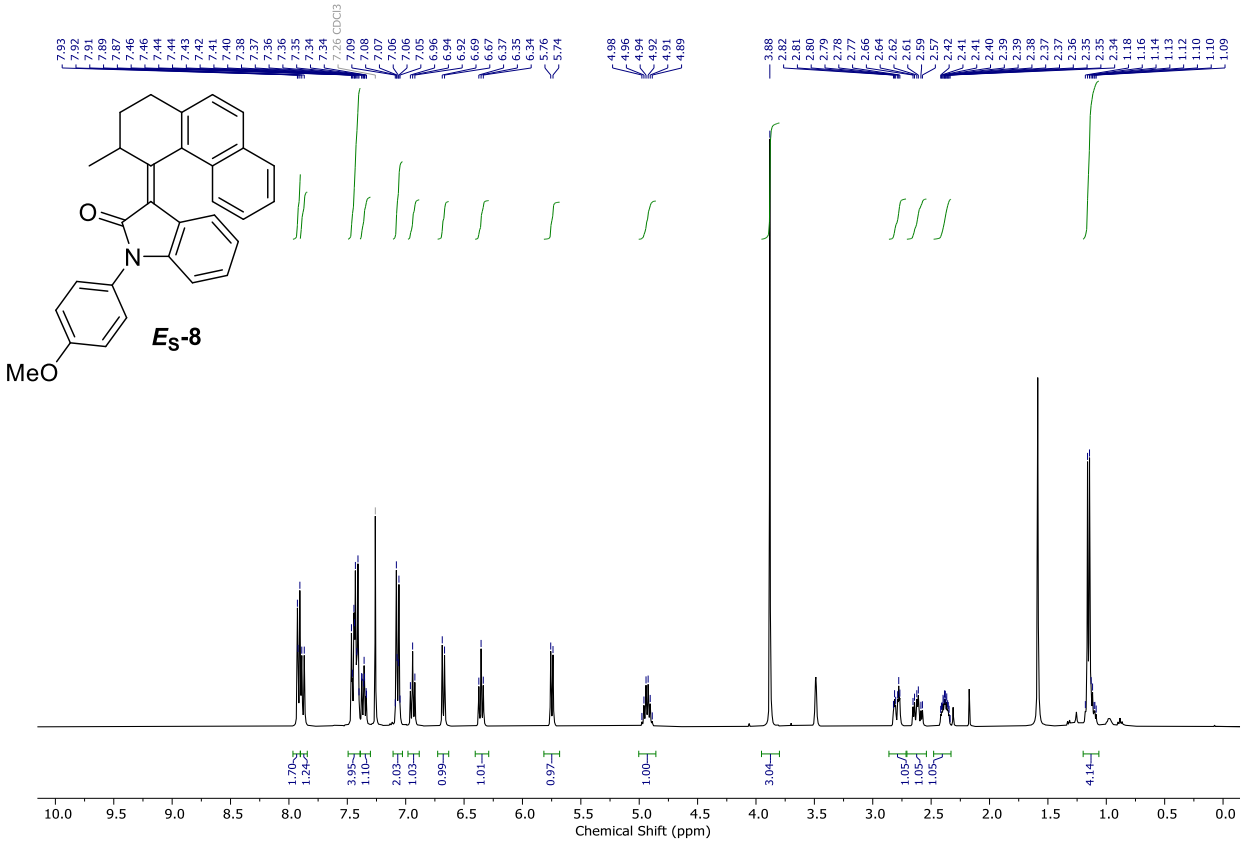
O
N
MeO
E_S-8
Chemical Shift (ppm)

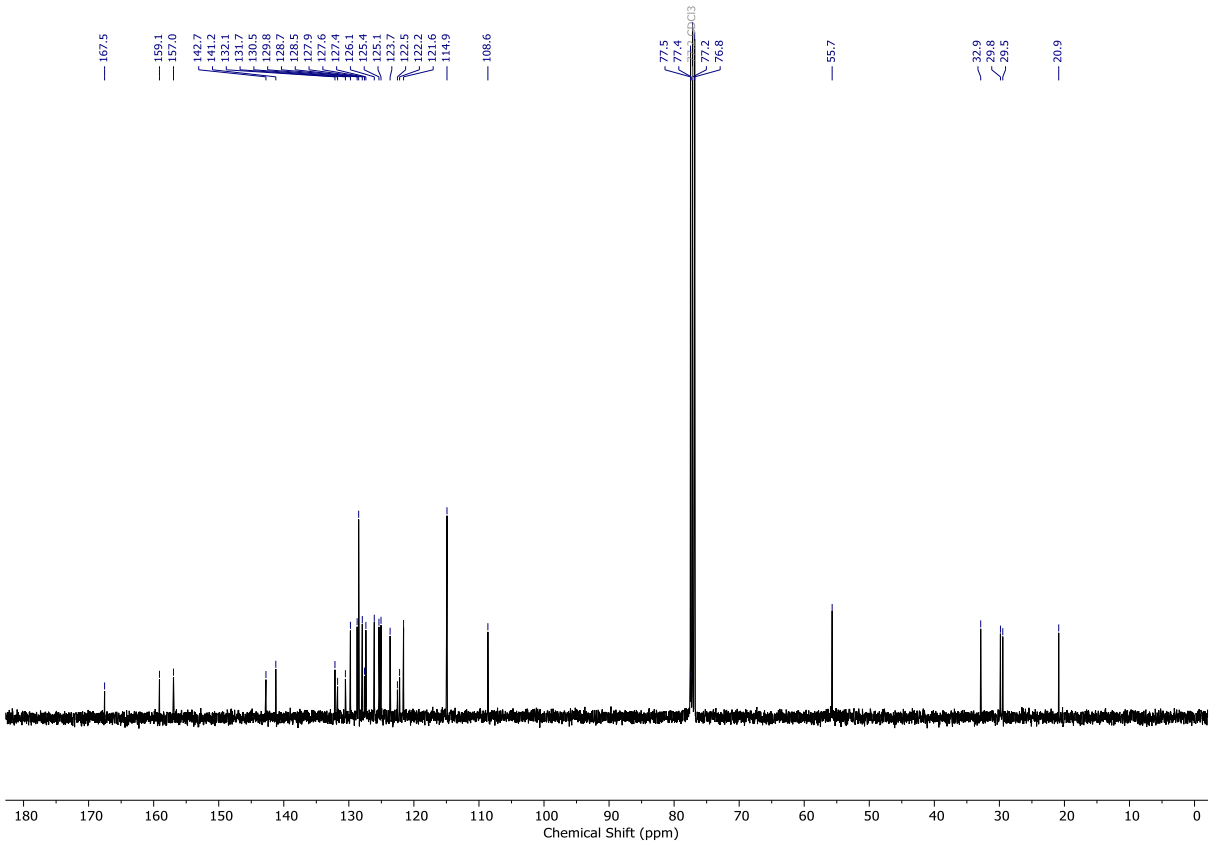
Chemical Shift (ppm)

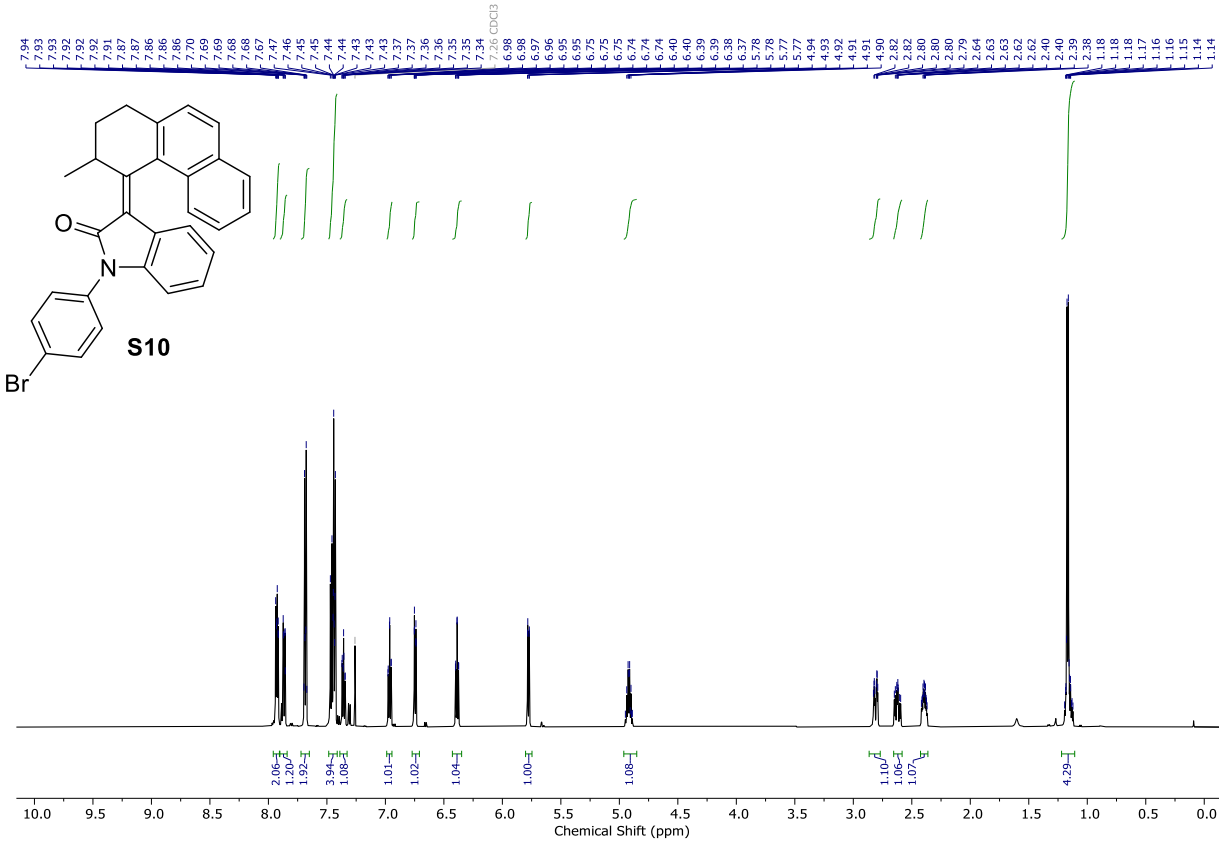
S10
Br
O
N
Chemical Shift (ppm)

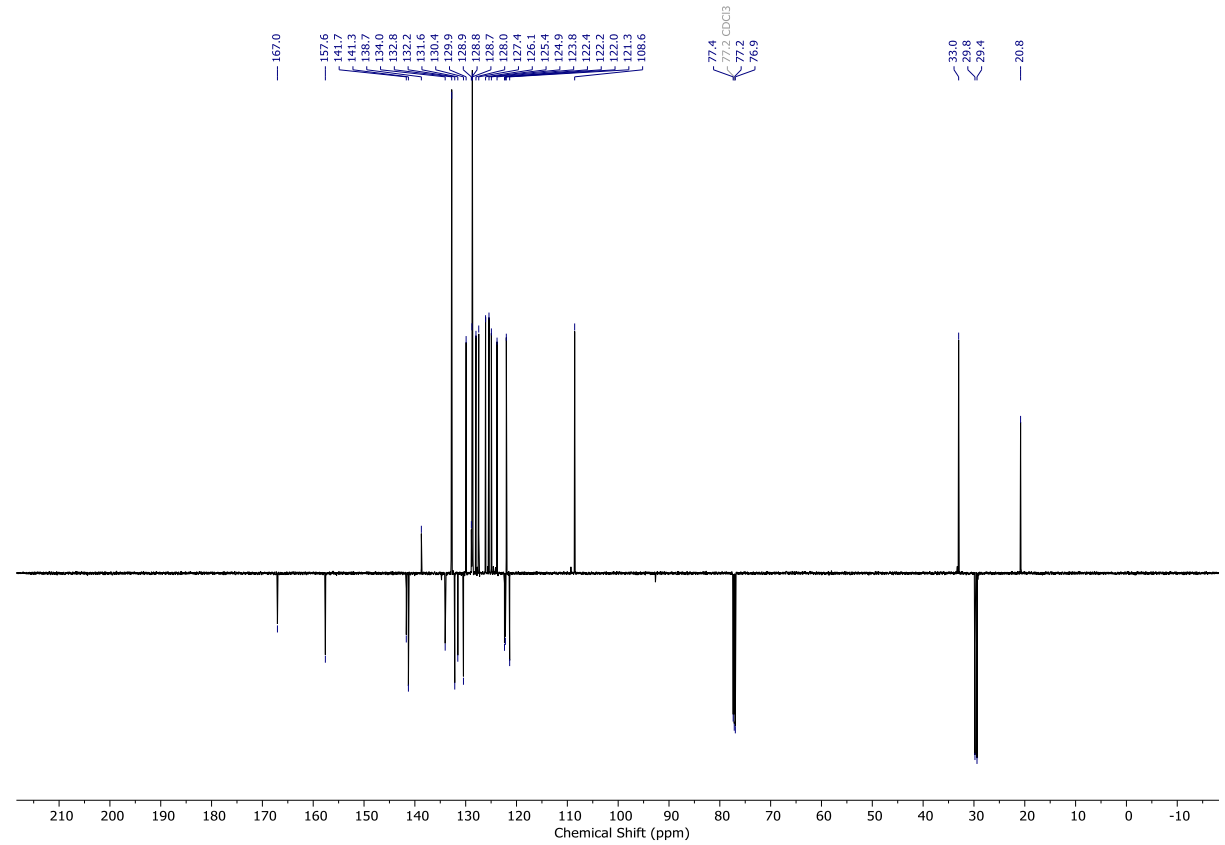
Chemical Shift (ppm)

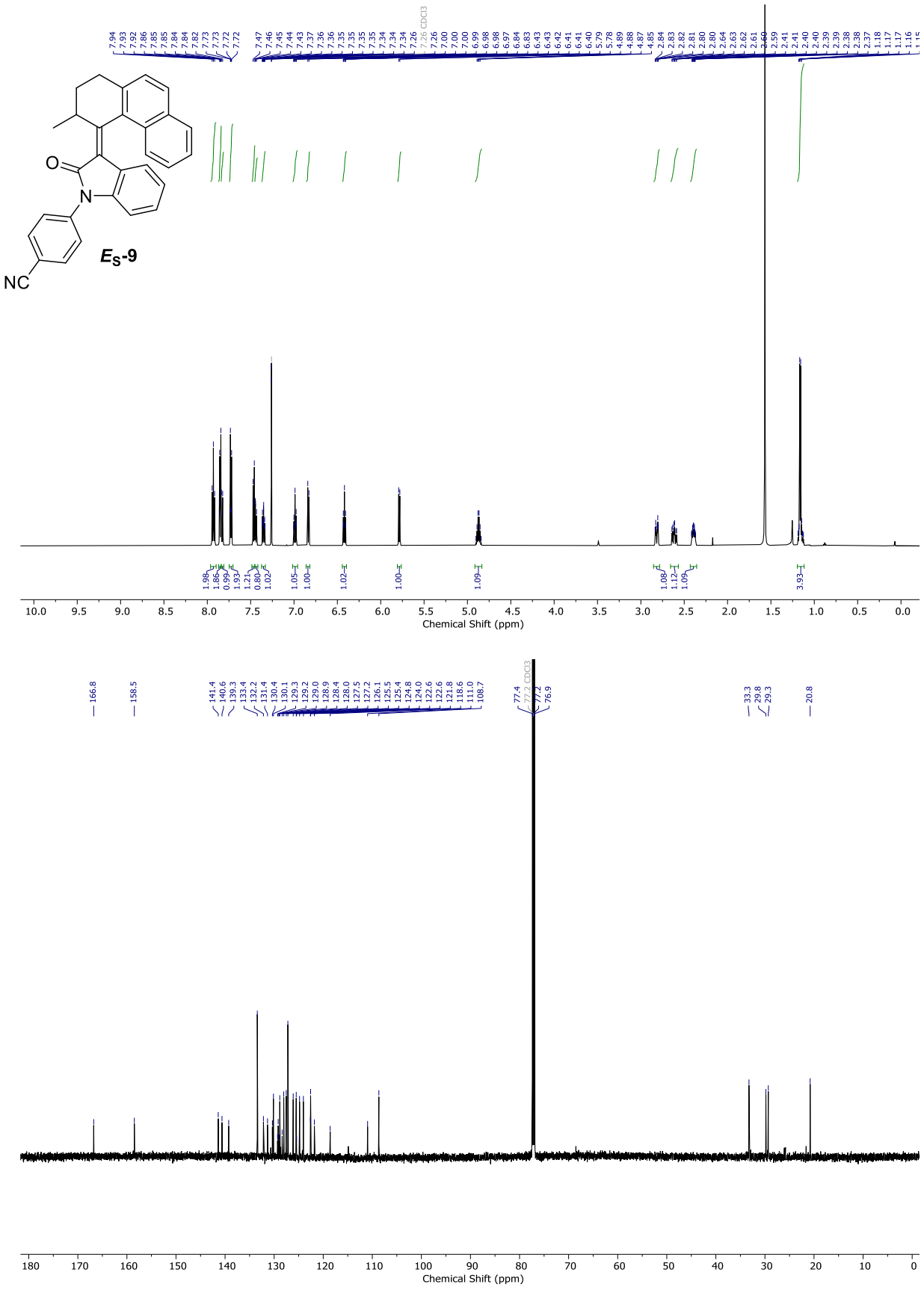
O
N
NC
E_S-9
Chemical Shift (ppm)
Chemical Shift (ppm)

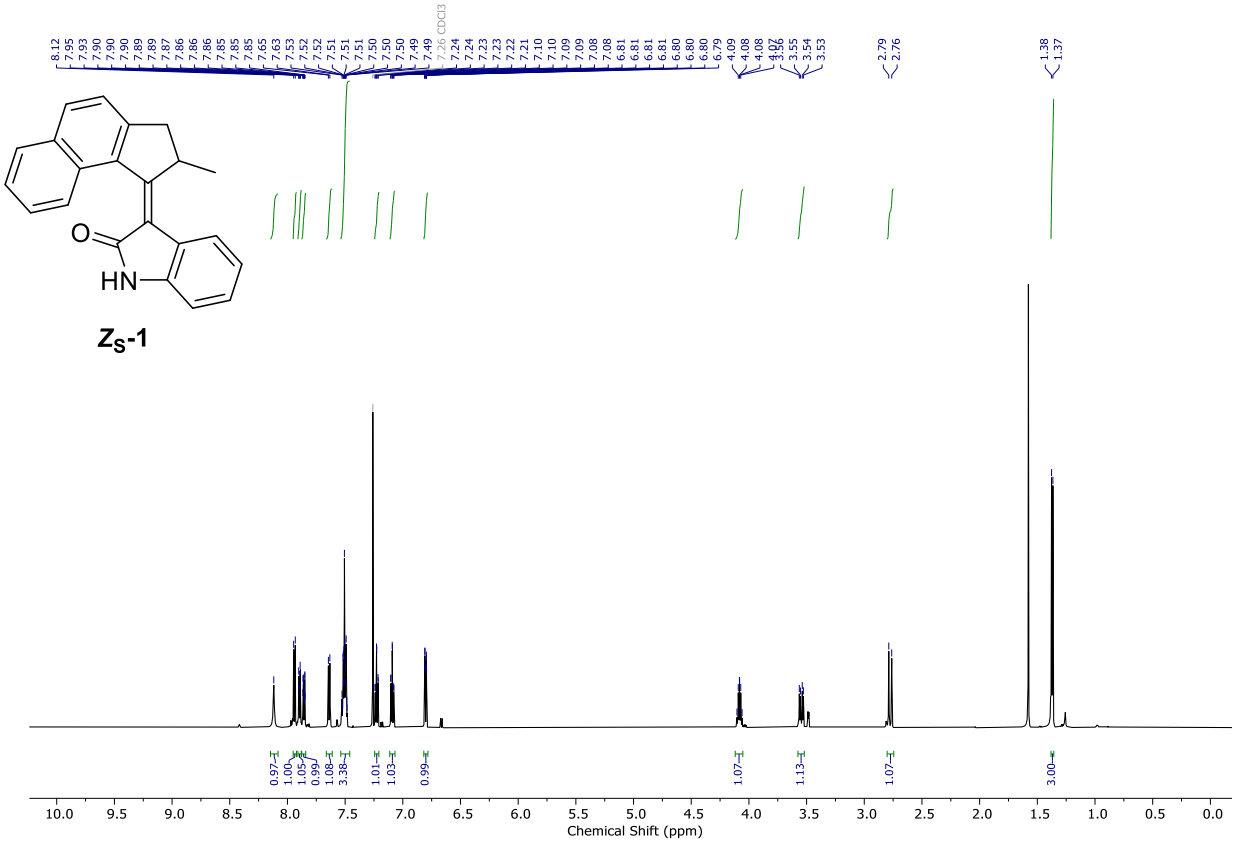
O
HN

Z_S-1

8.12
7.95
7.93
7.90
7.90
7.90
7.89
7.89
7.87
7.86
7.86
7.86
7.85
7.85
7.85
7.65
7.63
7.53
7.52
7.52
7.51
7.51
7.51
7.50
7.50
7.50
7.50
7.49
7.26 CDCl3
7.24
7.24
7.24
7.23
7.23
7.23
7.22
7.21
7.10
7.10
7.09
7.09
7.09
7.08
7.08
6.81
6.81
6.81
6.80
6.80
6.80
6.79
4.09
4.08
4.08
4.07
3.56
3.55
3.54
3.53
2.79
2.76
1.38
1.37
0.97
1.00
1.05
0.99
1.08
3.38
1.01
1.03
0.99
1.07
1.13
1.07
3.00
10.0
9.5
9.0
8.5
8.0
7.5
7.0
6.5
6.0
5.5
5.0
4.5
4.0
3.5
3.0
2.5
2.0
1.5
1.0
0.5
0.0
Chemical Shift (ppm)

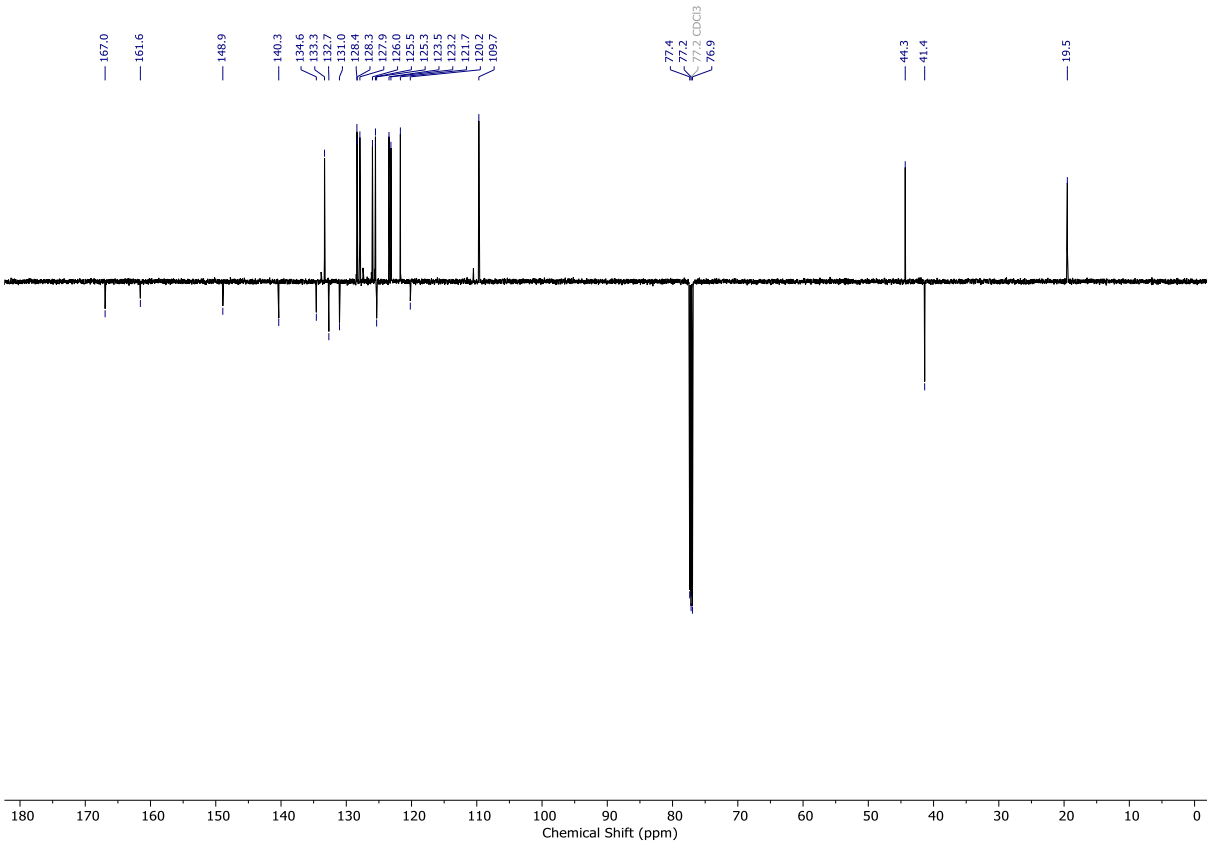
167.0
161.6
148.9
140.3
134.6
133.3
132.7
131.0
128.4
128.3
127.9
126.0
125.5
125.3
123.5
123.2
121.7
120.2
109.7
77.4
77.2
77.2 CDCl3
76.9
44.3
41.4
19.5
180
170
160
150
140
130
120
110
100
90
80
70
60
50
40
30
20
10
0
Chemical Shift (ppm)

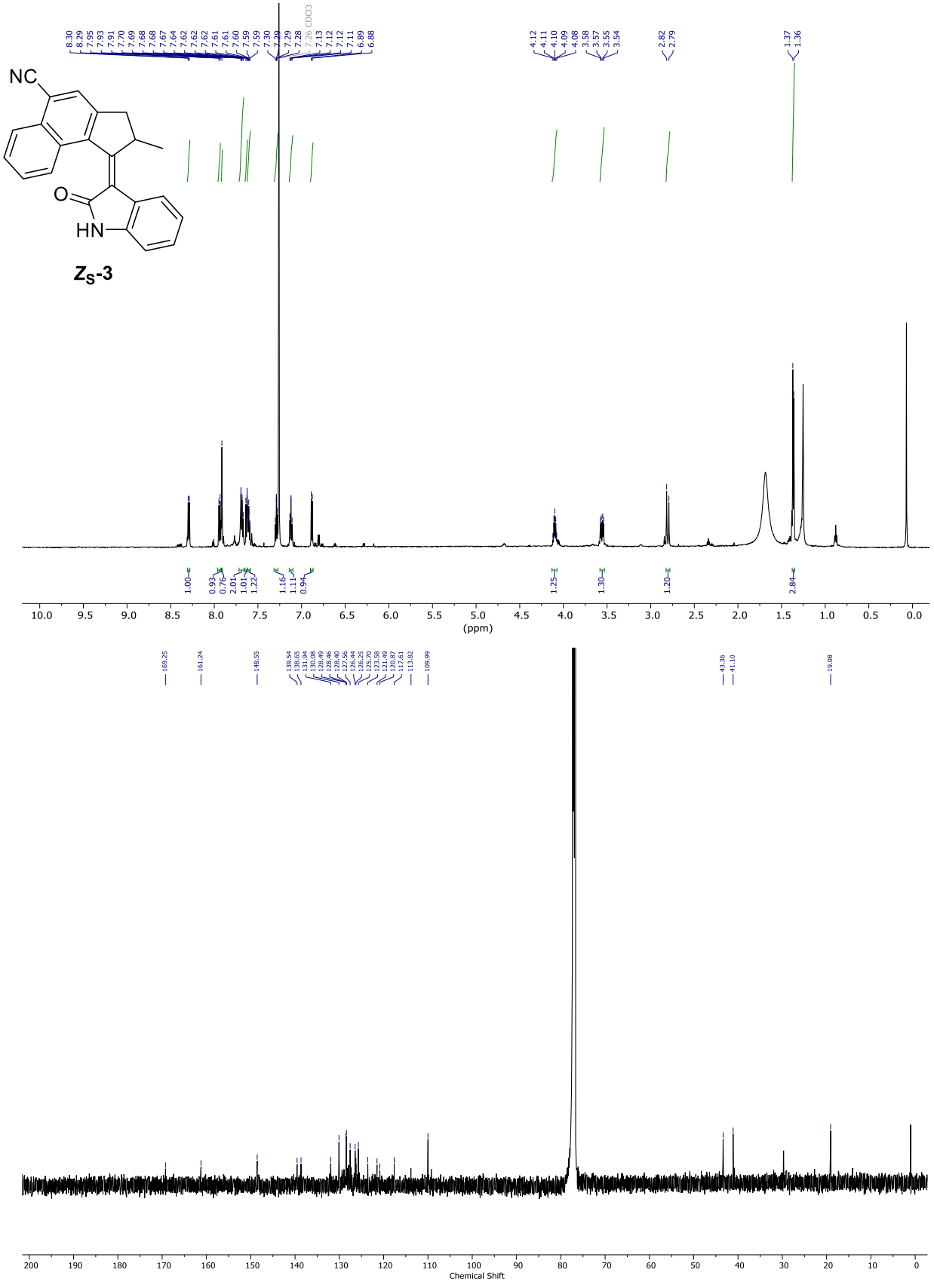
NC
O
HN
Z_S-3
(ppm)
Chemical Shift

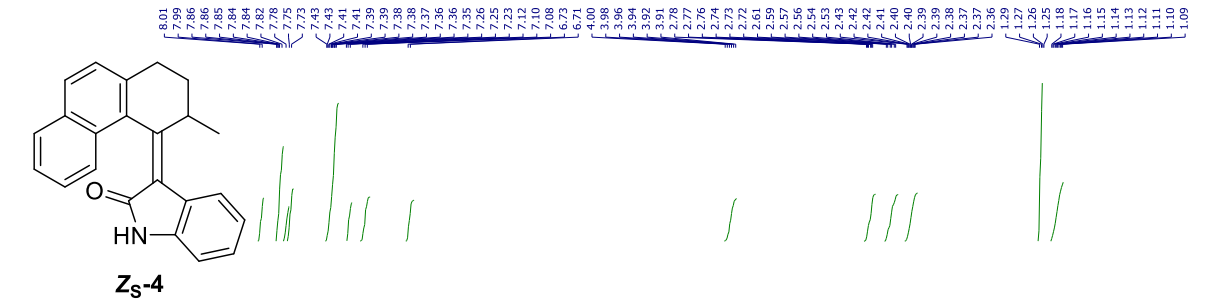
8.01 7.99 7.86 7.86 7.85 7.84 7.84 7.82 7.78 7.75 7.73 7.43 7.41 7.41 7.39 7.39 7.38 7.38 7.37 7.36 7.36 7.35 7.26 7.25 7.23 7.12 7.10 7.08 6.73 6.71 4.00 3.98 3.96 3.94 3.92 3.91 2.78 2.77 2.76 2.74 2.73 2.72 2.61 2.59 2.57 2.56 2.54 2.53 2.43 2.42 2.42 2.41 2.40 2.40 2.39 2.39 2.38 2.37 2.37 2.36 1.29 1.27 1.26 1.25 1.18 1.17 1.16 1.15 1.14 1.13 1.12 1.11 1.10 1.09
O
HN

Z_S-4

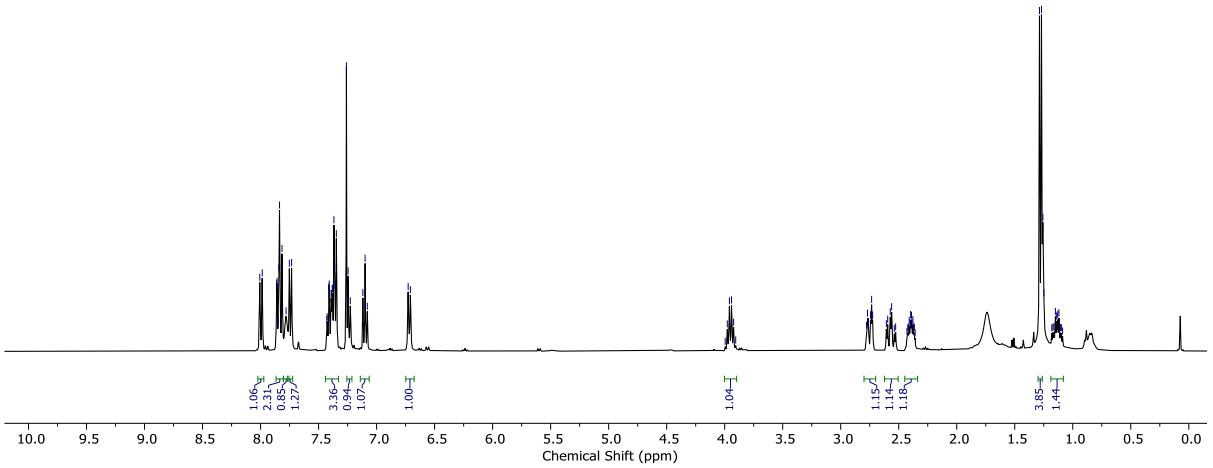
1.06 2.31 0.85 1.27 3.36 0.94 1.07 1.00 1.04 1.15 1.14 1.18 3.85 1.44
10.0 9.5 9.0 8.5 8.0 7.5 7.0 6.5 6.0 5.5 5.0 4.5 4.0 3.5 3.0 2.5 2.0 1.5 1.0 0.5 0.0
Chemical Shift (ppm)

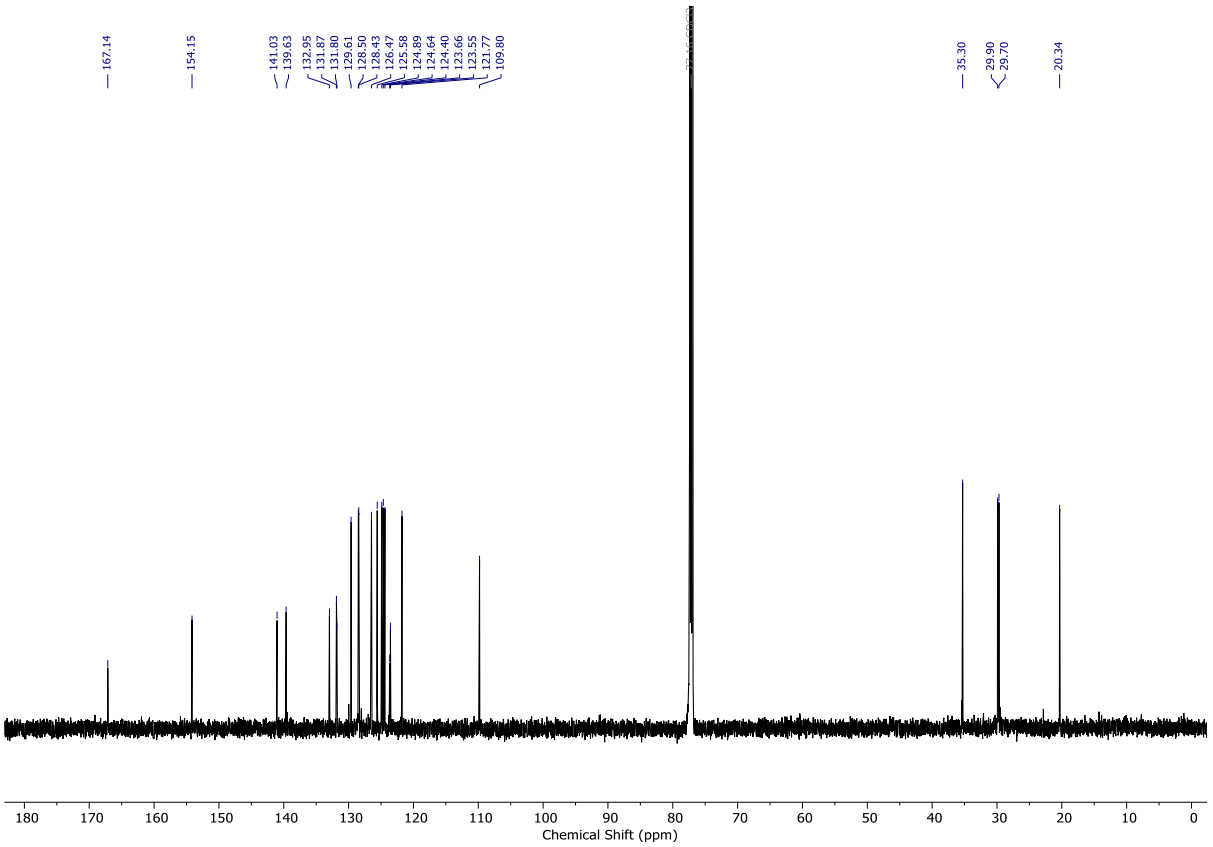
167.14 154.15 141.03 139.63 132.95 131.87 131.80 129.61 128.50 128.43 126.47 125.58 124.89 124.64 124.40 123.66 123.55 121.77 109.80 35.30 29.90 29.70 20.34
180 170 160 150 140 130 120 110 100 90 80 70 60 50 40 30 20 10 0
Chemical Shift (ppm)

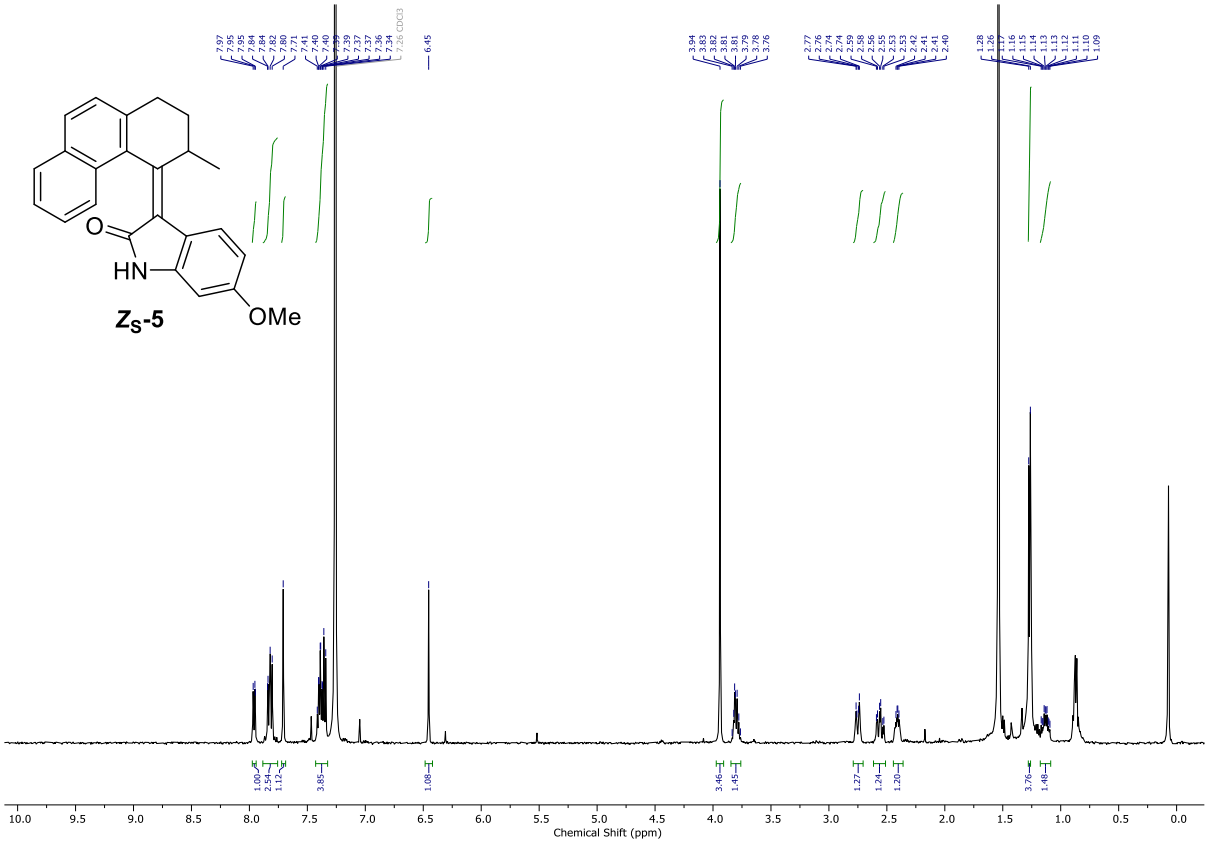
O
HN
OMe
Z_S-5
Chemical Shift (ppm)

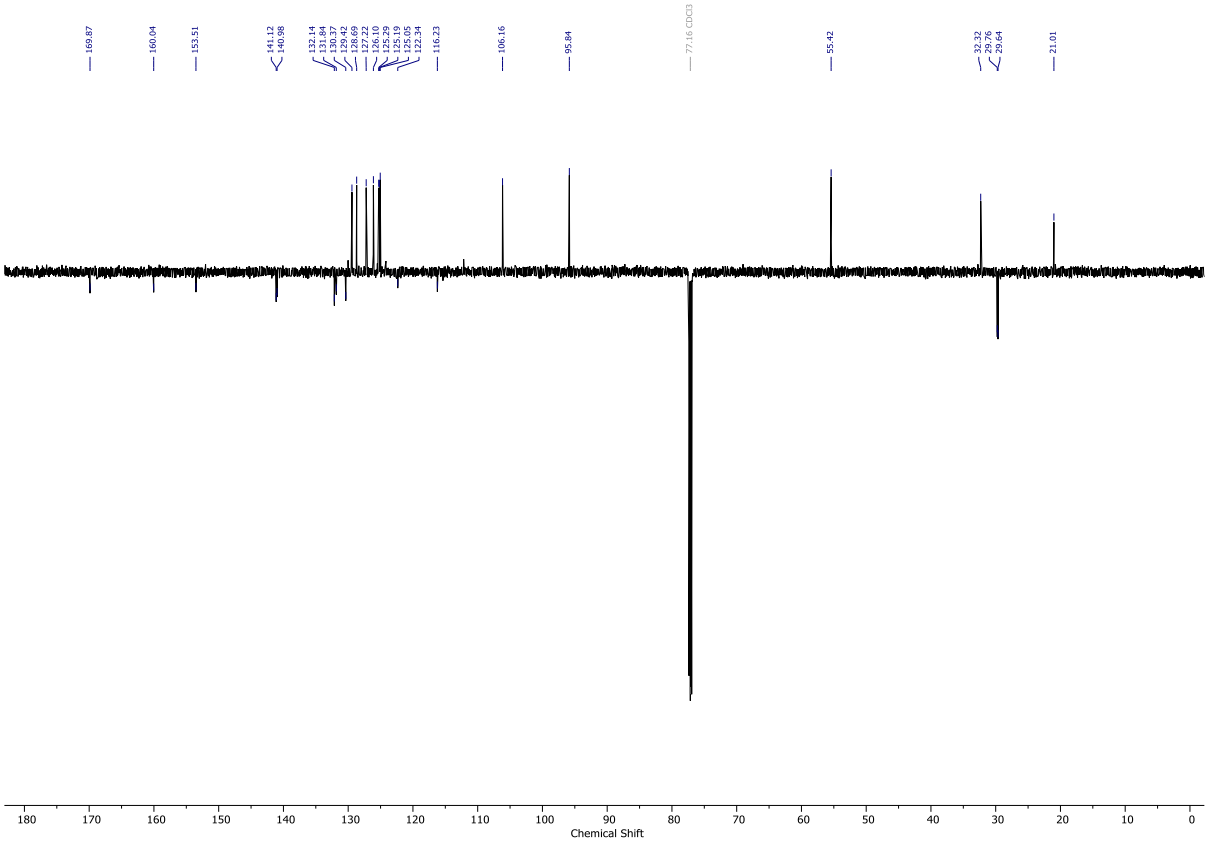
Chemical Shift

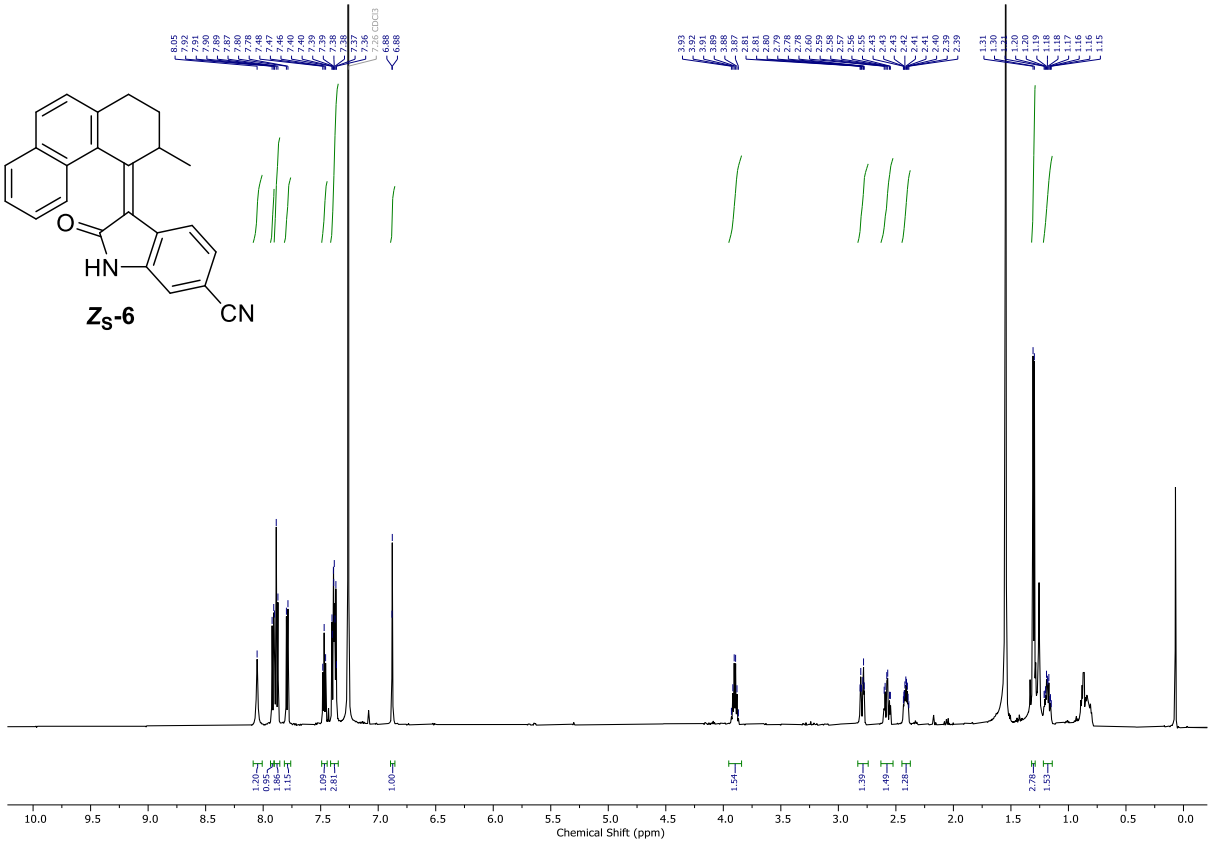
O
HN
CN
Z_S-6
Chemical Shift (ppm)

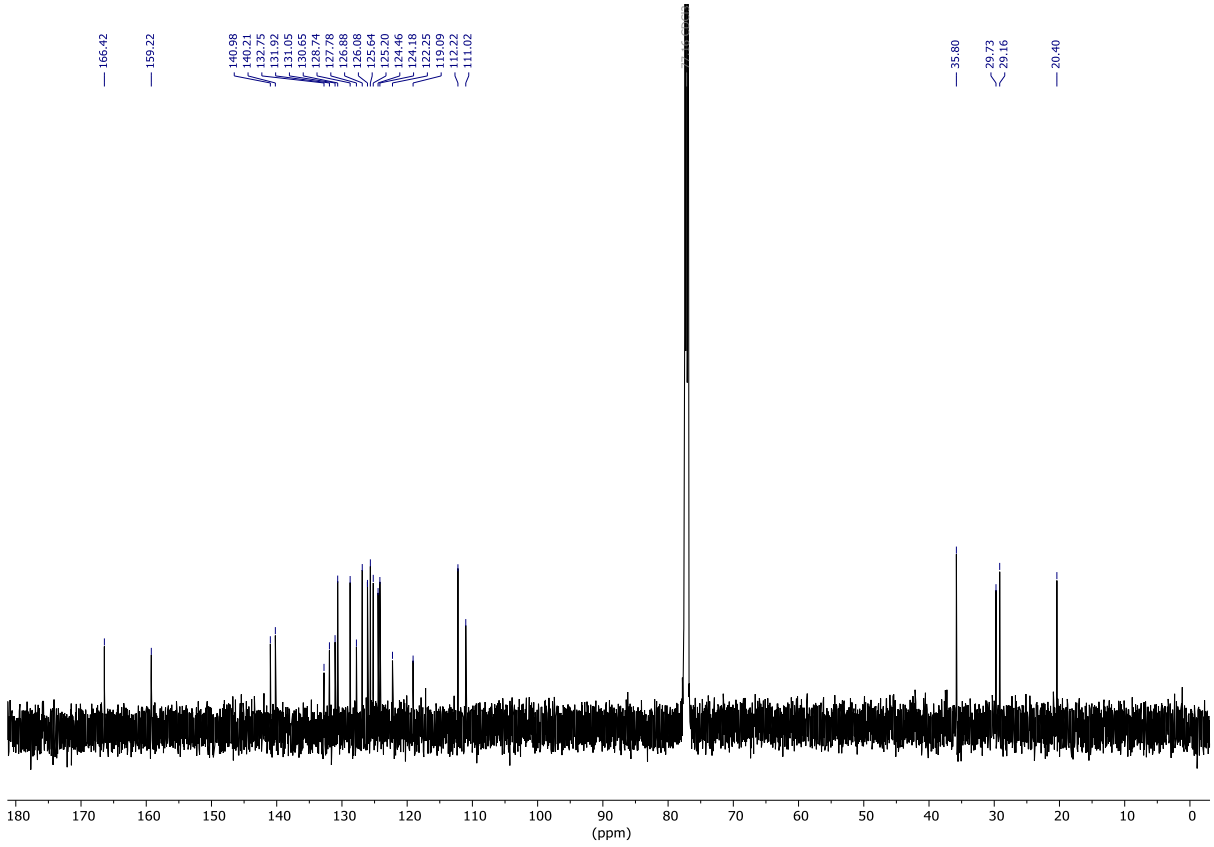
(ppm)

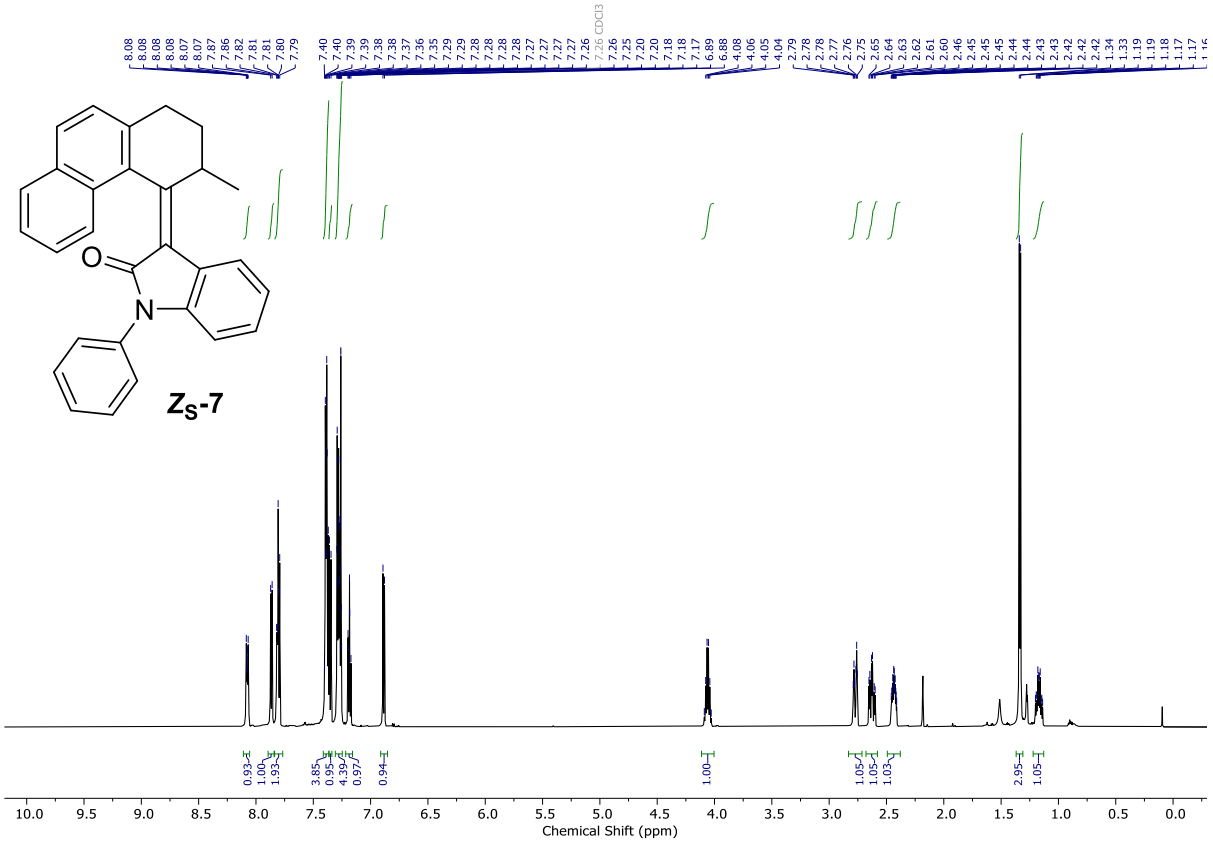
O
N
Z_S-7
Chemical Shift (ppm)

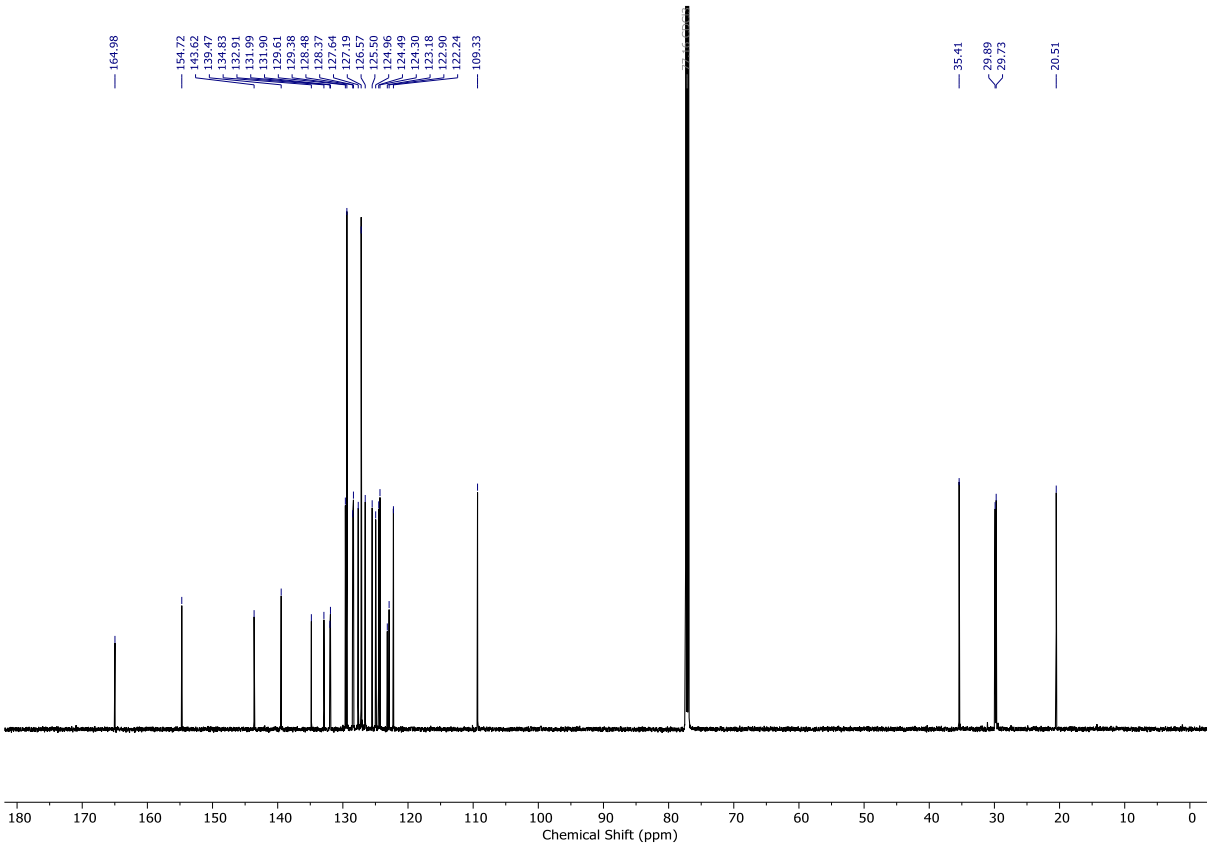
Chemical Shift (ppm)

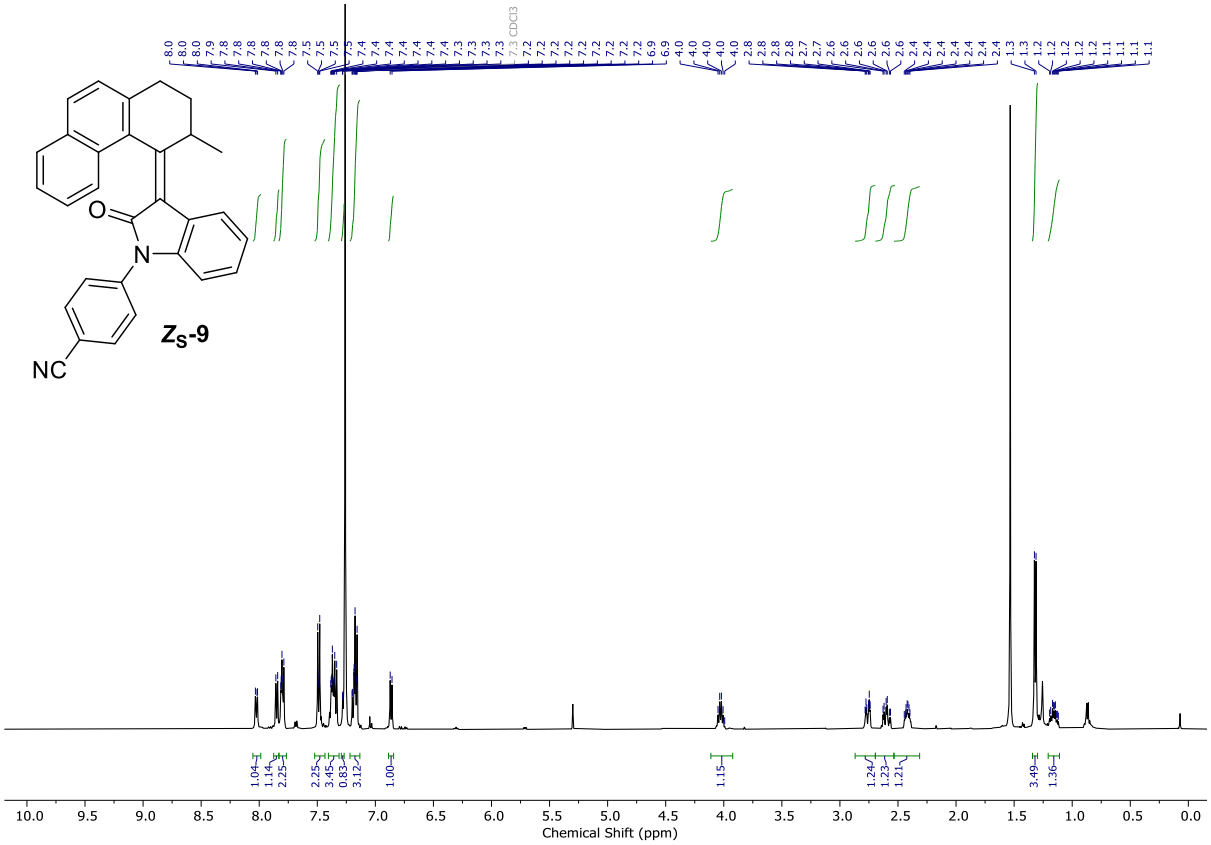
O
N
NC
Z_S-9
Chemical Shift (ppm)

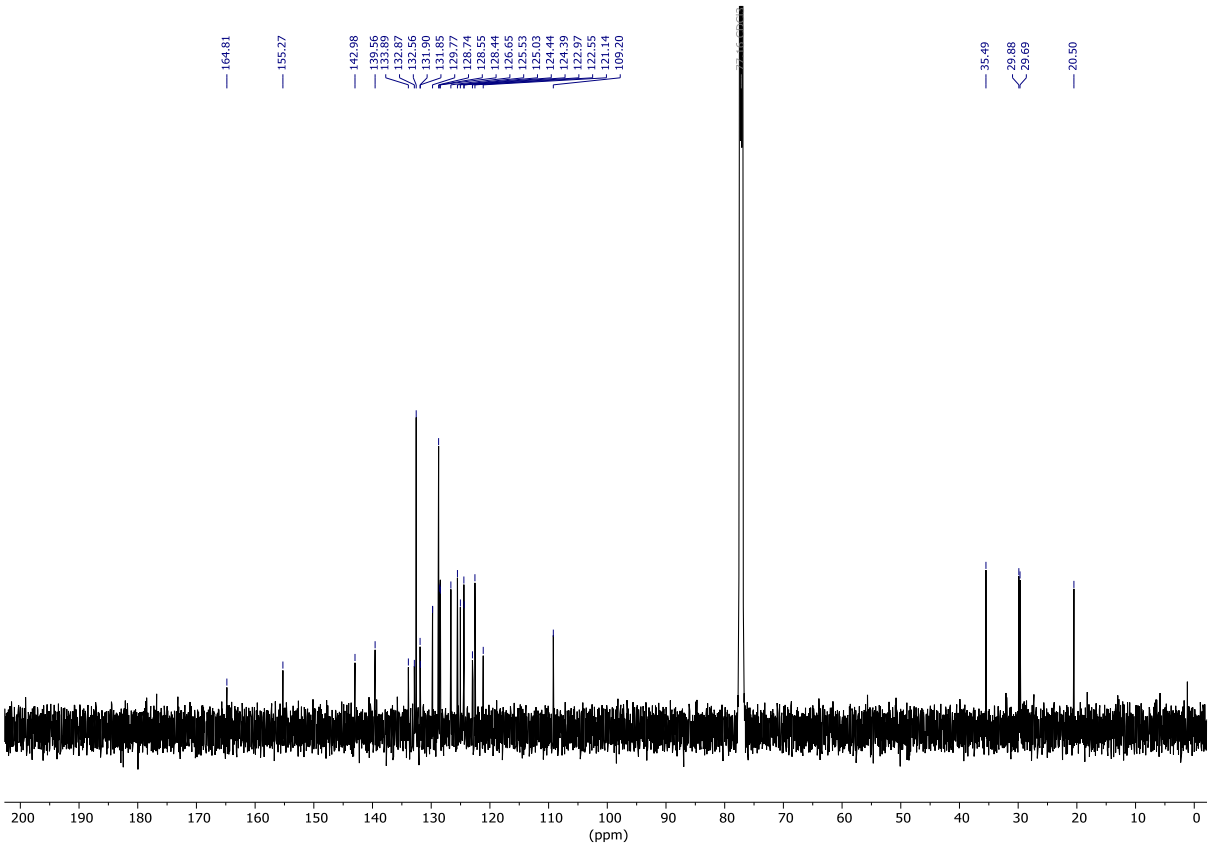
(ppm)

4. HPLC separation of stereoisomers

The *E*/*Z* isomers of **3**, **5**, **6**, and **9** were separated by semi-prep HPLC on a Phenomenex Luna 10 µm-PREP Silica(3) column (250 x 10.0 mm, particle size 100 Å).

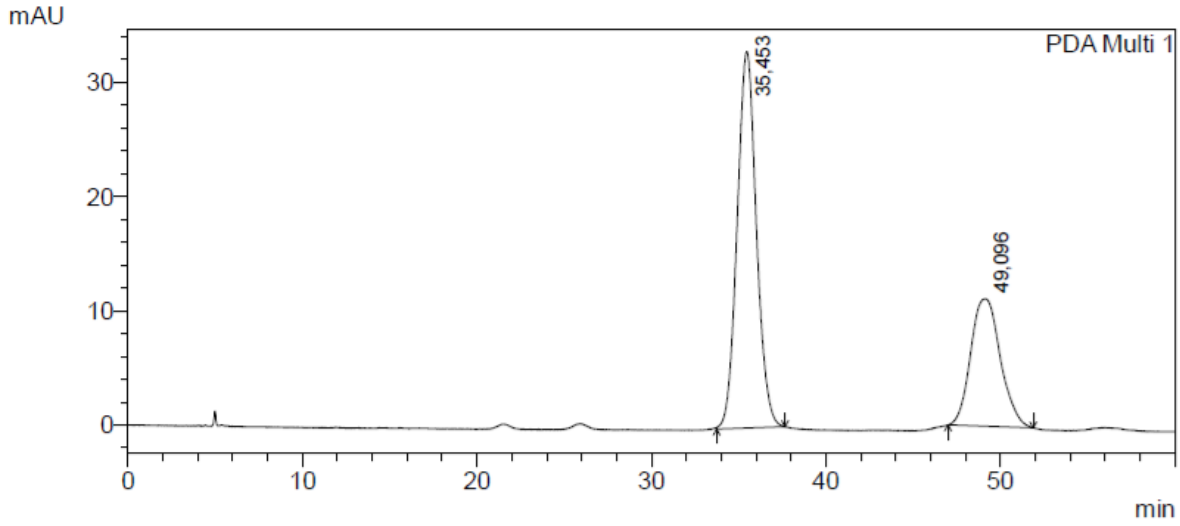

Figure S1: HPLC trace of the PSS of ***E***$_S$-**3**/***Z***$_S$-**3** (obtained irradiating the sample with a 365 nm LED) monitored at 400 nm. Conditions: heptane/propan-2-ol 99:1, 4.0 mL min^{-1}, 60 min, 40 °C. t_R^1 = 35.45 min (***E***$_S$-**3**); t_R^2 = 49.10 min (***Z***$_S$-**3**).

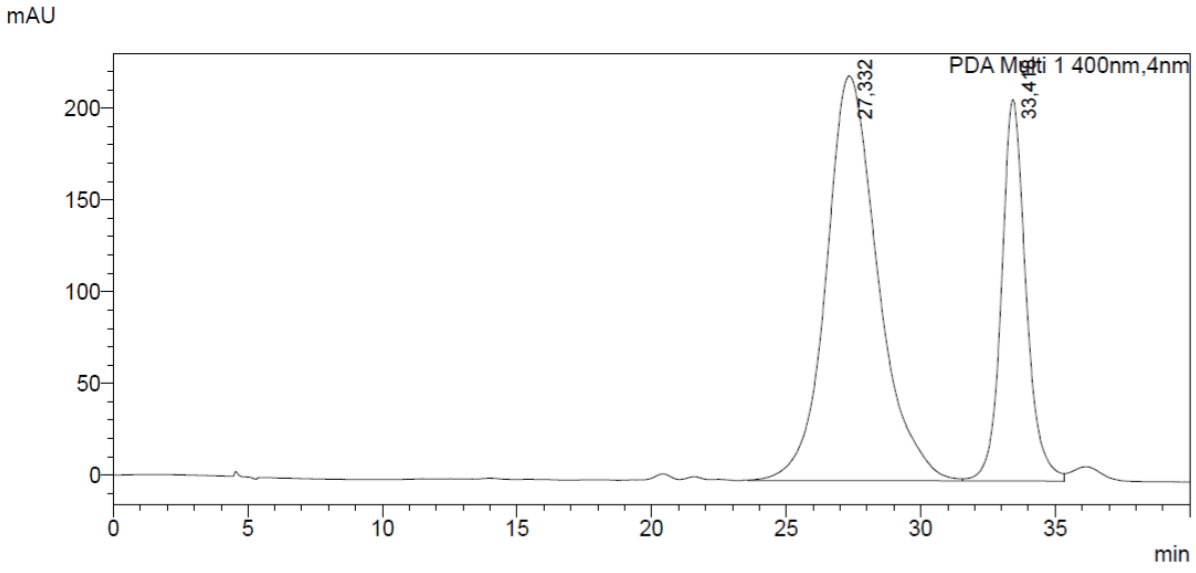

Figure S2: HPLC trace of the PSS of ***E***$_S$-**5**/***Z***$_S$-**5** (obtained irradiating the sample with a 365 nm LED and subsequently heating to reflux in EtOAc) monitored at 400 nm. Conditions: heptane/EtOAc 80:20, 3.5 mL min^{-1}, 40 min, 40 °C. t_R^1 = 27.33 min (***E***$_S$-**5**); t_R^2 = 33.42 min (***Z***$_S$-**5**).

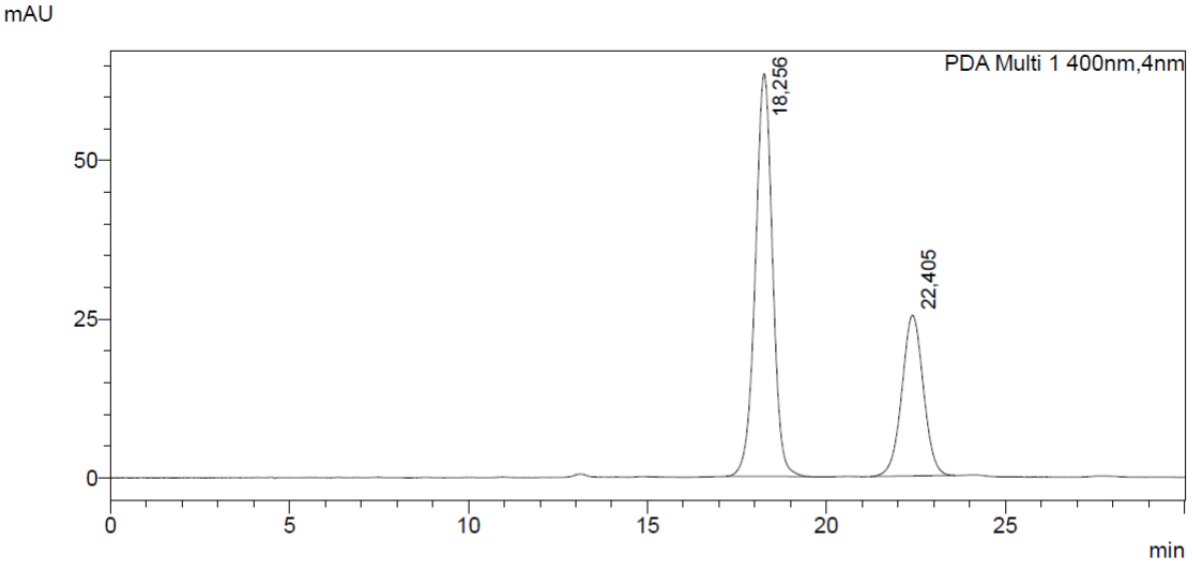

Figure S3: HPLC trace of the PSS of ***E*S-6/*Z*S-6** (obtained irradiating the sample with a 365 nm LED and subsequently heating to reflux in EtOAc) monitored at 400 nm. Conditions: heptane/EtOAc 80:20, 3.5 mL min^{-1}, 30 min, 40 °C. t_R^1 = 18.26 min (***E*S-6**); t_R^2 = 22.41 min (***Z*S-6**).

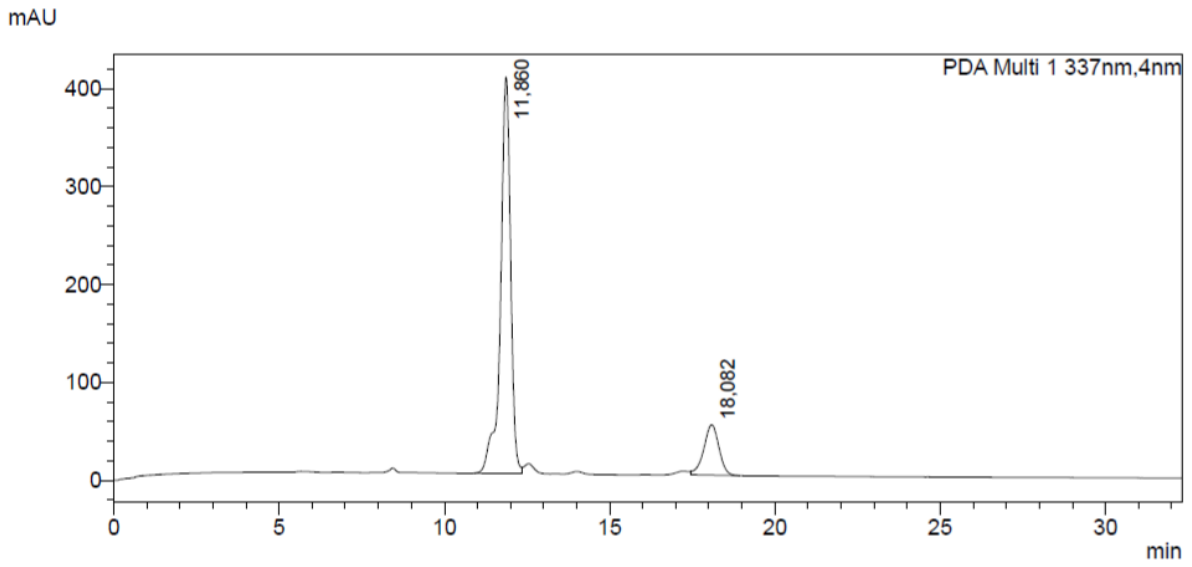

Figure S4: HPLC trace of the PSS of ***E*S-9/*Z*S-9** (obtained irradiating the sample with a 365 nm LED and subsequently heating to reflux in EtOAc) monitored at 337 nm. Conditions: heptane/EtOAc 97:3, 3.5 mL min^{-1}, 30 min, 40 °C. t_R^1 = 11.86 min (***E*S-9**); t_R^2 = 18.08 min (***Z*S-9**).

5. X-ray structures of ***E*s-3**, ***E*s-6** and ***E*s-9**

Single-crystals of ***E*S-3**, ***E*S-6** and ***E*S-9** were mounted on a cryoloop and placed in the nitrogen stream (100 K) of a Bruker-AXS D8 Venture diffractometer. Data collection and processing was carried out using the Bruker APEX3 software.[6] A multi-scan absorption correction was applied, based on the intensities of symmetry-related reflections measured at different angular settings (*SADABS*).[7] The structure was solved using *SHELXT*[8] and refinement was performed using *SHELXL*.[9] The hydrogen atoms were generated by geometrical considerations, constrained by idealised geometries and allowed to ride on their carrier atoms with an isotropic displacement parameter related to the equivalent displacement parameter of their carrier atoms. Contributions from disordered solvent present in structure of ***E*S-6** were removed using the PLATON/SQUEEZE routine.[10] No A- or B-level alerts were raised by CheckCIF for the fully refined structures.

A root mean squares deviation was calculated between the X-ray structures and their computed structures (DFT, ωB97X-D/def2-SVP, gas phase). The structures were compared without hydrogen atoms (see Figure S5).

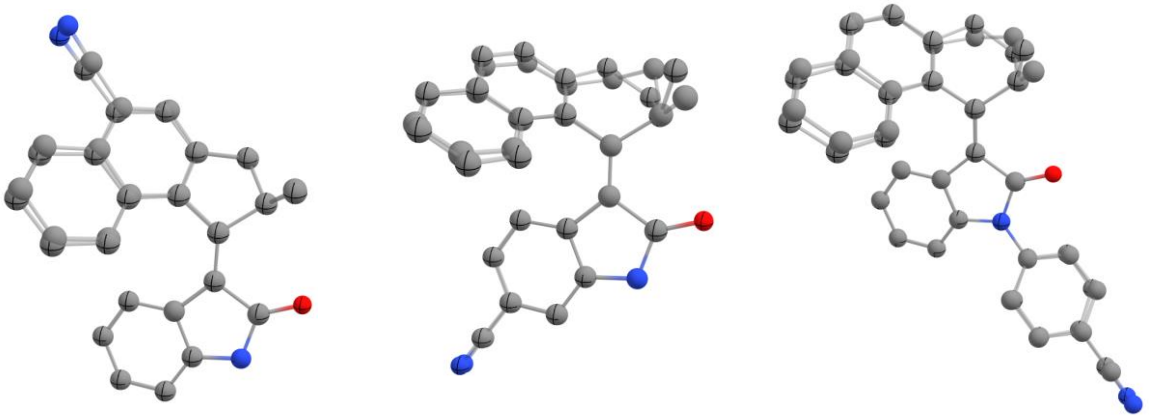

***E*S-3** ***E*S-6** ***E*S-9**

Figure S5: X-ray structures of ***E*S-3**, ***E*S-6** and ***E*S-9** with their optimised structures (DFT, ωB97X-D/def2-SVP) overlaid. Computed structures have grids on the atoms, experimentally determined X-ray structures have no grids on the atoms.

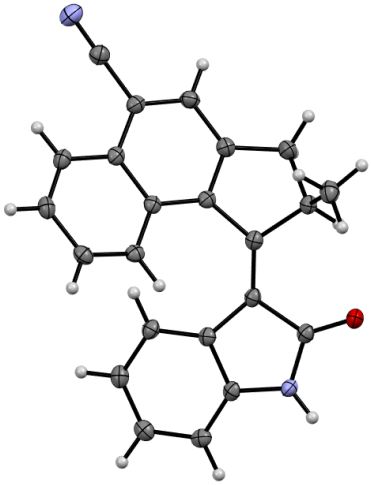

Figure S6: ORTEP image (ellipsoid at 50% probability) of ***E*S-3**.

Table S1: Crystal data and structure refinement for ***E*S-3**.

Empirical formula	$C_{23}H_{16}N_2O$
Formula weight	336.38
Temperature/K	100.0(2)
Crystal system	monoclinic
Space group	$P2_1/c$
a/Å	7.3794(3)
b/Å	17.1088(7)
c/Å	13.8545(5)
α/°	90
β/°	102.5930(10)
γ/°	90
Volume/Å^3	1707.09(12)
Z	4
ρ_{calc}g/cm^3	1.309
μ/mm^{-1}	0.639
F(000)	704.0
Crystal size/mm^3	0.363 × 0.33 × 0.14
Radiation	CuKα (λ = 1.54178)
2Θ range for data collection/°	8.334 to 144.884
Index ranges	-9 ≤ h ≤ 9, -21 ≤ k ≤ 21, -17 ≤ l ≤ 17
Reflections collected	34704
Independent reflections	3342 [R_{int} = 0.0403, R_{sigma} = 0.0215]
Data/restraints/parameters	3342/0/237
Goodness-of-fit on F^2	1.070
Final R indexes [I>=2σ (I)]	R_1 = 0.0363, wR_2 = 0.0913
Final R indexes [all data]	R_1 = 0.0384, wR_2 = 0.0931
Largest diff. peak/hole / e Å^{-3}	0.26/-0.29

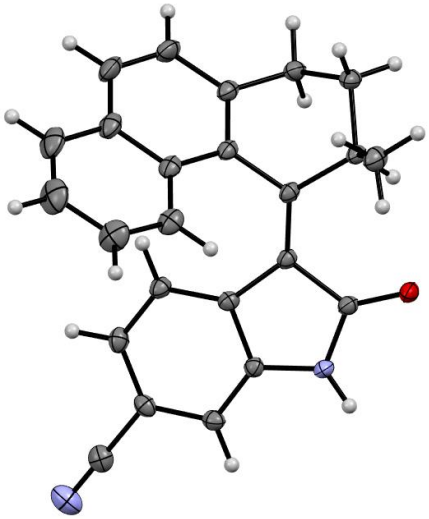

Figure S7: ORTEP image (ellipsoid at 50% probability) of ***E*S-6**.

Table 2: Crystal data and structure refinement for ***E*S-6**.

Empirical formula	$C_{24}H_{18}N_2O$
Formula weight	350.40
Temperature/K	100.00(2)
Crystal system	monoclinic
Space group	$P2_1/c$
a/Å	11.1398(4)
b/Å	8.6168(3)
c/Å	21.2050(7)
α/°	90
β/°	97.3040(10)
γ/°	90
Volume/Å^3	2018.94(12)
Z	4
ρ_{calc}g/cm^3	1.153
μ/mm^{-1}	0.559
F(000)	736.0
Crystal size/mm^3	0.519 × 0.38 × 0.27
Radiation	CuKα (λ = 1.54178)
2Θ range for data collection/°	11.096 to 144.086
Index ranges	-13 ≤ h ≤ 13, -10 ≤ k ≤ 10, -26 ≤ l ≤ 26
Reflections collected	34820
Independent reflections	3922 [R_{int} = 0.0505, R_{sigma} = 0.0283]
Data/restraints/parameters	3922/0/245
Goodness-of-fit on F^2	1.088
Final R indexes [I>=2σ (I)]	R_1 = 0.0508, wR_2 = 0.1453
Final R indexes [all data]	R_1 = 0.0531, wR_2 = 0.1472
Largest diff. peak/hole / e Å^{-3}	0.25/-0.42

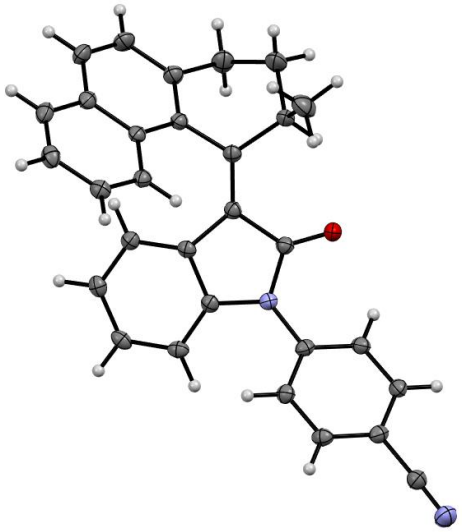

Figure S8: ORTEP image (ellipsoid at 50% probability) of ***E*S-9**.

Table S3: Crystal data and structure refinement for ***E*S-9**.

Empirical formula	$C_{30}H_{22}N_2O$
Formula weight	426.49
Temperature/K	100.00(2)
Crystal system	monoclinic
Space group	C2/c
a/Å	20.5250(6)
b/Å	7.5707(2)
c/Å	28.6634(9)
α/°	90
β/°	96.0020(10)
γ/°	90
Volume/Å^3	4429.6(2)
Z	8
ρ_{calc}g/cm^3	1.279
μ/mm^{-1}	0.607
F(000)	1792.0
Crystal size/mm^3	0.17 × 0.17 × 0.129
Radiation	CuKα (λ = 1.54178)
2Θ range for data collection/°	6.2 to 140.252
Index ranges	-24 ≤ h ≤ 24, -9 ≤ k ≤ 9, -34 ≤ l ≤ 34
Reflections collected	42392
Independent reflections	4167 [R_{int} = 0.0341, R_{sigma} = 0.0164]
Data/restraints/parameters	4167/0/299
Goodness-of-fit on F^2	1.046
Final R indexes [I>=2σ (I)]	R_1 = 0.0355, wR_2 = 0.0839
Final R indexes [all data]	R_1 = 0.0378, wR_2 = 0.0860
Largest diff. peak/hole / e Å^{-3}	0.28/-0.19

Figure S9: Single-crystal of ***E*S-3** (magnification x50)

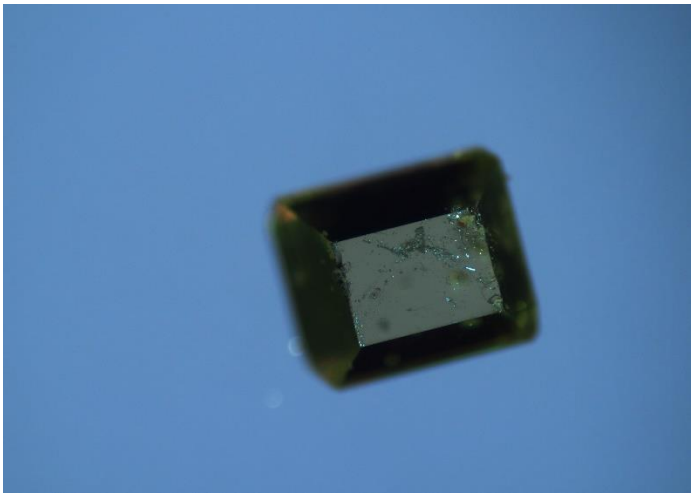

Figure S10: Single-crystal of ***E*S-6** (magnification x5)

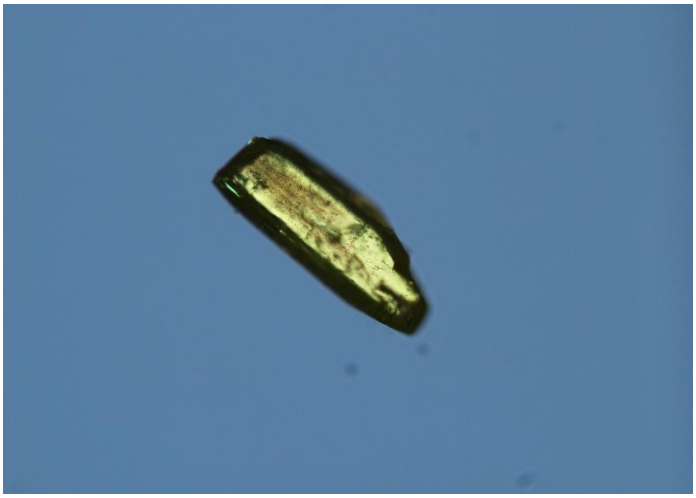

Figure S11: Single-crystal of ***E*S-9** (magnification x10)

6. NMR studies of rotation cycle

Solutions (~ 2 x 10^{-3} M) of the E_S isomers of motors **1** and **3** in degassed CD_2Cl_2 (freeze-pump-thaw × 3) were prepared and transferred into an NMR tube which was subsequently fitted with a glass optic fibre for *in situ* irradiation studies. The sample was place in a Varian Unity Plus 500 MHz NMR and cooled to –90 °C. 1H NMR spectra were recorded before irradiation, while irradiating at –90 °C, and at –90 °C after heating up to –45 °C for 15 min (for the THI step).

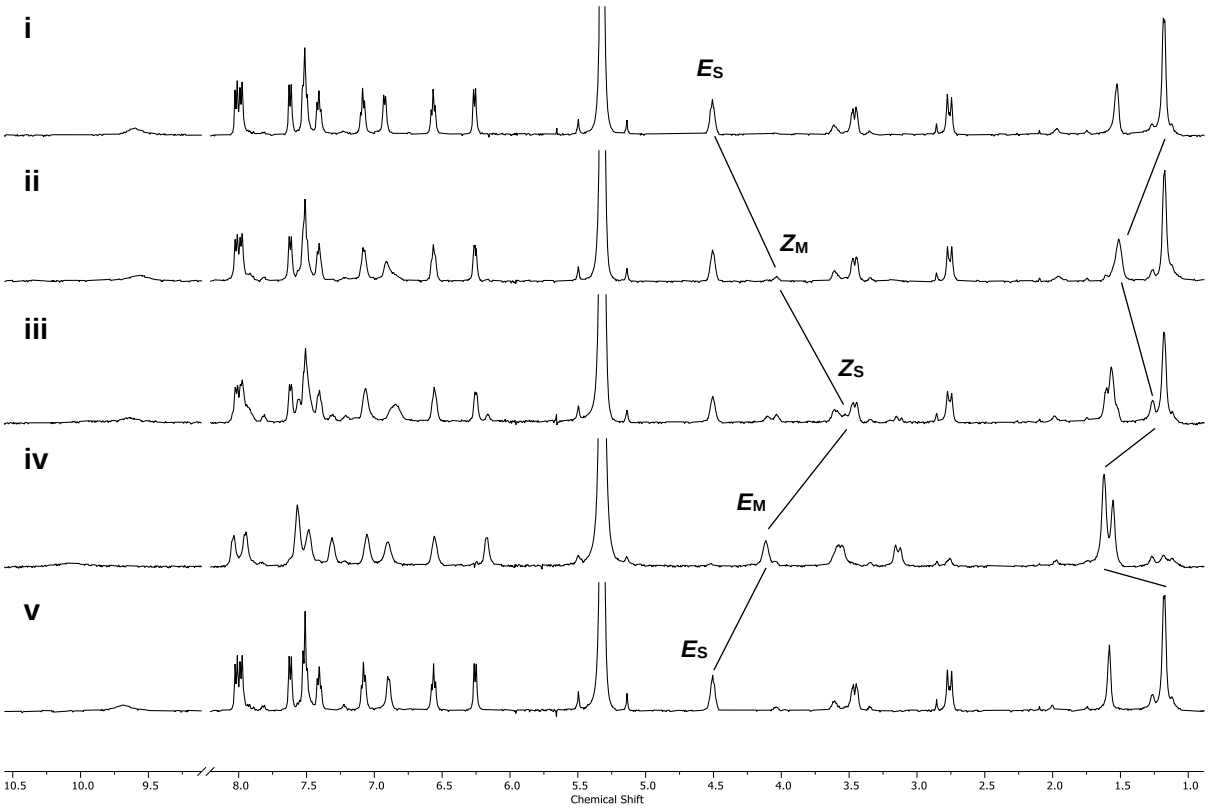

Figure S12: ^{1}H NMR irradiation studies of **1** in CD_2Cl_2 (c = 2.4 × 10^{-3} M). i) $\boldsymbol{E_S}$-**1** before irradiation; ii) 20 min irradiation 385 nm, emergence of $\boldsymbol{Z_M}$-**1**; iii) 60 min irradiation 385 nm, emergence of $\boldsymbol{Z_S}$-**1** and $\boldsymbol{E_M}$-**1**; iv) PSS_{385}; v) THI, –45 °C, 15 min.

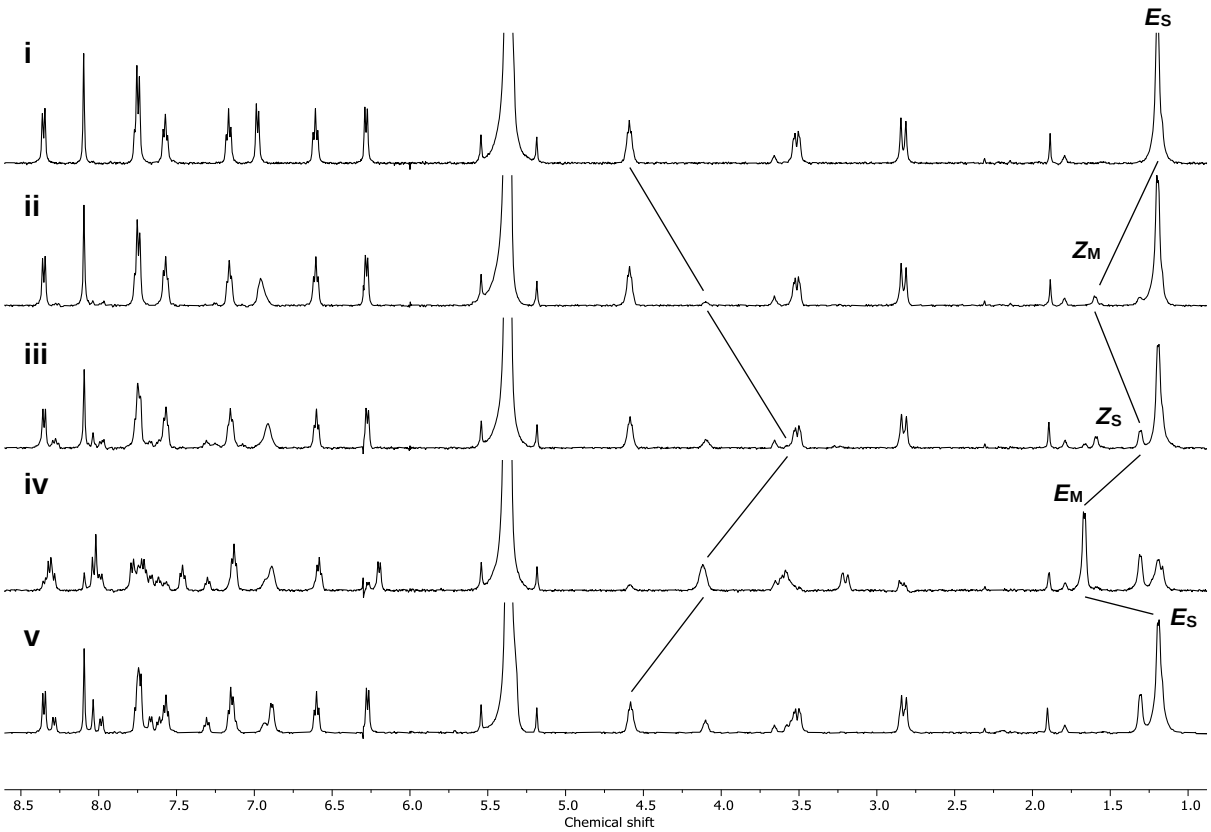

Figure S13: ^{1}H NMR irradiation studies of **3** in CD_2Cl_2 (c = 2.0 × 10^{-3} M). i) $\boldsymbol{E_S}$-**3** before irradiation; ii) 20 min irradiation 455 nm, emergence of $\boldsymbol{Z_M}$-**3**; iii) 60 min irradiation 455 nm, emergence of $\boldsymbol{Z_S}$-**3** and $\boldsymbol{E_M}$-**3**; iv) PSS_{455}; v) THI, –45 °C, 15 min.

Solutions (~ 2 × 10^{-3} M) of the E_S isomers of motors **4** – **9** in degassed DMSO (freeze-pump-thaw × 3) were prepared and transferred into an NMR tube which was subsequently fitted with a glass optic fibre for *in situ* irradiation studies. The sample was placed in a Varian Unity Plus 500 MHz NMR at room temperature. ^{1}H NMR spectra were recorded before irradiation at 25 °C and while irradiating to PSS at 25 °C. After PSS was reached, the sample was removed from the NMR, and heated to 70 °C in an oil bath for the THI step. Then the sample was placed back into the NMR at 25 °C and irradiation to PSS was resumed again. After PSS was reached, the sample was taken out of the spectrometer and heated to 100 °C in an oil bath for the second THI step, and then a final spectrum was taken in the NMR at 25 °C.

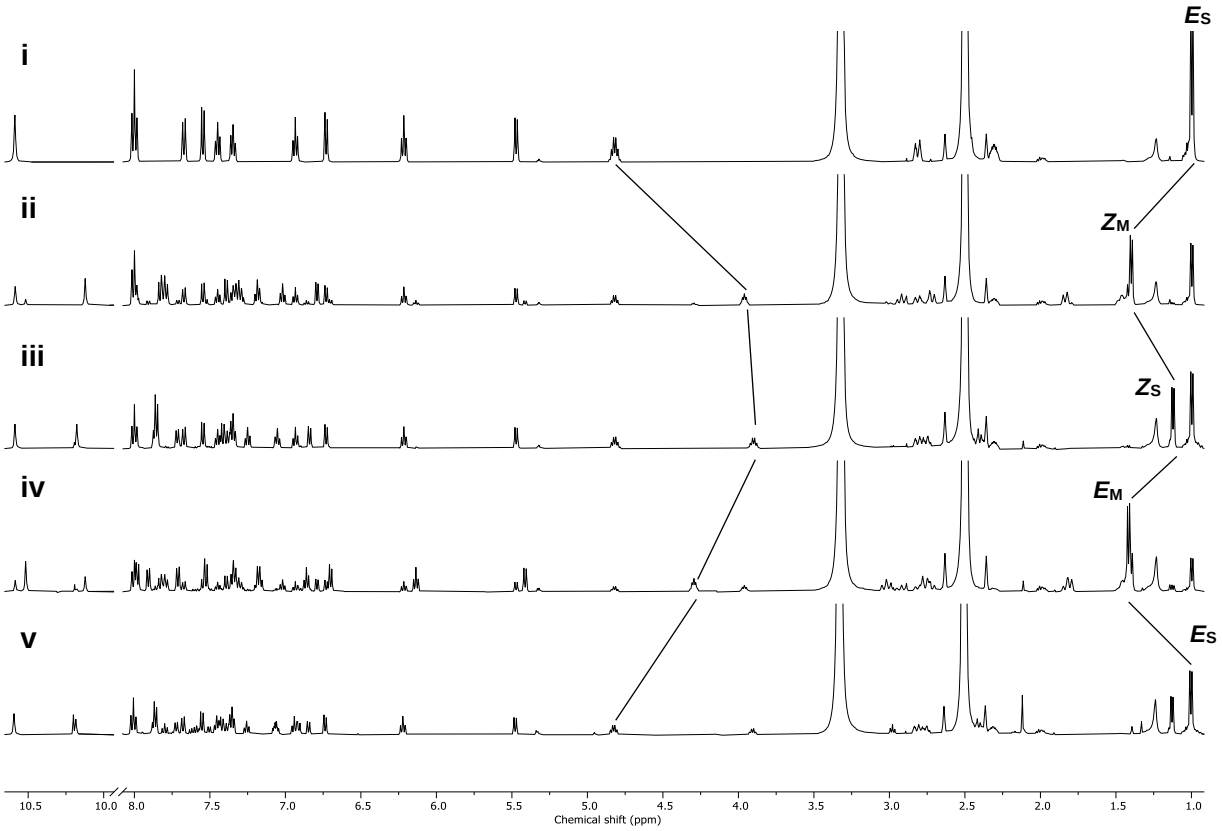

Figure S14: ^{1}H NMR irradiation studies of **4** in DMSO-d_6 (c = 2.4 × 10^{-3} M). i) ***E*S-4** before irradiation; ii) PSS_{395} = 52:48 (***E*S-4** : ***Z*M-4**); iii) THI, 70 °C, 60 min; iv) PSS_{395} = 4:96 (***Z*S-4** : *E*M-**4**); v) THI, 100 °C, 180 min.

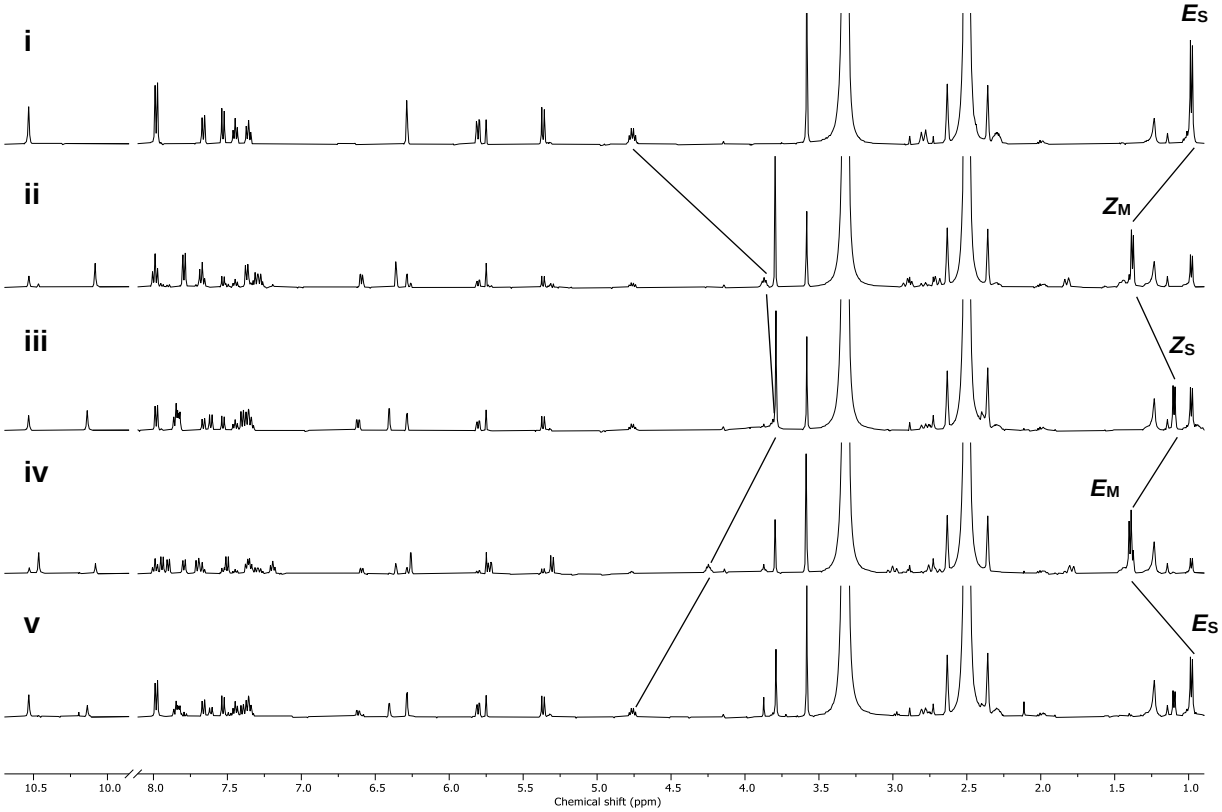

Figure S15: ^{1}H NMR irradiation studies of **5** in DMSO-d_6 (c = 1.8 × 10^{-3} M). i) ***E*$_S$-5** before irradiation; ii) PSS_{405} = 29:71 (***E*$_S$-5** : ***Z*$_M$-5**); iii) THI, 70 °C, 60 min; iv) PSS_{405} >99:1 (***E*$_M$-5** : ***Z*$_S$-5**); v) THI, 100 °C, 180 min.

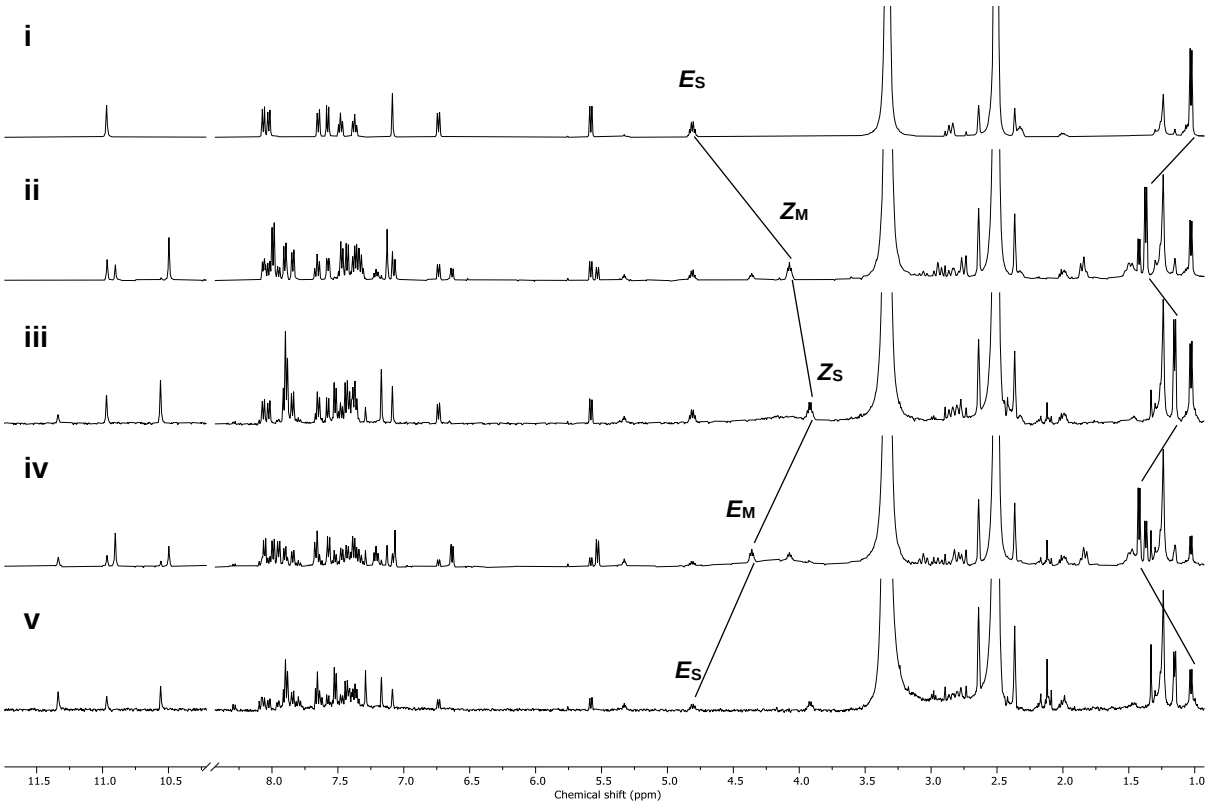

Figure S16: ^{1}H NMR irradiation studies of **6** in DMSO-d_6 (c = 2.5 × 10^{-3} M). i) ***E*$_S$-6** before irradiation; ii) PSS_{420} = 36:64 (***E*$_S$-6** : ***Z*$_M$-6**); iii) THI, 70 °C, 60 min; iv) PSS_{420} = 22:78 (***Z*$_S$-6** : ***E*$_M$-6**); v) THI, 100 °C, 180 min.

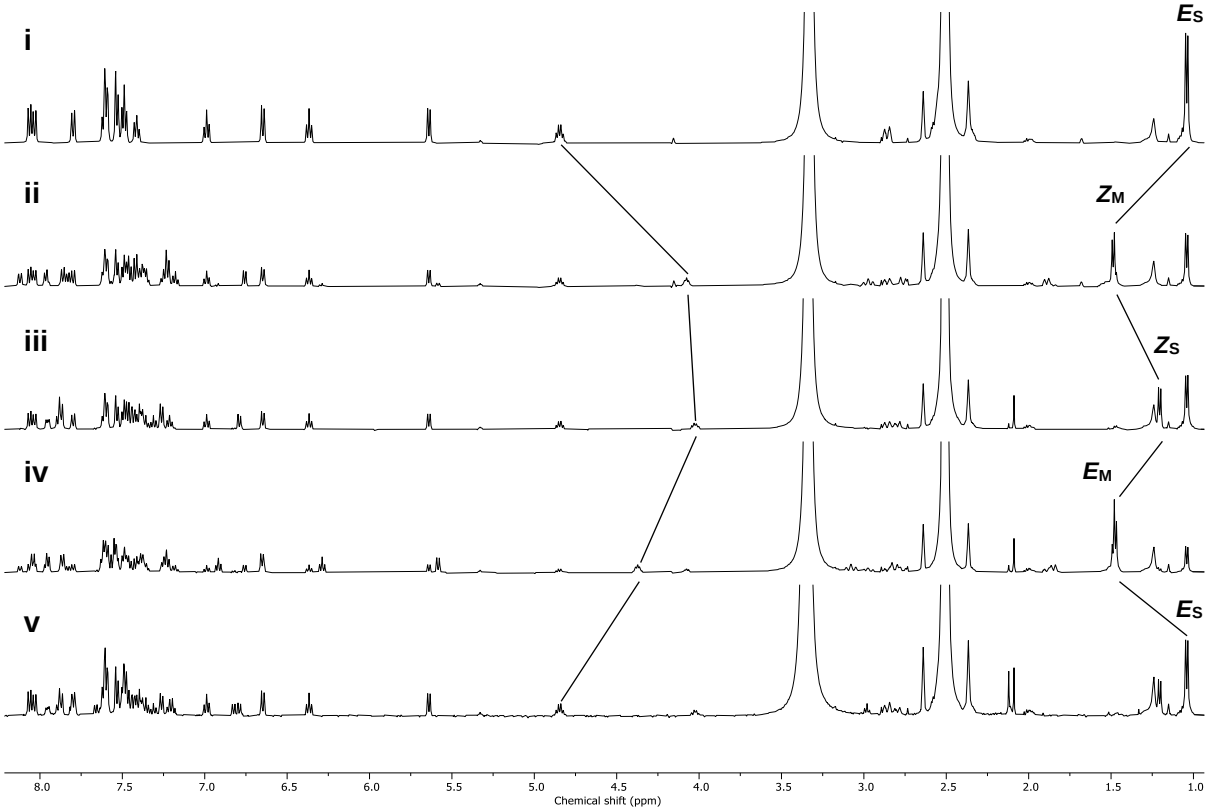

Figure S17: ^{1}H NMR irradiation studies of **7** in DMSO-d_6 (c = 2.5 × 10^{-3} M). i) ***E*$_S$-7** before irradiation; ii) PSS_{395} = 48:52 (***E*$_S$-7** : ***Z*$_M$-7**); iii) THI, 70 °C, 60 min; iv) PSS_{395} = 13:87 (***Z*$_S$-7** : ***E*$_M$-7**); v) THI, 100 °C, 180 min.

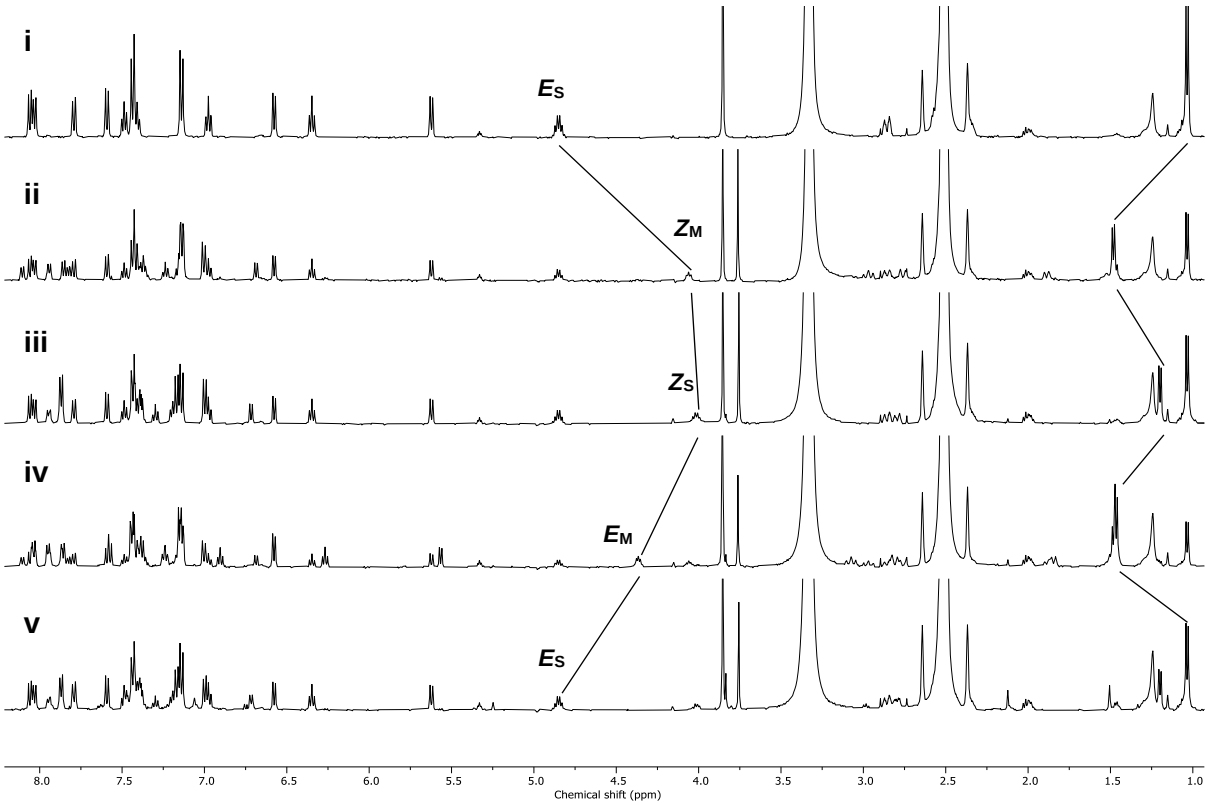

Figure S18: ^{1}H NMR irradiation studies of **8** in DMSO-d_6 (c = 1.2 × 10^{-3} M). i) ***E*$_S$-8** before irradiation; ii) PSS_{395} = 58:42 (***E*$_S$-8** : ***Z*$_M$-8**); iii) THI, 70 °C, 60 min; iv) PSS_{395} = 16:84 (***Z*$_S$-8** : ***E*$_M$-8**); v) THI, 100 °C, 180 min.

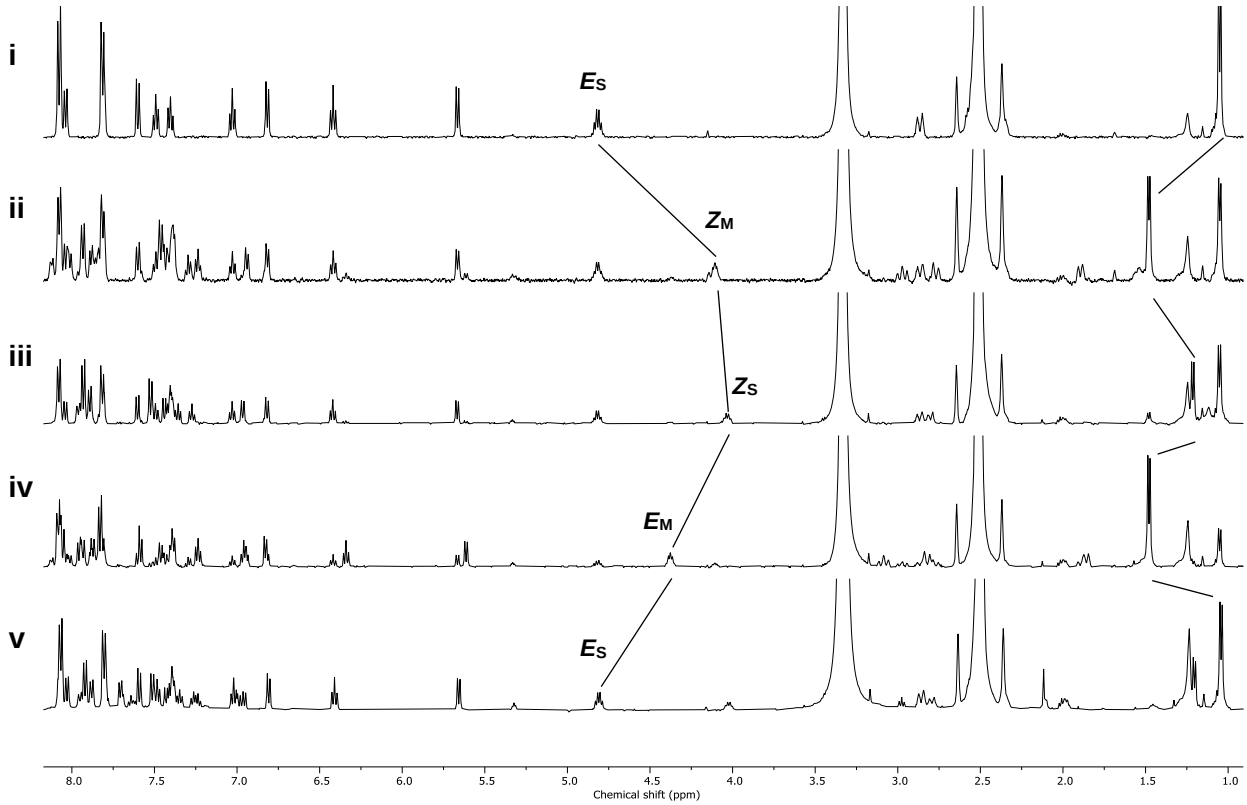

Figure S19: ^{1}H NMR irradiation studies of **9** in DMSO-d_6 (c = 2.3 x 10^{-3} M). i) ***E*$_S$-9** before irradiation; ii) PSS_{395} = 49:51 (***E*$_S$-9** : ***Z*$_M$-9**); iii) THI, 70 °C, 60 min; iv) PSS_{395} = 5:95 (***Z*$_S$-9** : ***E*$_M$-9**); v) THI, 100 °C, 180 min.

7. UV-Vis spectra

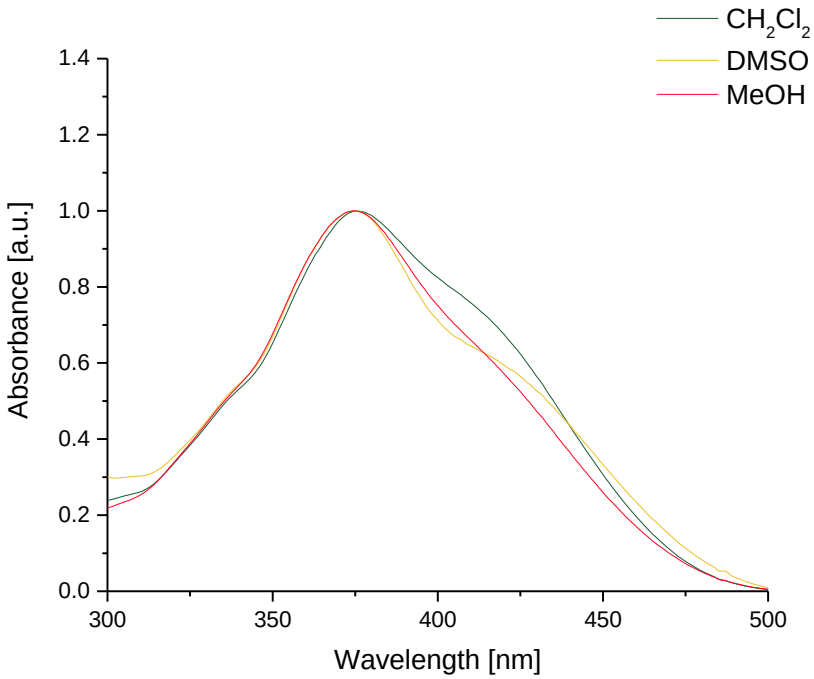

Figure S20: Normalised UV-Vis absorption spectra of motor ***E*S-1** in CH_2Cl_2, DMSO and MeOH.

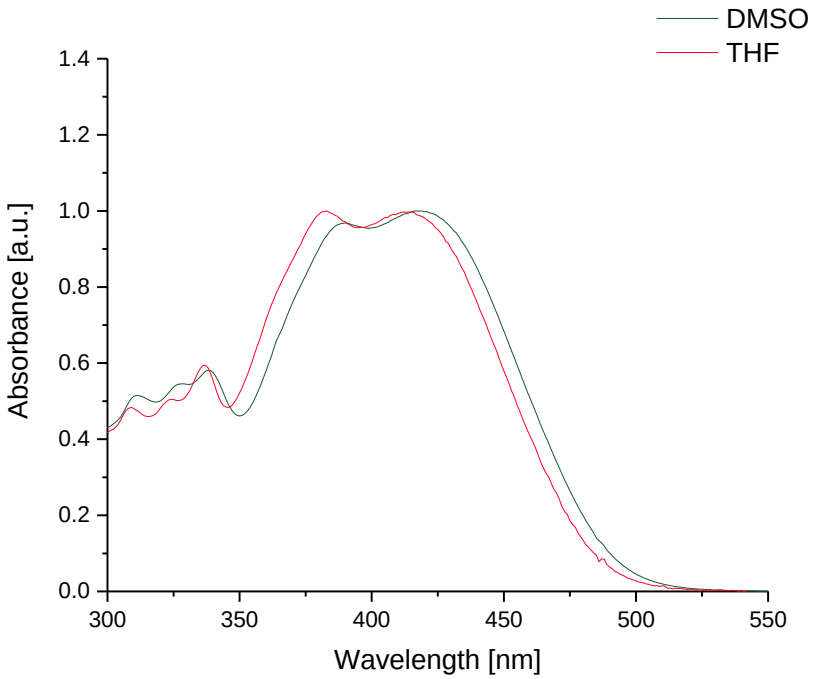

Figure S21: Normalised UV-Vis absorption spectra of motor ***E*S-2** in DMSO and THF.

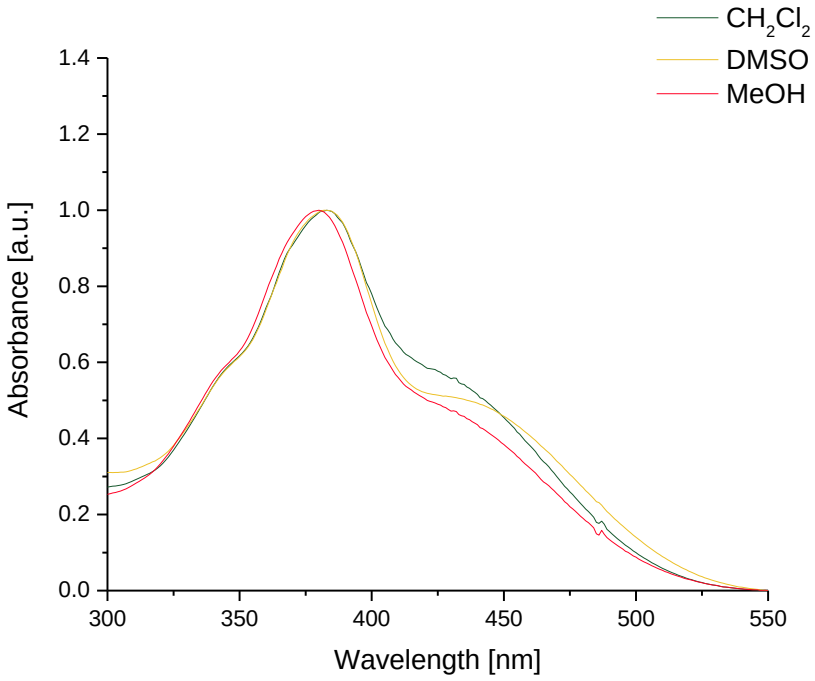

Figure S22: Normalised UV-Vis absorption spectra of motor ***E*S-3** in CH_2Cl_2, DMSO and MeOH.

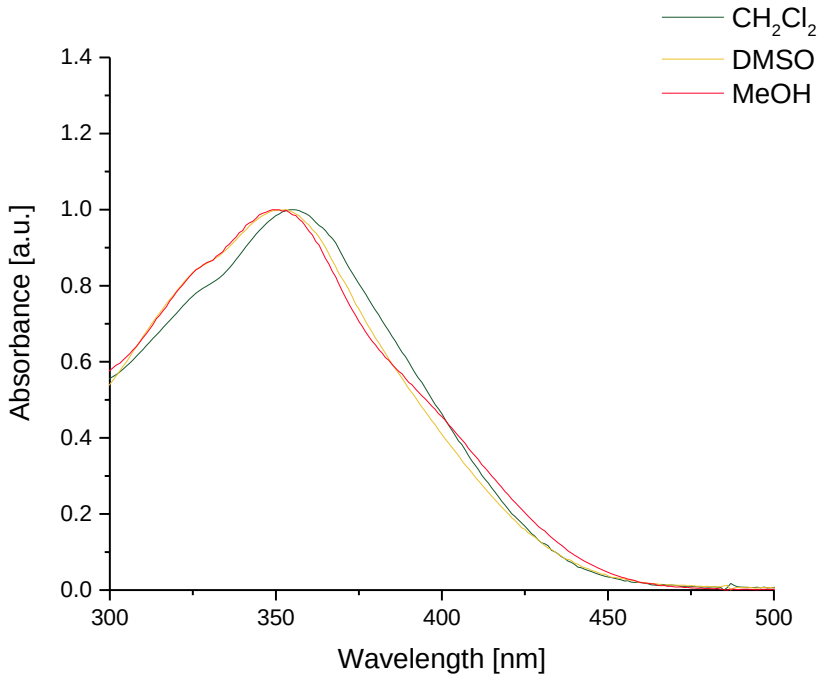

Figure S23: Normalised UV-Vis absorption spectra of motor ***E*S-4** in CH_2Cl_2, DMSO and MeOH.

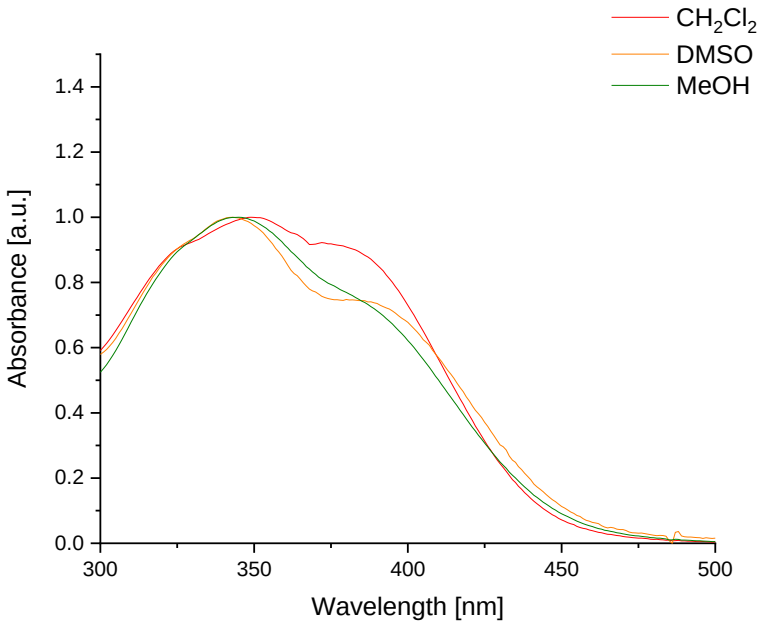

Figure S24: Normalised UV-Vis absorption spectra of motor ***E*S-5** in CH_2Cl_2, DMSO and MeOH.

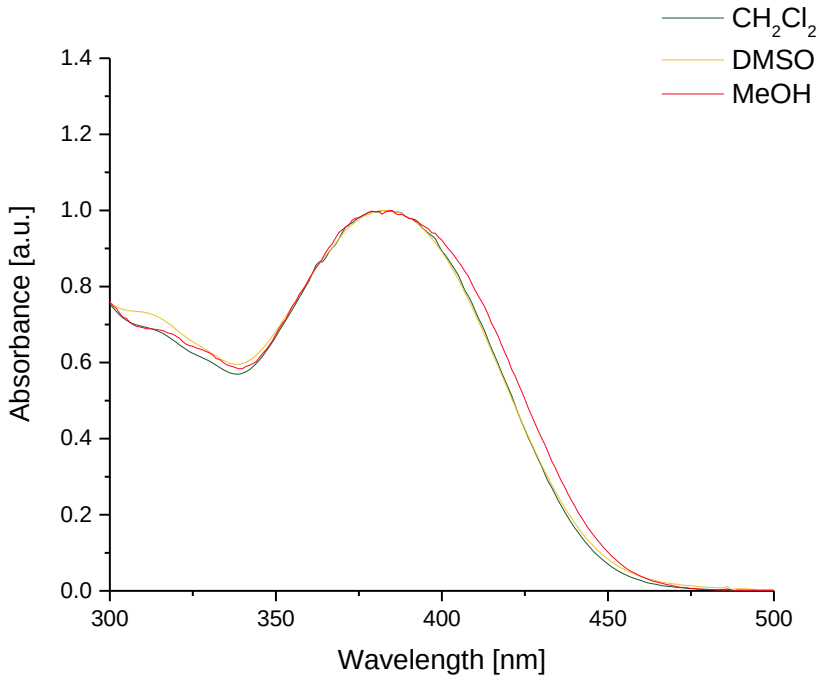

Figure S25: Normalised UV-Vis absorption spectra of motor ***E*S-6** in CH_2Cl_2, DMSO and MeOH.

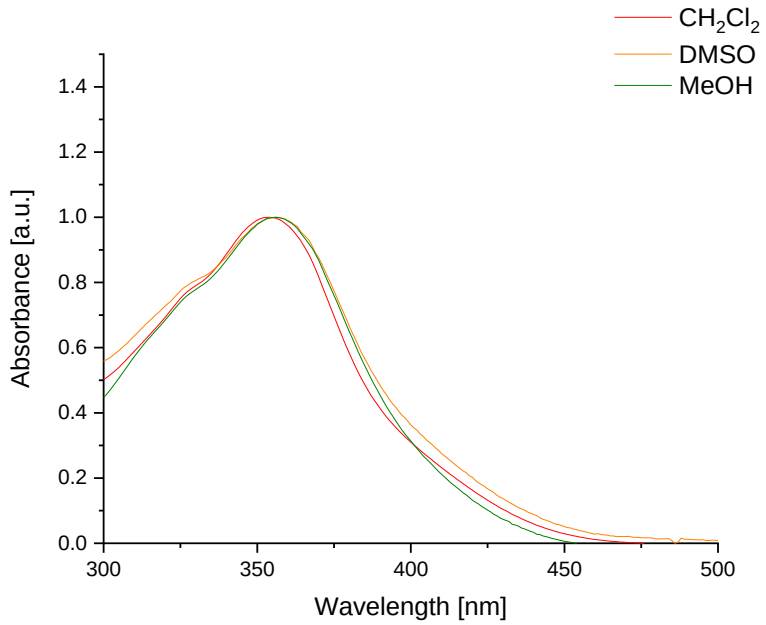

Figure S26: Normalised UV-Vis absorption spectra of motor ***E*S-7** in CH_2Cl_2, DMSO and MeOH.

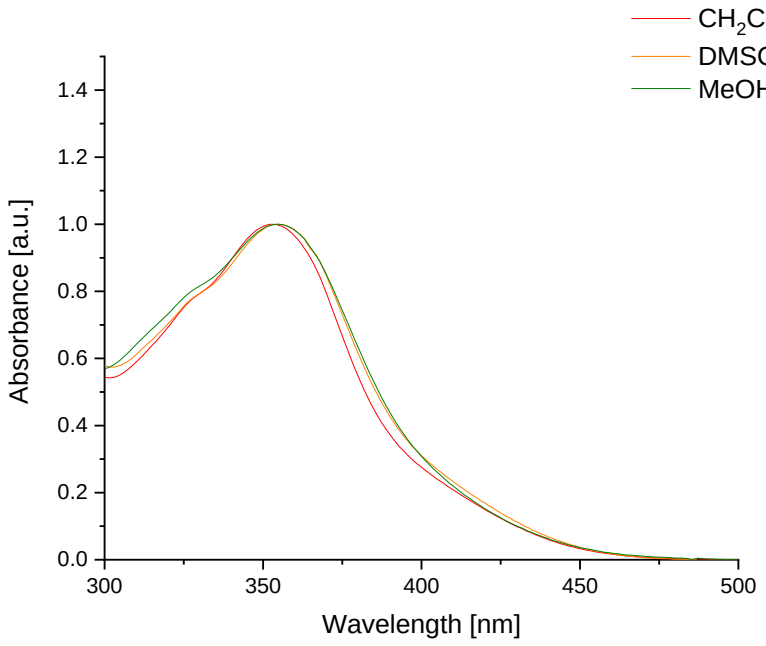

Figure S27: Normalised UV-Vis absorption spectra of motor ***E*S-8** in CH_2Cl_2, DMSO and MeOH.

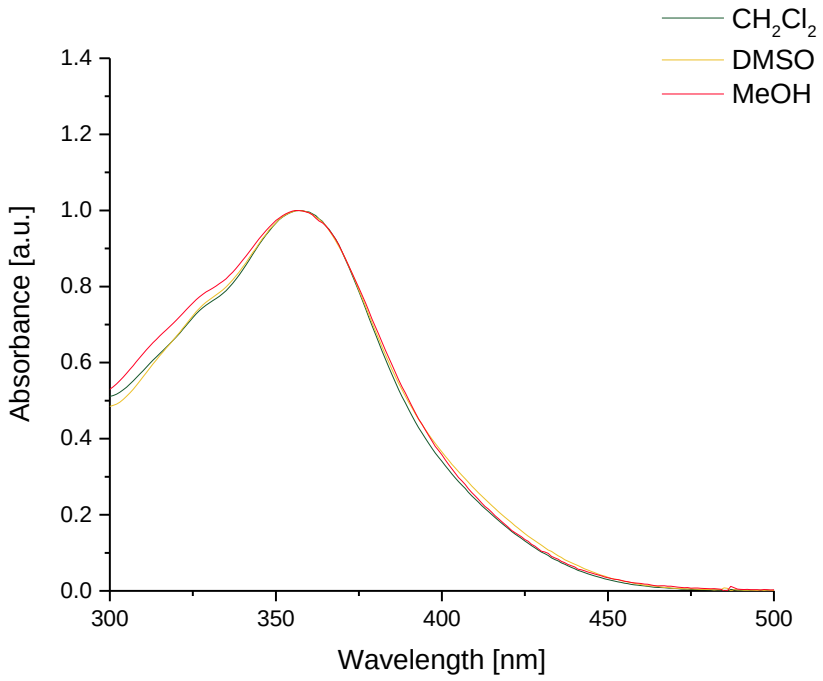

Figure S28: Normalised UV-Vis absorption spectra of motor ***E*S-9** in CH_2Cl_2, DMSO and MeOH.

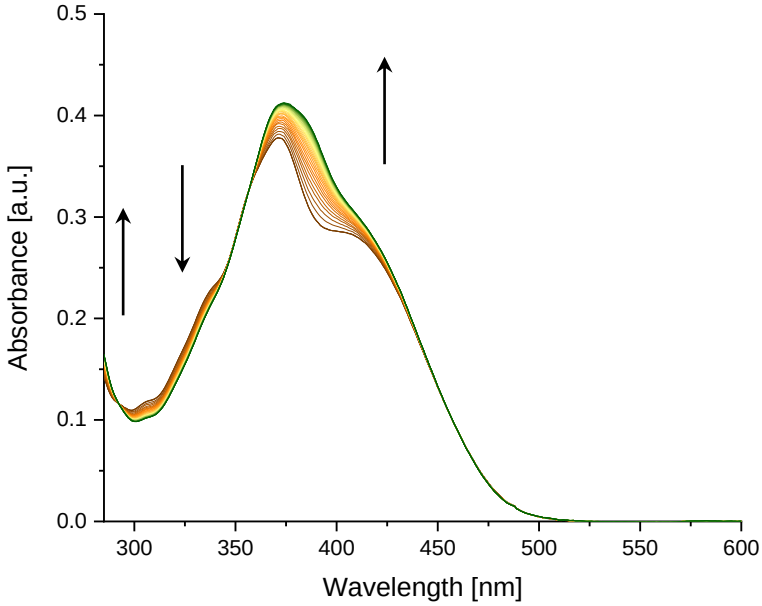

Figure S29: UV-Vis irradiation of **1** in toluene (c = ~ 1 × 10^{-5} M) at 20 °C with λ = 365 nm.

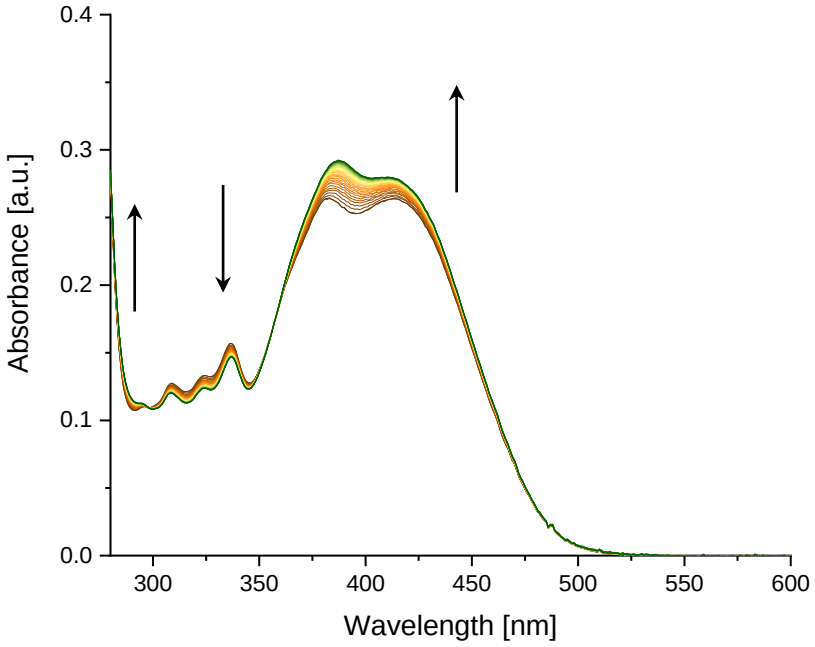

Figure S30: UV-Vis irradiation of **2** in THF (c = ~ 1 × 10^{-5} M) at 20 °C with λ = 365 nm.

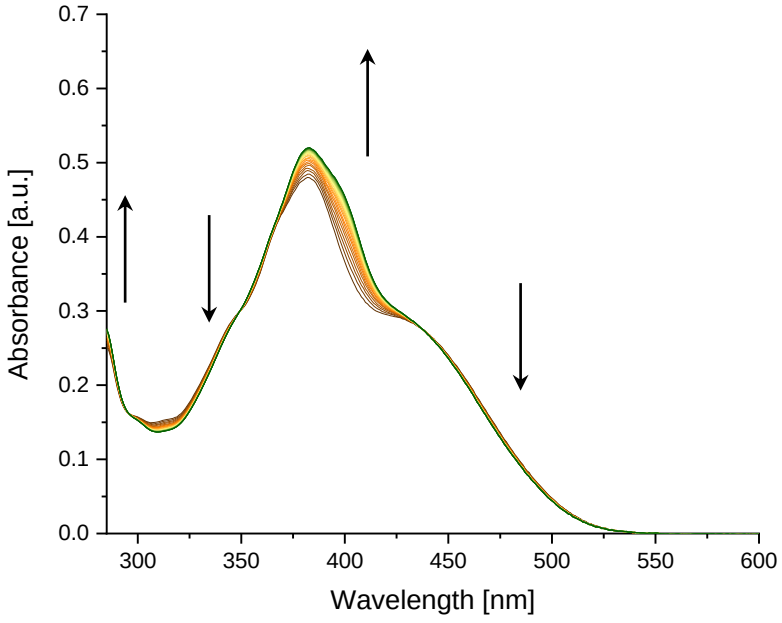

Figure S31: UV-Vis irradiation of **3** in toluene (c = ~ 1 × 10^{-5} M) at 20 °C with λ = 365 nm.

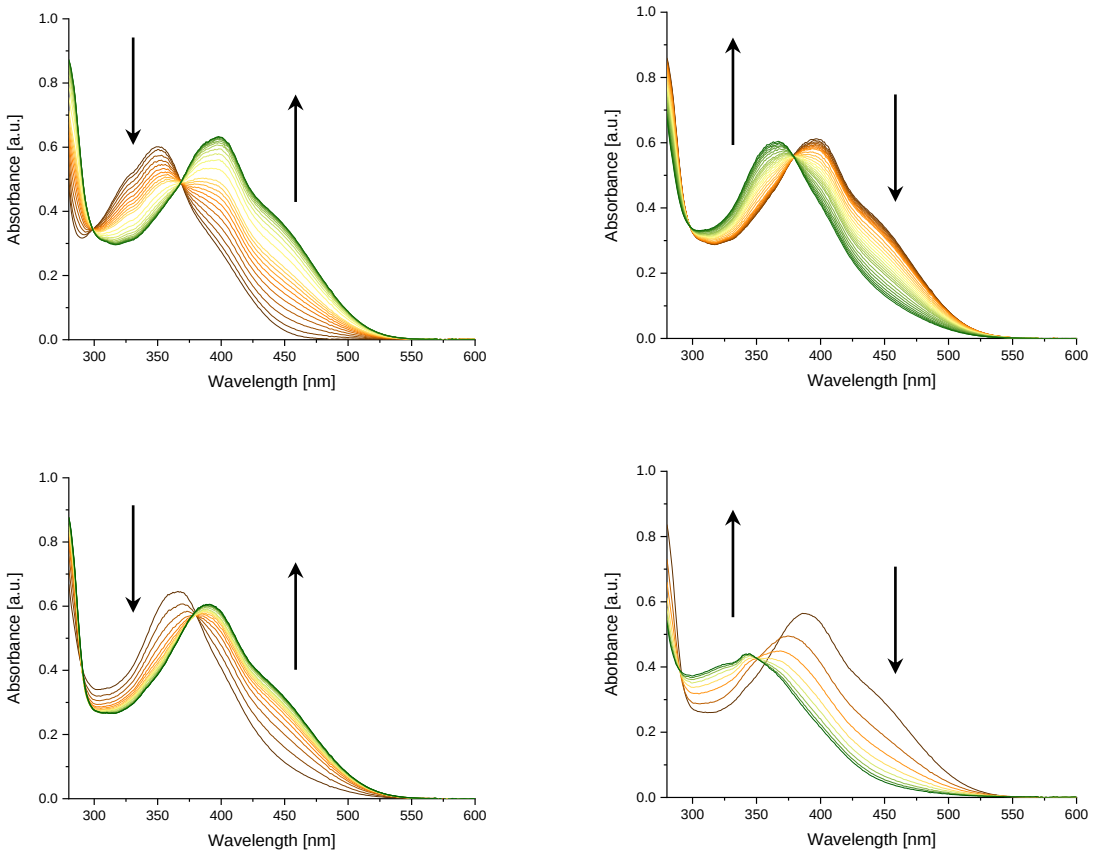

Figure S32: UV-Vis analysis of the rotation cycle of **4** in DMSO (c = ~ 2 × 10^{-5} M). Top left: irradiation to PSS with λ = 365 nm; top right: heating to 60 °C, THI; bottom left: irradiation to PSS with λ = 365 nm; bottom right: heating to 100 °C, THI.

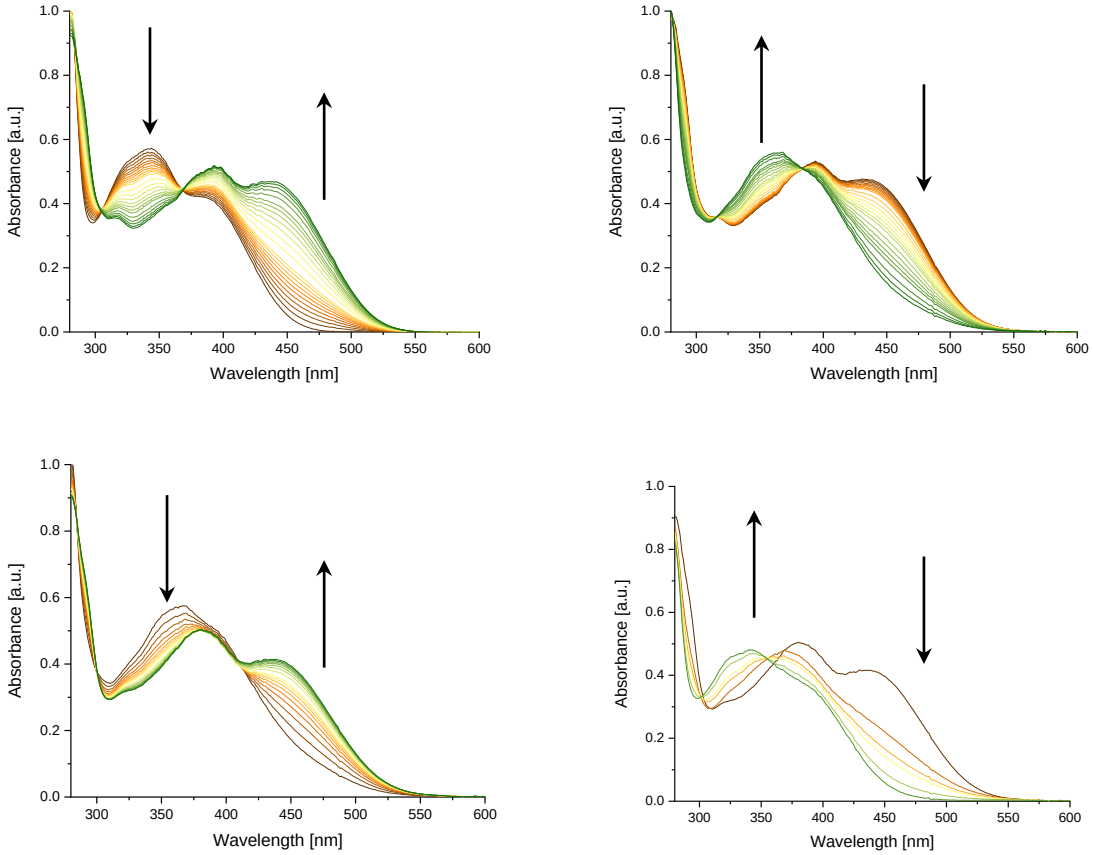

Figure S33: UV-Vis analysis of the rotation cycle of **5** in DMSO (c = ~ 2 × 10^{-5} M). Top left: irradiation to PSS with λ = 365 nm; top right: heating to 60 °C, THI; bottom left: irradiation to PSS with λ = 365 nm; bottom right: heating to 100 °C, THI.

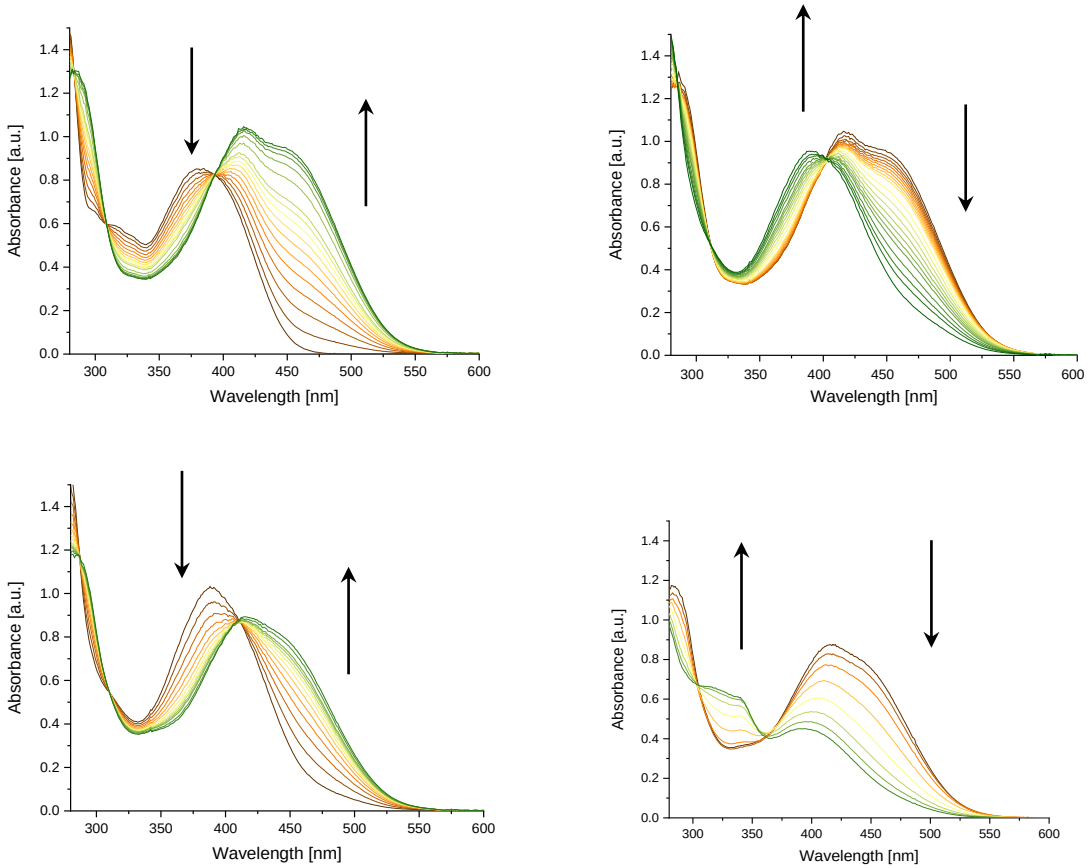

Figure S34: UV-Vis analysis of the rotation cycle of **6** in DMSO (c = ~ 4 × 10^{-5} M). Top left: irradiation to PSS with λ = 365 nm; top right: heating to 60 °C, THI; bottom left: irradiation to PSS with λ = 365 nm; bottom right: heating to 100 °C, THI.

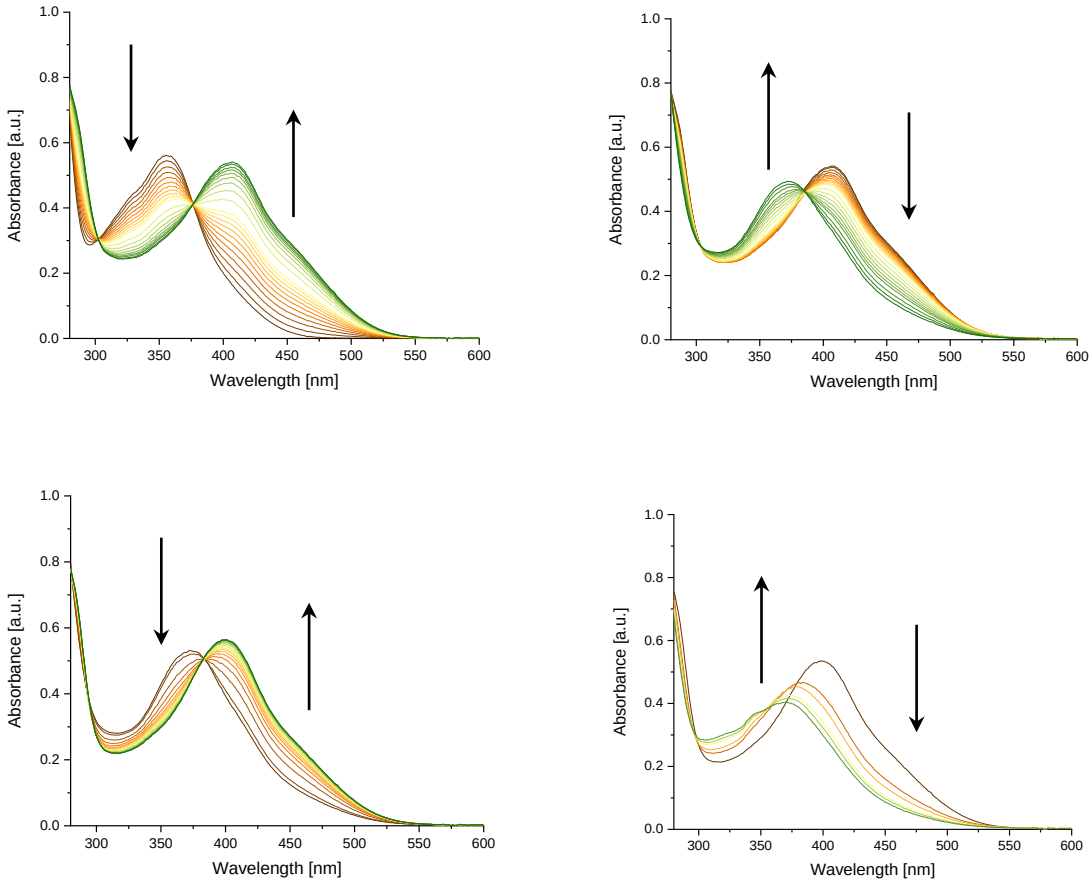

Figure S35: UV-Vis analysis of the rotation cycle of **7** in DMSO (c = ~ 2 × 10^{-5} M). Top left: irradiation to PSS with λ = 365 nm; top right: heating to 60 °C, THI; bottom left: irradiation to PSS with λ = 365 nm; bottom right: heating to 100 °C, THI.

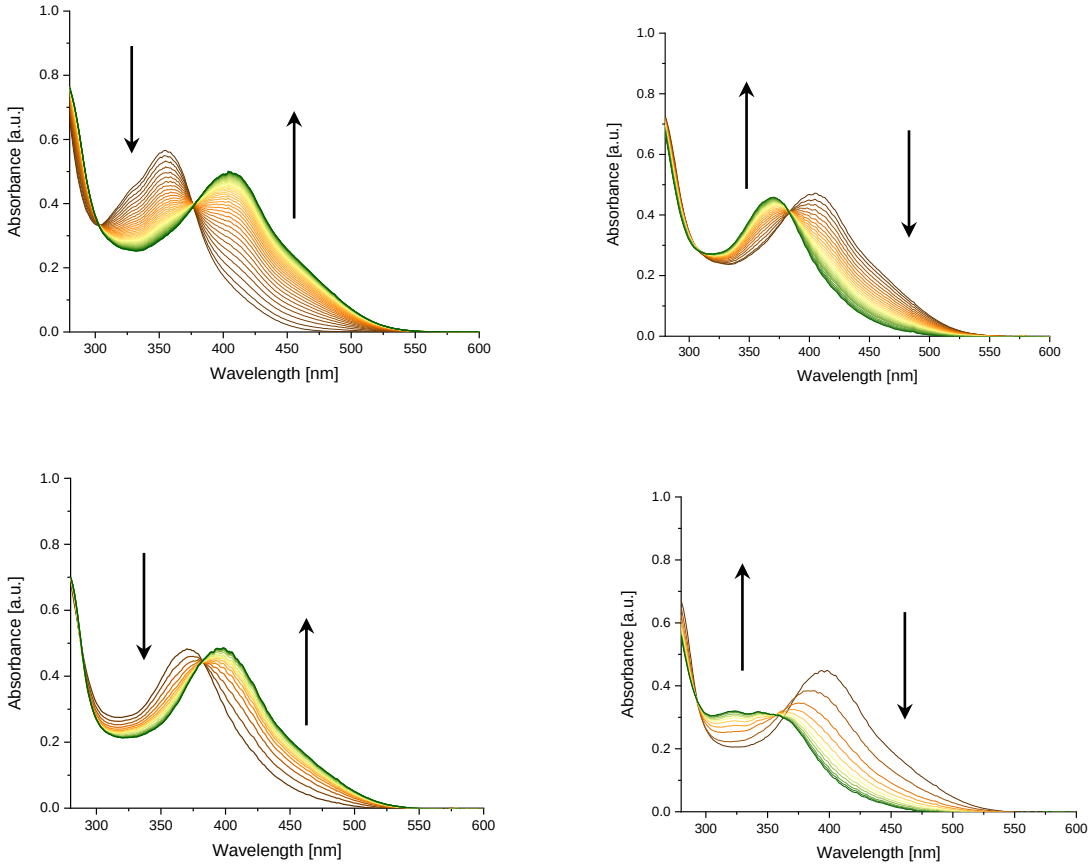

Figure S36: UV-Vis analysis of the rotation cycle of **8** in DMSO (c = ~ 2 × 10^{-5} M). Top left: irradiation to PSS with λ = 365 nm; top right: heating to 60 °C, THI; bottom left: irradiation to PSS with λ = 365 nm; bottom right: heating to 100 °C, THI.

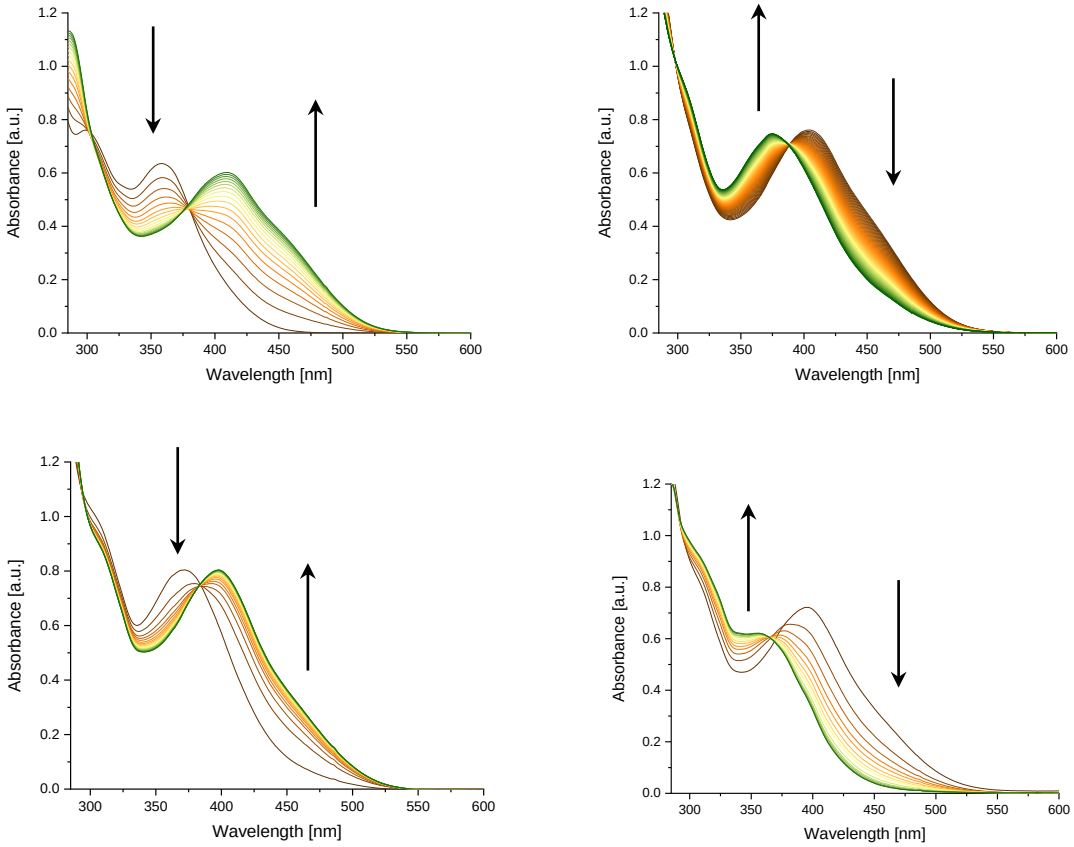

Figure S37: UV-Vis analysis of the rotation cycle of **9** in DMSO (c = ~ 2 × 10^{-5} M). Top left: irradiation to PSS with λ = 365 nm; top right: heating to 60 °C, THI; bottom left: irradiation to PSS with λ = 365 nm; bottom right: heating to 100 °C, THI.

8. Eyring analysis

NMR samples of motors **1** and **3** in d_4-methanol (~ 1 × 10^{-3} M) were irradiated with a Thorlabs LED (M365F1) for five runs at different constant temperatures (between −41.14 and −51.93 °C) to approach PSS. The temperature of the NMR probe was measured measuring the relative distance between the residual solvent signals. The thermal helix inversion was followed plotting the decay of the integrals of ***E*M-1** and ***E*M-3** after switching off the irradiation, in order to extract the rate constants used for the Eyring plots. A least squares analysis was performed on the Eyring equation to retrieve the ΔG‡ of THI.

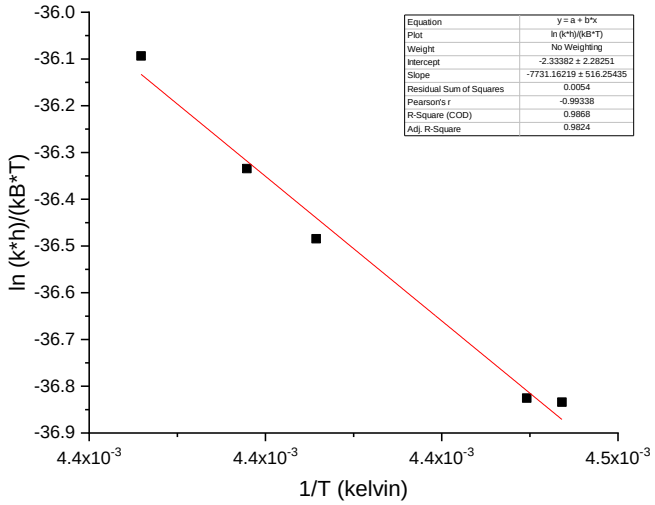

Figure S38: Eyring plot analysis of ***E*M-1** to ***E*S-1** in d_4-methanol.

Table S4: Activation parameters of **1** at 20 °C.

	***E*M-1 → *E*S-1**
ΔG‡ (kcal mol^{-1})	17 ± 1
ΔH‡ (kcal mol^{-1})	15 ± 1
ΔS‡ (cal K^{-1} mol^{-1})	–5 ± 6
$t_{1/2}$	300 ms

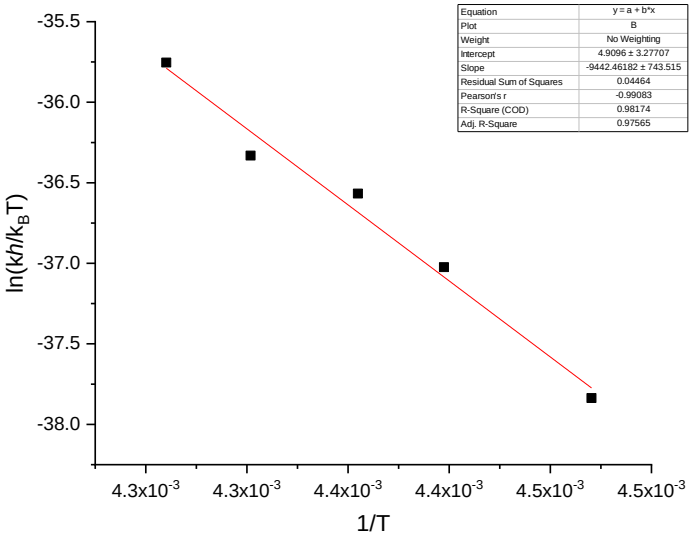

Figure S39: Eyring plot analysis of ***E*$_M$-3** to ***E*$_S$-3** in d_4-methanol.

Table 5: Activation parameters of **1** at 20 °C.

	***E*$_M$-3 → *E*$_S$-3**
$\Delta G^{\ddagger}$ (kcal mol^{-1})	16 ± 1
$\Delta H^{\ddagger}$ (kcal mol^{-1})	19 ± 1
$\Delta S^{\ddagger}$ (cal K^{-1} mol^{-1})	10 ± 7
$t_{1/2}$	100 ms

Eyring plot analysis of the thermal isomerisation processes of motors **4**–**9** was performed by monitoring the decrease in absorption of a UV-Vis sample over time. The rate constants (*k*) of the first order decay at five temperatures were obtained by fitting to $Y = Ae^{(-k \cdot t)} + Y0$ using Origin software. A least squares analysis was performed on the Eyring equation to retrieve the $\Delta G^{\ddagger}$ of THI.

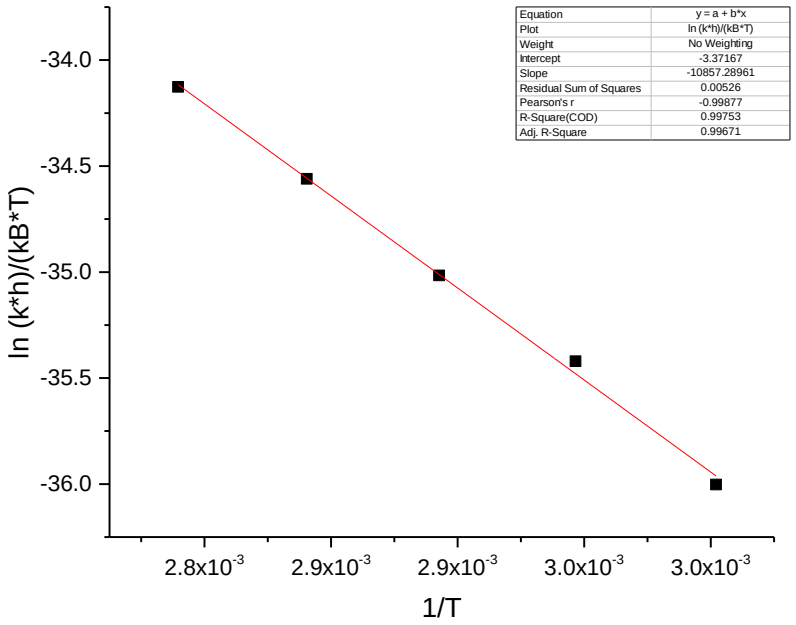

Figure S40: Eyring plot analysis of Z_M-**4** to Z_S-**4**, monitoring decrease in absorption at λ = 400 nm in toluene at 60, 65, 70, 75 and 80 °C.

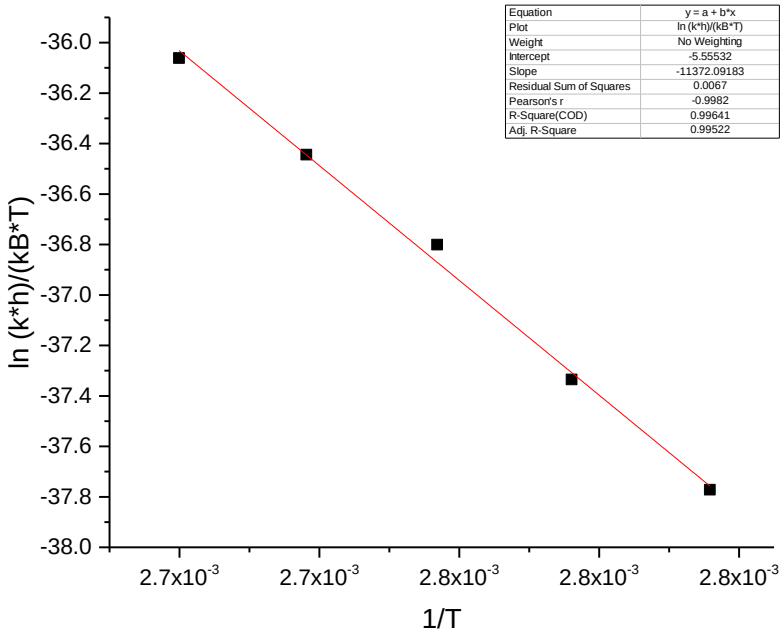

Figure S41: Eyring plot analysis of E_M-**4** to E_S-**4**, monitoring decrease in absorption at λ = 400 nm in toluene at 80, 85, 90, 95 and 100 °C.

Table S6: Activation parameters of **4** at 20 °C

	Z_M-**4** → Z_S-**4**	E_M-**4** → E_S-**4**
$\Delta G^{‡}$ (kcal mol^{-1})	23.5 ± 0.3	25.8 ± 0.5
$\Delta H^{‡}$ (kcal mol^{-1})	21.6 ± 0.6	22.6 ± 0.8
$\Delta S^{‡}$ (cal K^{-1} mol^{-1})	–7 ± 2	–11 ± 2
$t_{1/2}$	11 h	24 d

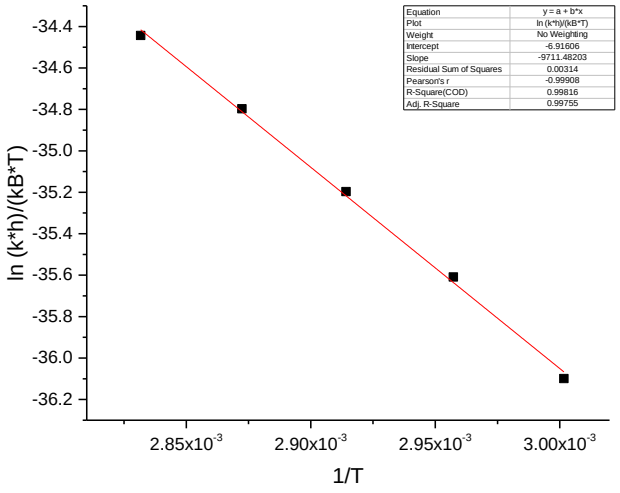

Figure S42: Eyring plot analysis of Z_M-**5** to Z_S-**5**, monitoring decrease in absorption at λ = 450 nm in toluene at 60, 65, 70, 75 and 80 °C.

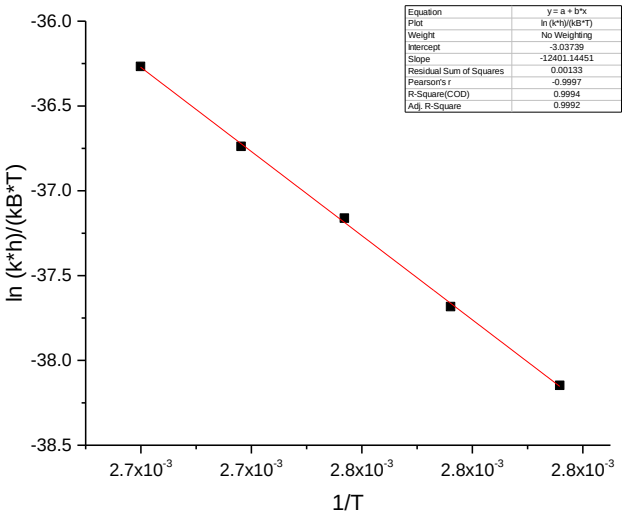

Figure S43: Eyring plot analysis of E_M-**5** to E_S-**5**, monitoring decrease in absorption at λ = 450 nm in toluene at 80, 85, 90, 95 and 100 °C.

Table S7: Activation parameters of **5** at 20 °C

	Z_M-**5** → Z_S-**5**	E_M-**5** → E_S-**5**
$\Delta G^{‡}$ (kcal mol^{-1})	23.3 ± 0.2	26.4 ± 0.2
$\Delta H^{‡}$ (kcal mol^{-1})	19.3 ± 0.5	24.6 ± 0.4
$\Delta S^{‡}$ (cal K^{-1} mol^{-1})	–14 ± 1	–6 ± 1
$t_{1/2}$	8 h	64 d

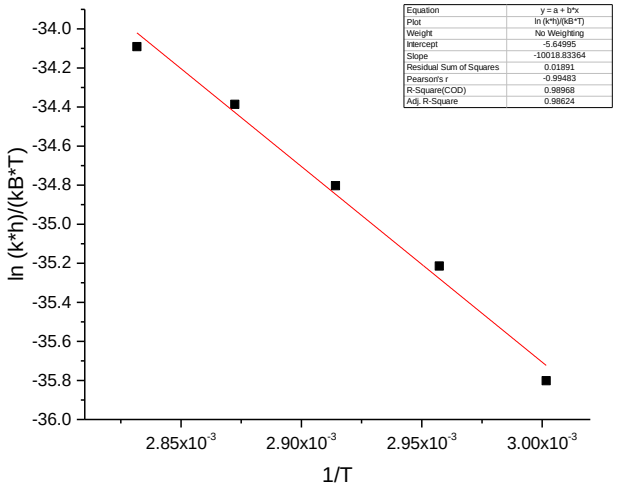

Figure S44: Eyring plot analysis of Z_M-**6** to Z_S-**6**, monitoring decrease in absorption at λ = 450 nm in toluene at 60, 65, 70, 75 and 80 °C.

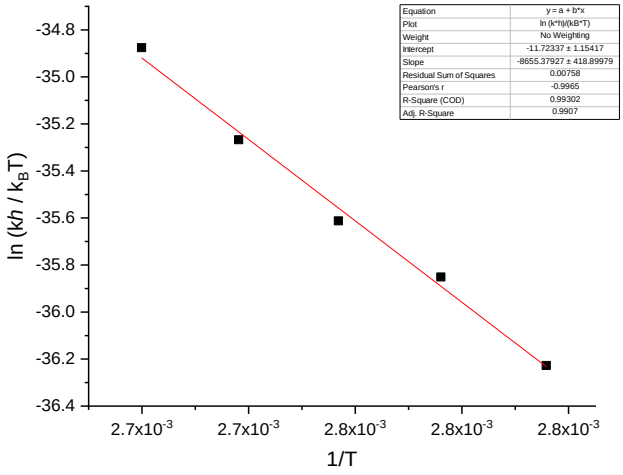

Figure S45: Eyring plot analysis of E_M-**6** to E_S-**6**, monitoring decrease in absorption at λ = 450 nm in toluene at 80, 85, 90, 95 and 100 °C.

Table S8: Activation parameters of **6** at 20 °C

	Z_M-**6** → Z_S-**6**	E_M-**6** → E_S-**6**
$\Delta G^{‡}$ (kcal mol^{-1})	23.2 ± 0.6	24.0 ± 0.5
$\Delta H^{‡}$ (kcal mol^{-1})	20 ± 1	17.2 ± 0.8
$\Delta S^{‡}$ (cal K^{-1} mol^{-1})	–11 ± 3	–23 ± 2
$t_{1/2}$	6 h	27 h

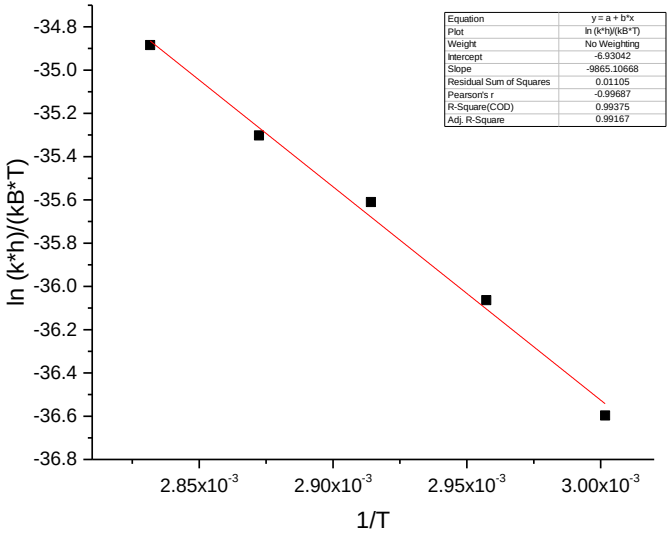

Figure S46: Eyring plot analysis of Z_M-**7** to Z_S-**7** monitoring decrease in absorption at λ = 400 nm in toluene at 60, 65, 70, 75 and 80 °C.

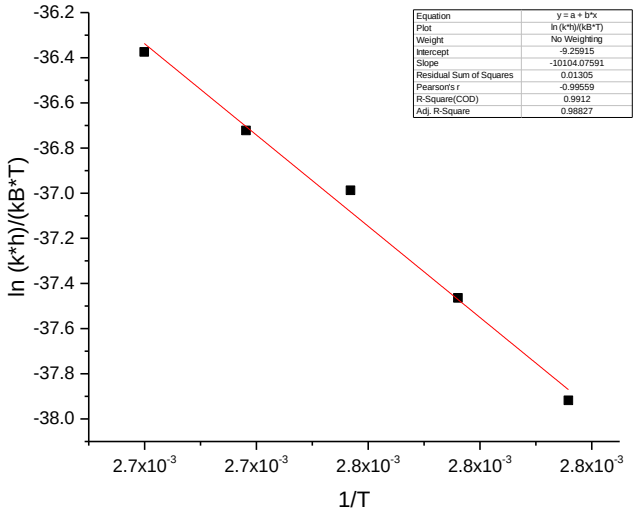

Figure S47: Eyring plot analysis of E_M-**7** to E_S-**7** monitoring decrease in absorption at λ = 400 nm in toluene at 80, 85, 90, 95 and 100 °C.

Table S9: Activation parameters of **7** at 20 °C

	Z_M-**7** → Z_S-**7**	E_M-**7** → E_S-**7**
$\Delta G^{‡}$ (kcal mol^{-1})	23.6 ± 0.4	25.5 ± 0.7
$\Delta H^{‡}$ (kcal mol^{-1})	19.6 ± 0.9	20 ± 1
$\Delta S^{‡}$ (cal K^{-1} mol^{-1})	–14 ± 3	–18 ± 3
$t_{1/2}$	13 h	13 d

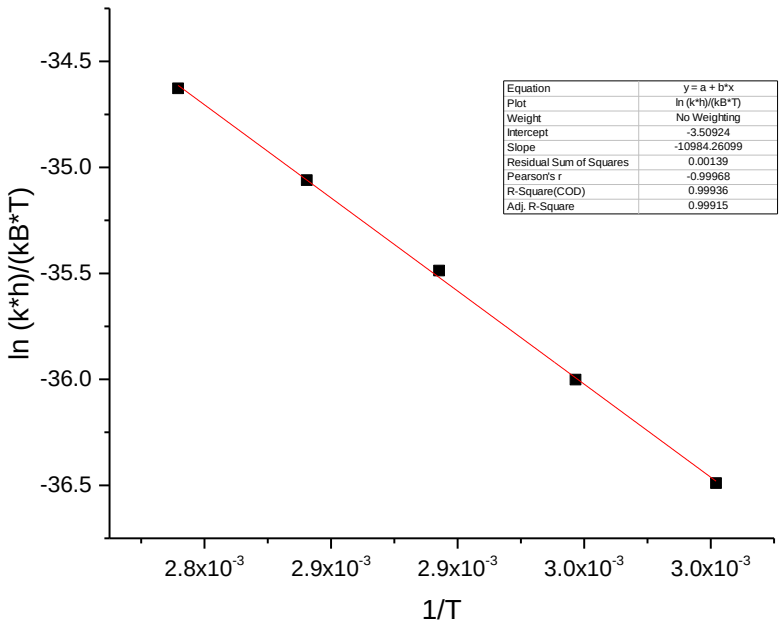

Figure S48: Eyring plot analysis of Z_M-**8** to Z_S-**8** monitoring decrease in absorption at λ = 400 nm in toluene at 60, 65, 70, 75 and 80 °C.

Table S10: Activation parameters of Z_M-**8** to Z_S-**8** at 20 °C.

$\Delta G^{\ddagger}$ (kcal mol^{-1})	23.9 ± 0.1
$\Delta H^{\ddagger}$ (kcal mol^{-1})	21.8 ± 0.3
$\Delta S^{\ddagger}$ (cal K^{-1} mol^{-1})	–7.0 ± 0.9
$t_{1/2}$	20 h

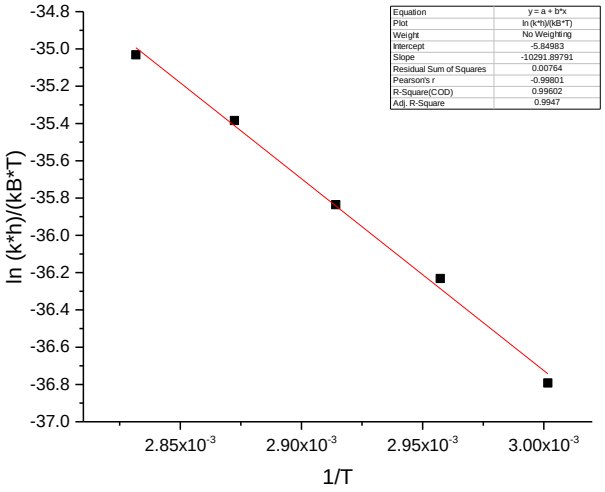

Figure S49: Eyring plot analysis of Z_M-**9** to Z_S-**9** monitoring decrease in absorption at λ = 400 nm in toluene at 60, 65, 70, 75 and 80 °C.

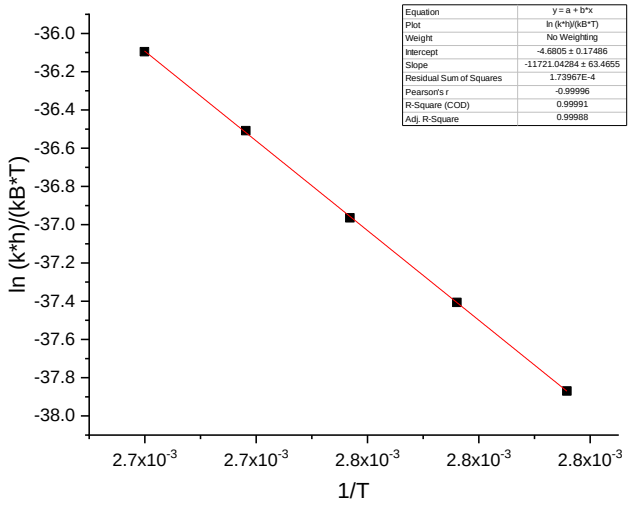

Figure S50: Eyring plot analysis of E_M-**9** to E_S-**9** monitoring decrease in absorption at λ = 400 nm in toluene at 80, 85, 90, 95 and 100 °C.

Table S11: Activation parameters of **9** at 20 °C

	Z_M-**9** → Z_S-**9**	E_M-**9** → E_S-**9**
$\Delta G^{‡}$ (kcal mol^{-1})	23.9 ± 0.4	26.02 ± 0.08
$\Delta H^{‡}$ (kcal mol^{-1})	20.5 ± 0.7	23.3 ± 0.1
$\Delta S^{‡}$ (cal K^{-1} mol^{-1})	–12 ± 2	–9.3 ± 0.3
$t_{1/2}$	20 h	33 d

9. Quantum yield determination

Chemical actinometry

A modification of a standard protocol was applied for the determination of the photon flux.[11,12] An aqueous H_2SO_4 solution (0.05 M) containing freshly recrystallised $K_3[Fe(C_2O_4)_3]$ (41 mM, 2 mL, 1 cm quartz cuvette) was irradiated at 20 °C for a given period of time in the dark with a 365 nm LED. The solution was then diluted with 1.0 mL of an aqueous H_2SO_4 solution (0.5 M) containing phenanthroline (1 g/L) and NaOAc (122.5 g/L) and left to react for 10 min. The absorption at λ = 510 nm was measured and compared to an identically prepared non-irradiated sample. The concentration of $[Fe(phenanthroline)_3]^{2+}$ complex was calculated using its molar absorptivity (ε = 11100 M^{-1} cm^{-1}) and considering the dilution. The quantity of Fe^{2+} ions expressed in mol was plotted versus time (expressed in seconds, s) and the slope, obtained by linear fitting the data points to the equation y = ax + b, equals the rate of formation of the Fe^{2+} ion at the given wavelength. This rate can be converted into the photon flux (I) by dividing it by the quantum yield of $[Fe(phenanthroline)_3]^{2+}$ complex at 365 nm (Φ^{365nm} = 121%)[13] and by the probability of photon absorption at 365 nm of the Fe^{3+} complex (approximated to 1 as we were working in the total absorption regime). The obtained molar photon flux was I = 4.21 × 10^{-8} mol s^{-1}.

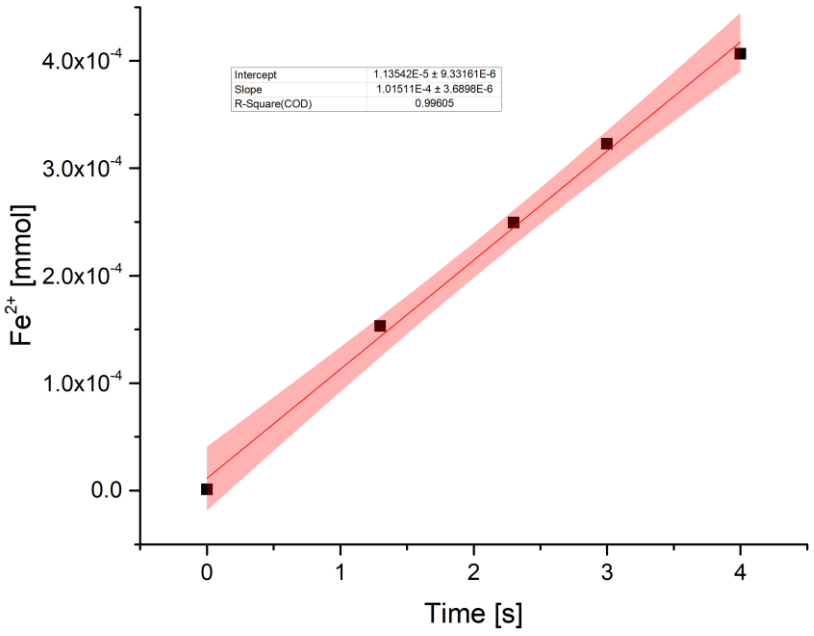

Figure S51: Linear fitting of the Fe^{2+} moles generated upon irradiation at different irradiation times with the associated confidence interval (95%). The fitting afforded a molar photon flux I = 4.21 x 10^{-8} mol s^{-1}.

Quantum yield determination

For motors **1**-**3**, obtaining a direct quantum yield of isomerisation is challenging, due to the prohibitive THI barriers between the stable and metastable states meaning the concentration of the metastable states at room temperature is negligible. Considering this, we measure two approximated quantum yields directly connecting the E_S and Z_S states of these motors, and neglecting the contribution of the metastable states. This gives the following approximation:

$$\boldsymbol{E}_{\mathbf{S}} \underset{QY_{ZE}}{\overset{QY_{EZ}}{\rightleftharpoons}} \boldsymbol{Z}_{\mathbf{S}}$$

Solutions of the E_S states in toluene (~ 2×10^{-5} M) were irradiated with a 365 nm LED, and the spectra were collected over the first *ca.* 100 s of constant irradiation (until PSS was reached), following the evolution of the absorption maximum. UV-Vis spectra were recorded every second. Baseline corrections were carried out to account for baseline drifting, and the absorbance at 365 nm over the course of the measurement was extracted. The data was subsequently processed in Copasi, using a method outlined by Stranius & Börjesson, based on Equation 1:[11]

$$\frac{d[A]}{dt} = -\frac{QY_{EZ} \cdot I \cdot \beta_E(t)}{N_A \cdot V} + \frac{QY_{ZE} \cdot I \cdot \beta_Z(t)}{N_A \cdot V}$$

Equation 1

Where I is the molar photon flux (previously determined by chemical actinometry), N_A is Avogadro's constant, V is the total volume of the irradiated solution (2 mL), and β is the fraction of photons absorbed by either the E_S or Z_S isomer, a number that is determined using the PSS ratio and the corresponding molar extinction coefficients for each isomer. This equation was used to determine the approximated QYs in the cases of motors **1**–**3**.

For motors **4**–**9**, the same method was used to calculate the QYs of the stable and their corresponding metastable states, which are thermally stable at room temperature ($t_{1/2}$ = hours – days). UV-Vis measurements were taken every 5 s over the first *ca.* 150 – 500 s of constant irradiation until PSS was reached, extracting the absorbance at 365 nm. In these cases, there is no approximation required and the QYs of all isomers in the rotation cycle could be determined:

$$\boldsymbol{E}_{\mathbf{S}} \underset{QY_{backwards}}{\overset{QY_{forwards}}{\rightleftharpoons}} \boldsymbol{Z}_{\mathbf{M}} \qquad\qquad \boldsymbol{Z}_{\mathbf{S}} \underset{QY_{backwards}}{\overset{QY_{forwards}}{\rightleftharpoons}} \boldsymbol{E}_{\mathbf{M}}$$

The data shown in Tables S12 and S13 show averaged QY data over three separate runs. Figures S52 – S80 show individual representative runs of these data.

Table S12: Molar extinction coefficients at 365 nm, PSS at 365 nm and QYs for motors **1**–**3**. The bold QY is the average of the measurements repeated in triplicate.

Motor	$\varepsilon_{(Es)}$ ($M^{-1}\,cm^{-1}$)	$\varepsilon_{(Zs)}$ ($M^{-1}\,cm^{-1}$)	PSS_{365} (E_S : Z_S)	QY (%) $E_S \rightarrow Z_S$	QY (%) $Z_S \rightarrow E_S$
1	9700	12400	75:25	6.01 6.57 7.58 **6.72**	14.94 17.89 17.84 **16.89**
2	8200	9000	64:36	9.36 9.80 11.24 **10.13**	14.53 14.66 15.55 **14.91**
3	10100	10600	69:31	11.45 9.97 10.94 **10.79**	23.21 20.92 23.30 **22.48**

Table S13: Molar extinction coefficients at 365 nm, PSS at 365 nm and QYs for motors **4**–**9**. The bold QY is the average of the measurements repeated in triplicate.

Motor	$\varepsilon_{(Es)}$	$\varepsilon_{(Zm)}$	PSS_{365} (E_S : Z_M)	QY $E_S \rightarrow Z_M$	QY $Z_M \rightarrow E_S$	$\varepsilon_{(Zs)}$	$\varepsilon_{(Em)}$	PSS_{365} (Z_S : E_M)	QY (%) $Z_S \rightarrow E_M$	QY (%) $E_M \rightarrow Z_S$
4	8600	7200	17:83	6.82 6.19 6.95 **6.65**	1.67 1.42 1.63 **1.57**	11000	7100	12:88	13.21 12.56 12.90 **12.89**	3.09 3.14 3.09 **3.11**
5	7700	6900	23:77	5.22 5.31 5.49 **5.34**	1.34 2.09 1.83 **1.76**	8800	6400	10:90	11.39 11.29 11.63 **11.44**	1.46 1.55 1.69 **1.57**
6	8400	4800	12:88	7.37 7.11 7.34 **7.27**	1.91 1.78 1.40 **1.70**	8400	5100	10:90	19.24 16.33 18.98 **18.18**	3.28 2.80 4.03 **3.37**
7	9300	6000	16:84	3.95 4.00 3.83 **3.93**	0.99 1.42 1.11 **1.17**	8200	5900	5:95	17.42 18.06 17.80 **17.76**	1.33 1.42 1.40 **1.38**
8	10600	6900	17:83	3.35 3.13 3.13 **3.20**	0.85 1.05 0.98 **0.96**	8700	-	7:92	-	-
9	10100	4800	18:82	3.18 3.13 3.22 **3.18**	1.32 1.54 1.34 **1.40**	8300	6200	2:98	16.32 15.63 16.41 **16.12**	0.82 1.12 0.76 **0.90**

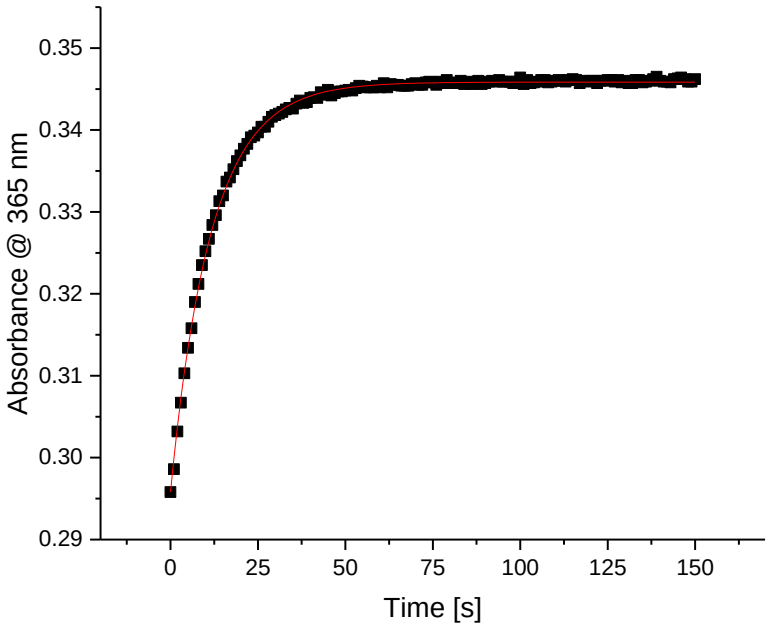

Figure S52: Change in absorbance at 365 nm during the irradiation of ***E*S-1** with a 365 nm LED. The red line represents the fit as exported from Copasi.

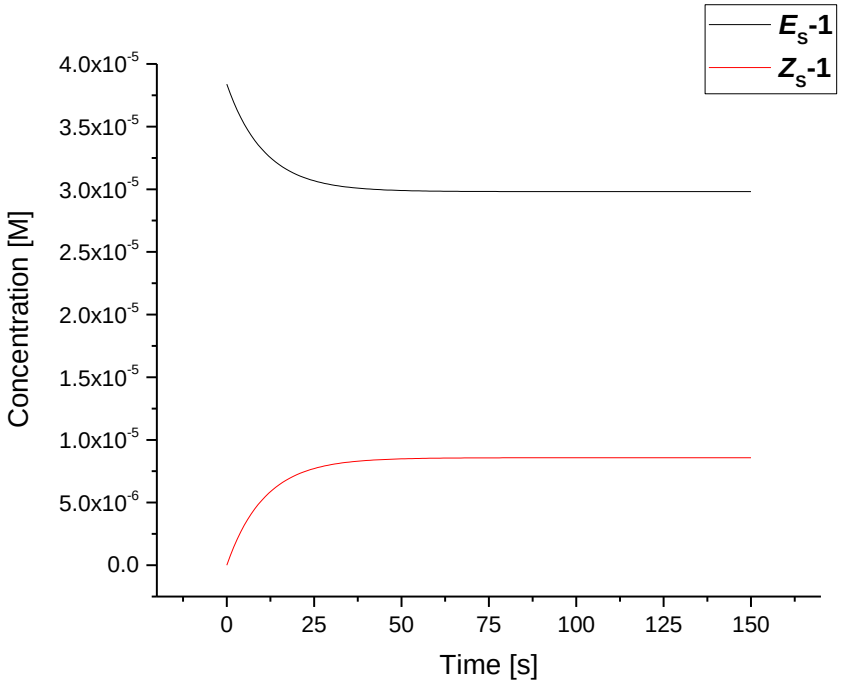

Figure S53: Evolution of the concentration of ***E*S-1** and ***Z*S-1** during the irradiation of ***E*S-1** with a 365 nm LED as fitted by Equation 1 in Copasi.

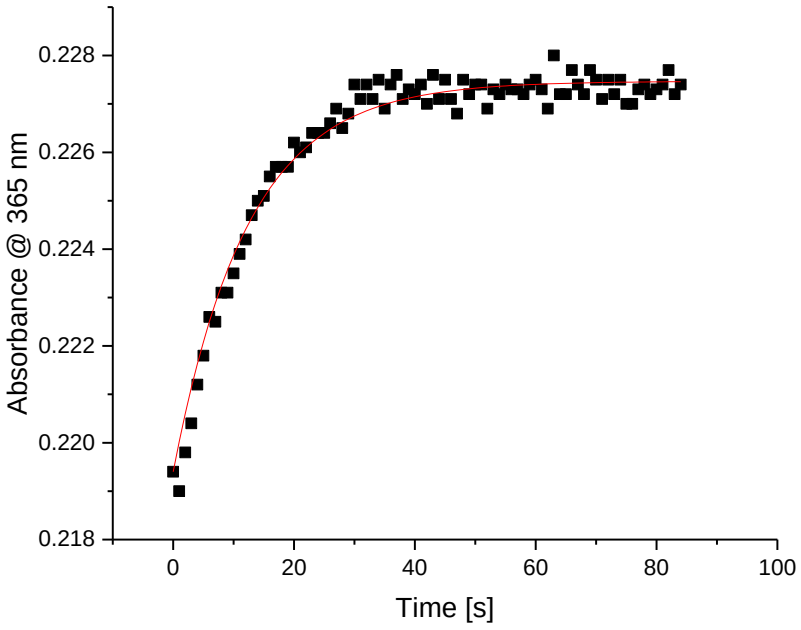

e

Figure S54: Change in absorbance at 365 nm during the irradiation of ***E*S-2** with a 365 nm LED. The red line represents the fit as exported from Copasi.

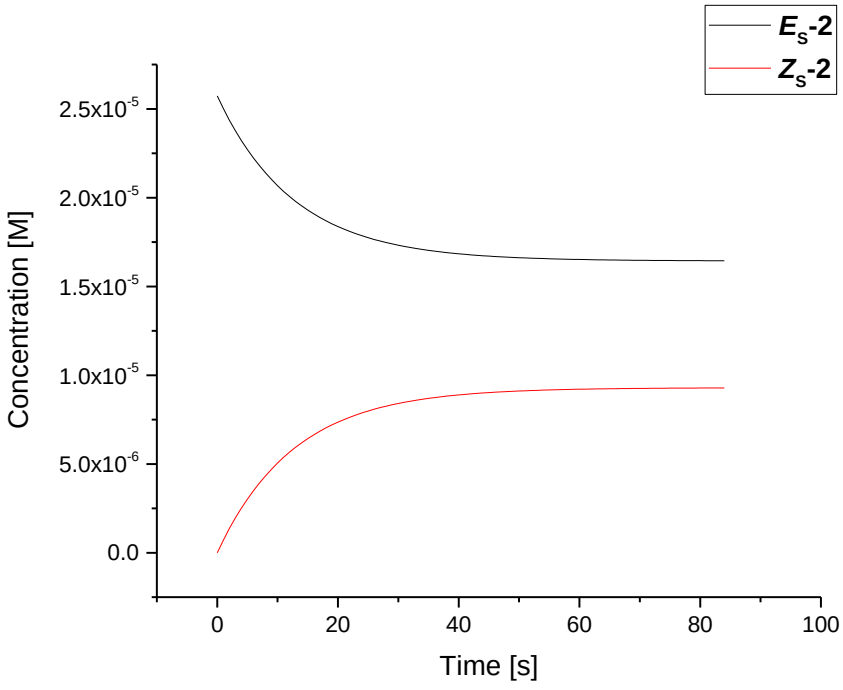

Figure S55: Evolution of the concentration of ***E*S-2** and ***Z*S-2** during the irradiation of ***E*S-2** with a 365 nm LED as fitted by Equation 1 in Copasi.

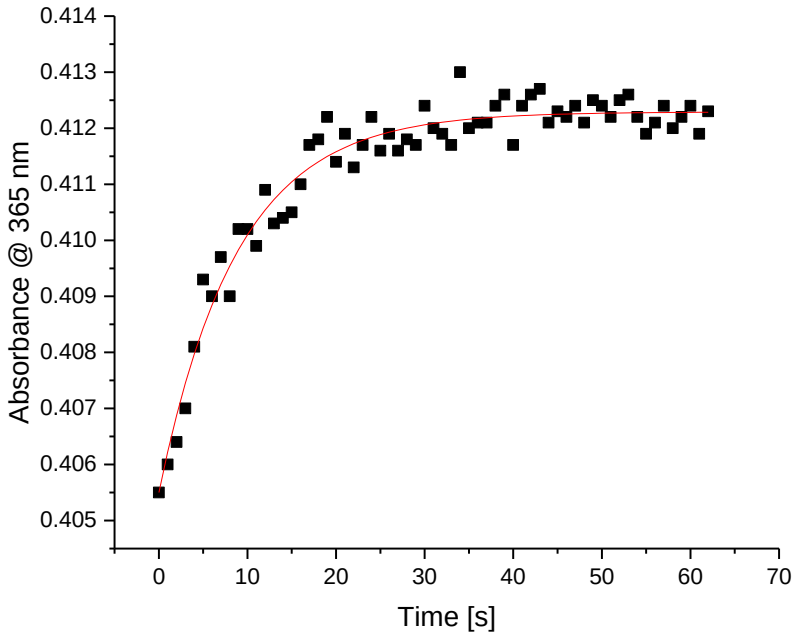

Figure S56: Change in absorbance at 365 nm during the irradiation of ***E*S-3** with a 365 nm LED. The red line represents the fit as exported from Copasi.

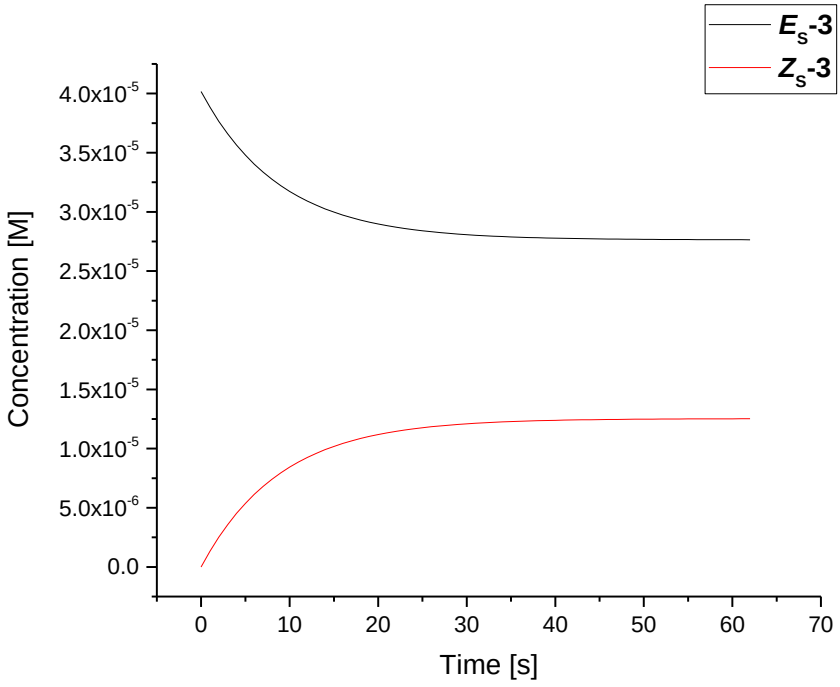

Figure S57: Evolution of the concentration of ***E*S-3** and ***Z*S-3** during the irradiation of ***E*S-3** with a 365 nm LED as fitted by Equation 1 in Copasi.

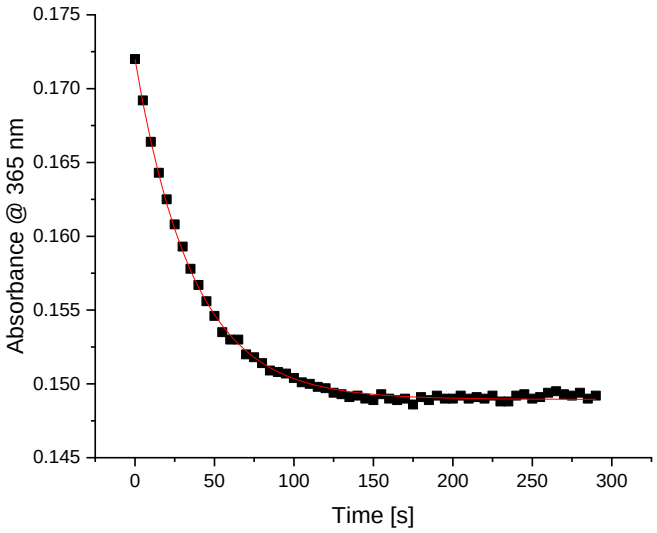

Figure S58: Change in absorbance at 365 nm during the irradiation of ***E*S-4** with a 365 nm LED. The red line represents the fit as exported from Copasi.

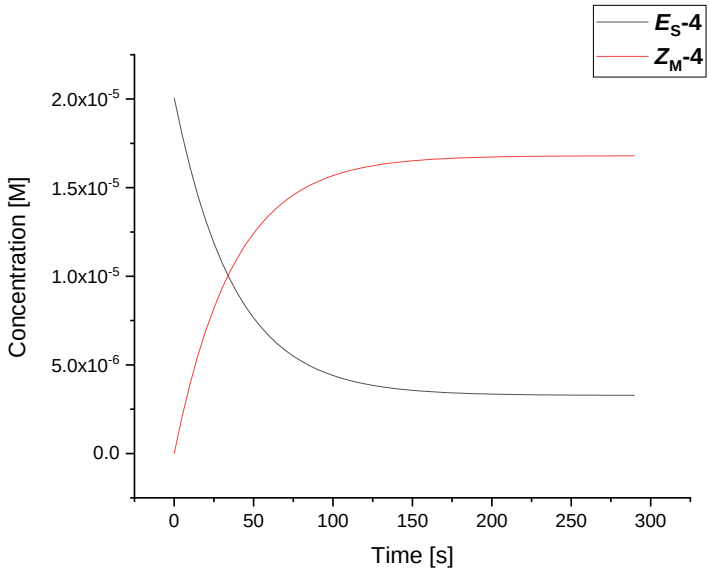

Figure S59: Evolution of the concentration of ***E*S-4** and ***Z*M-4** during the irradiation of ***E*S-4** with a 365 nm LED as fitted by Equation 1 in Copasi.

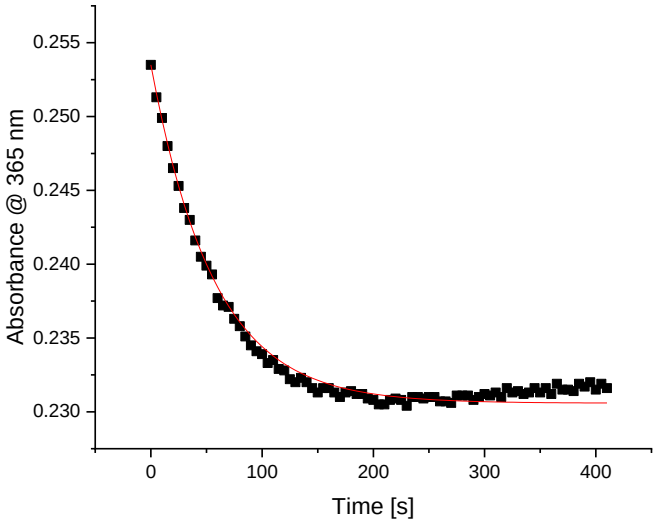

Figure S60: Change in absorbance at 365 nm during the irradiation of ***E*S-5** with a 365 nm LED. The red line represents the fit as exported from Copasi.

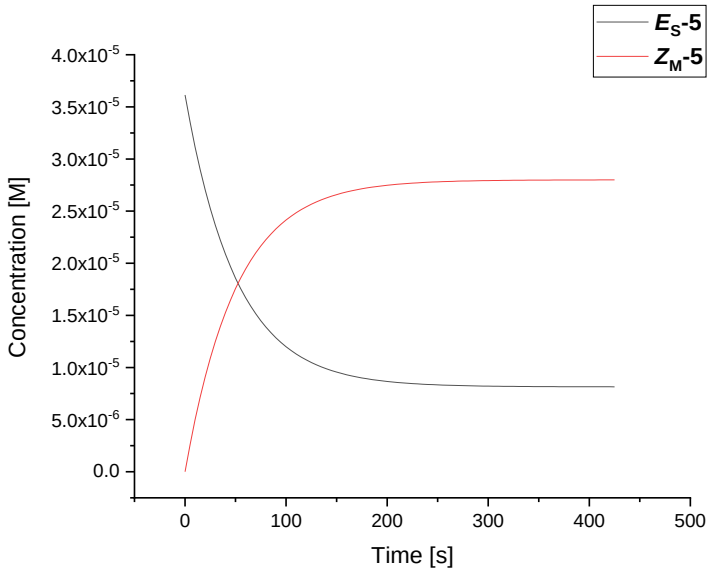

Figure S61: Evolution of the concentration of ***E*S-5** and ***Z*M-5** during the irradiation of ***E*S-5** with a 365 nm LED as fitted by Equation 1 in Copasi.

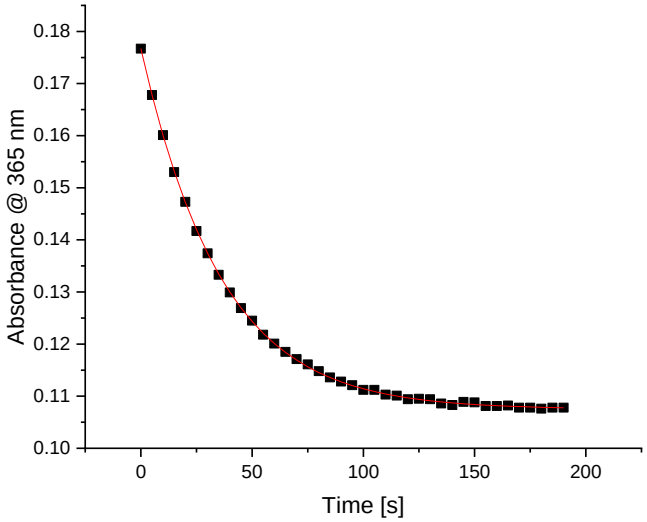

Figure S62: Change in absorbance at 365 nm during the irradiation of ***E*S-6** with a 365 nm LED. The red line represents the fit as exported from Copasi.

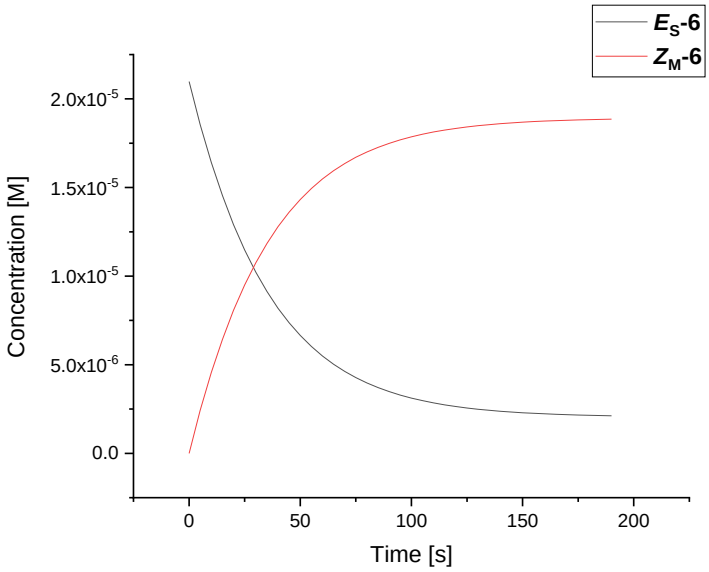

Figure S63: Figure 64: Evolution of the concentration of ***E*S-6** and ***Z*M-6** during the irradiation of ***E*S-6** with a 365 nm LED as fitted by Equation 1 in Copasi.

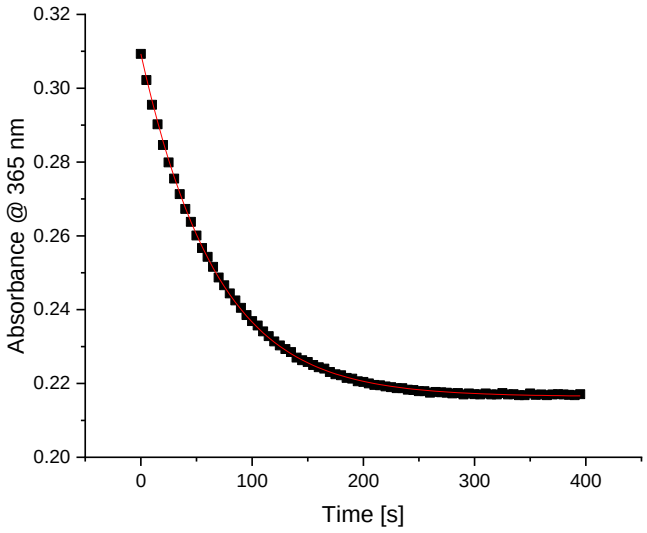

Figure S65: Change in absorbance at 365 nm during the irradiation of ***E*S-7** with a 365 nm LED. The red line represents the fit as exported from Copasi.

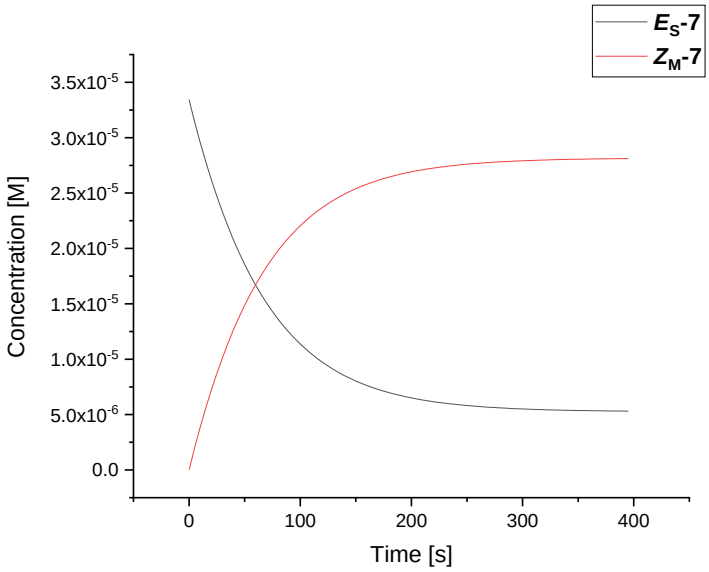

Figure S66: Evolution of the concentration of ***E*S-7** and ***Z*M-7** during the irradiation of ***E*S-7** with a 365 nm LED as fitted by Equation 1 in Copasi.

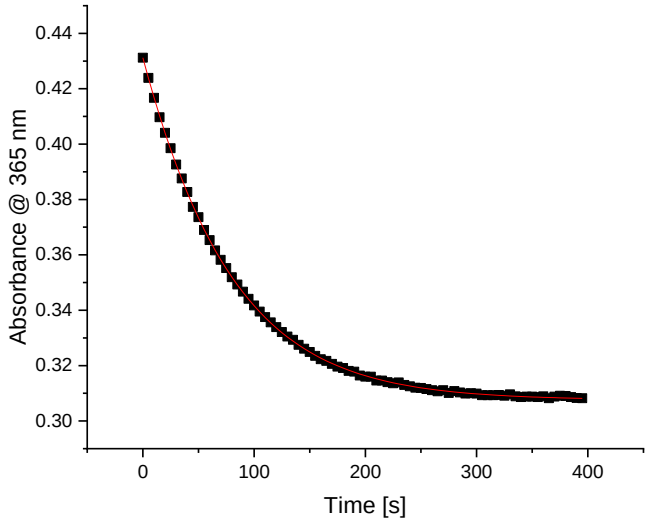

Figure S67: Change in absorbance at 365 nm during the irradiation of ***E*S-8** with a 365 nm LED. The red line represents the fit as exported from Copasi.

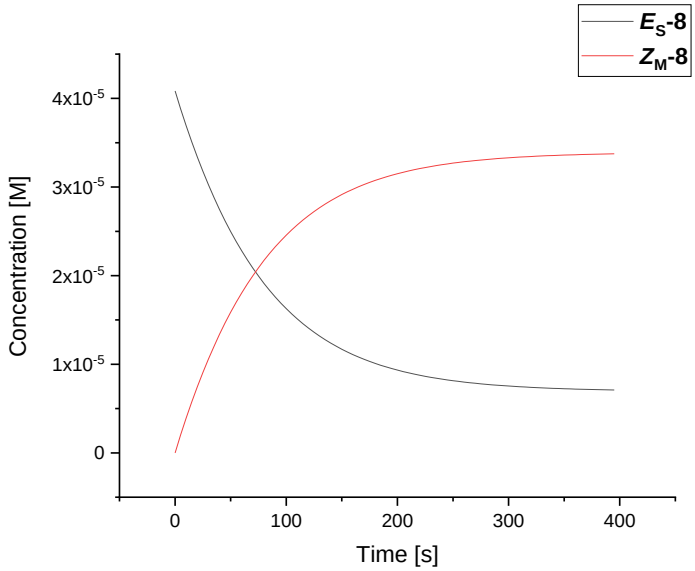

Figure S68: Evolution of the concentration of ***E*S-8** and ***Z*M-8** during the irradiation of ***E*S-8** with a 365 nm LED as fitted by Equation 1 in Copasi.

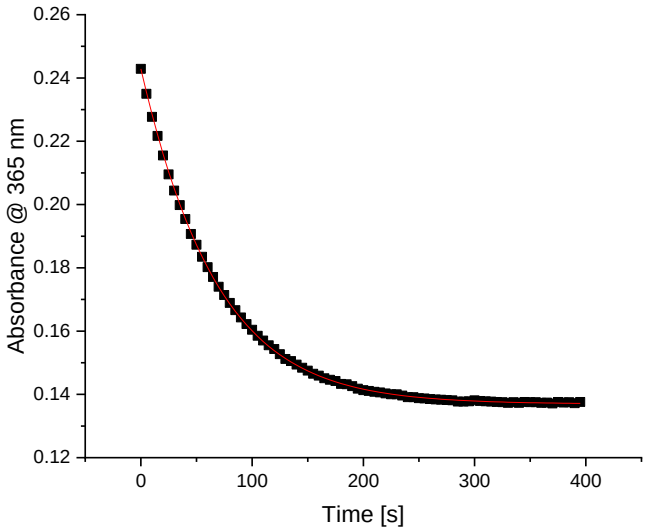

Figure S69: Change in absorbance at 365 nm during the irradiation of ***E*S-9** with a 365 nm LED. The red line represents the fit as exported from Copasi.

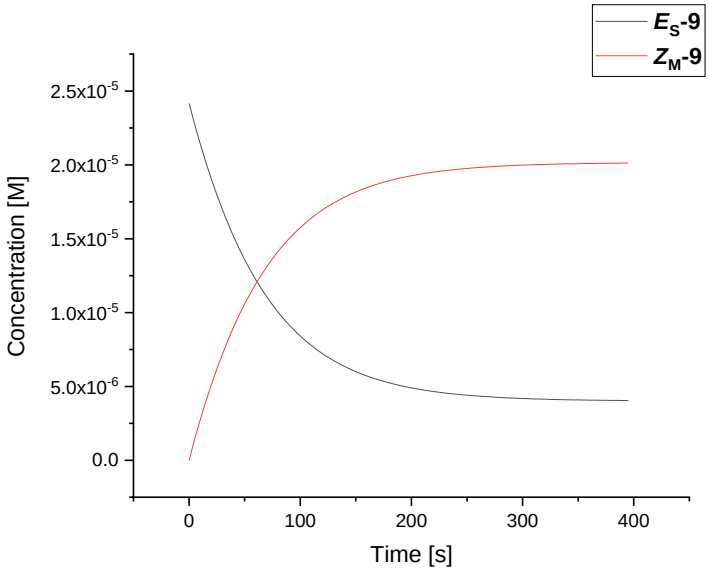

Figure S70: Evolution of the concentration of ***E*S-9** and ***Z*M-9** during the irradiation of ***E*S-9** with a 365 nm LED as fitted by Equation 1 in Copasi.

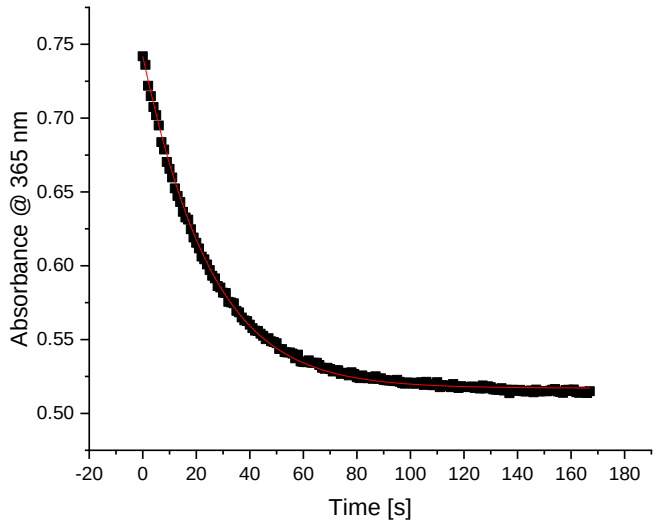

Figure S71: Change in absorbance at 365 nm during the irradiation of ***Z*S-4** with a 365 nm LED. The red line represents the fit as exported from Copasi.

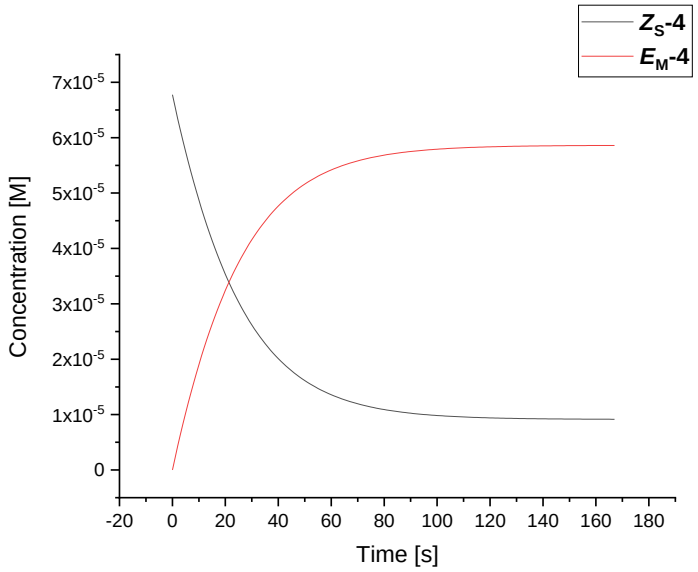

Figure S72: Evolution of the concentration of ***Z*S-4** and ***E*M-4** during the irradiation of ***Z*S-4** with a 365 nm LED as fitted by Equation 1 in Copasi.

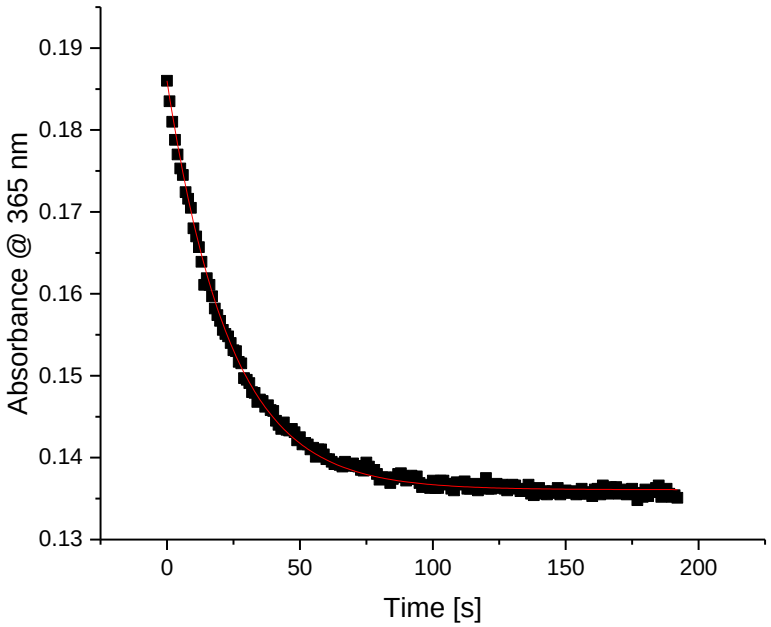

Figure S73: Change in absorbance at 365 nm during the irradiation of ***Z*S-5** with a 365 nm LED. The red line represents the fit as exported from Copasi.

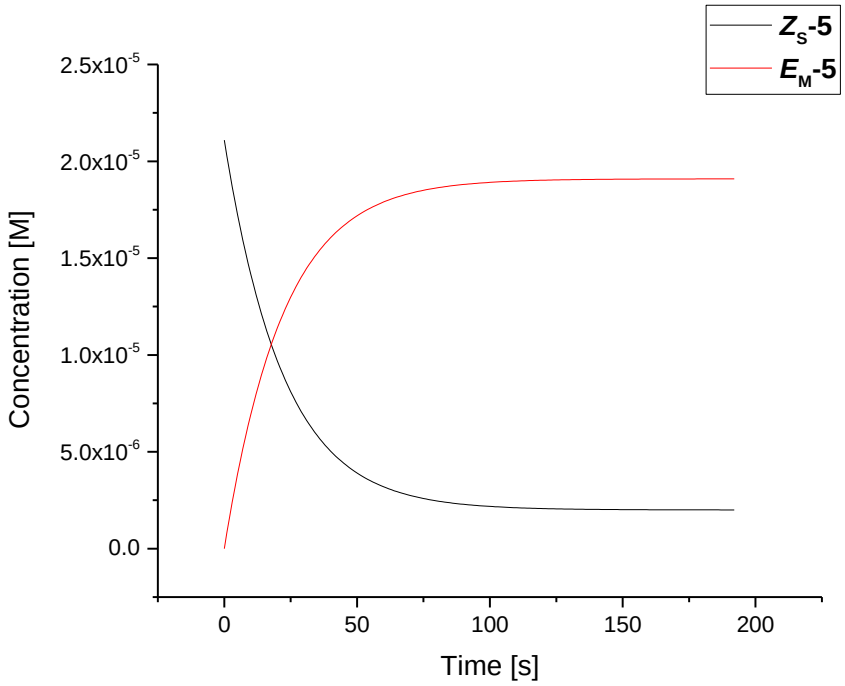

Figure S74: Evolution of the concentration of ***Z*S-5** and ***E*M-5** during the irradiation of ***Z*S-5** with a 365 nm LED as fitted by Equation 1 in Copasi.

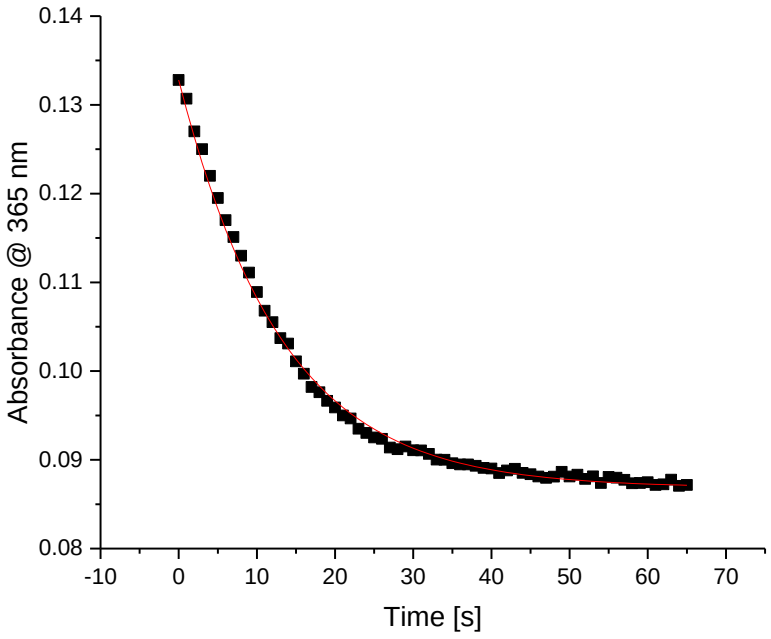

Figure S75: Change in absorbance at 365 nm during the irradiation of ***Z*S-6** with a 365 nm LED. The red line represents the fit as exported from Copasi.

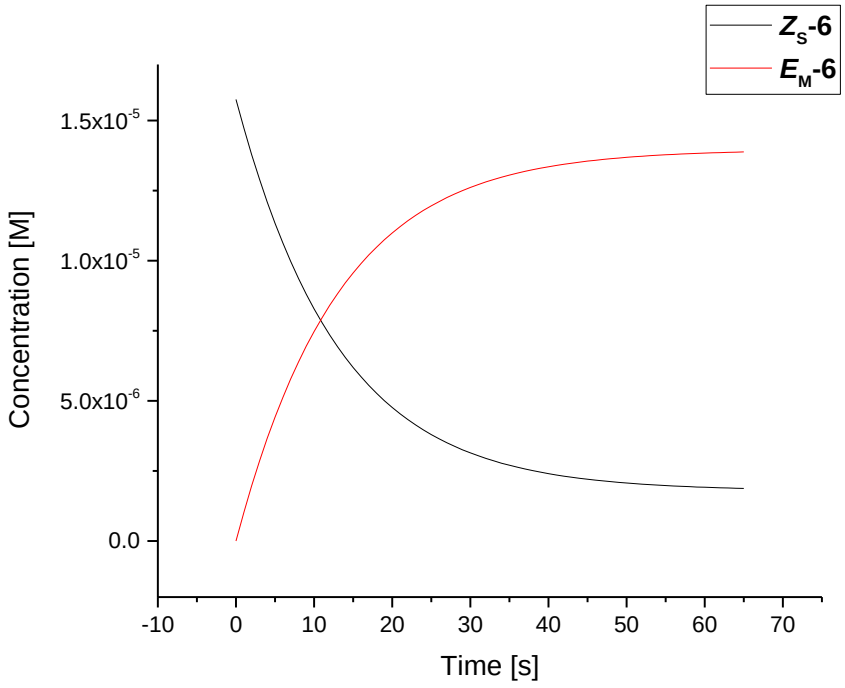

Figure S76: Evolution of the concentration of ***Z*S-6** and ***E*M-6** during the irradiation of ***Z*S-6** with a 365 nm LED as fitted by Equation 1 in Copasi.

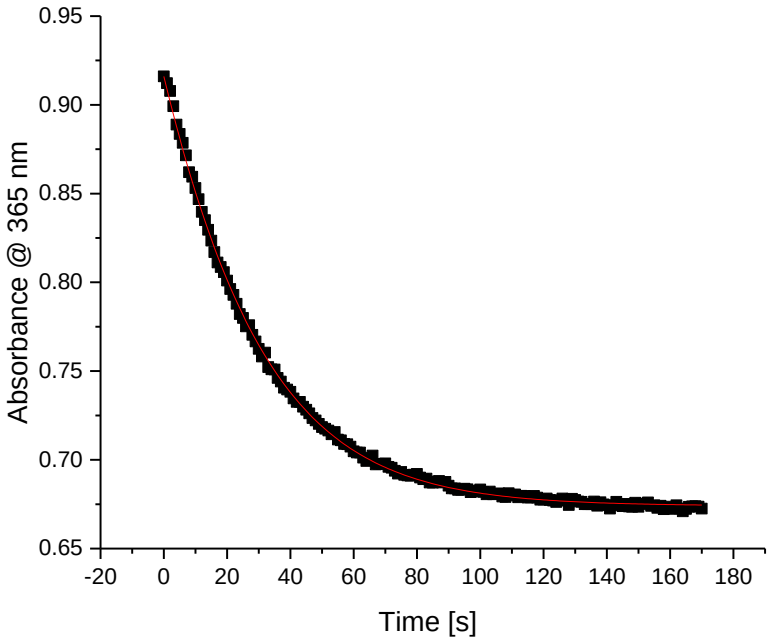

Figure S77: Change in absorbance at 365 nm during the irradiation of ***Z*S-7** with a 365 nm LED. The red line represents the fit as exported from Copasi.

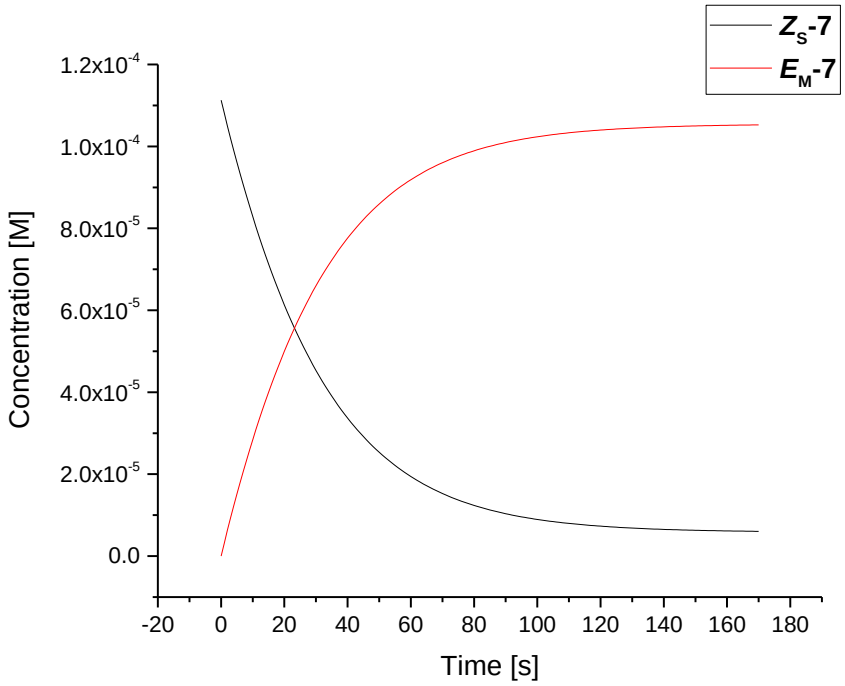

Figure S78: Evolution of the concentration of ***Z*S-7** and ***E*M-7** during the irradiation of ***Z*S-7** with a 365 nm LED as fitted by Equation 1 in Copasi.

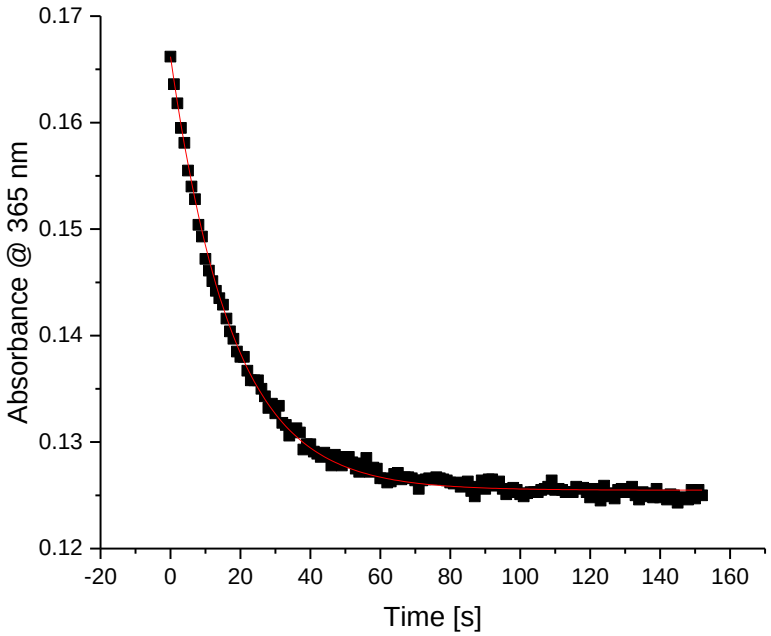

Figure S79: Change in absorbance at 365 nm during the irradiation of ***Z*S-9** with a 365 nm LED. The red line represents the fit as exported from Copasi.

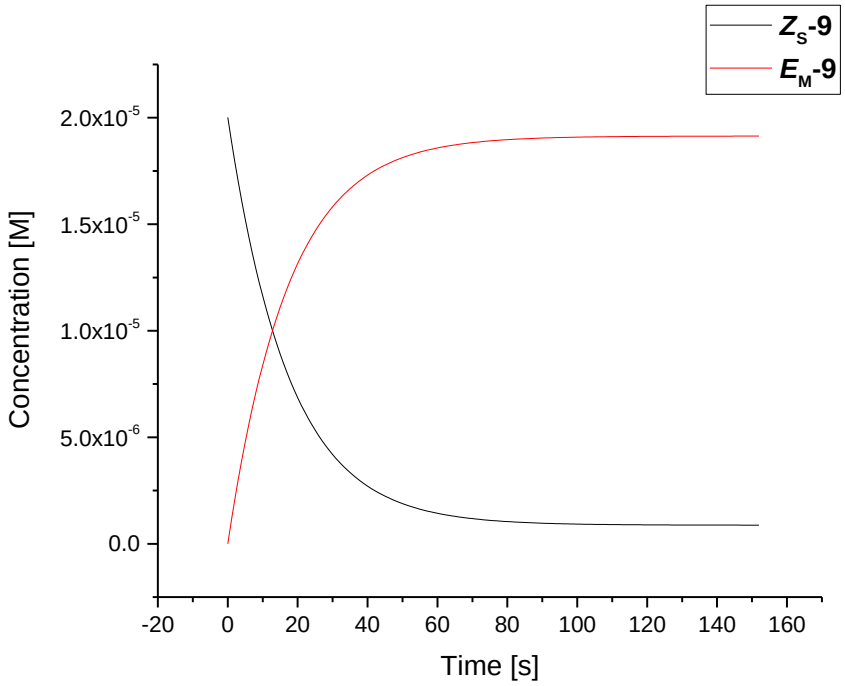

Figure S80: Evolution of the concentration of ***Z*S-9** and ***E*M-9** during the irradiation of ***Z*S-9** with a 365 nm LED as fitted by Equation 1 in Copasi.

10. Computational analysis and simulated UV-Vis spectra

Computational analysis was carried out using the Gaussian 16, Rev B.01 software package.[14] Motors **1**–**9**, were optimised considering all of the states involved in the thermal helix inversion step of a molecular motor (stable and metastable, connected by the THI transition state) for both configurations, *E* and *Z* (Figure S81). All xyz coordinates are provided as additional supplementary files.

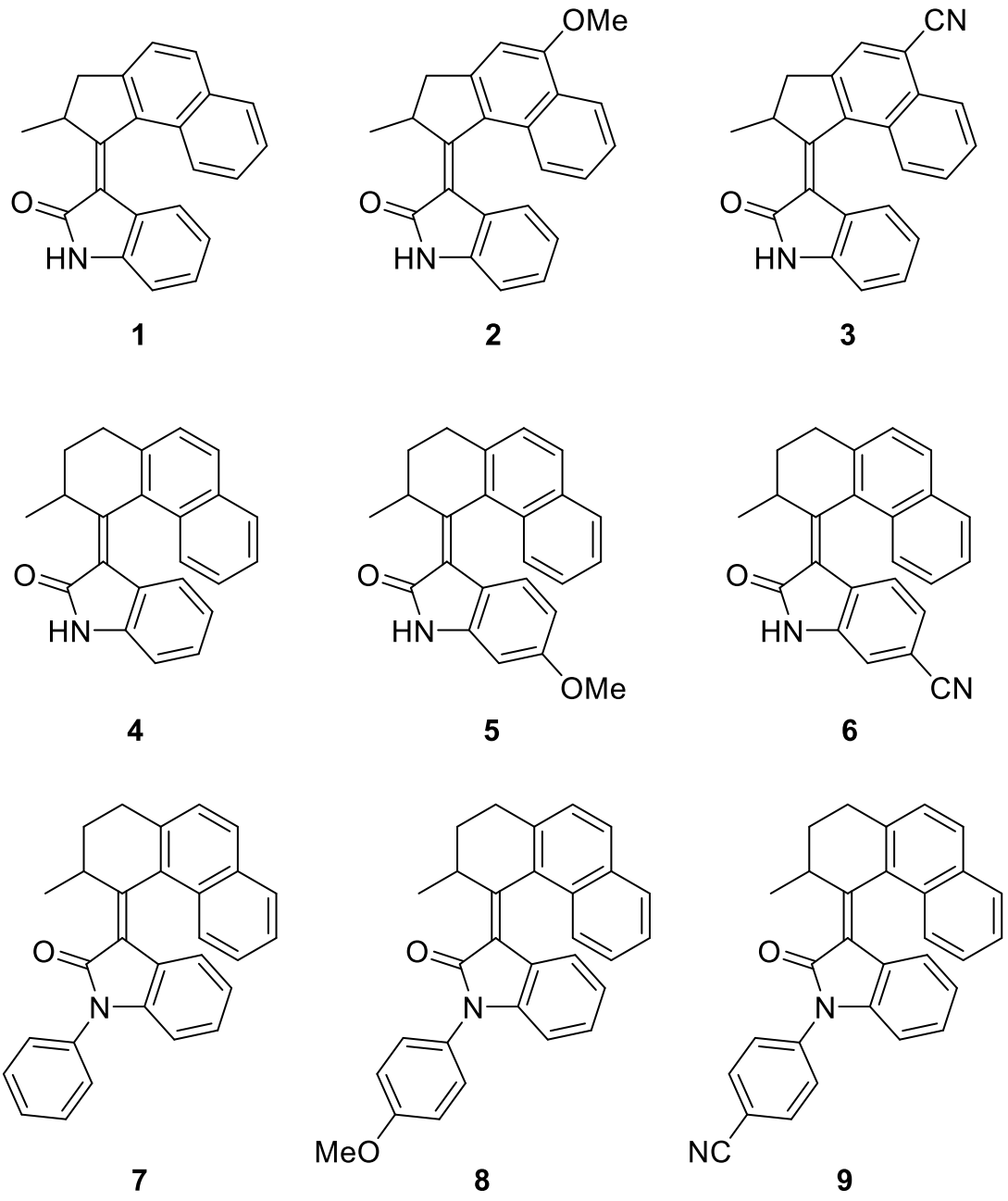

Figure S81

The configurations of each compound were numbered accordingly (e.g. ***E*$_S$-1** for the stable *E* configuration of motor **1**) and their structures optimised with DFT at the ωB97X-D/def2-SVP level. All stationary points were confirmed to be such due to the number of imaginary frequencies obtained after the Hessian calculation (0 for minima, 1 for transition states). The optimised structures of motor **1** are shown in Figure S82 as representative examples.

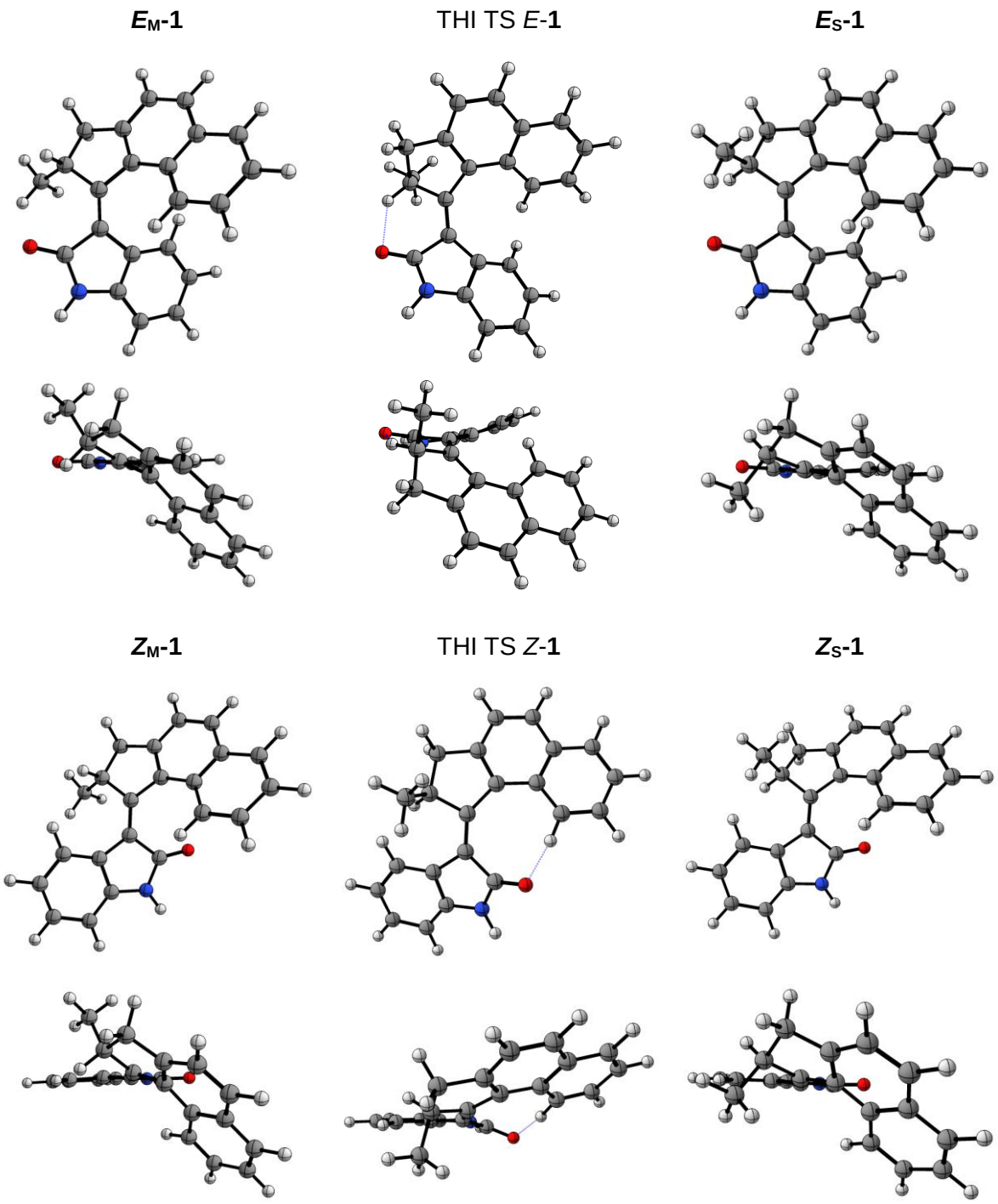

Figure S82: DFT optimised structures of minima and THI transition states of motor **1**. Side view (top row) and top view (bottom row)

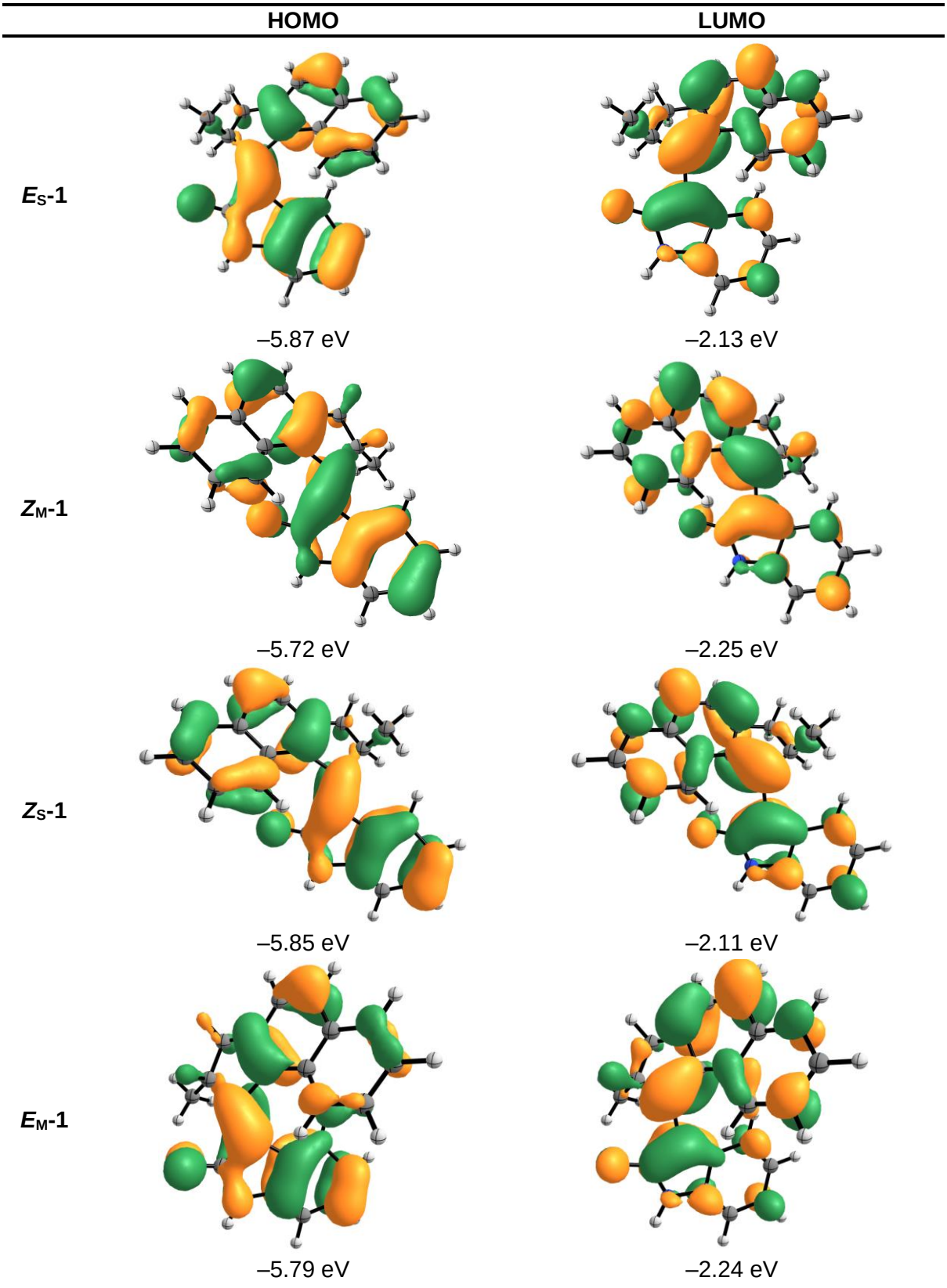

Figure S83: Frontier orbitals of motor **1** (PBE0/def2-TZVP, SMD = DMSO)

	HOMO	LUMO
E_S-4	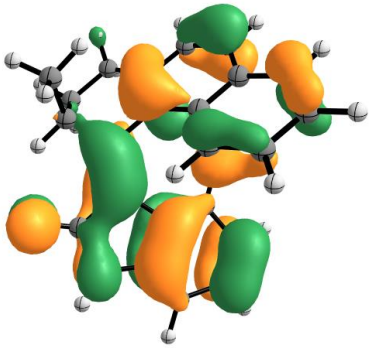 –5.98 eV	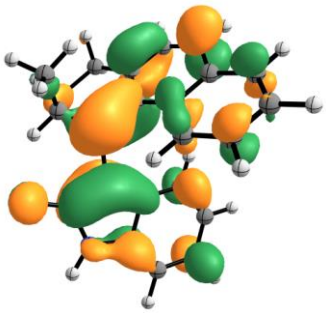 –1.96 eV
Z_M-4	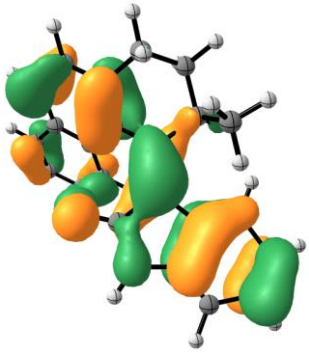 –5.87 eV	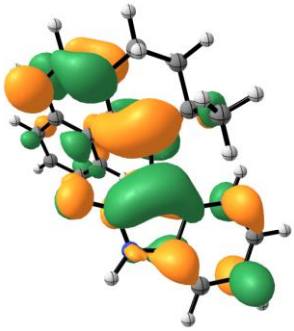 –1.99 eV
Z_S-4	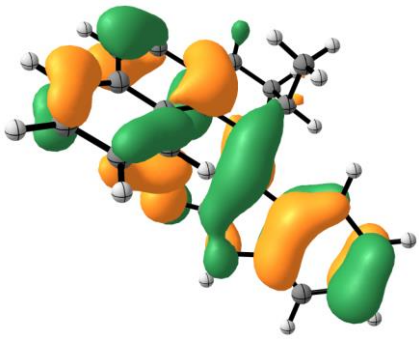 –5.88 eV	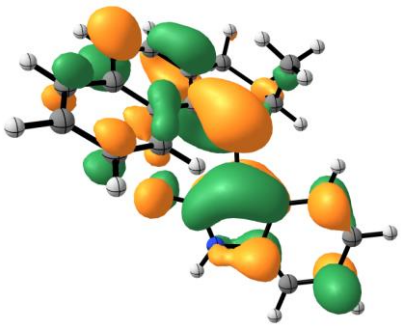 –0.96 eV
E_M-4	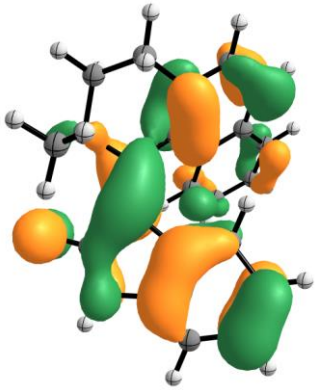 –5.77 eV	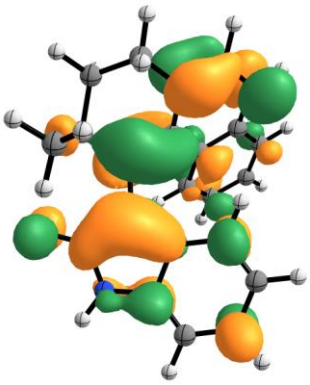 –2.17 eV

Figure S84: Frontier orbitals of motor **4** (PBE0/def2-TZVP, SMD = DMSO).

	HOMO	LUMO
E_S-7	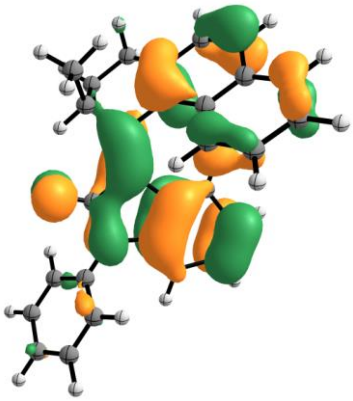	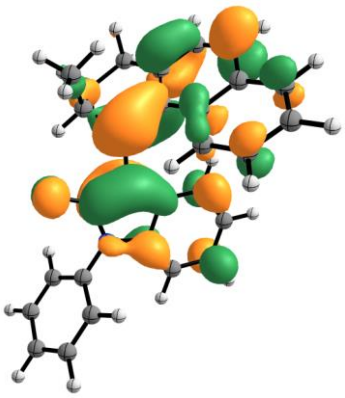
	–5.98 eV	–2.03 eV
Z_M-7	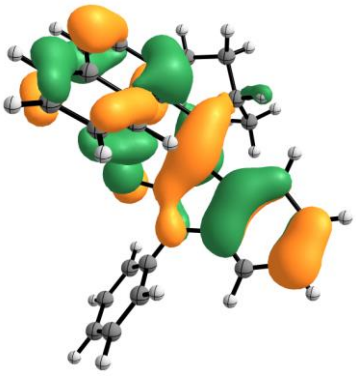	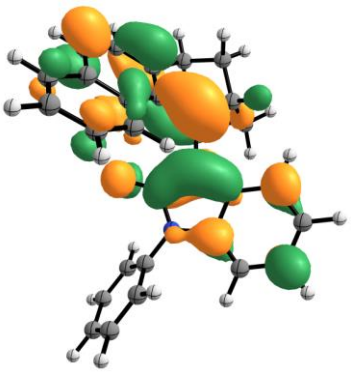
	–5.78 eV	–2.23 eV
Z_S-7	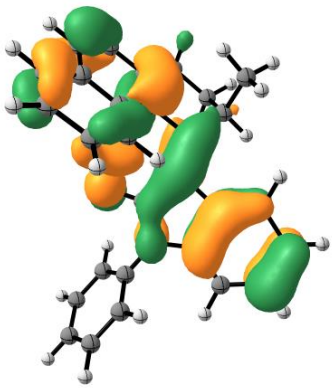	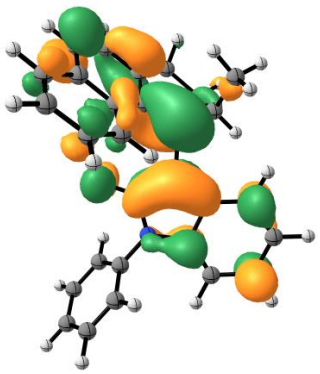
	–5.88 eV	–2.05 eV
E_M-7	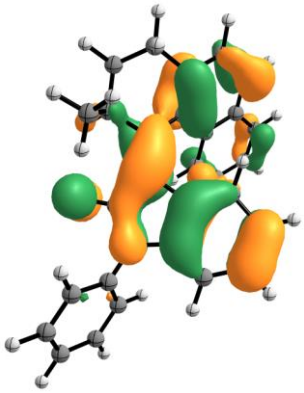	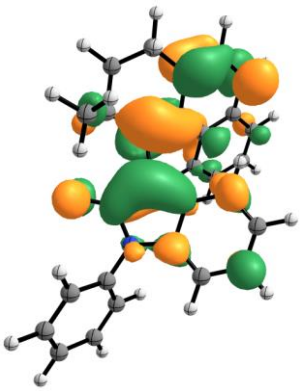
	–5.89 eV	–2.25 eV

Figure S85: Frontier orbitals of motor **7** (PBE0/def2-TZVP, SMD = DMSO).

Solvent corrections were introduced by means of the SMD model, affording results in CH_2Cl_2, DMSO and MeOH. The Gibbs free energy correction was applied to all the electronic energies, the results are shown in Table S14. The UV-Vis spectra of stable and metastable states were calculated at the TD-DFT PBE0/def2-TZVP level over the first 15 singlet transitions on the geometries calculated in the different solvents. The simulated UV-Vis for stable and metastable compounds are reported below (top left CH_2Cl_2, top right DMSO, bottom MeOH). The calculated absorption maxima for the first excited state are tabulated in Table S15.

Table S14: DFT calculated barriers for the THI steps in motors **1**–**9**.

	Gas phase		CH_2Cl_2		MeOH	
	$\Delta G^{\ddagger}_{calc}$ (*Z*) / kcal mol^{-1}	$\Delta G^{\ddagger}_{calc}$ (*E*) / kcal mol^{-1}	$\Delta G^{\ddagger}_{calc}$ (*Z*) / kcal mol^{-1}	$\Delta G^{\ddagger}_{calc}$ (*E*) / kcal mol^{-1}	$\Delta G^{\ddagger}_{calc}$ (*Z*) / kcal mol^{-1}	$\Delta G^{\ddagger}_{calc}$ (*E*) / kcal mol^{-1}
1	11.0	17.1	11.8	16.8	13.4	14.6
2	11.1	17.4	11.9	16.5	13.7	16.7
3	11.7	17.1	12.9	16.8	14.0	17.3
4	26.6	31.0	26.7	30.3	27.4	30.6
5	26.7	29.6	27.3	29.1	28.3	29.3
6	25.4	30.5	26.0	29.4	26.4	29.6
7	26.2	31.1	26.9	30.6	27.1	31.0
8	26.5	30.8	26.9	28.2	26.9	31.2
9	26.6	30.5	27.3	29.8	27.7	30.1

Table S15: DFT calculated absorption maxima for the HOMO-LUMO transition of motors **1**–**9**.

	DMSO				CH_2Cl_2				MeOH			
	E_S	Z_M	Z_S	E_M	E_S	Z_M	Z_S	E_M	E_S	Z_M	Z_S	E_M
1	412	451	412	443	413	451	412	444	410	449	410	446
2	415	451	416	447	415	451	416	447	415	451	416	447
3	452	490	448	482	451	488	446	482	446	484	443	482
4	388	440	405	430	389	441	405	430	389	440	405	428
5	401	449	412	448	401	449	412	448	402	450	413	447
6	406	457	423	441	406	459	425	441	409	456	423	441
7	396	445	410	436	397	447	411	437	397	445	410	443
8	395	444	408	435	396	446	410	437	395	445	408	433
9	396	447	410	434	397	449	412	435	398	448	412	433

***E*$_S$-1**

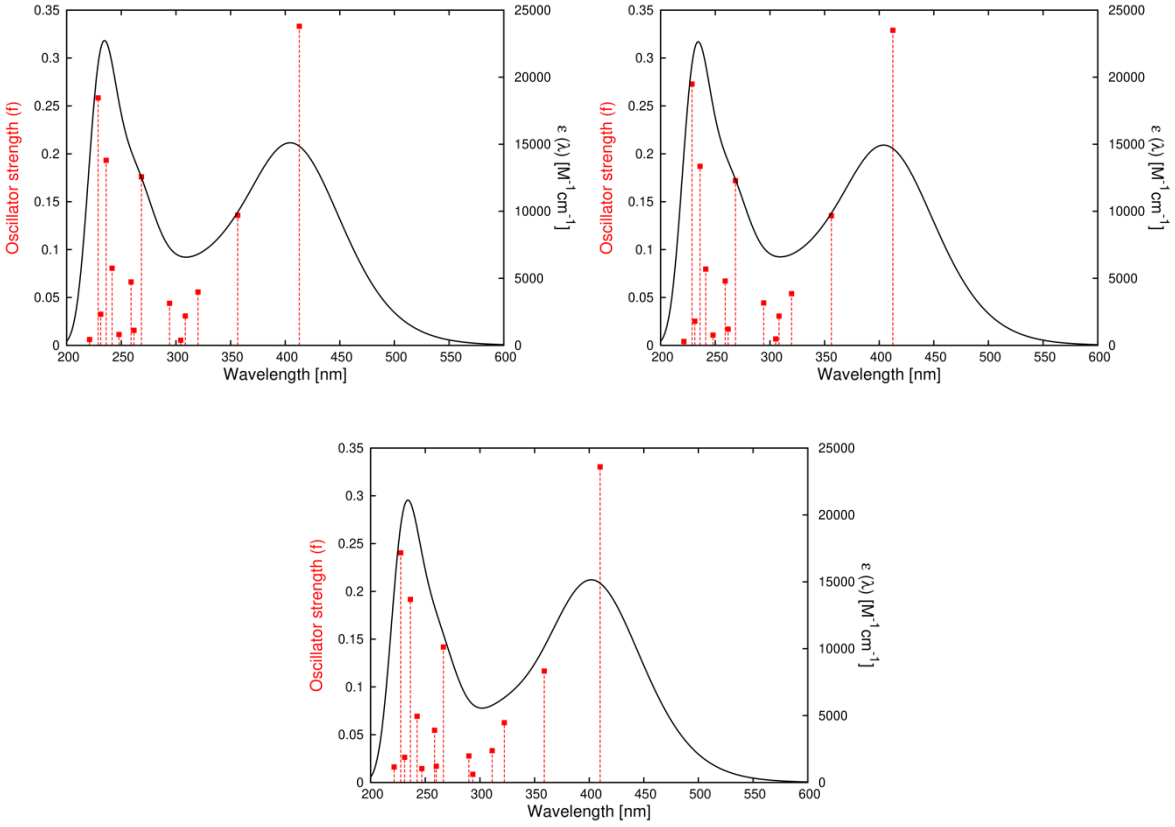
Oscillator strength (f)
ε (λ) [M^{-1}cm^{-1}]
Wavelength [nm]

***E*$_M$-1**

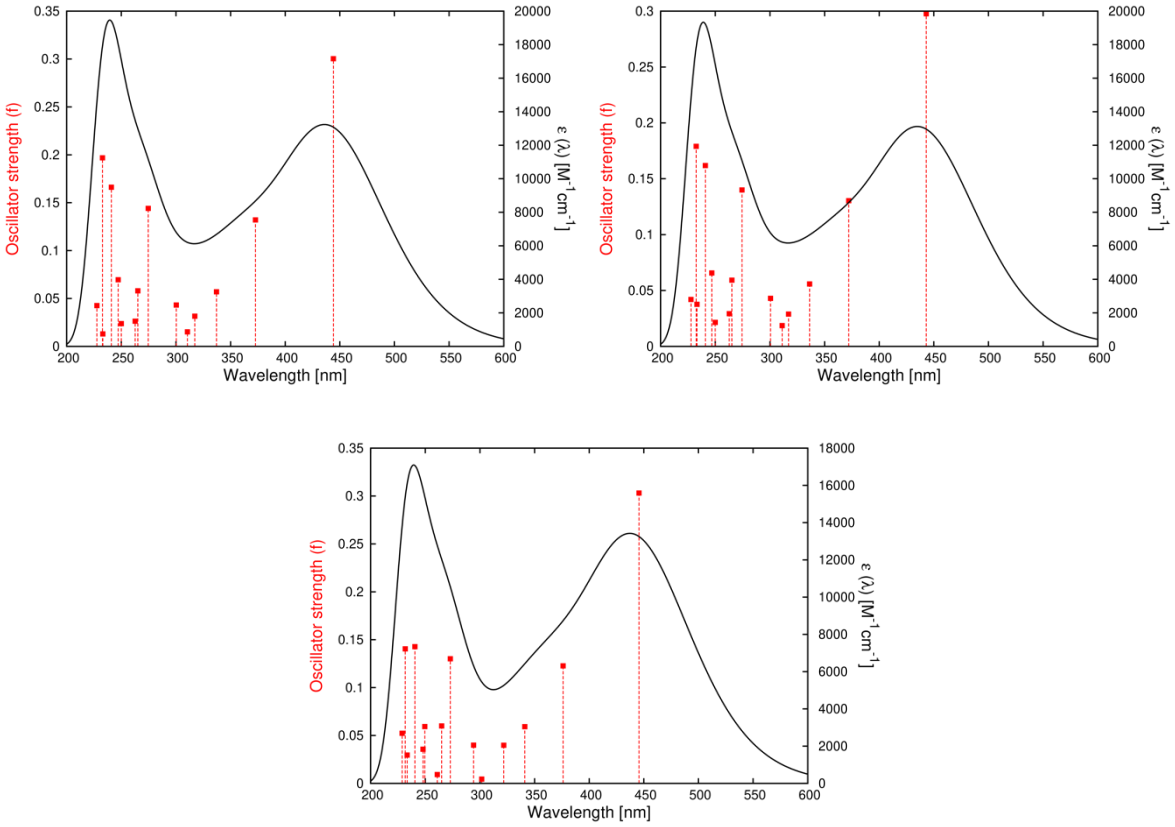
Oscillator strength (f)
ε (λ) [M^{-1}cm^{-1}]
Wavelength [nm]

Z_S-1

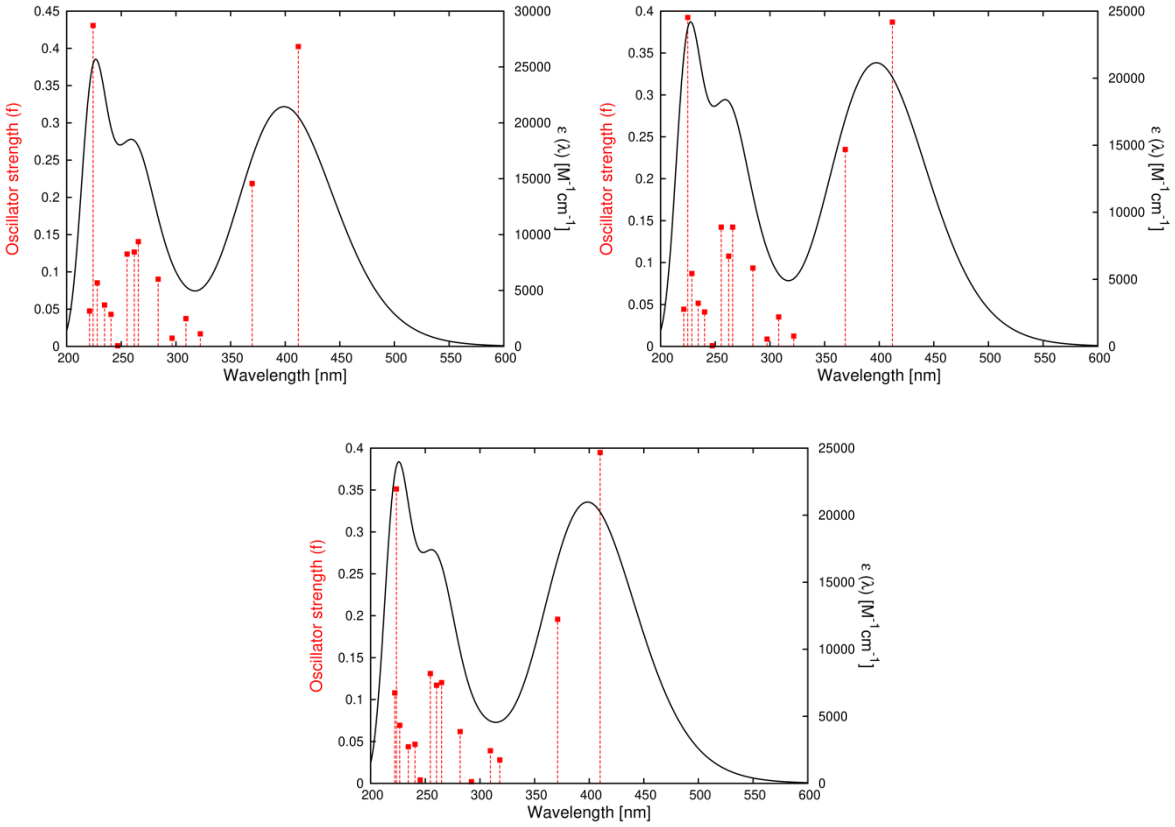
Oscillator strength (f)
ε (λ) [M-1cm-1]
Wavelength [nm]

Z_M-1

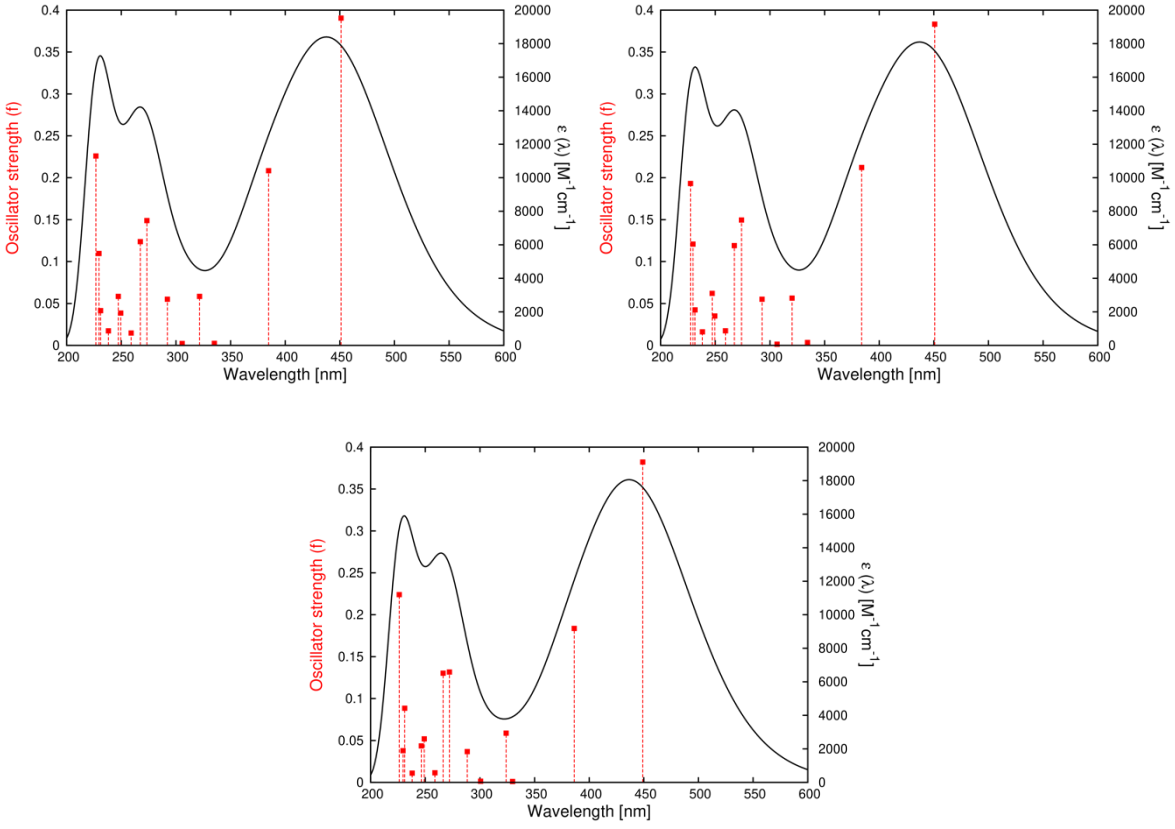
Oscillator strength (f)
ε (λ) [M-1cm-1]
Wavelength [nm]

E_S-2

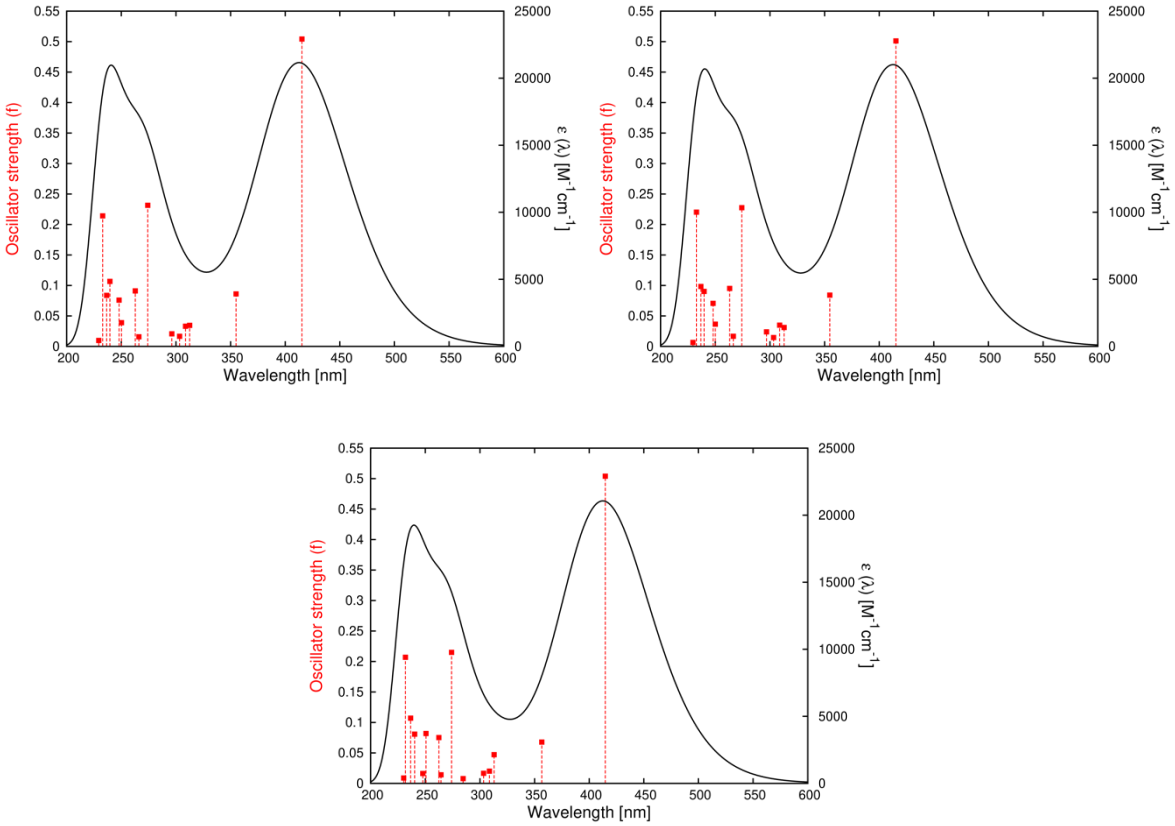
Oscillator strength (f)
ε (λ) [M-1cm-1]
Wavelength [nm]

E_M-2

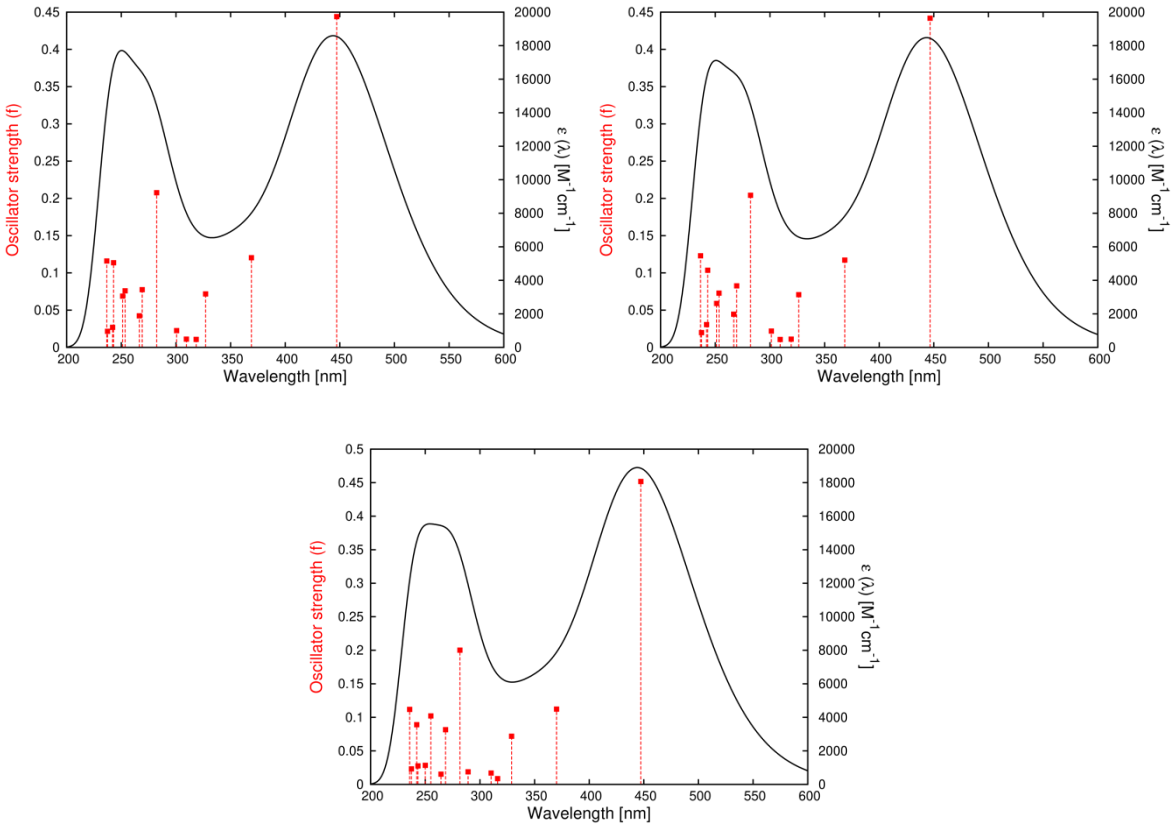
Oscillator strength (f)
ε (λ) [M-1cm-1]
Wavelength [nm]

Z_S-2

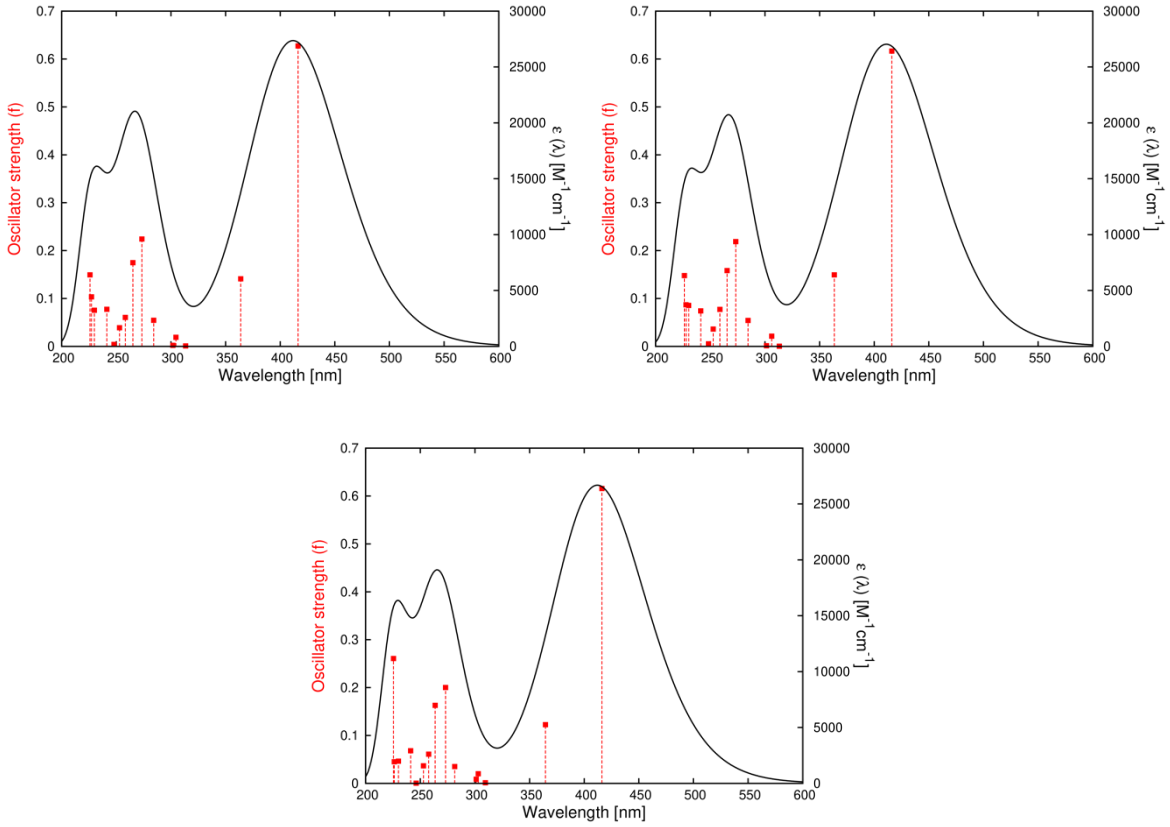
Oscillator strength (f)
ε (λ) [M-1cm-1]
Wavelength [nm]

Z_M-2

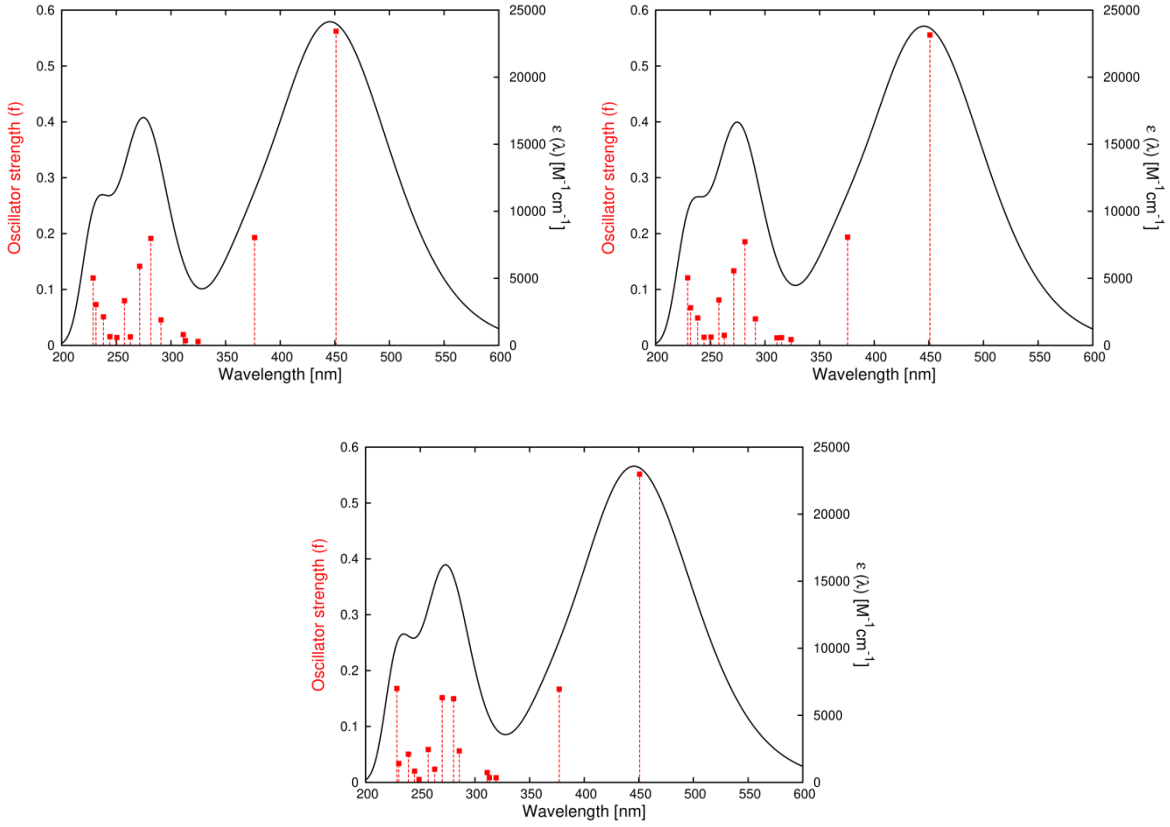
Oscillator strength (f)
ε (λ) [M-1cm-1]
Wavelength [nm]

***E*$_S$-3**

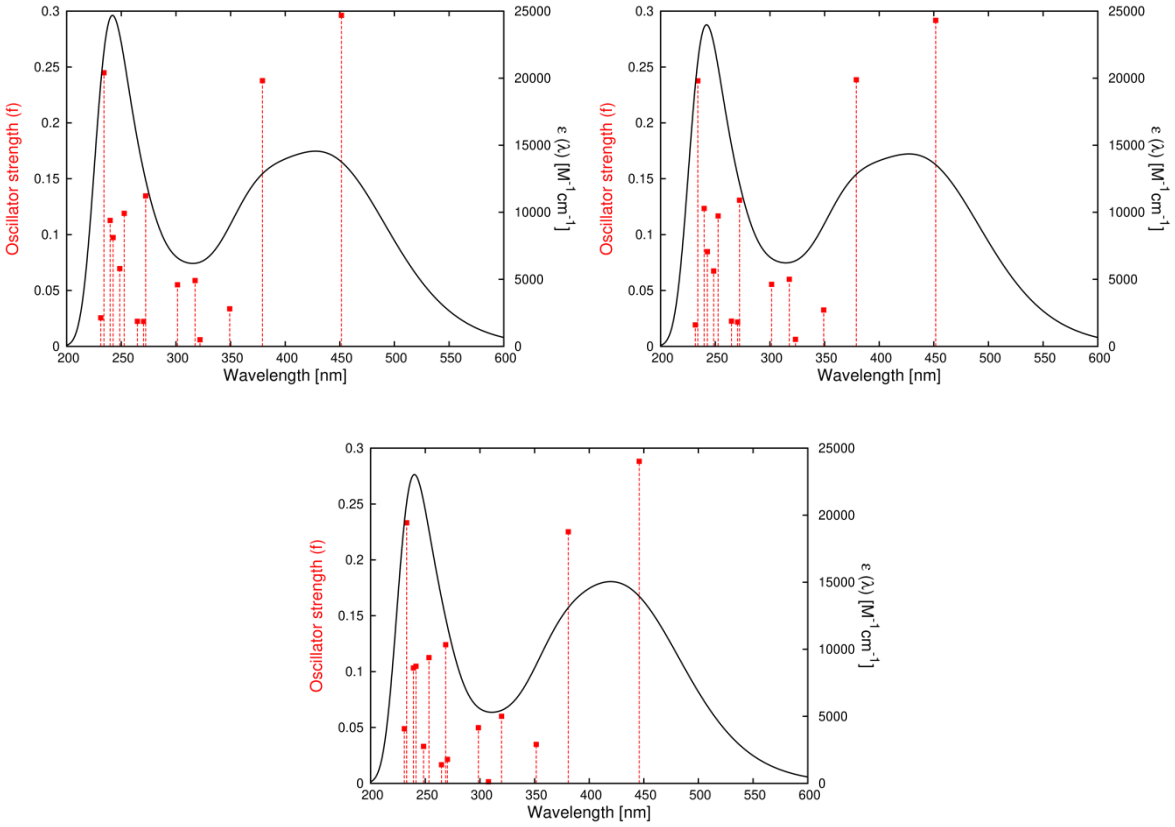
Oscillator strength (f)
ε (λ) [M^{-1}cm^{-1}]
Wavelength [nm]

***E*$_M$-3**

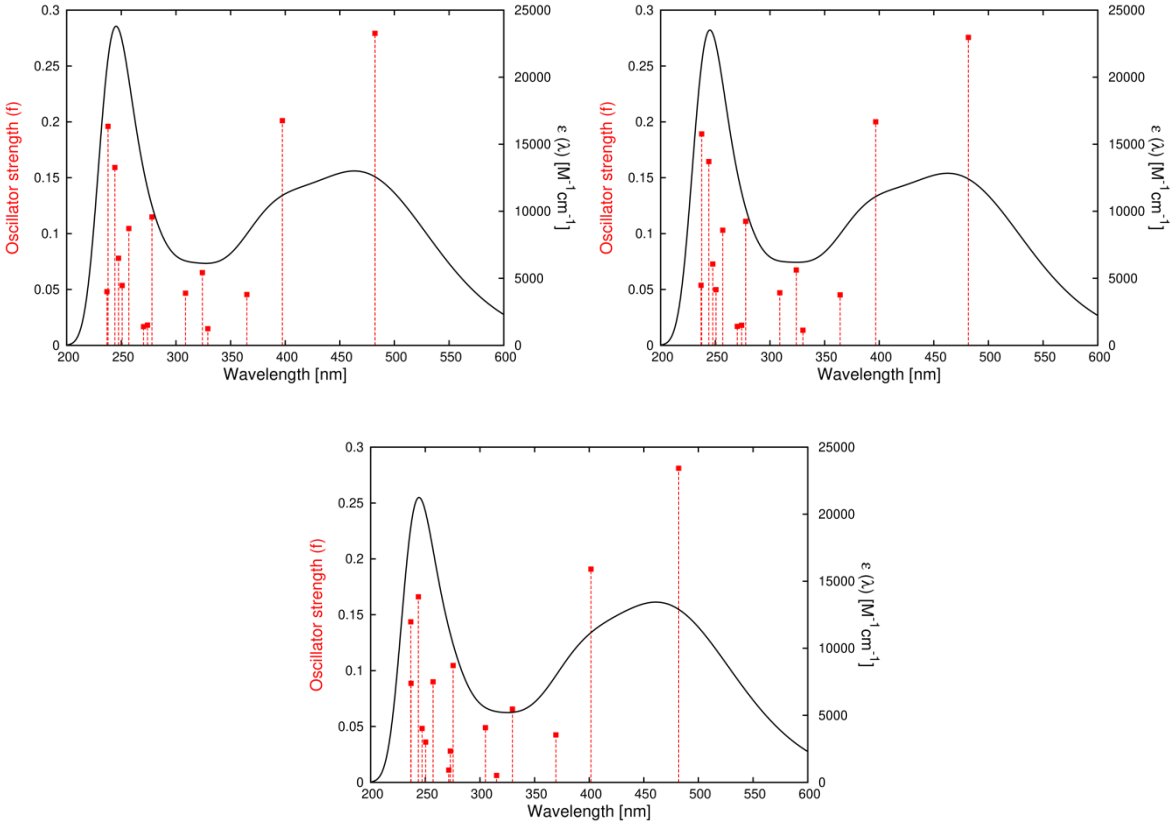
Oscillator strength (f)
ε (λ) [M^{-1}cm^{-1}]
Wavelength [nm]

Z_S-3

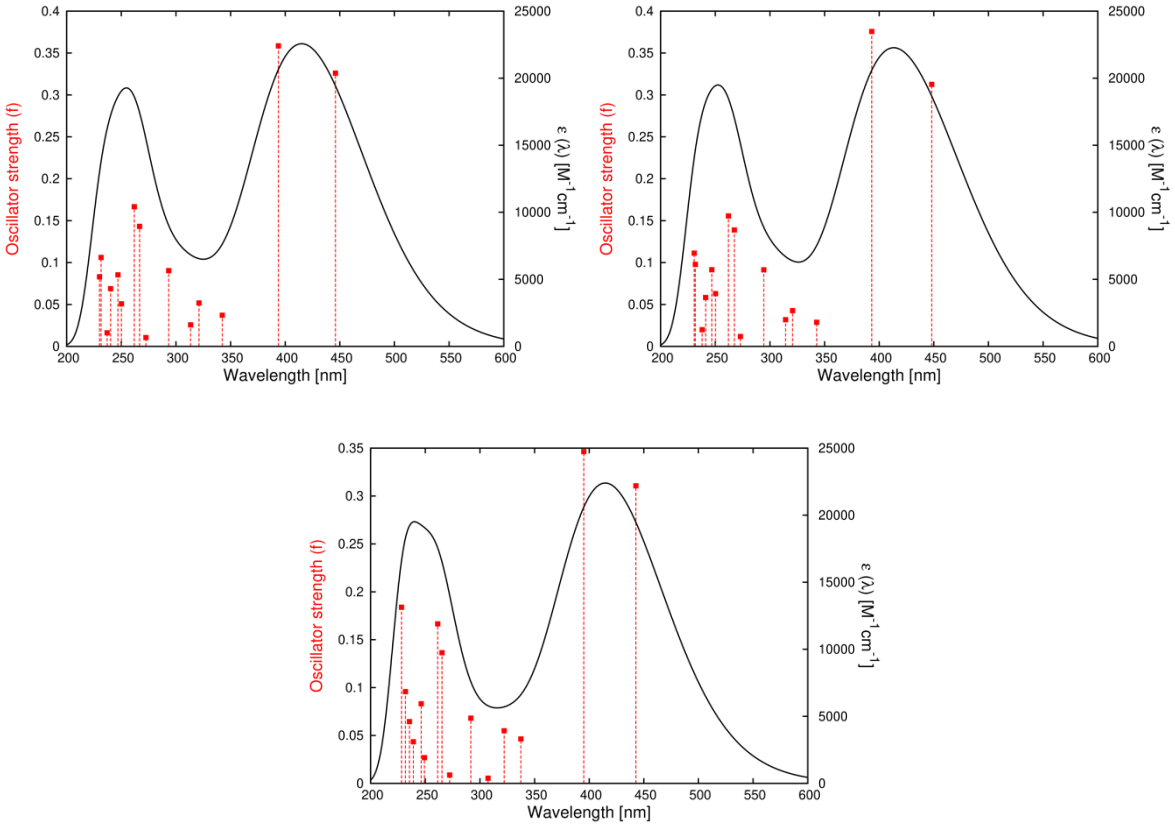
Oscillator strength (f)
ε (λ) [M-1cm-1]
Wavelength [nm]

Z_M-3

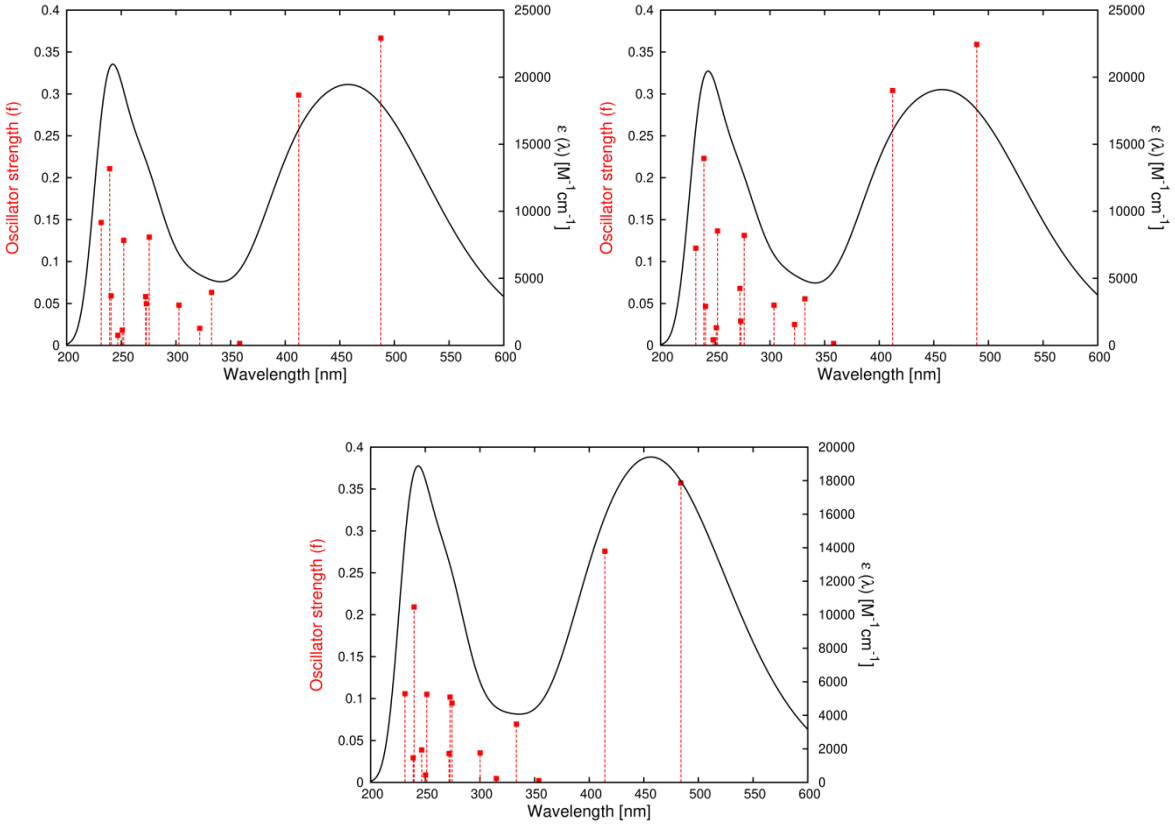
Oscillator strength (f)
ε (λ) [M-1cm-1]
Wavelength [nm]

***E*$_S$-4**

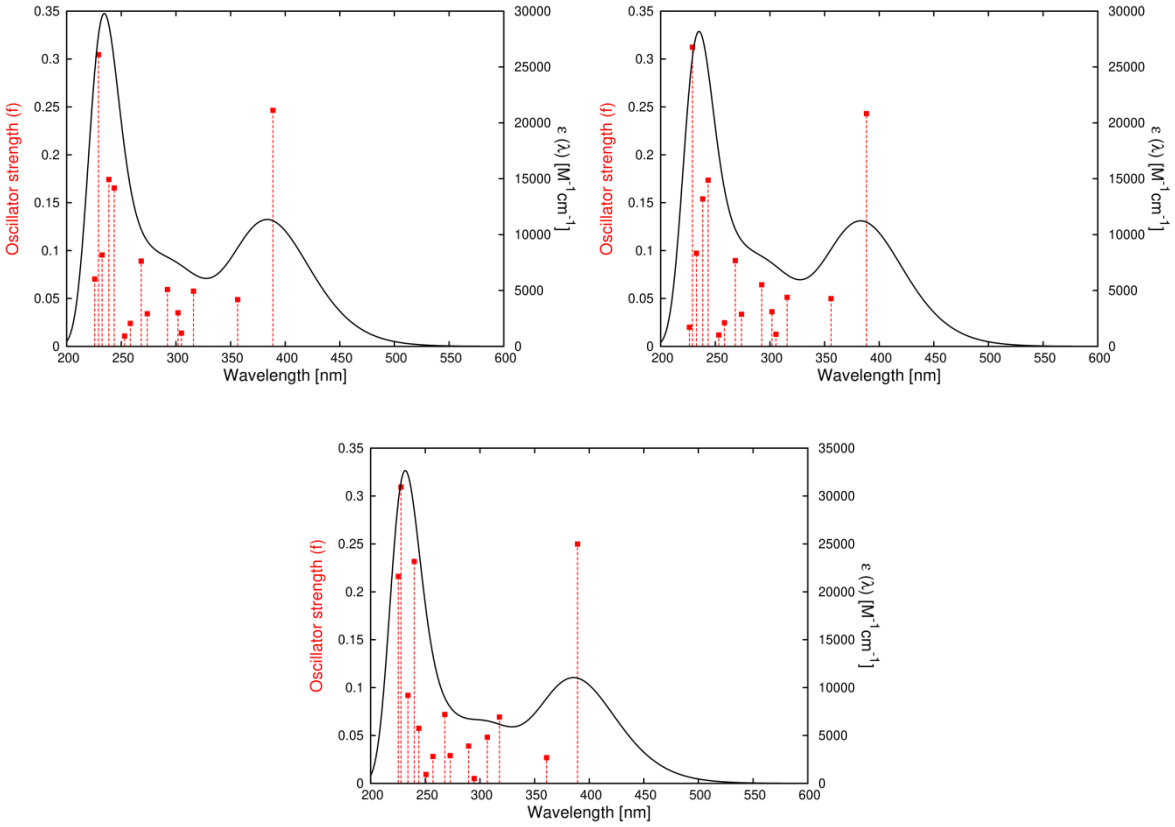
Oscillator strength (f)
ε (λ) [M^{-1}cm^{-1}]
Wavelength [nm]

***E*$_M$-4**

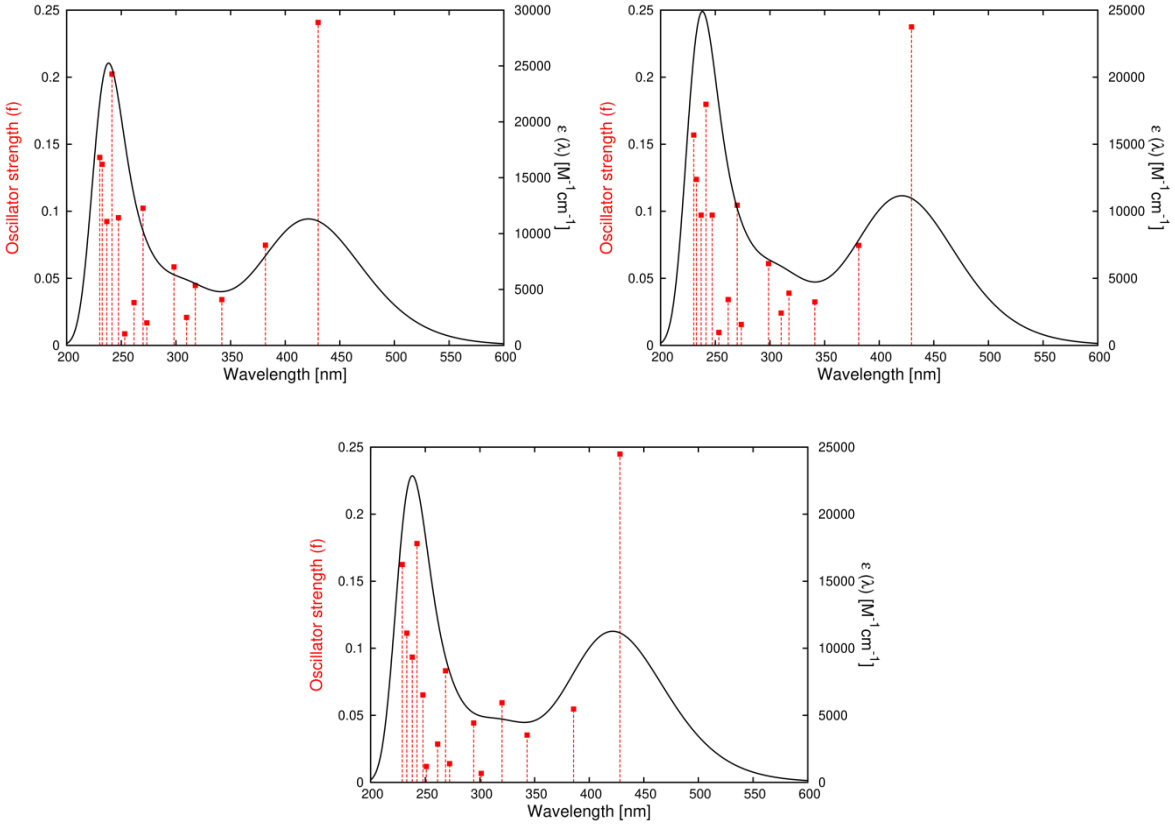
Oscillator strength (f)
ε (λ) [M^{-1}cm^{-1}]
Wavelength [nm]

Z_S-4

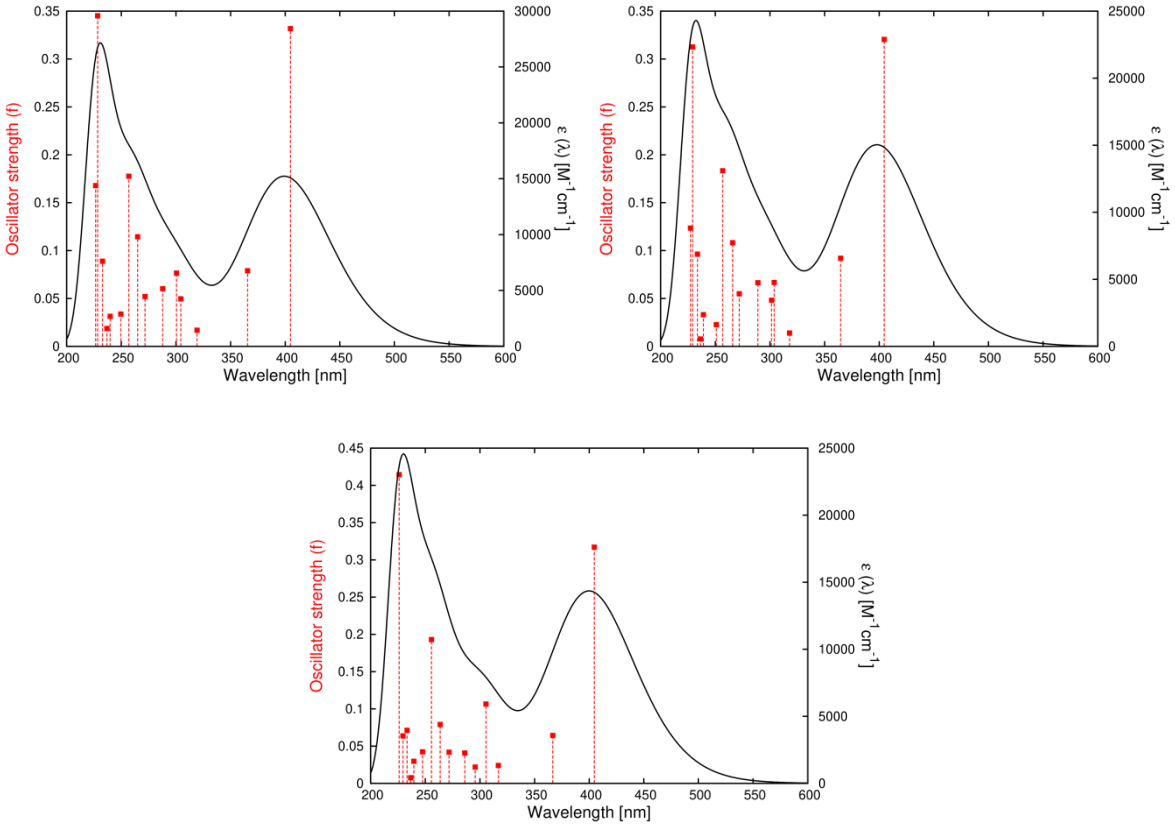
Oscillator strength (f)
ε (λ) [M-1cm-1]
Wavelength [nm]

Z_M-4

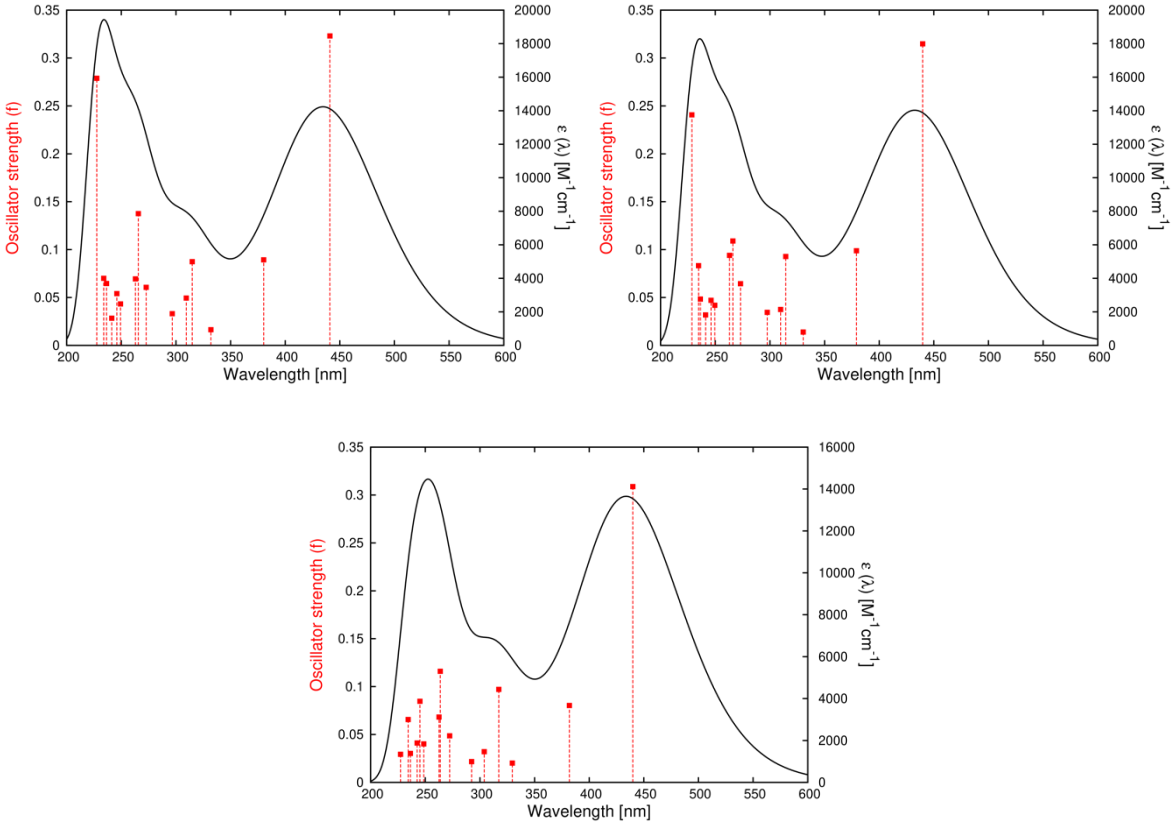
Oscillator strength (f)
ε (λ) [M-1cm-1]
Wavelength [nm]

E_S-5

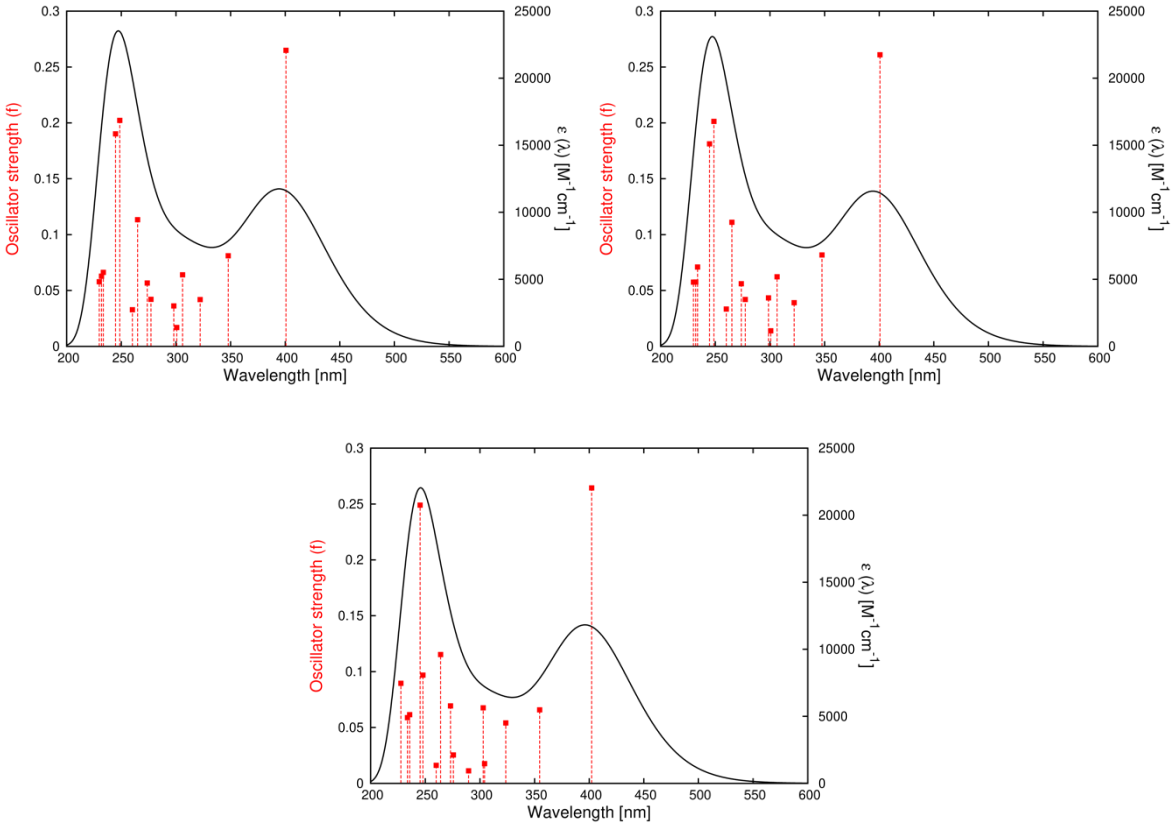
Oscillator strength (f)
ε (λ) [M-1cm-1]
Wavelength [nm]

E_M-5

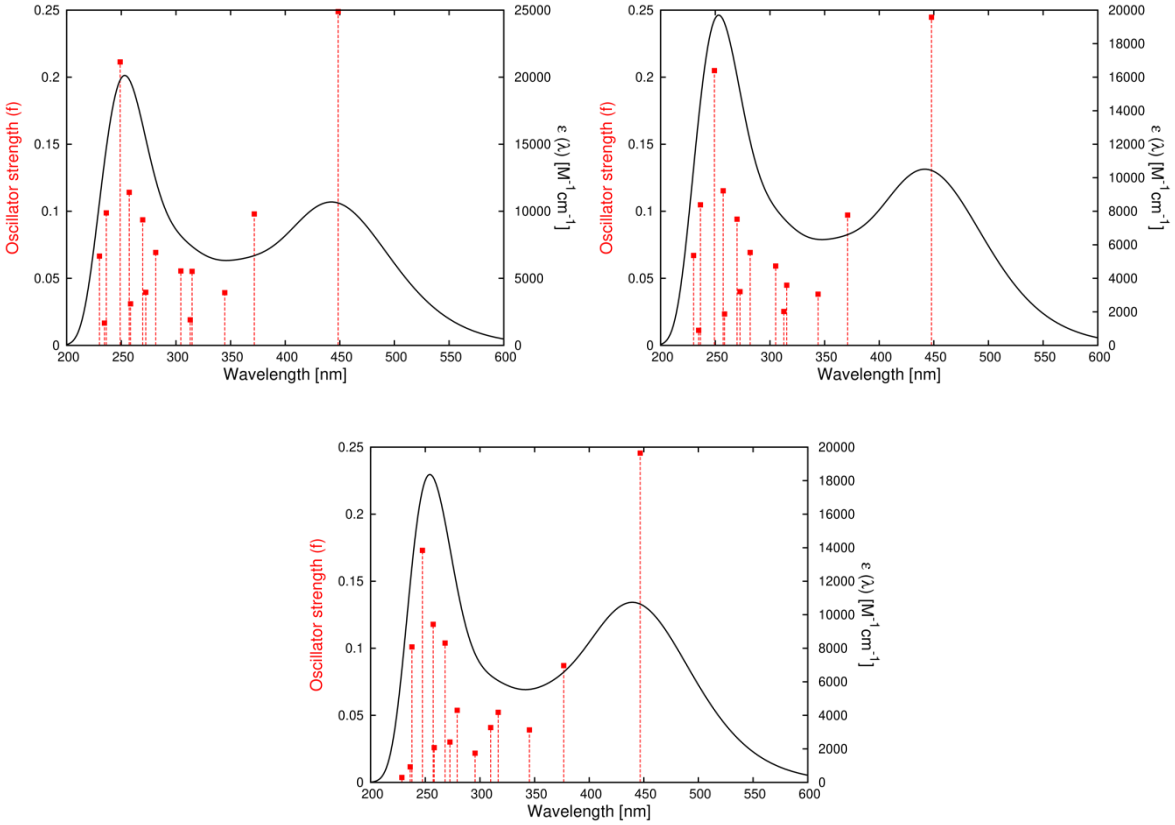
Oscillator strength (f)
ε (λ) [M-1cm-1]
Wavelength [nm]

Z_S-5

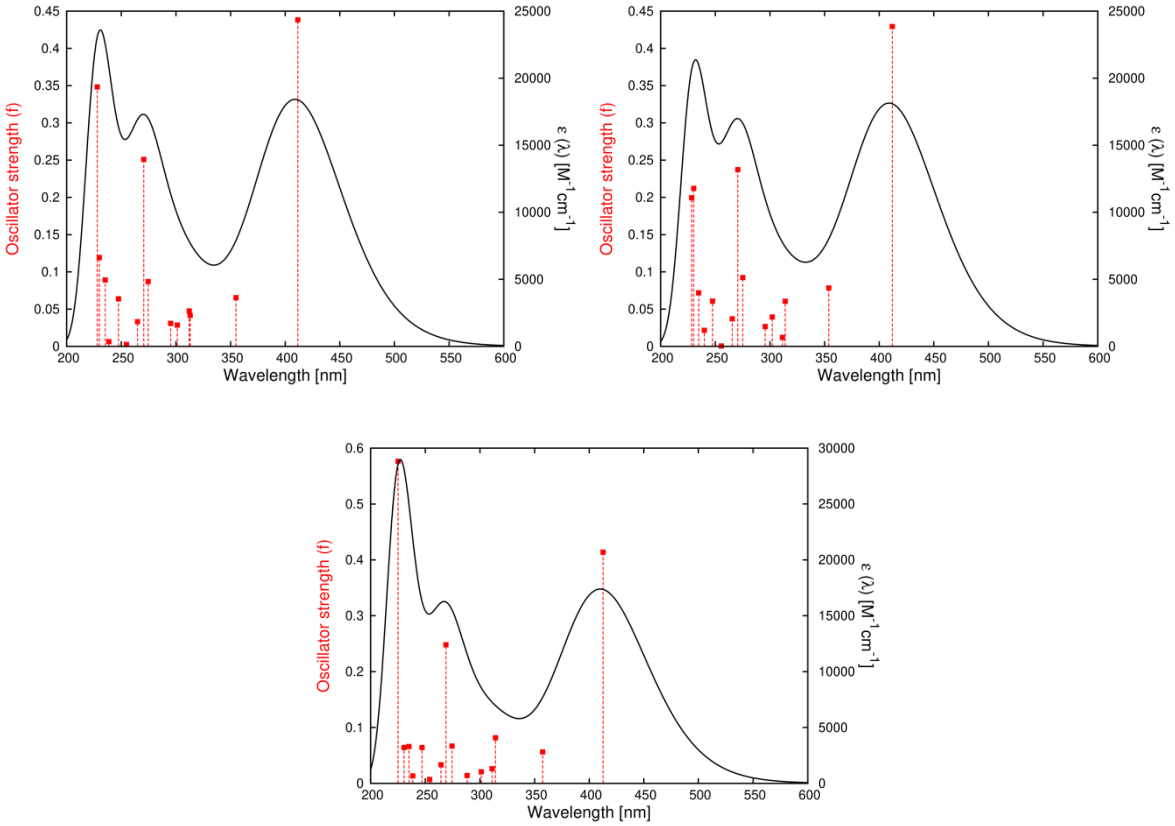
Oscillator strength (f)
ε (λ) [M-1cm-1]
Wavelength [nm]

Z_M-5

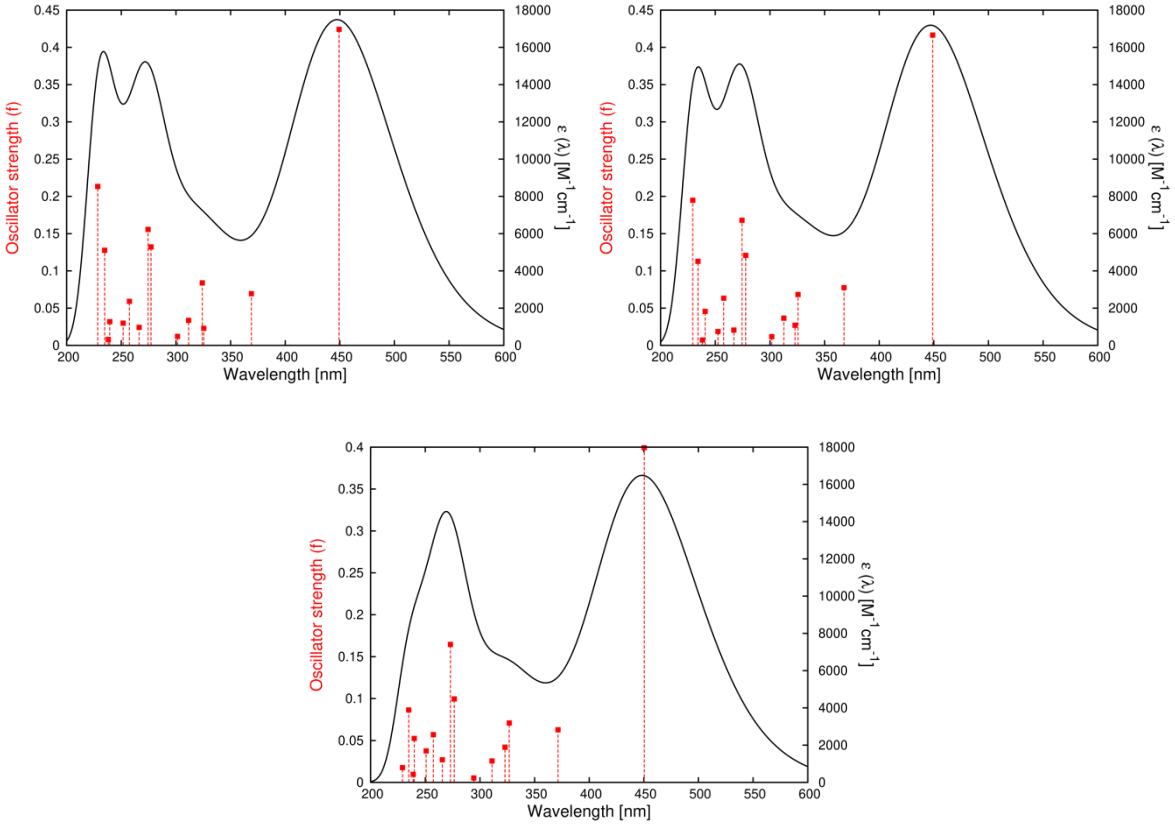
Oscillator strength (f)
ε (λ) [M-1cm-1]
Wavelength [nm]

E_S-6

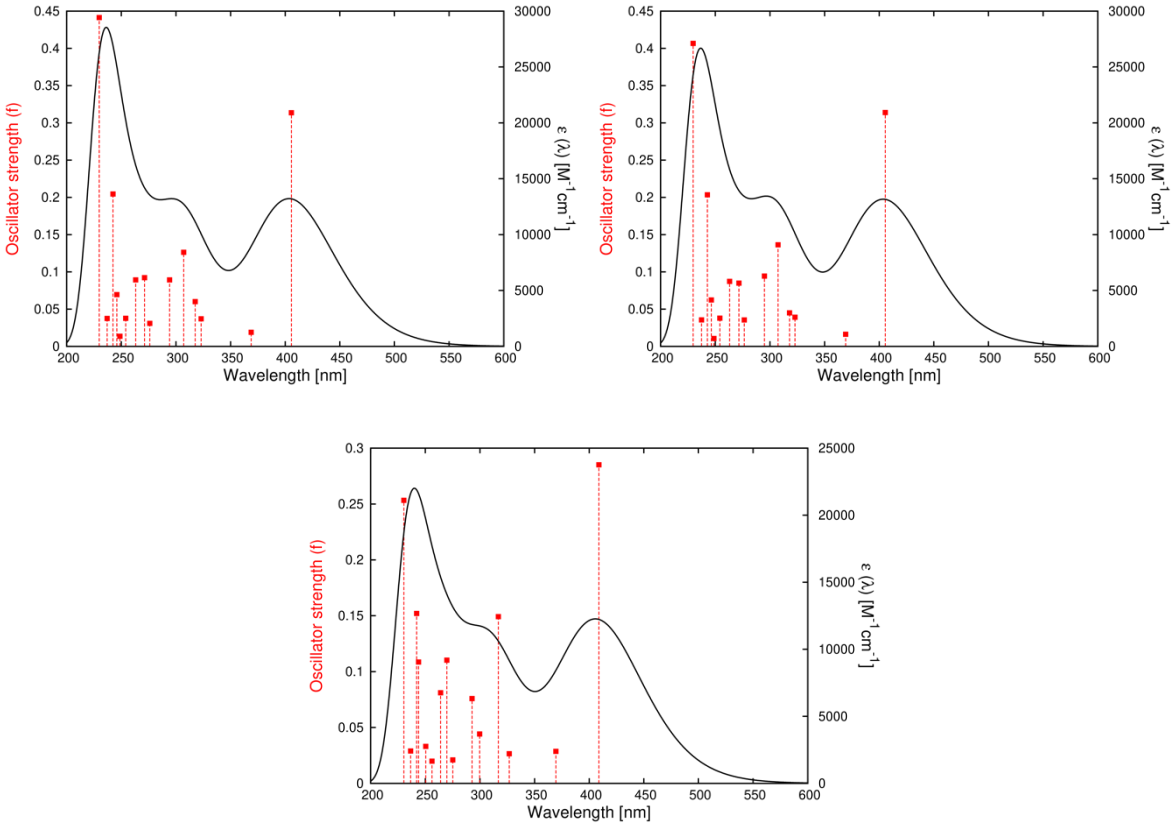
Oscillator strength (f)
ε (λ) [M-1cm-1]
Wavelength [nm]

E_M-6

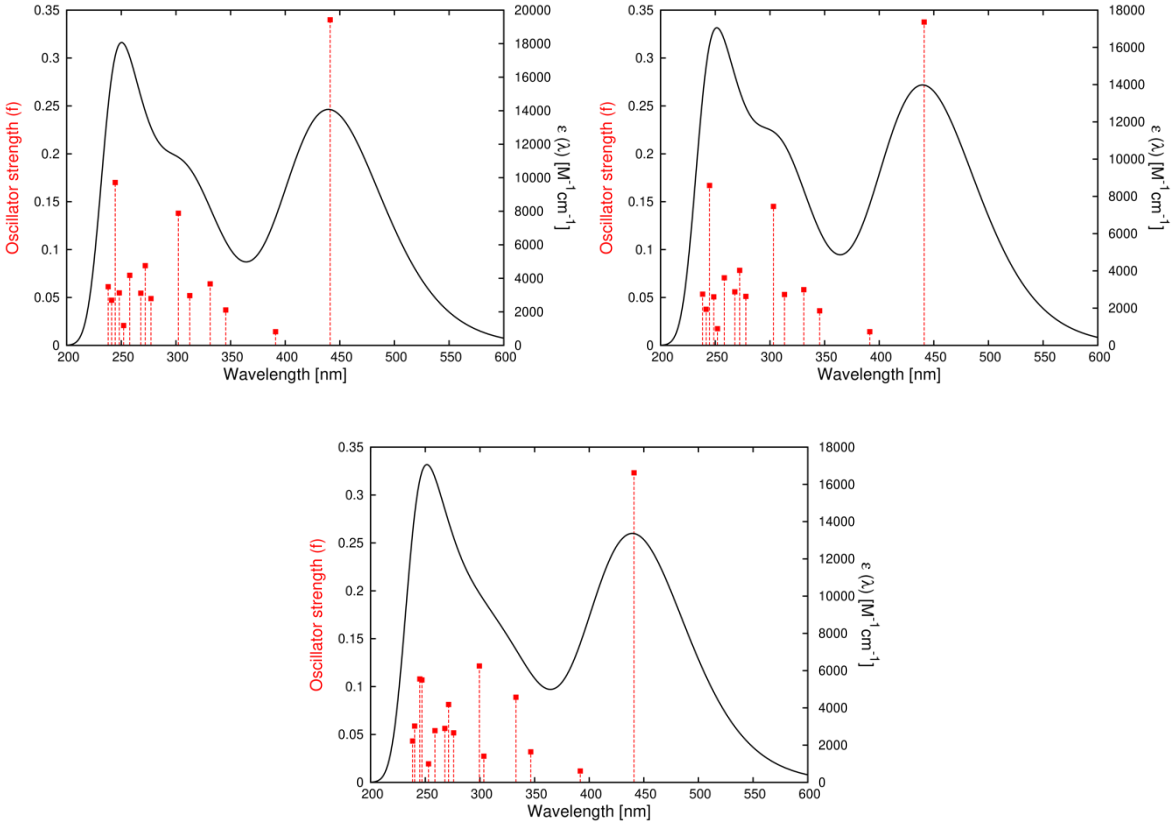
Oscillator strength (f)
ε (λ) [M-1cm-1]
Wavelength [nm]

Z_S-6

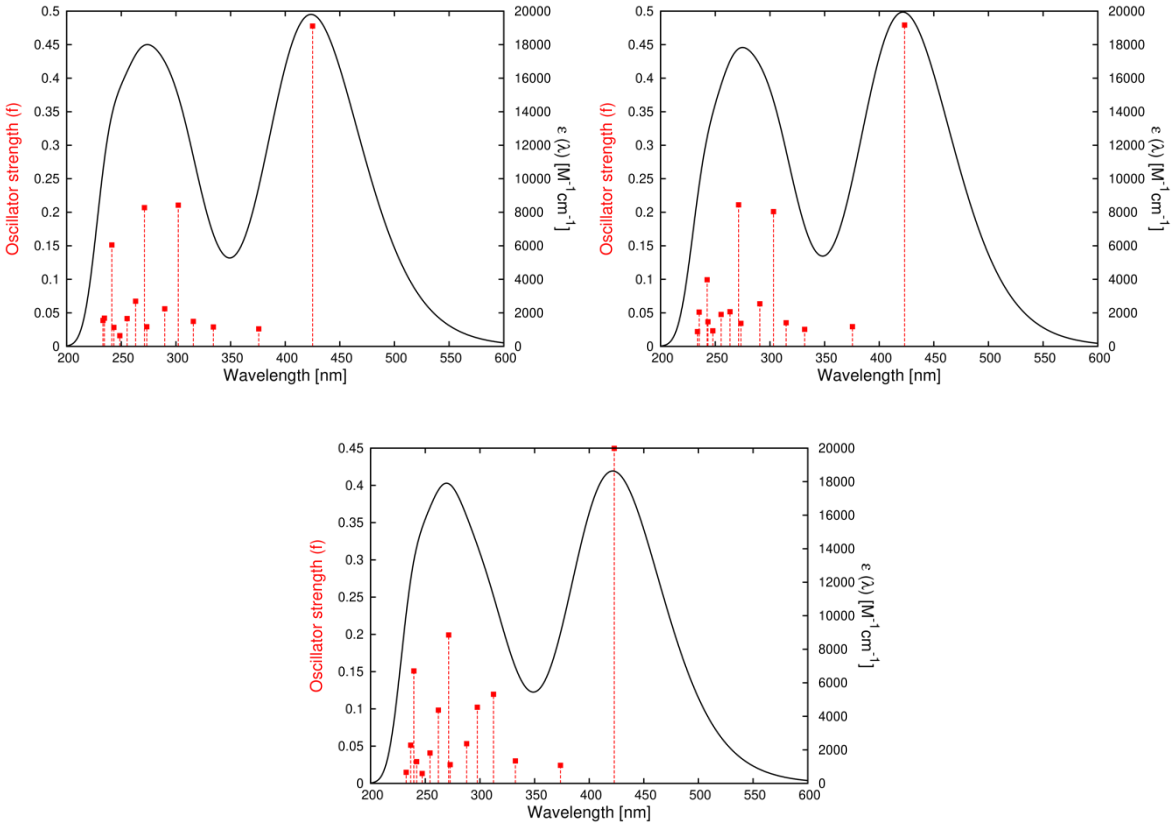
Oscillator strength (f)
ε (λ) [M-1cm-1]
Wavelength [nm]

Z_M-6

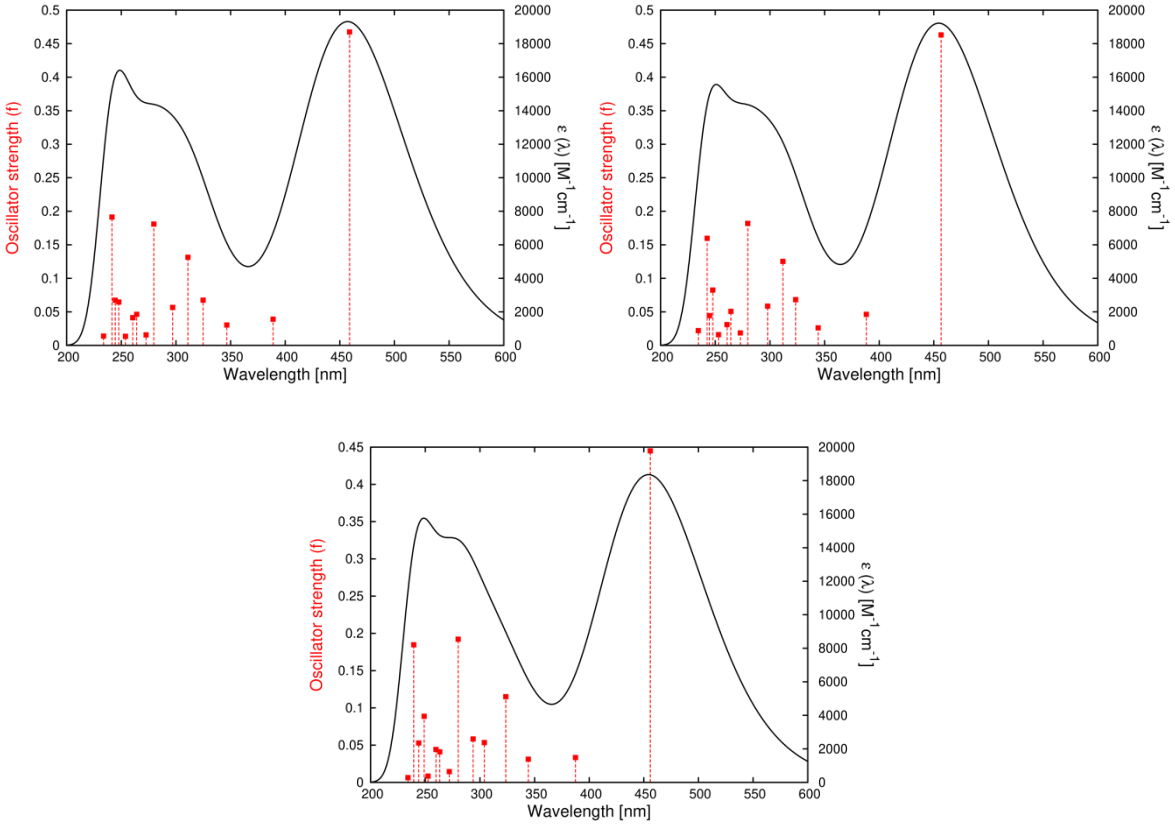
Oscillator strength (f)
ε (λ) [M-1cm-1]
Wavelength [nm]

E_S-7

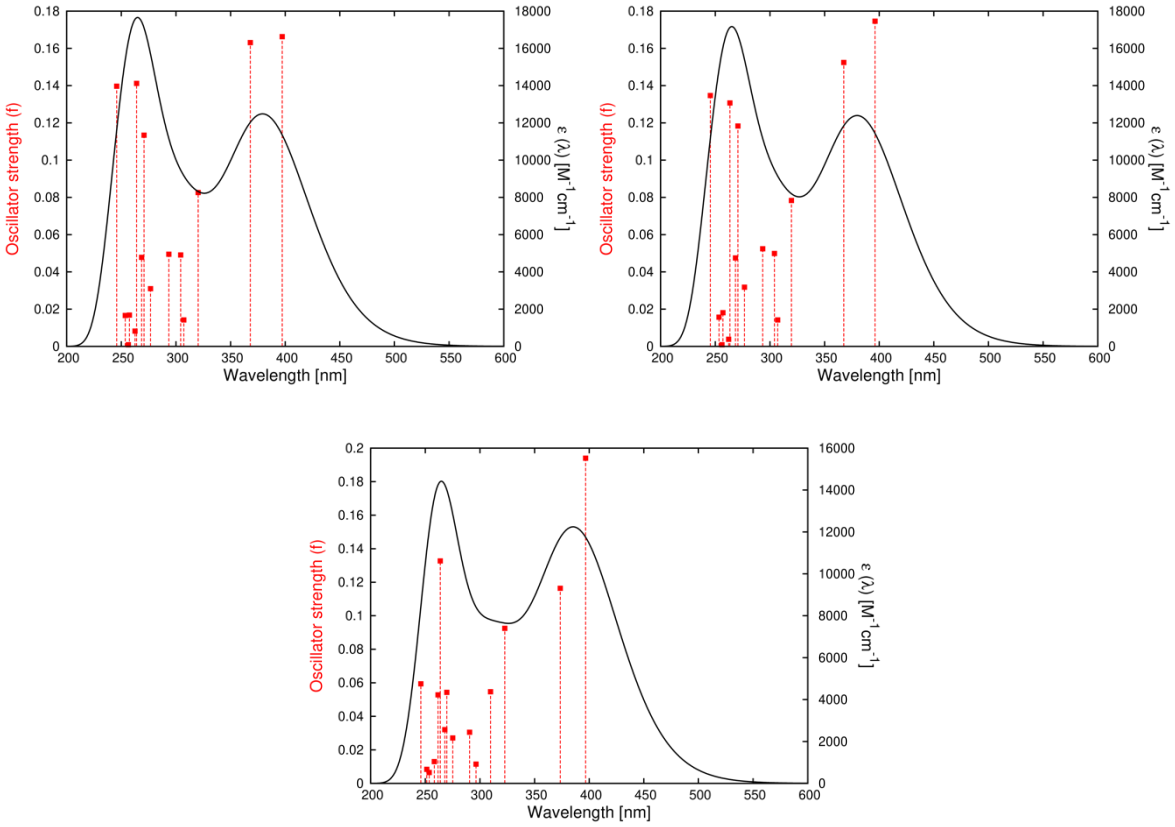
Oscillator strength (f)
ε (λ) [M-1cm-1]
Wavelength [nm]

E_M-7

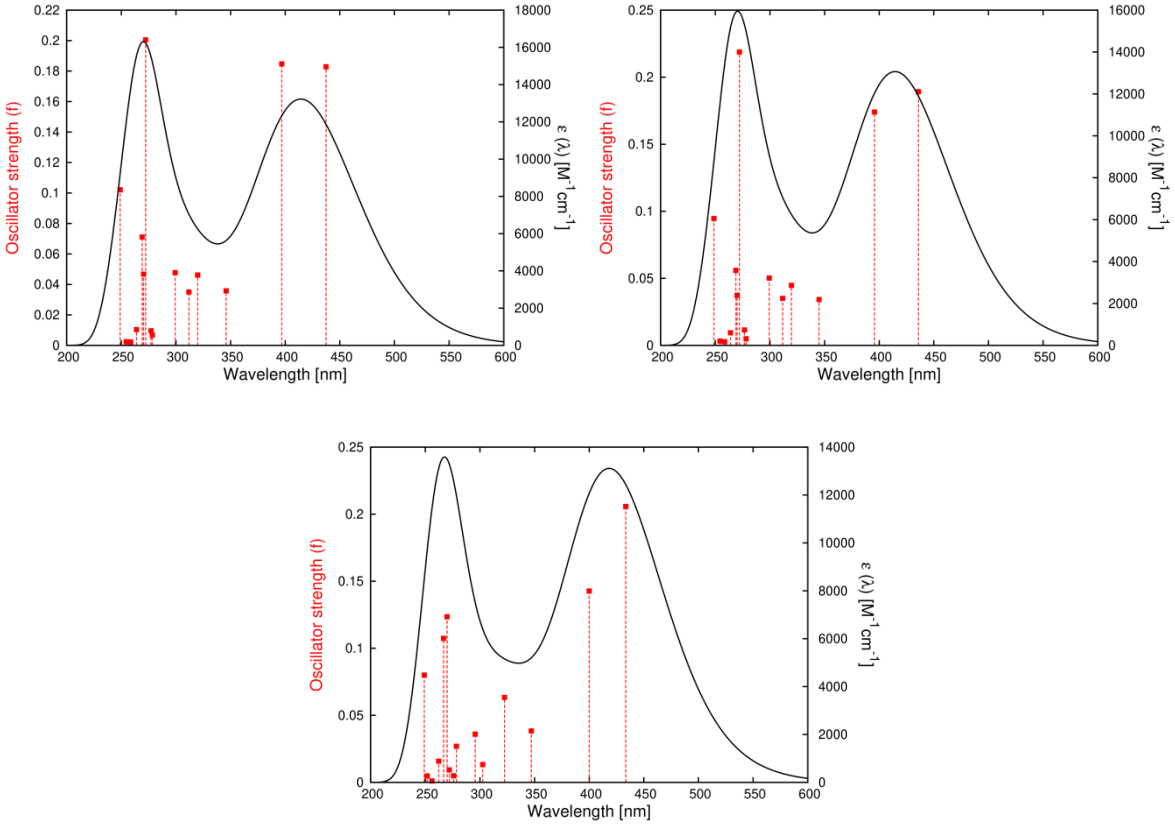
Oscillator strength (f)
ε (λ) [M-1cm-1]
Wavelength [nm]

***Z*S-7**

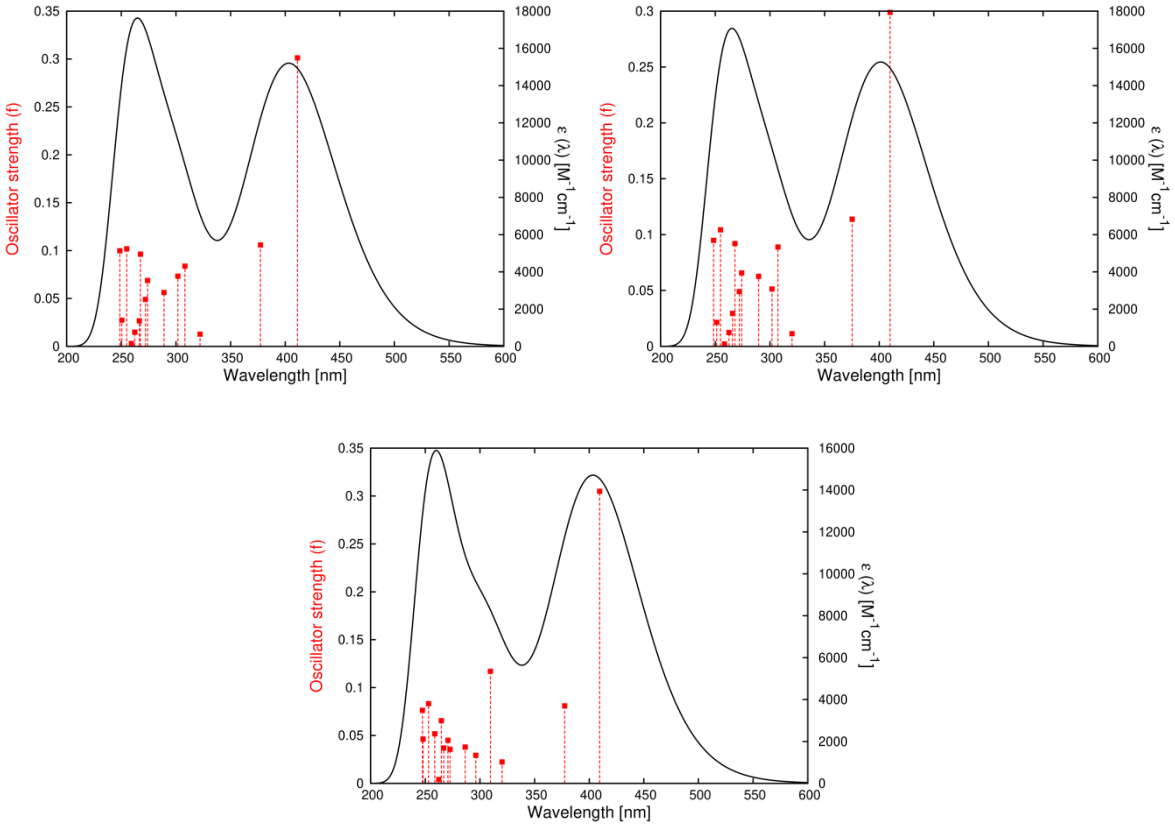
Oscillator strength (f)
ε (λ) [M-1cm-1]
Wavelength [nm]

***Z*M-7**

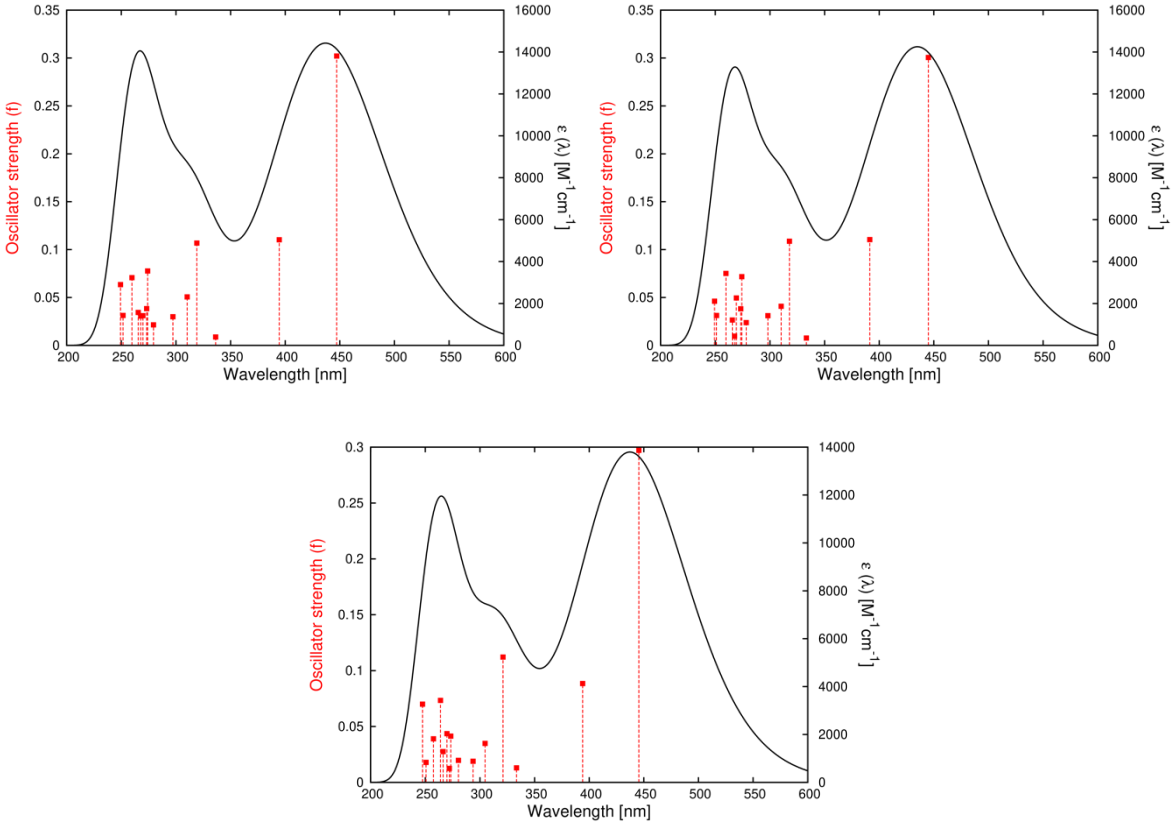
Oscillator strength (f)
ε (λ) [M-1cm-1]
Wavelength [nm]

E_S-8

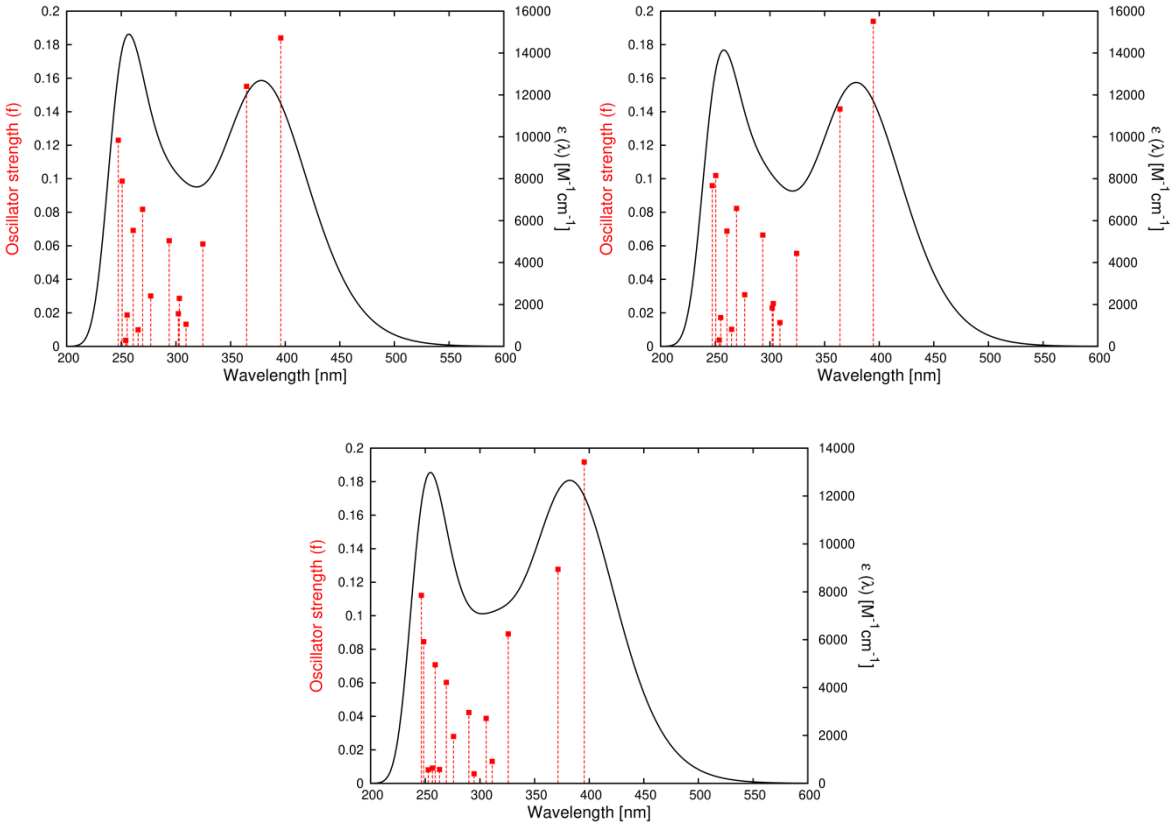
Oscillator strength (f)
ε (λ) [M-1cm-1]
Wavelength [nm]

E_M-8

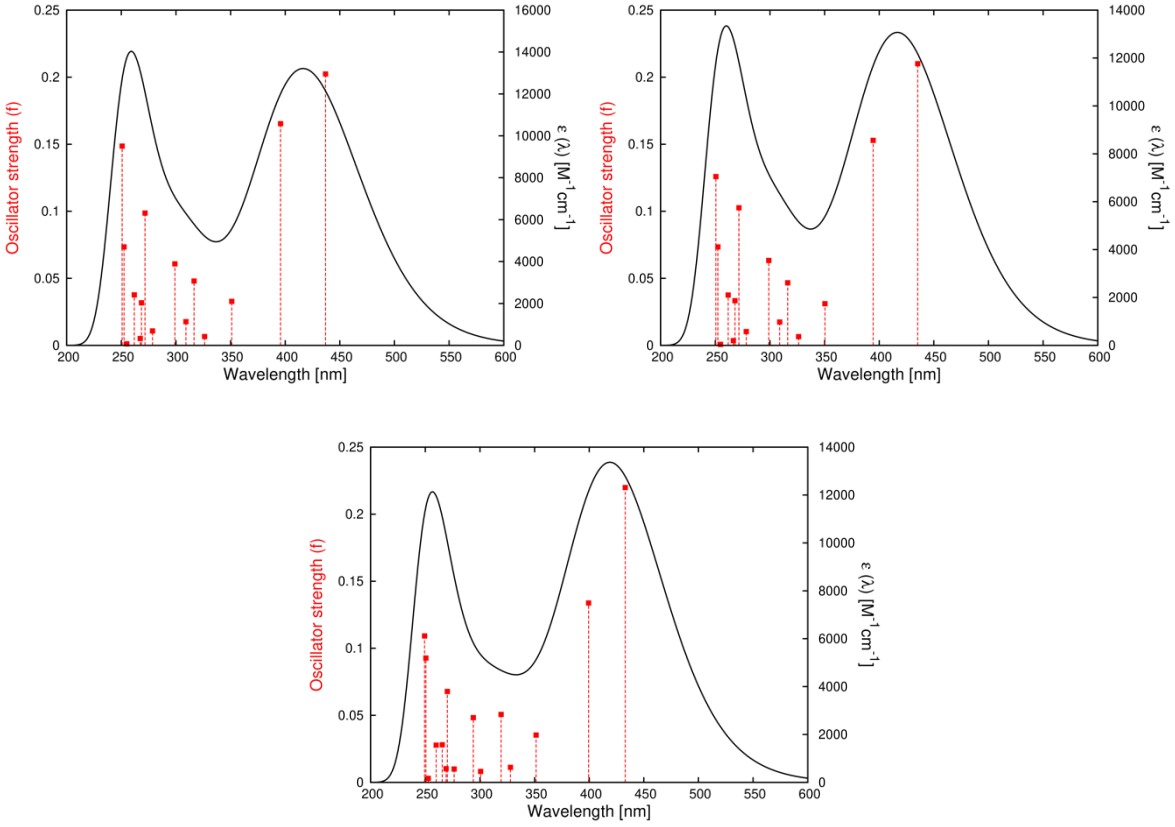
Oscillator strength (f)
ε (λ) [M-1cm-1]
Wavelength [nm]

Z_S-8

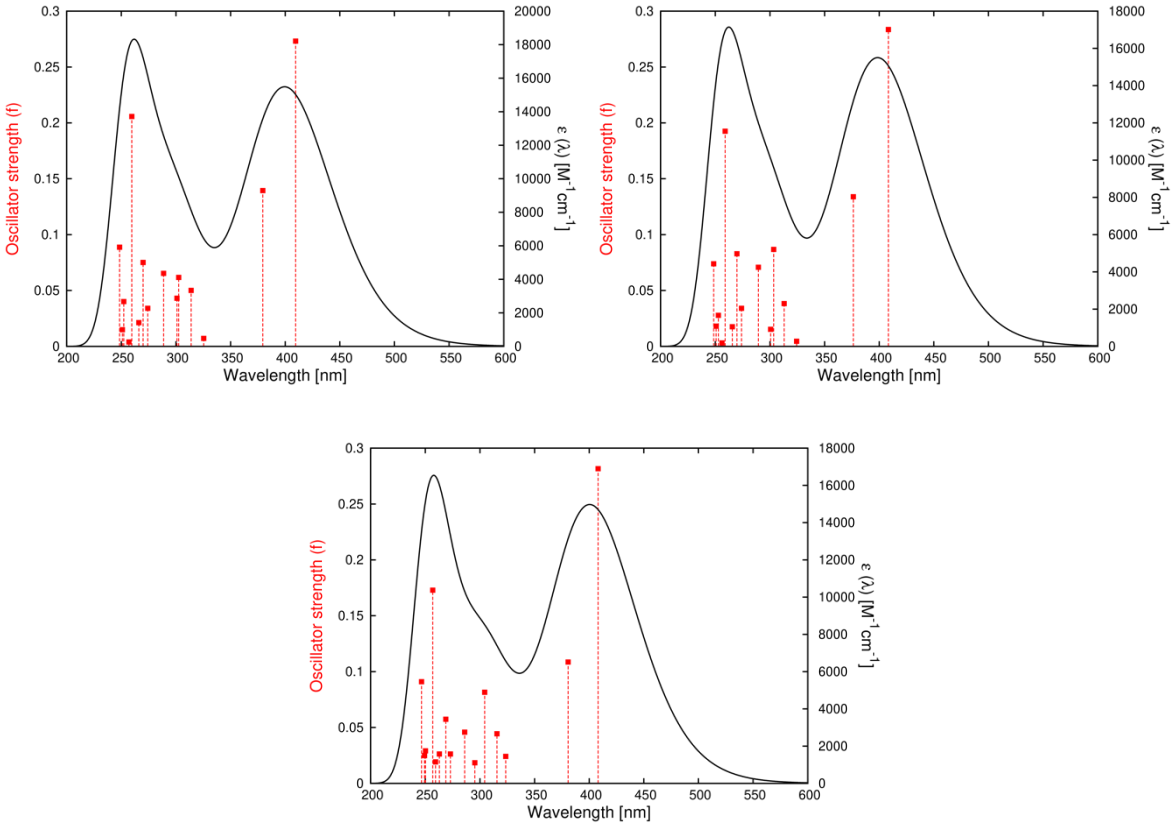
Oscillator strength (f)
ε (λ) [M⁻¹cm⁻¹]
Wavelength [nm]

Z_M-8

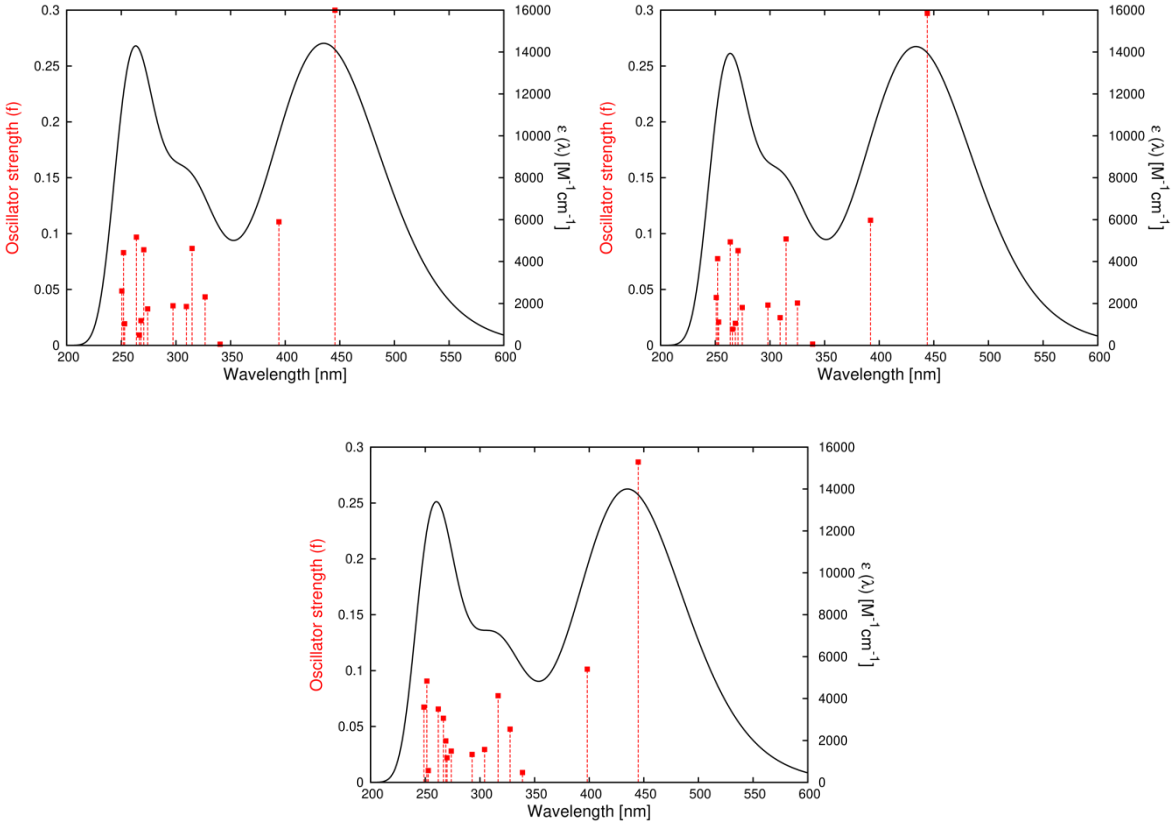
Oscillator strength (f)
ε (λ) [M⁻¹cm⁻¹]
Wavelength [nm]

E_S-9

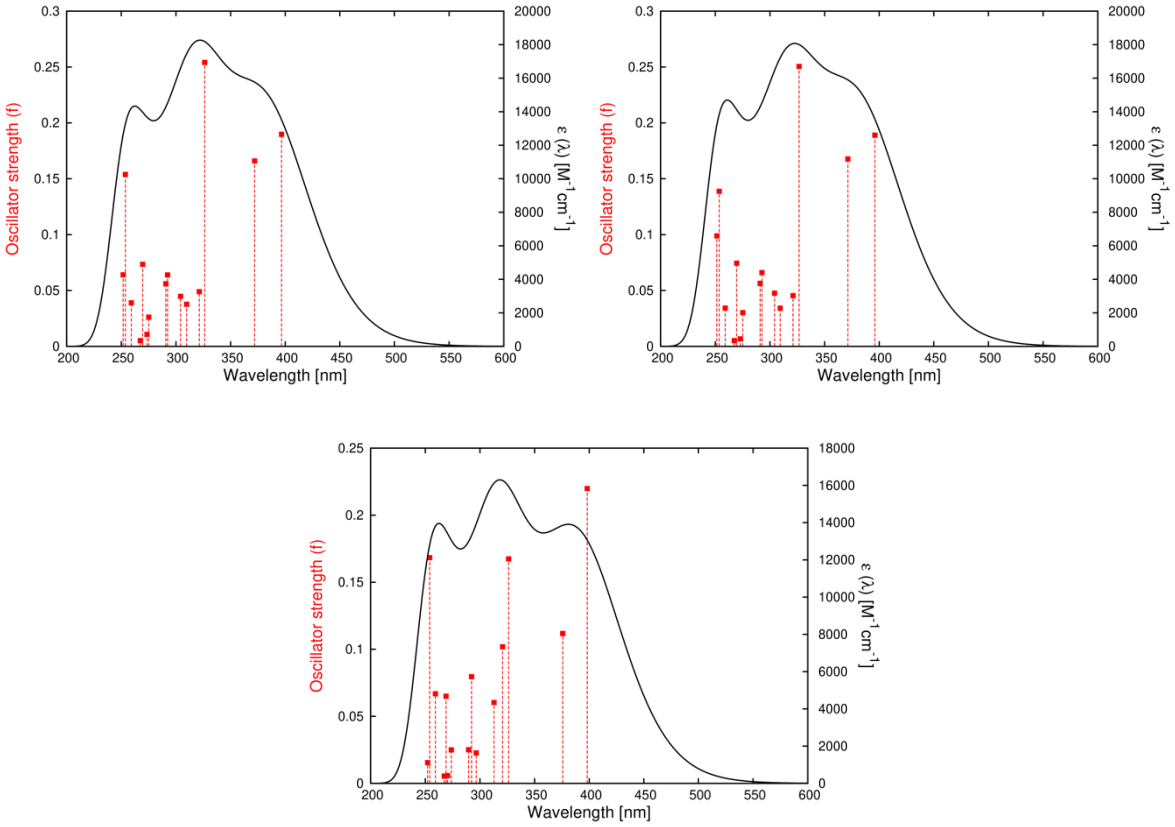
Oscillator strength (f)
ε (λ) [M-1cm-1]
Wavelength [nm]

E_M-9

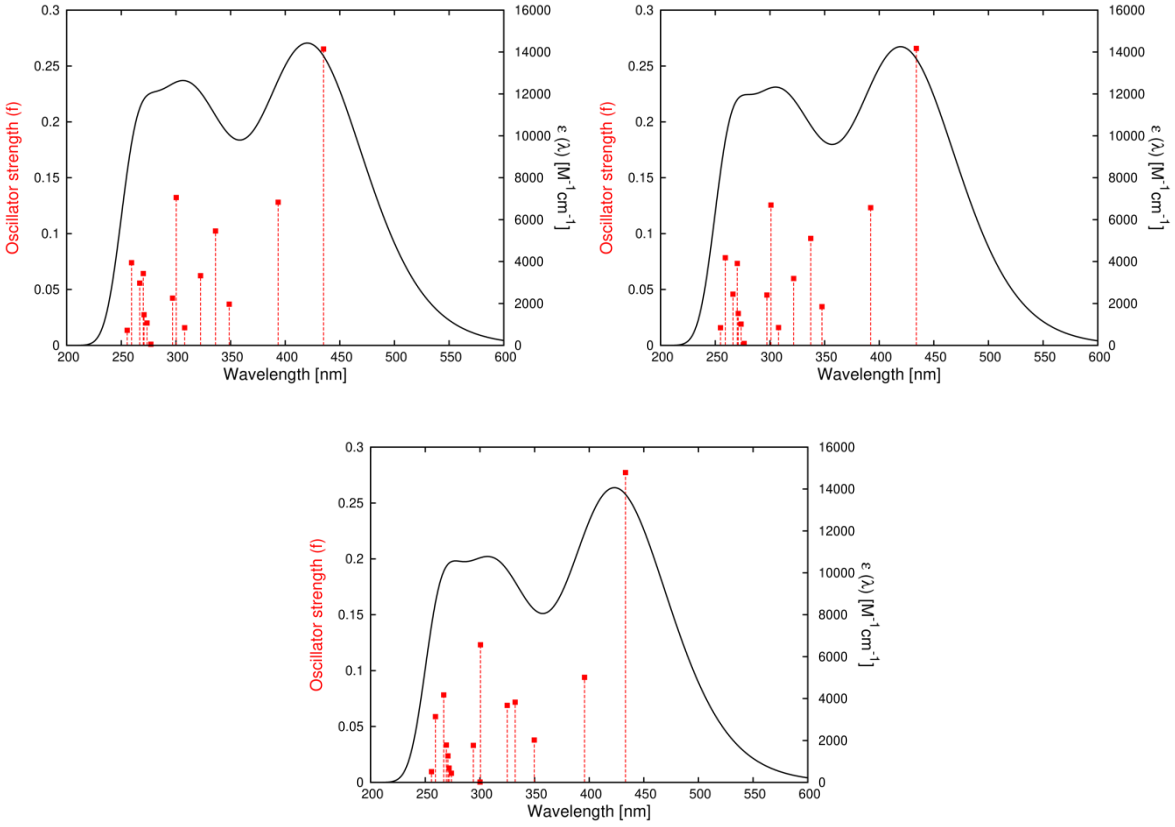
Oscillator strength (f)
ε (λ) [M-1cm-1]
Wavelength [nm]

Z_S-9

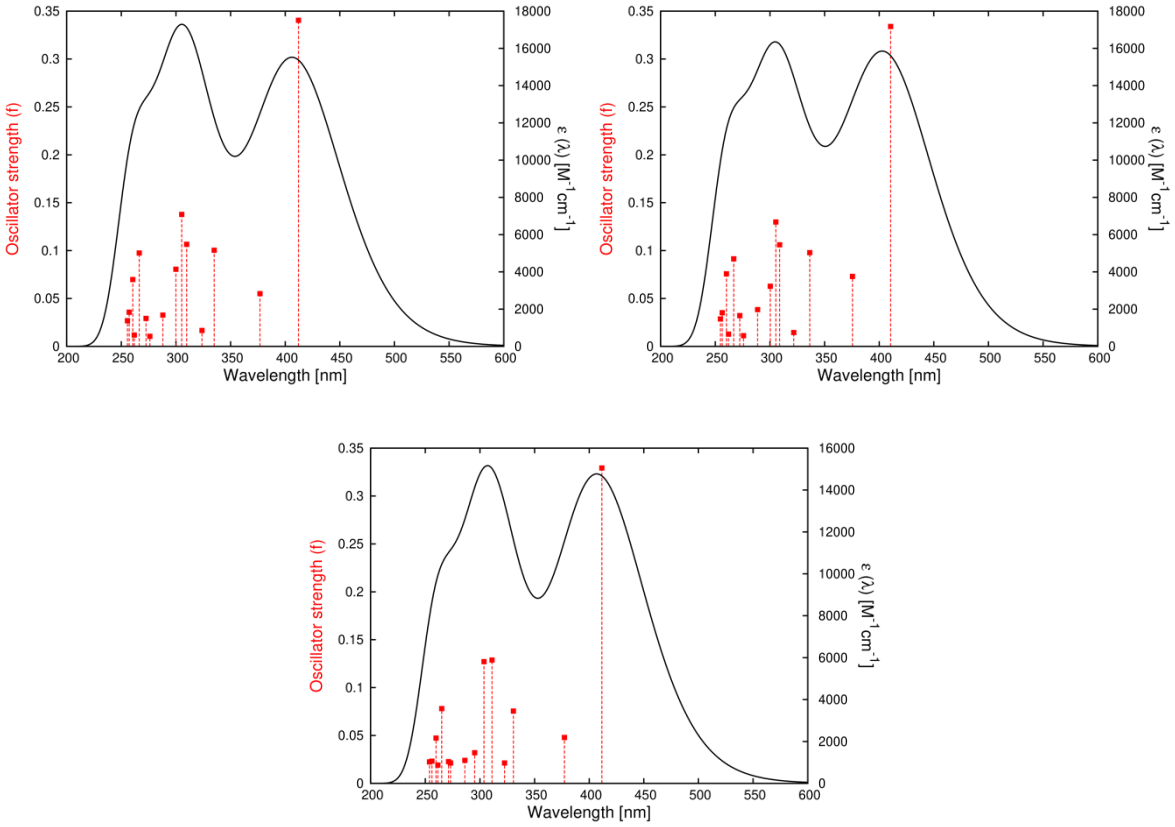
Oscillator strength (f)
ε (λ) [M-1cm-1]
Wavelength [nm]

Z_M-9

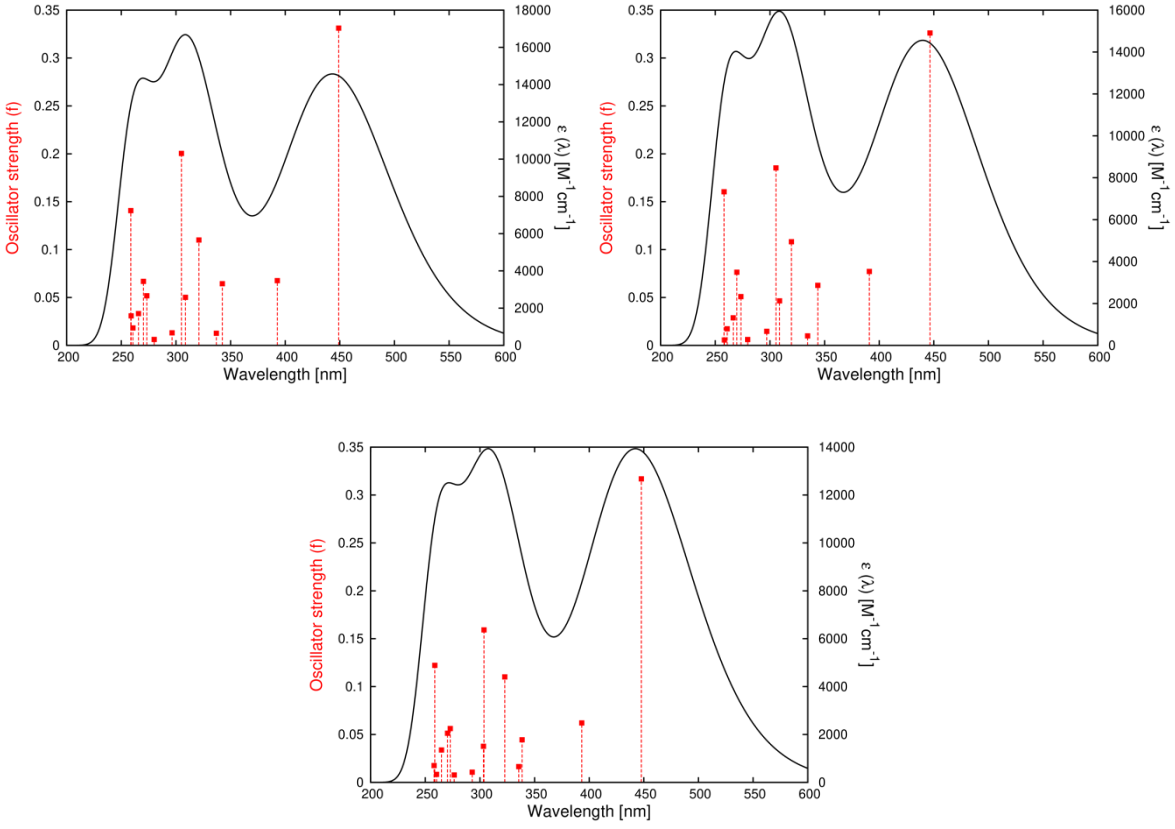
Oscillator strength (f)
ε (λ) [M-1cm-1]
Wavelength [nm]

11. References

1 P. Štacko, J. C. M. Kistemaker and B. L. Feringa, *Chem. Eur. J.*, 2017, **23**, 6643–6653.

2 L. Pfeifer, M. Scherübl, M. Fellert, W. Danowski, J. Cheng, J. Pol and B. L. Feringa, *Chem. Sci.*, 2019, **10**, 8768–8773.

3 J. C. M. Kistemaker, S. F. Pizzolato, T. van Leeuwen, T. C. Pijper and B. L. Feringa, *Chem. Eur. J.*, 2016, **22**, 13478–13487.

4 D. P. Phillips, A. R. Hudson, B. Nguyen, T. L. Lau, M. H. McNeill, J. E. Dalgard, J. H. Chen, R. J. Penuliar, T. A. Miller and L. Zhi, *Tetrahedron Lett.*, 2006, **47**, 7137–7138.

5 R. A. Altman, A. M. Hyde, X. Huang and S. L. Buchwald, *J. Am. Chem. Soc.*, 2008, **130**, 9613–9620.

6 Bruker, 2016. APEX3 (V2016.1-0), SAINT (Version 8.37A) and SADABS (Version 2014/15). Bruker AXS Inc., Madison, Wisconsin, USA.

7 L. Krause, R. Herbst-Irmer, G. M. Sheldrick and D. Stalke, *J. Appl. Crystallogr.*, 2015, **48**, 3–10.

8 G. M. Sheldrick and IUCr, *Acta Crystallogr. Sect. A Found. Adv.*, 2015, **71**, 3–8.

9 G. M. Sheldrick, *Acta Crystallogr Sect. A*, 2008, **A64**, 112–122.

10 A. L. Spek, *Acta Crystallogr. Sect. C Struct. Chem.*, 2015, **71**, 9–18.

11 K. Stranius and K. Börjesson, *Sci. Rep.*, 2017, **7**, 1–9.

12 H. J. Kuhn, S. E. Braslavsky and R. Schmidt, *Pure Appl. Chem.*, 2004, **76**, 2105–2146.

13 M. Montalti, A. Credi, L. Prodi and M. T. Gandolfi, *Handbook of Photochemistry*, CRC Press, 2006.

14 Gaussian 16, Revision B.01, M. J. Frisch, G. W. Trucks, H. B. Schlegel, G. E. Scuseria, M. A. Robb, J. R. Cheeseman, G. Scalmani, V. Barone, G. A. Petersson, H. Nakatsuji, X. Li, M. Caricato, A. V. Marenich, J. Bloino, B. G. Janesko, R. Gomperts, B. Mennucci, H. P. Hratchian, J. V. Ortiz, A. F. Izmaylov, J. L. Sonnenberg, D. Williams-Young, F. Ding, F. Lipparini, F. Egidi, J. Goings, B. Peng, A. Petrone, T. Henderson, D. Ranasinghe, V. G. Zakrzewski, J. Gao, N. Rega, G. Zheng, W. Liang, M. Hada, M. Ehara, K. Toyota, R. Fukuda, J. Hasegawa, M. Ishida, T. Nakajima, Y. Honda, O. Kitao, H. Nakai, T. Vreven, K. Throssell, J. A. Montgomery, Jr., J. E. Peralta, F. Ogliaro, M. J. Bearpark, J. J. Heyd, E. N. Brothers, K. N. Kudin, V. N. Staroverov, T. A. Keith, R. Kobayashi, J. Normand, K. Raghavachari, A. P. Rendell, J. C. Burant, S. S. Iyengar, J. Tomasi, M. Cossi, J. M. Millam, M. Klene, C. Adamo, R. Cammi, J. W. Ochterski, R. L. Martin, K. Morokuma, O. Farkas, J. B. Foresman, and D. J. Fox, Gaussian, Inc., Wallingford CT, 2016.

12. Appendix

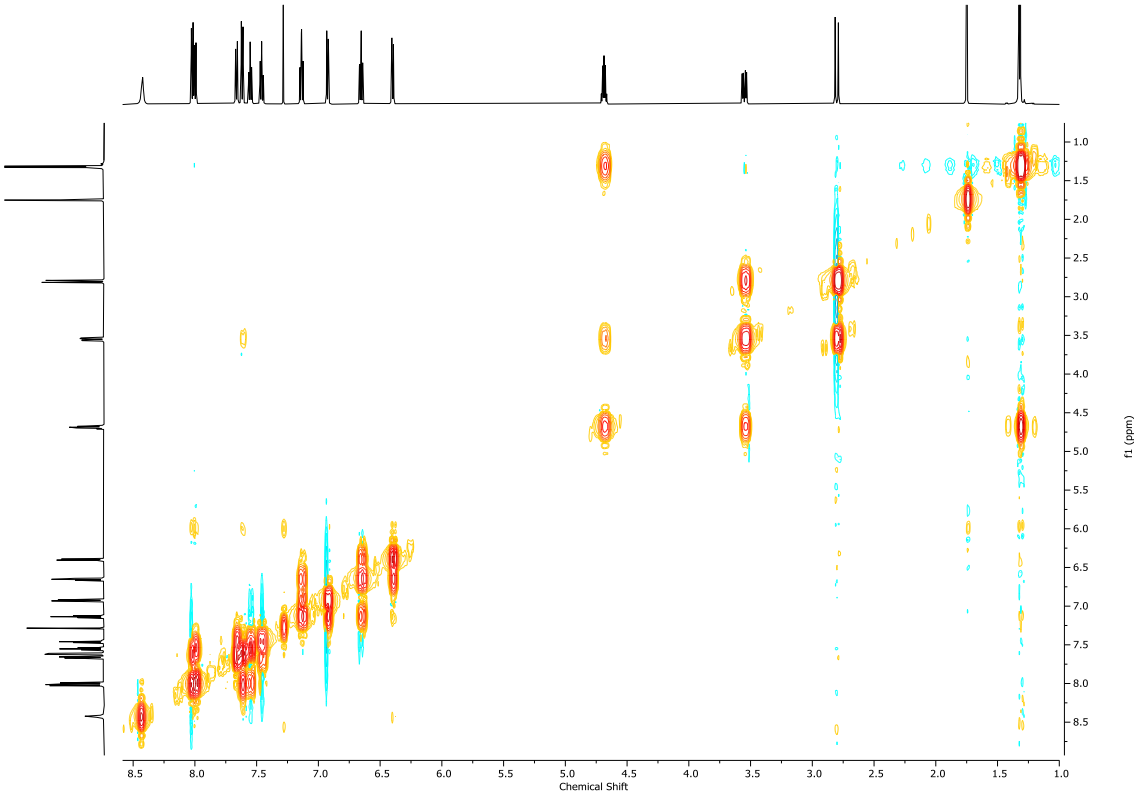

Figure S86: COSY spectrum of ***E*S-1** in $CDCl_3$.

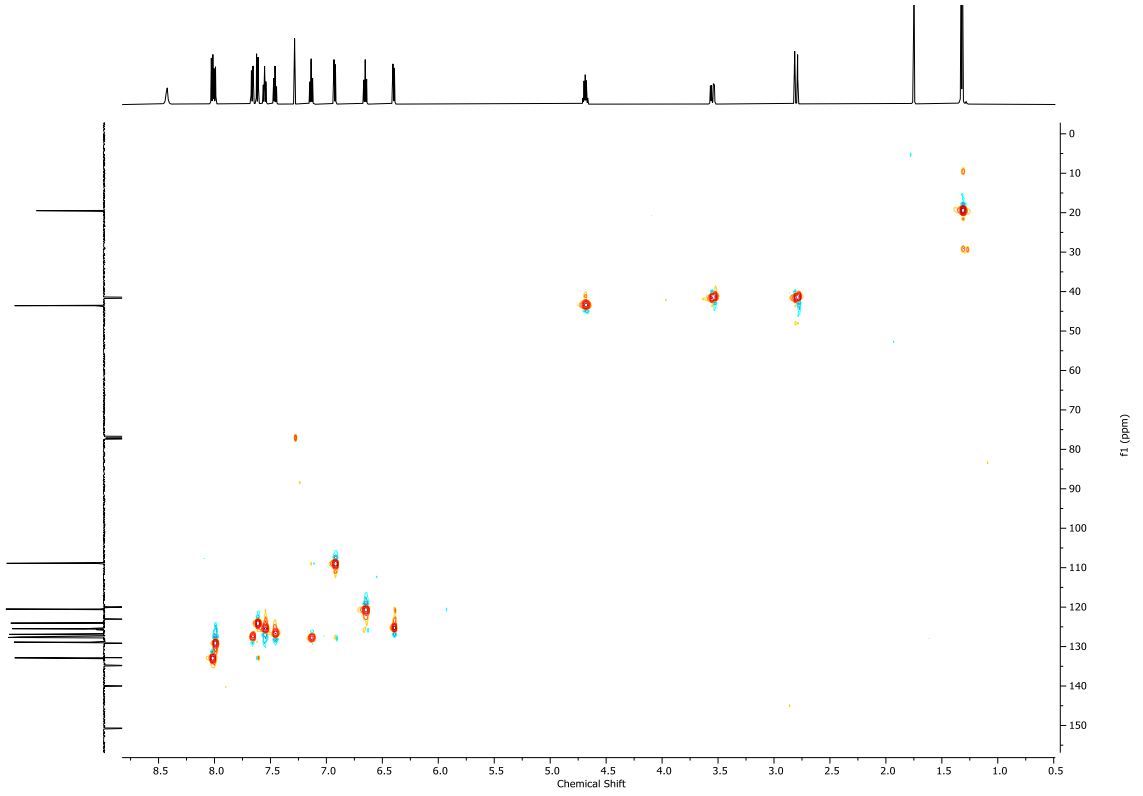

Figure S87: HSQC spectrum of ***E*S-1** in $CDCl_3$.

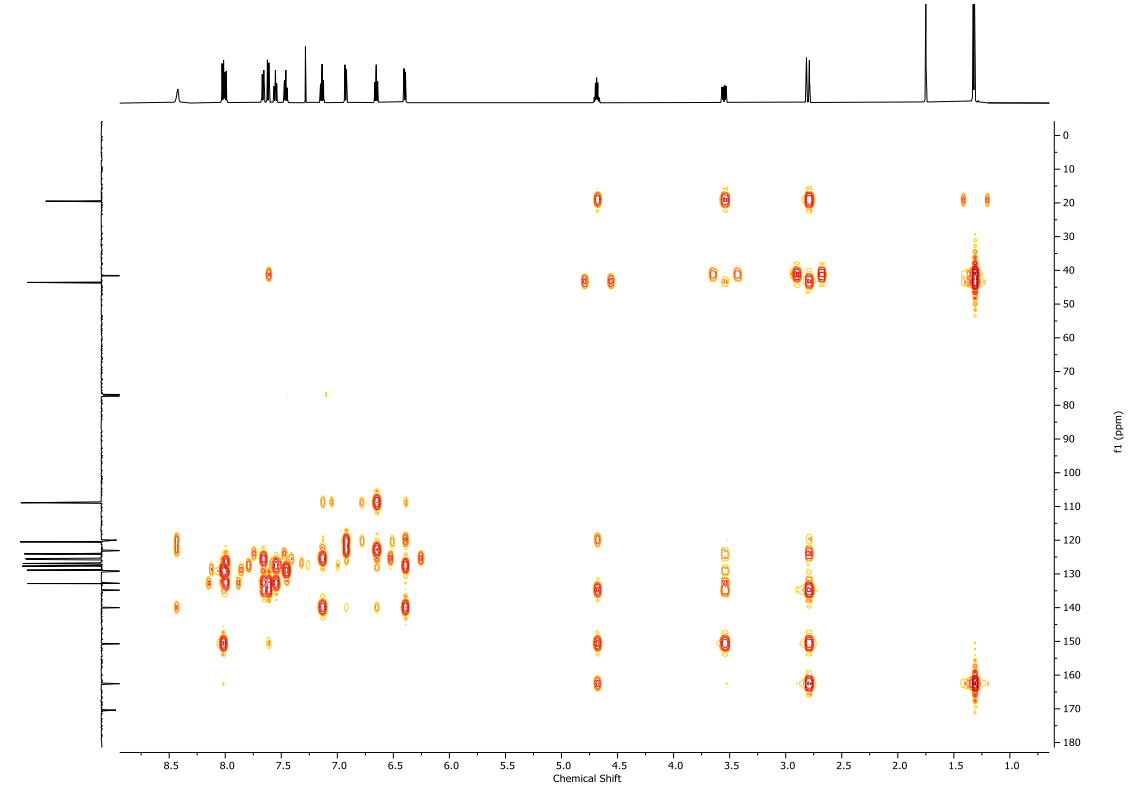

Figure S88: HMBC spectrum of ***E*S-1** in $CDCl_3$.

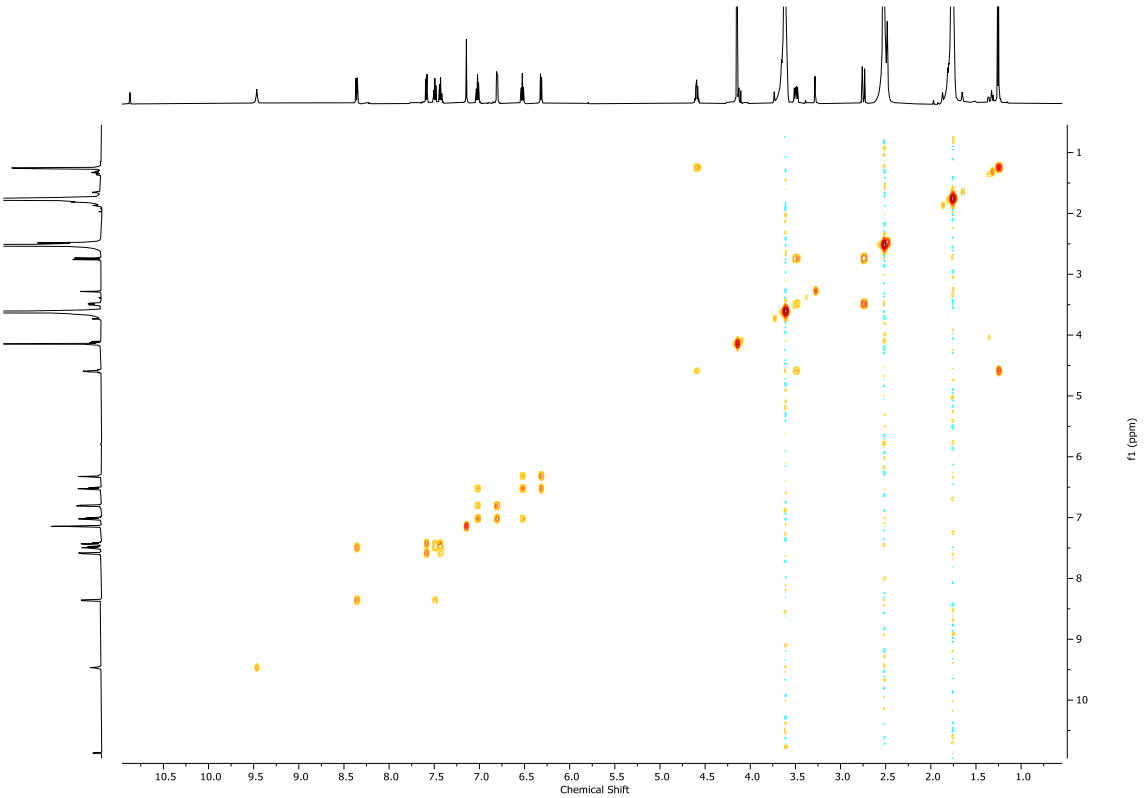

Figure S89: COSY spectrum of ***E*S-2** in d_8-THF.

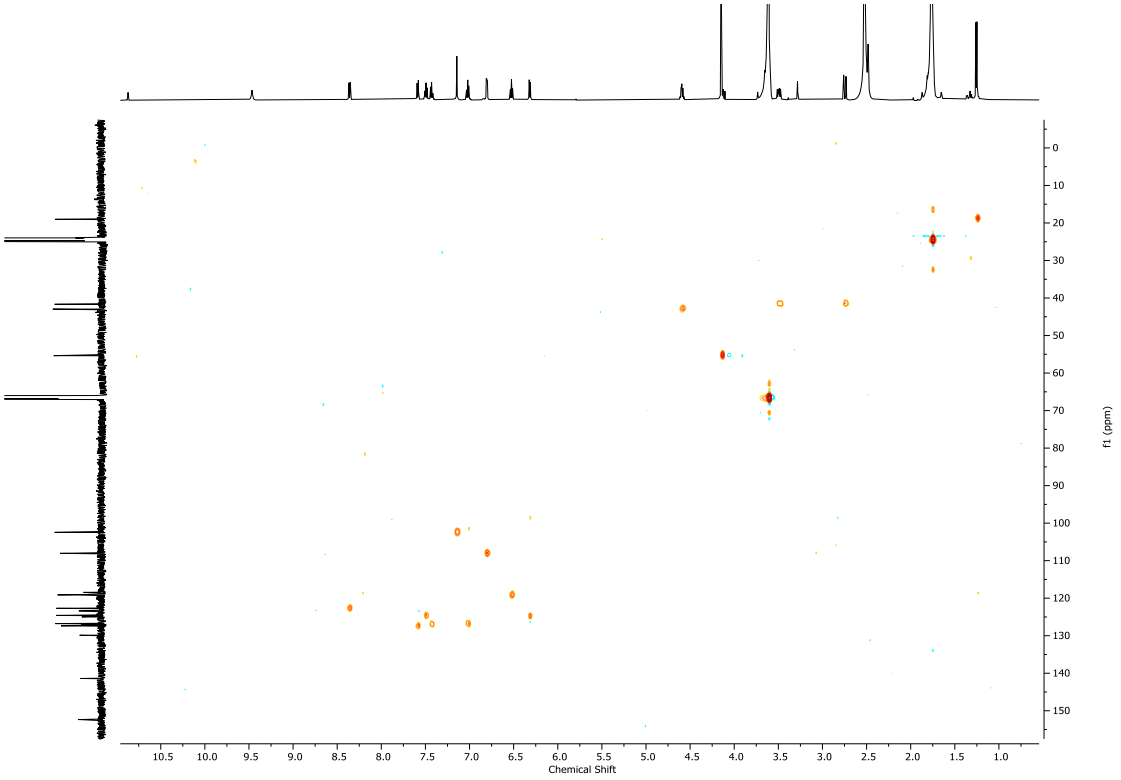

Figure S90: HSQC spectrum of ***E*S-2** in d_8-THF.

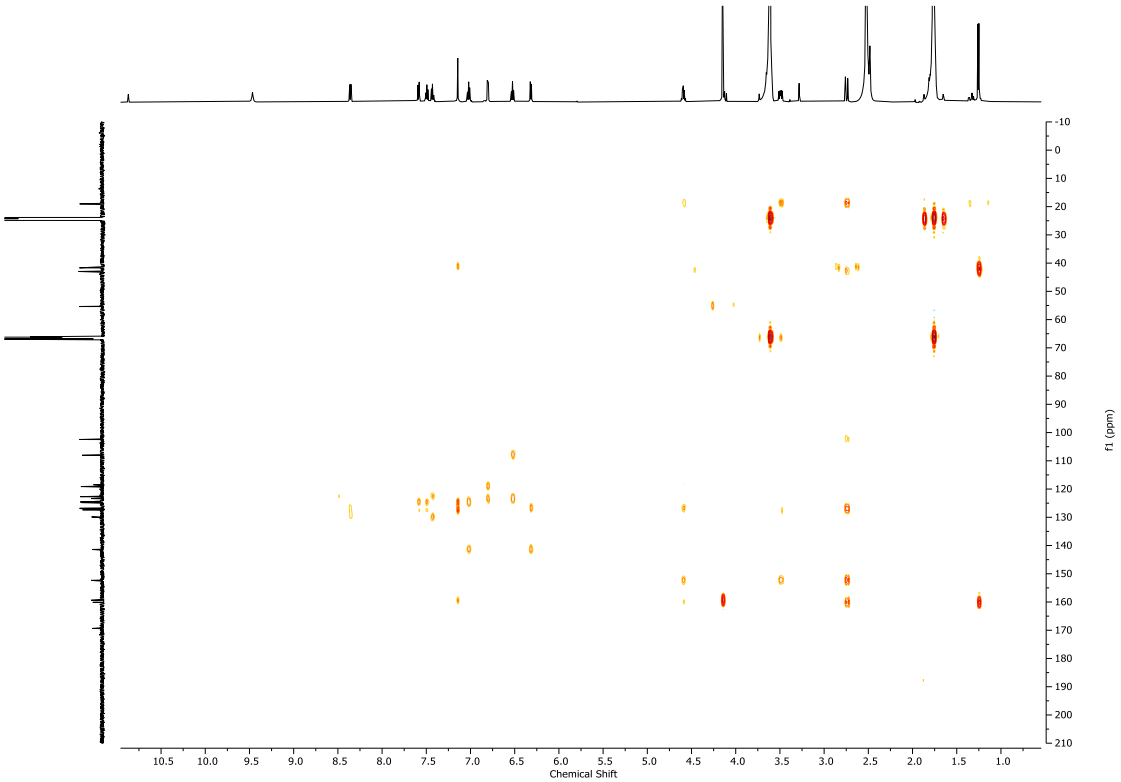

Figure S91: HMBC spectrum of ***E*S-2** in d_8-THF.

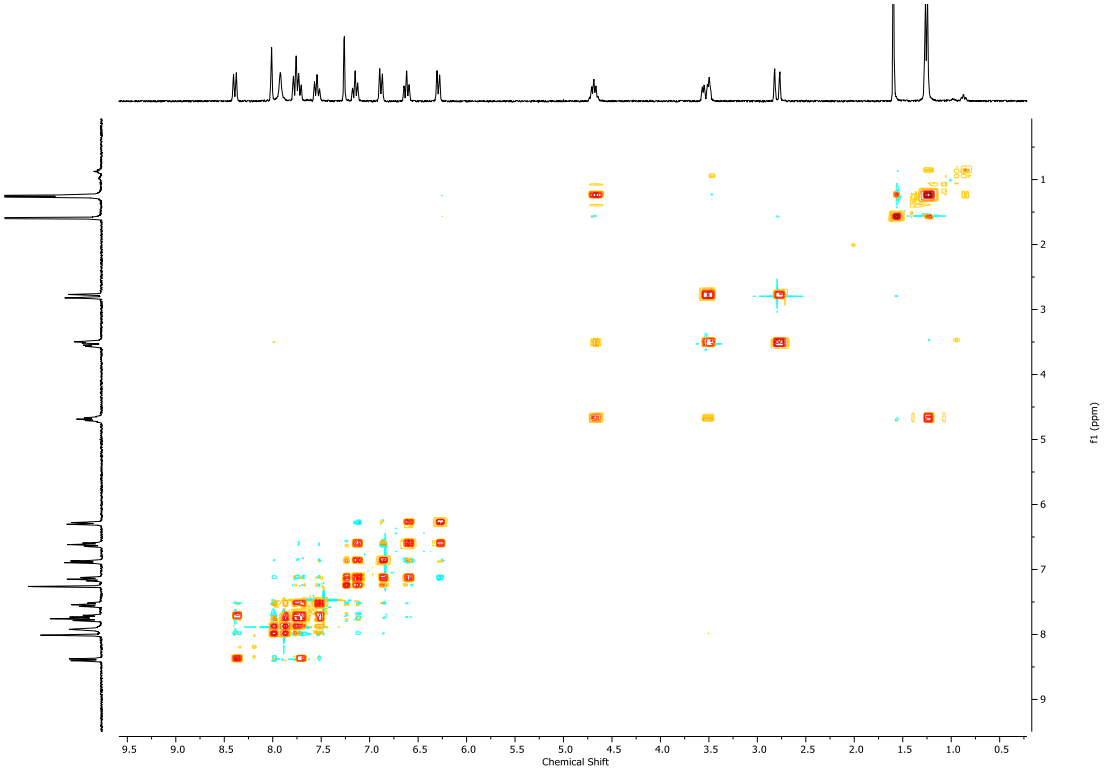

Figure S92: COSY spectrum of ***E*S-3** in $CDCl_3$.

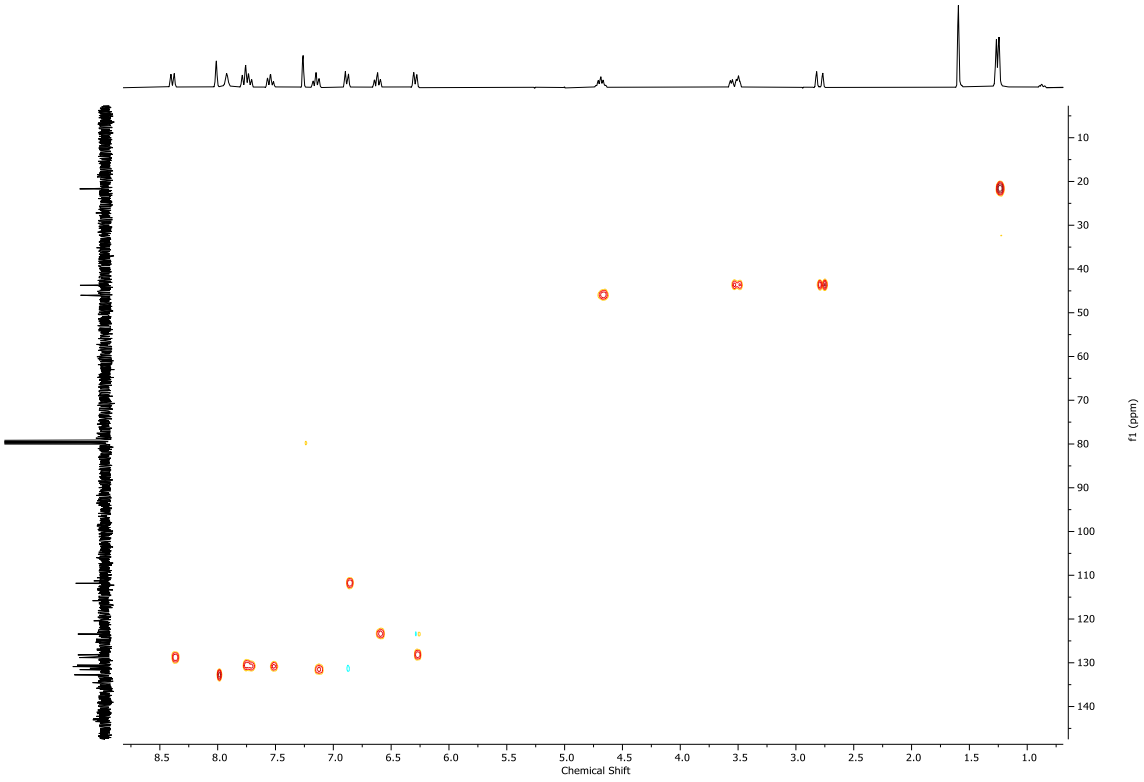

Figure S93: HSQC spectrum of ***E*S-3** in $CDCl_3$.

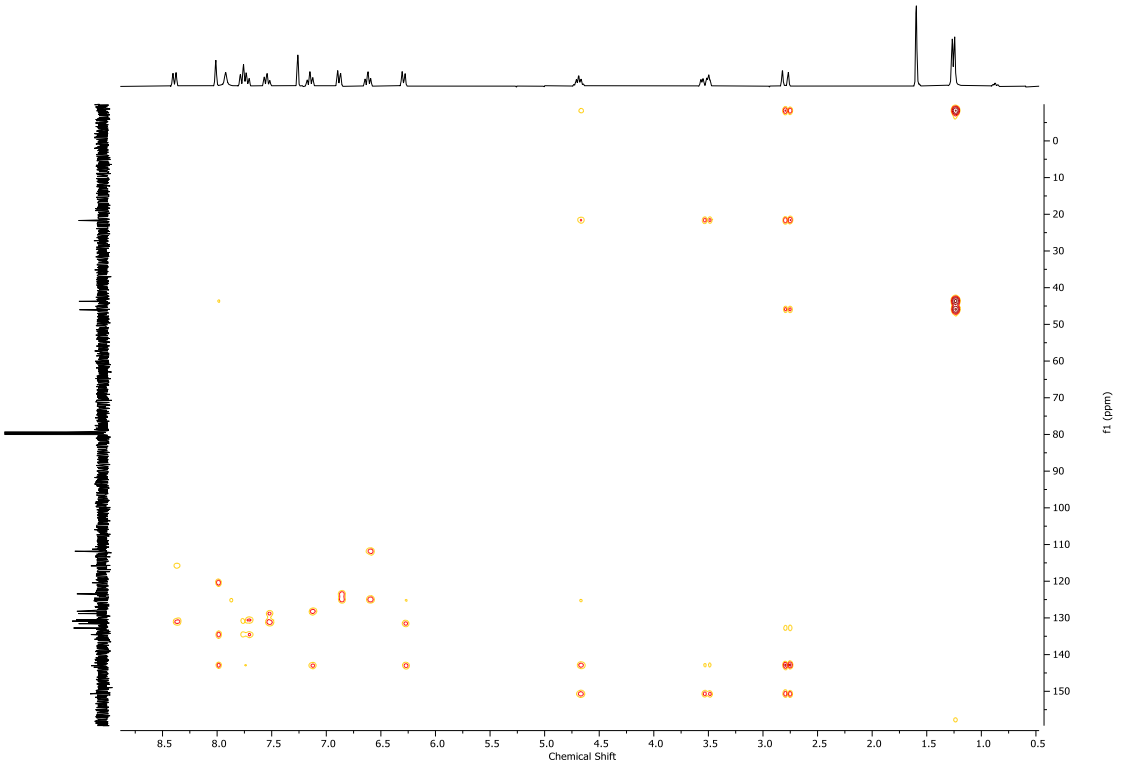

Figure S94: HMBC spectrum of ***E*S-3** in $CDCl_3$.

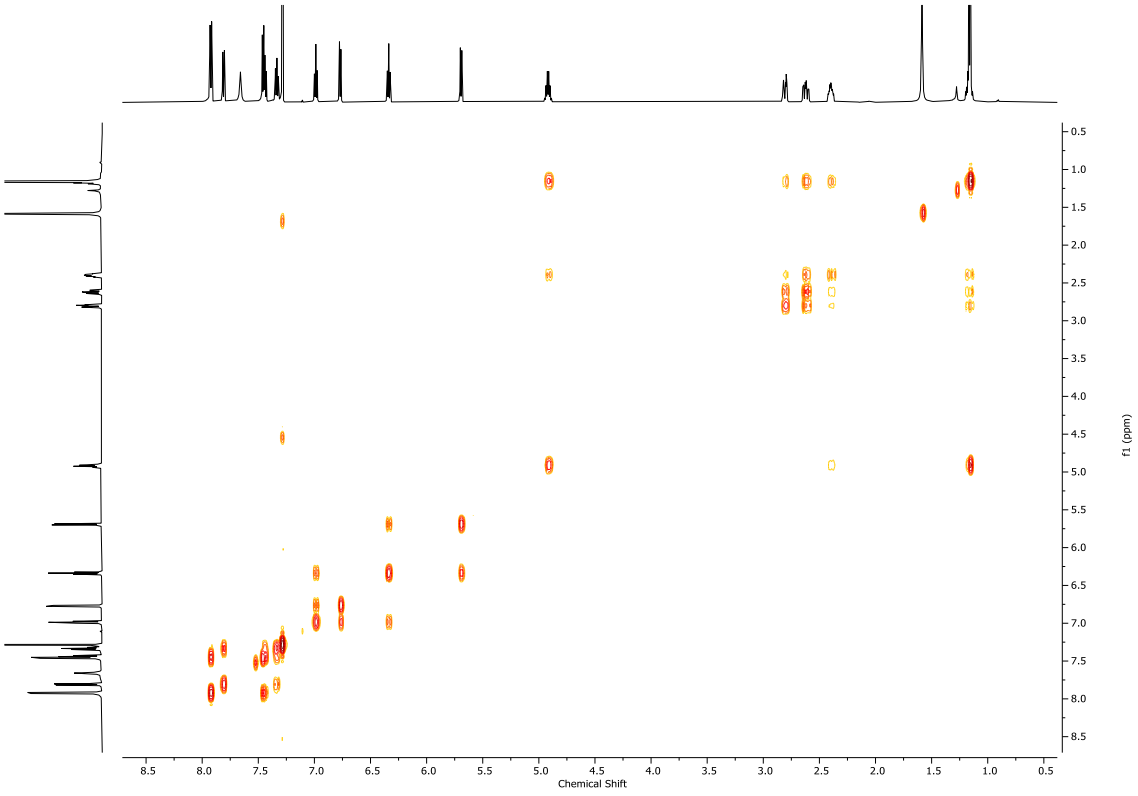

Figure S95: COSY spectrum of ***E*S-4** in $CDCl_3$.

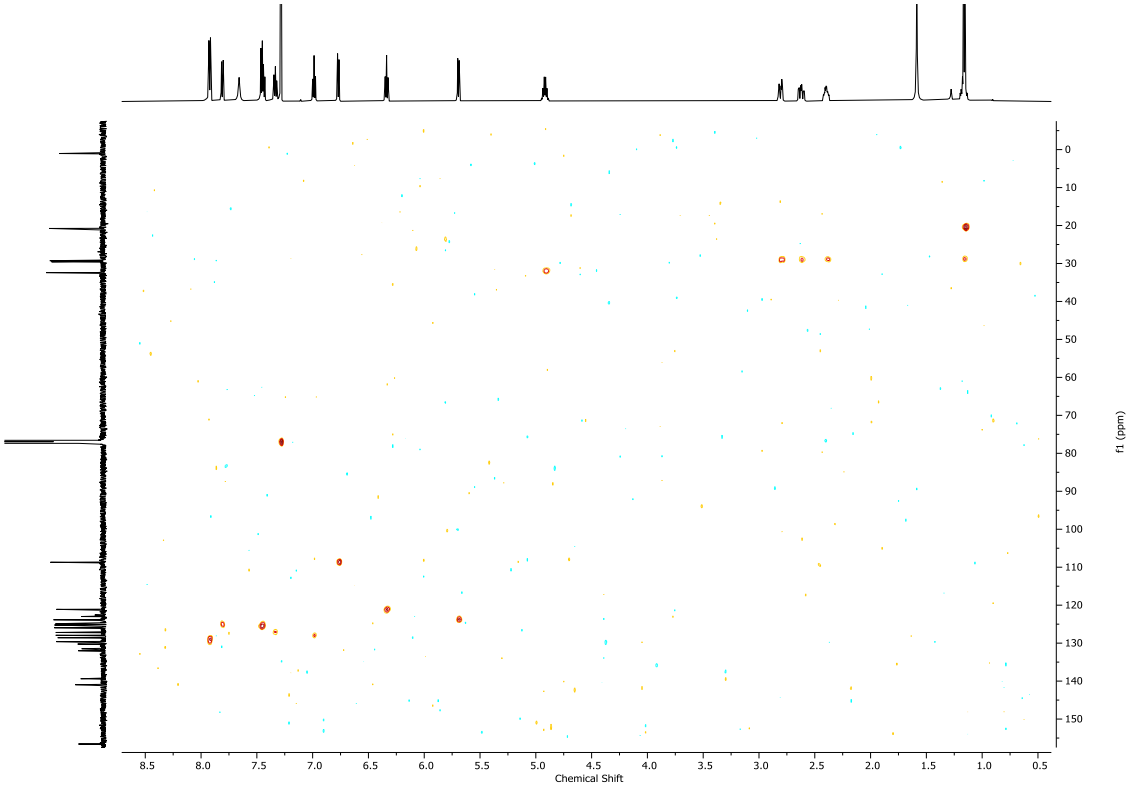

Figure S96: HSQC spectrum of ***E*S-4** in $CDCl_3$.

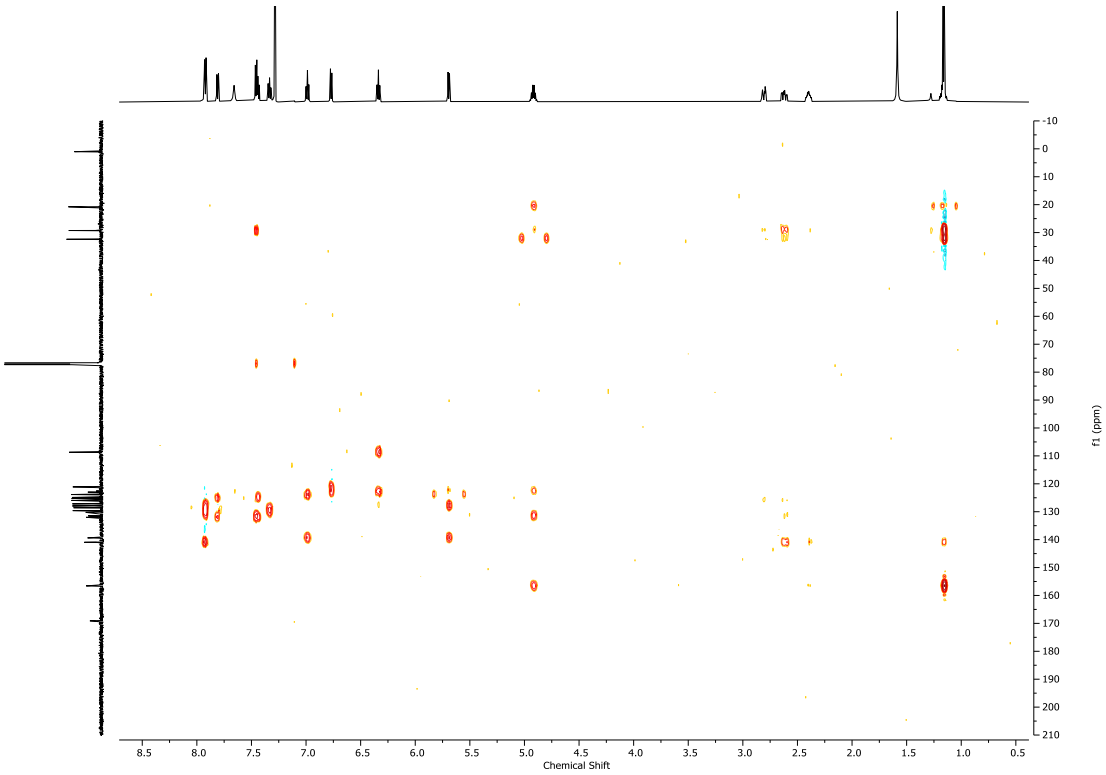

Figure S97: HMBC spectrum of ***E*S-4** in $CDCl_3$.

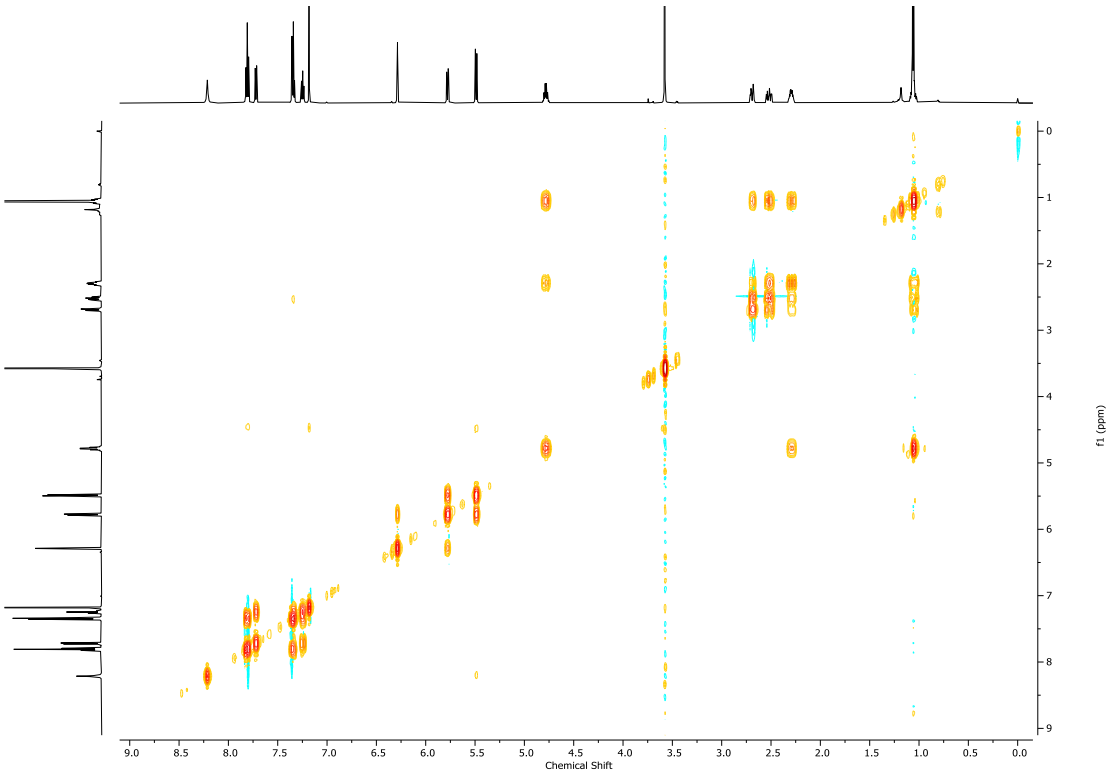

Figure S98: COSY spectrum of ***E*S-5** in $CDCl_3$.

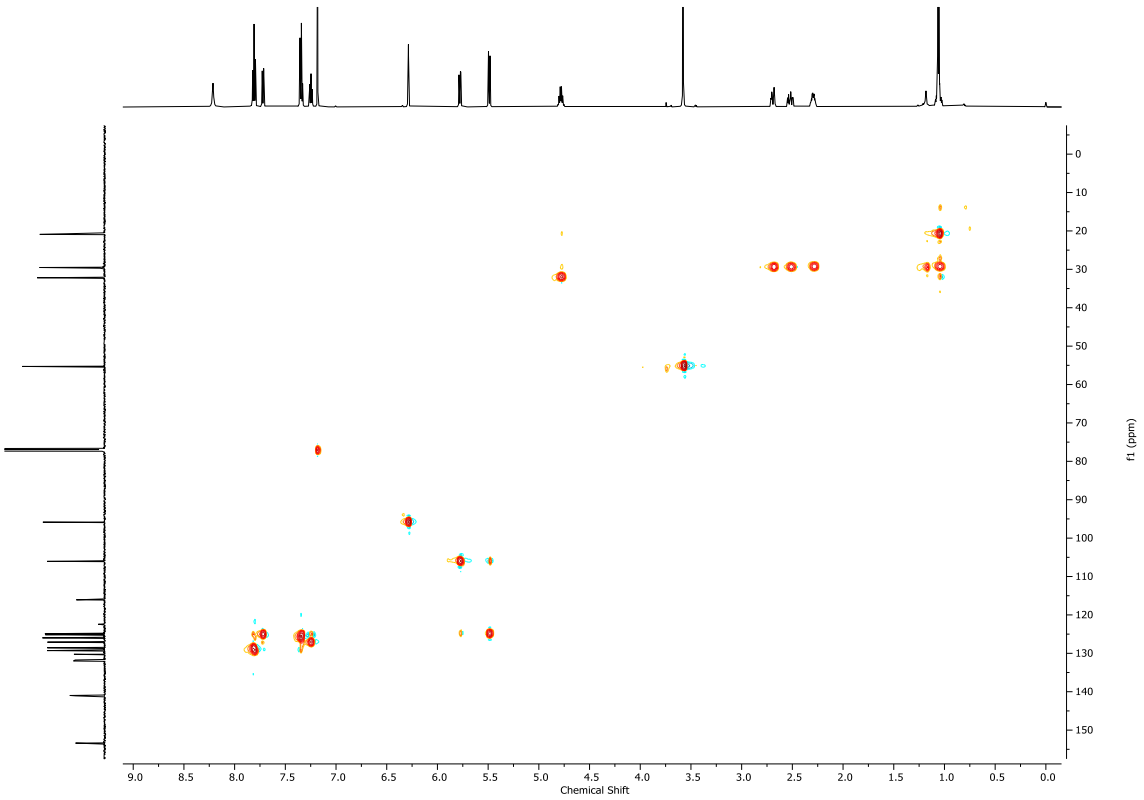

Figure S99: HSQC spectrum of ***E*S-5** in $CDCl_3$.

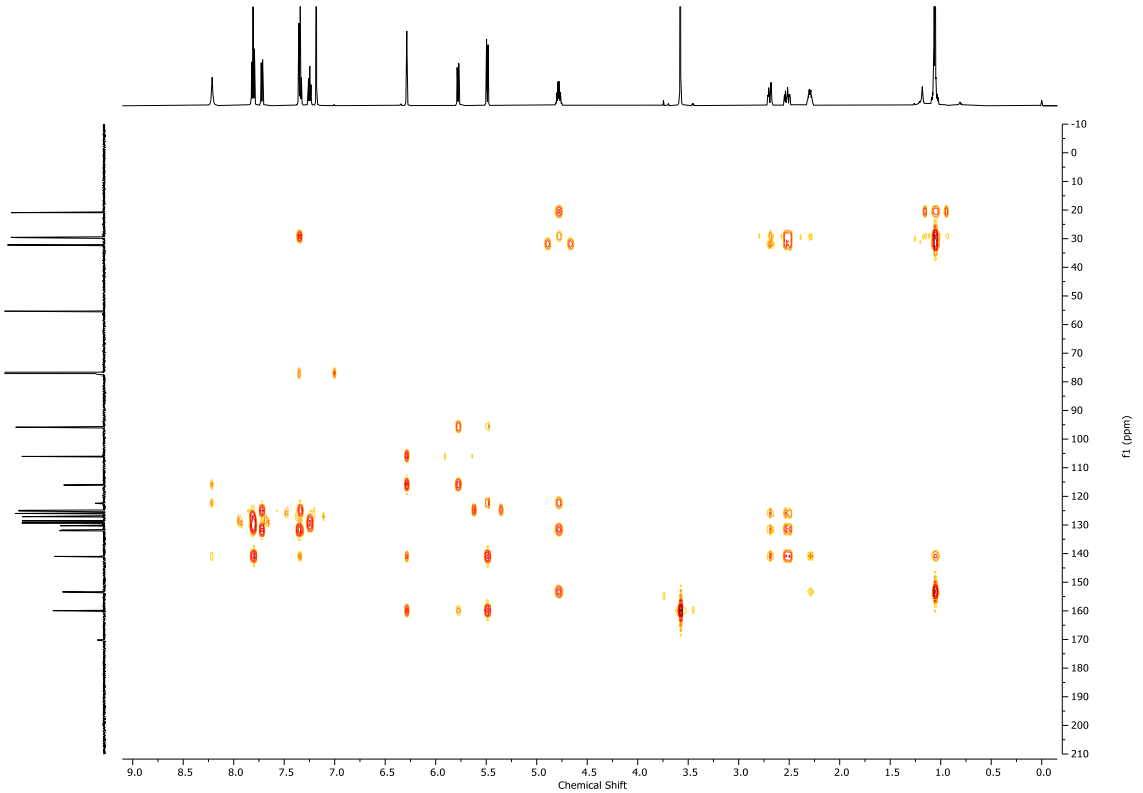

Figure S100: HMBC spectrum of ***E*S-5** in $CDCl_3$.

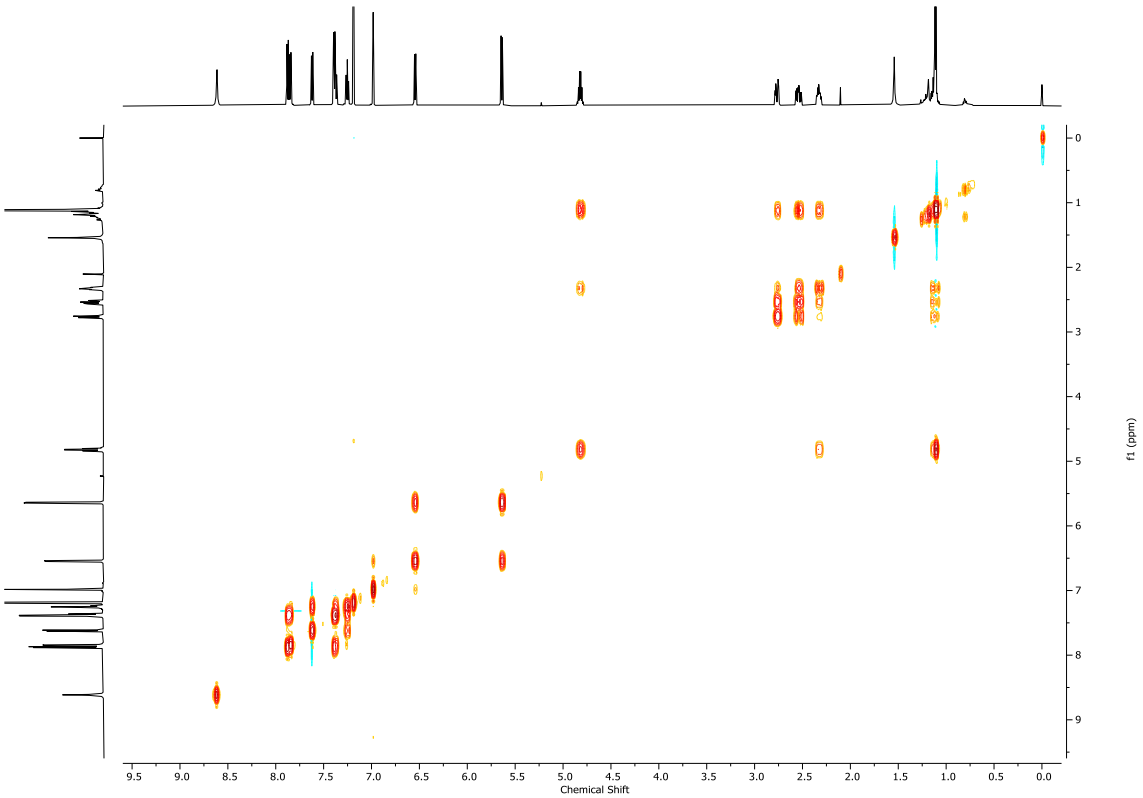

Figure S101: COSY spectrum of ***E*S-6** in $CDCl_3$.

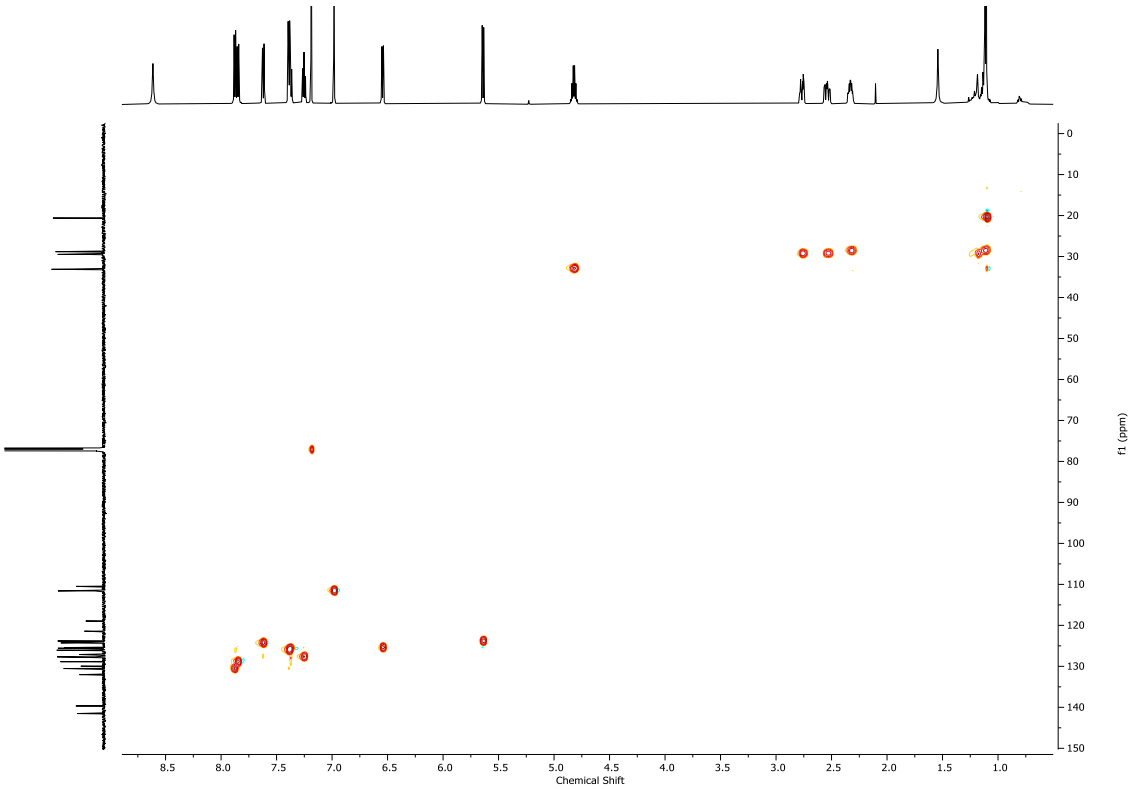

Figure S102: HSQC spectrum of ***E*S-6** in $CDCl_3$.

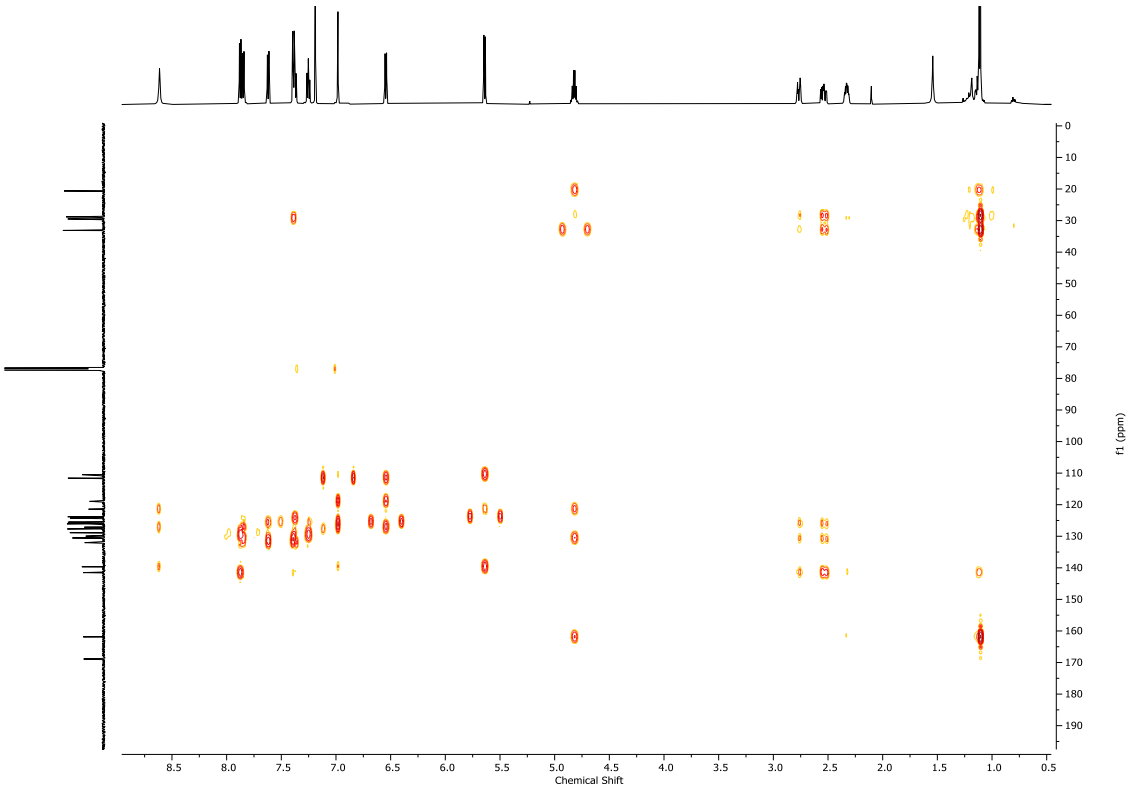

Figure S103: HMBC spectrum of ***E*S-6** in $CDCl_3$.

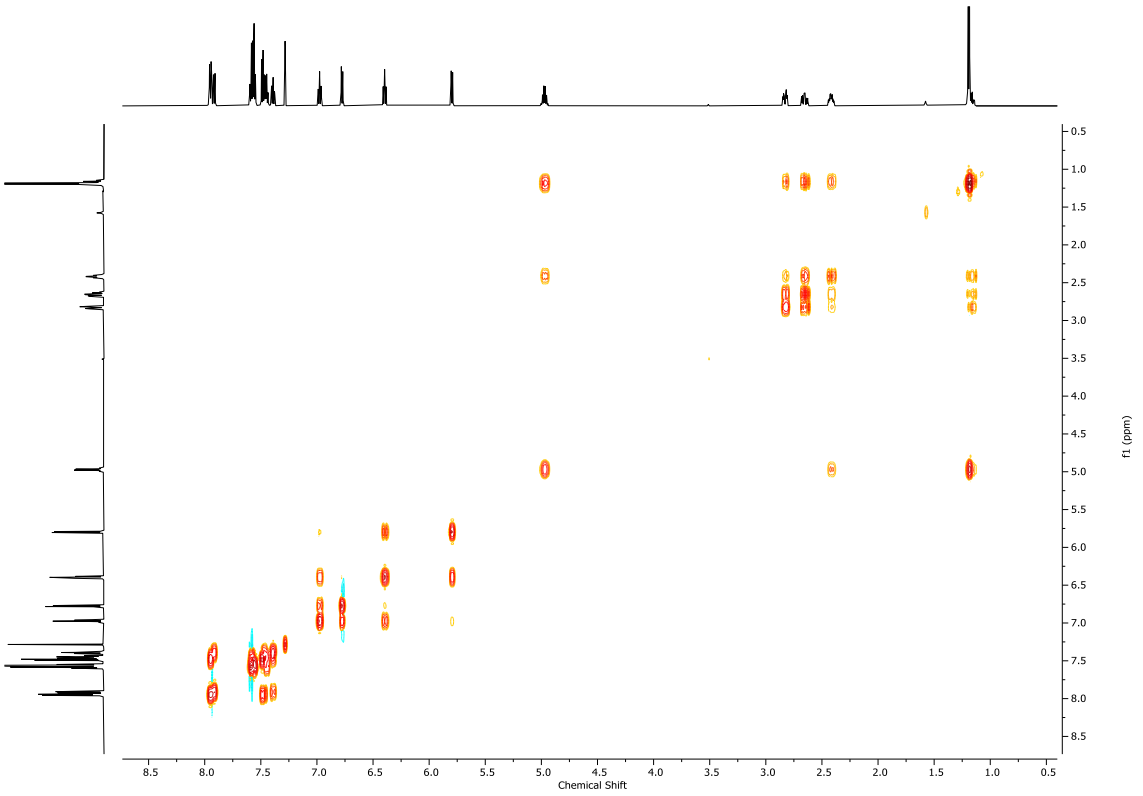

Figure S104: COSY spectrum of ***E*S-7** in $CDCl_3$.

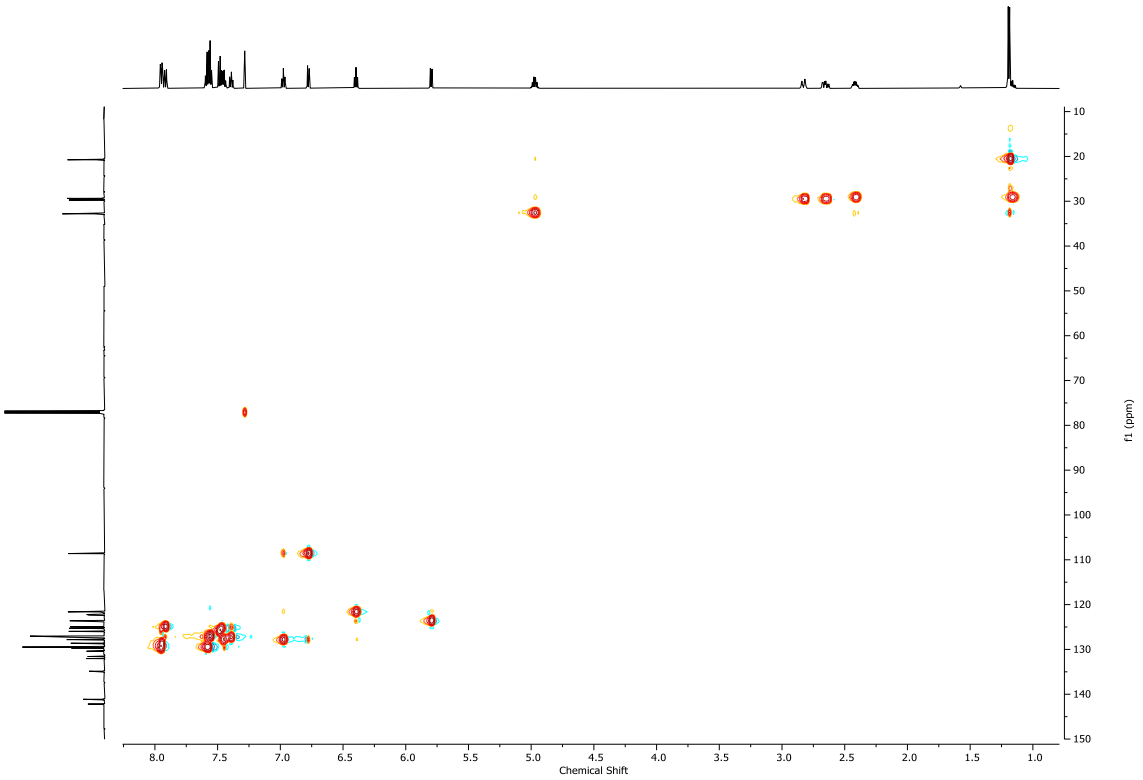

Figure S105: HSQC spectrum of ***E*S-7** in $CDCl_3$.

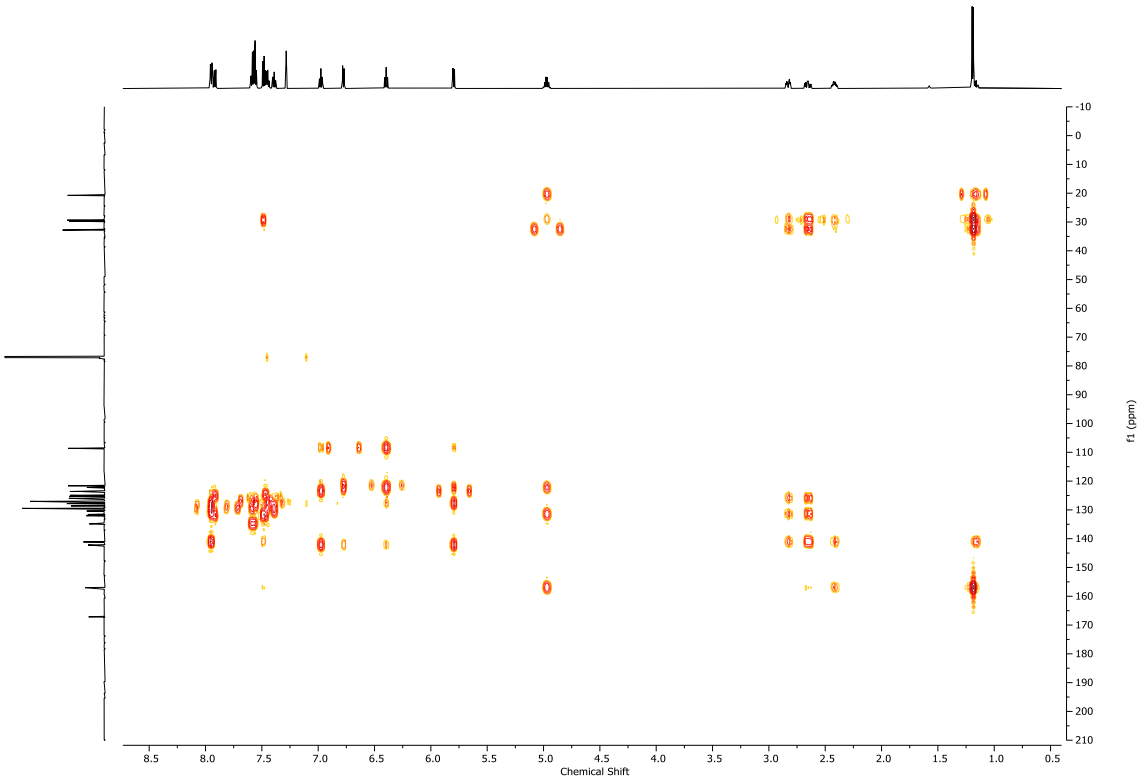

Figure S106: HMBC spectrum of ***E*S-7** in $CDCl_3$.

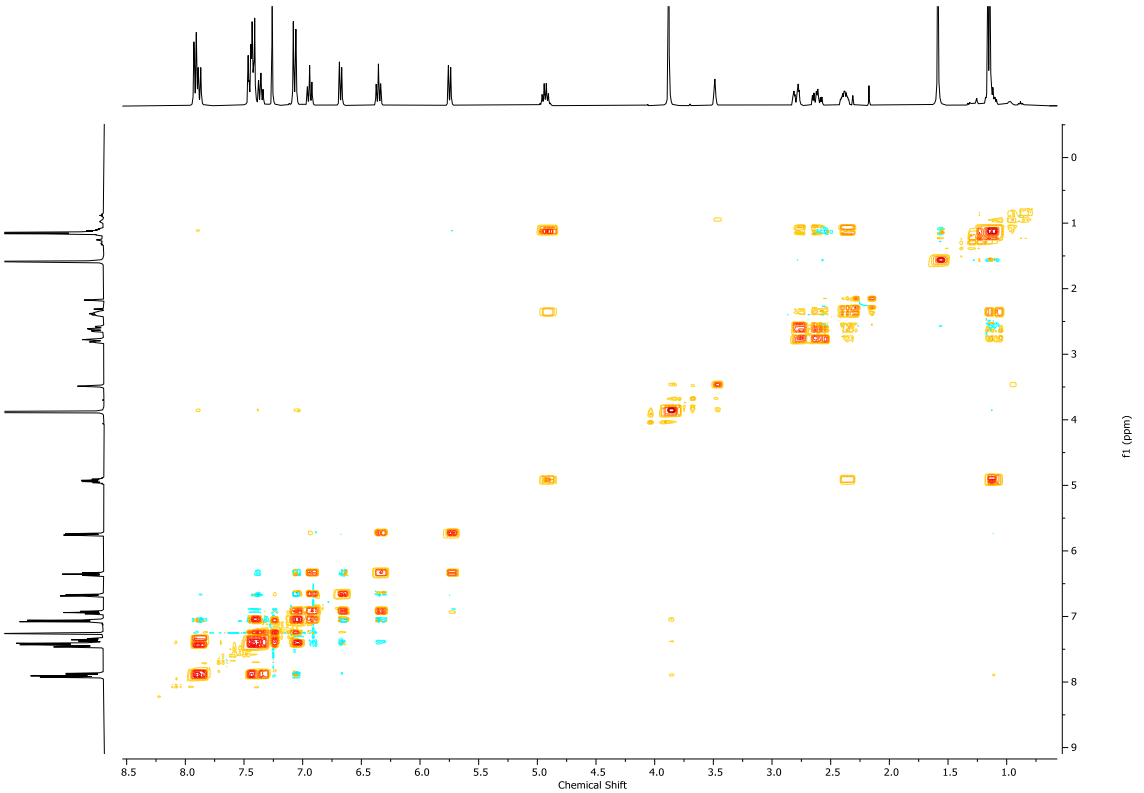

Figure S107: COSY spectrum of ***E*S-8** in $CDCl_3$.

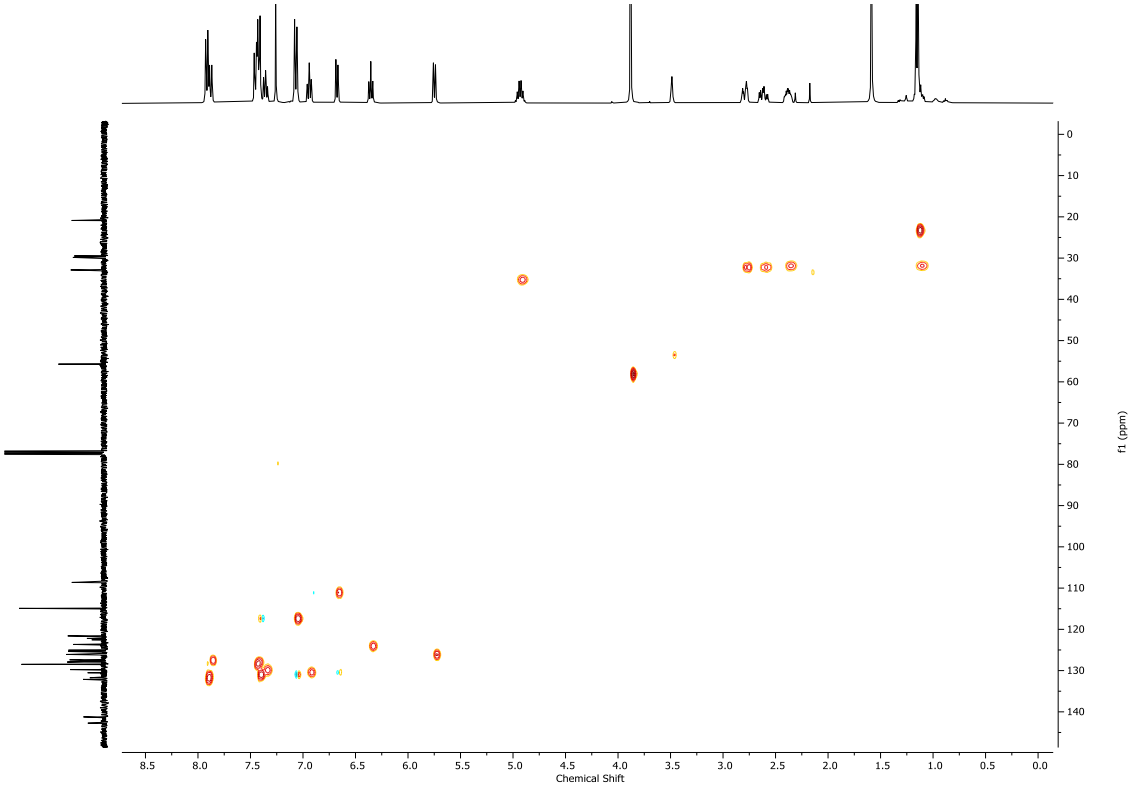

Figure S108: HSQC spectrum of ***E*S-8** in $CDCl_3$.

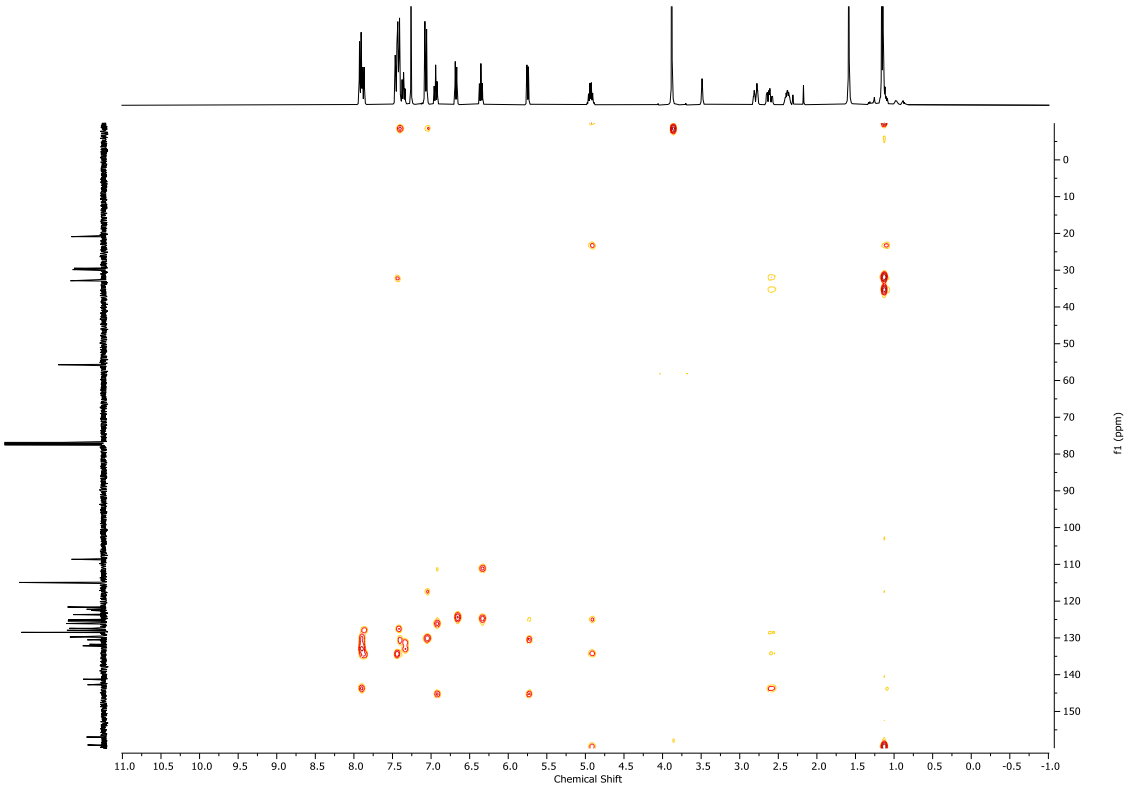

Figure S109: HMBC spectrum of ***E*S-8** in $CDCl_3$.

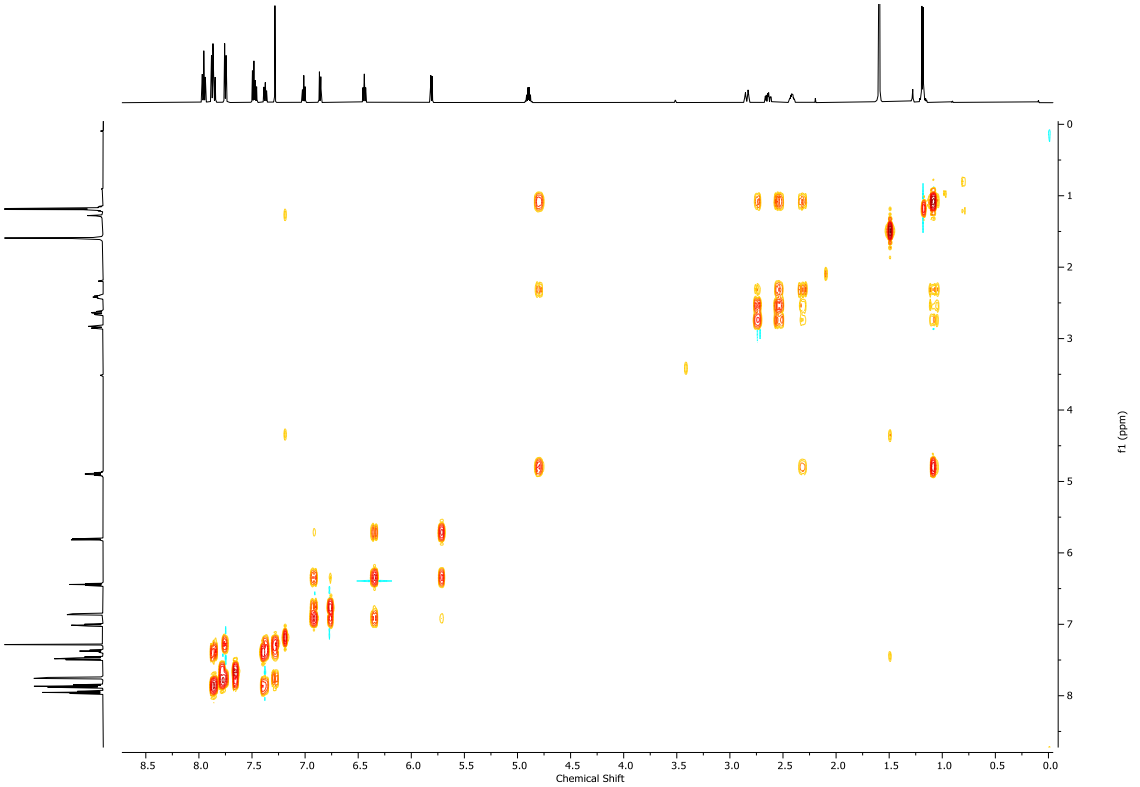

Figure S110: COSY spectrum of ***E*S-9** in $CDCl_3$.

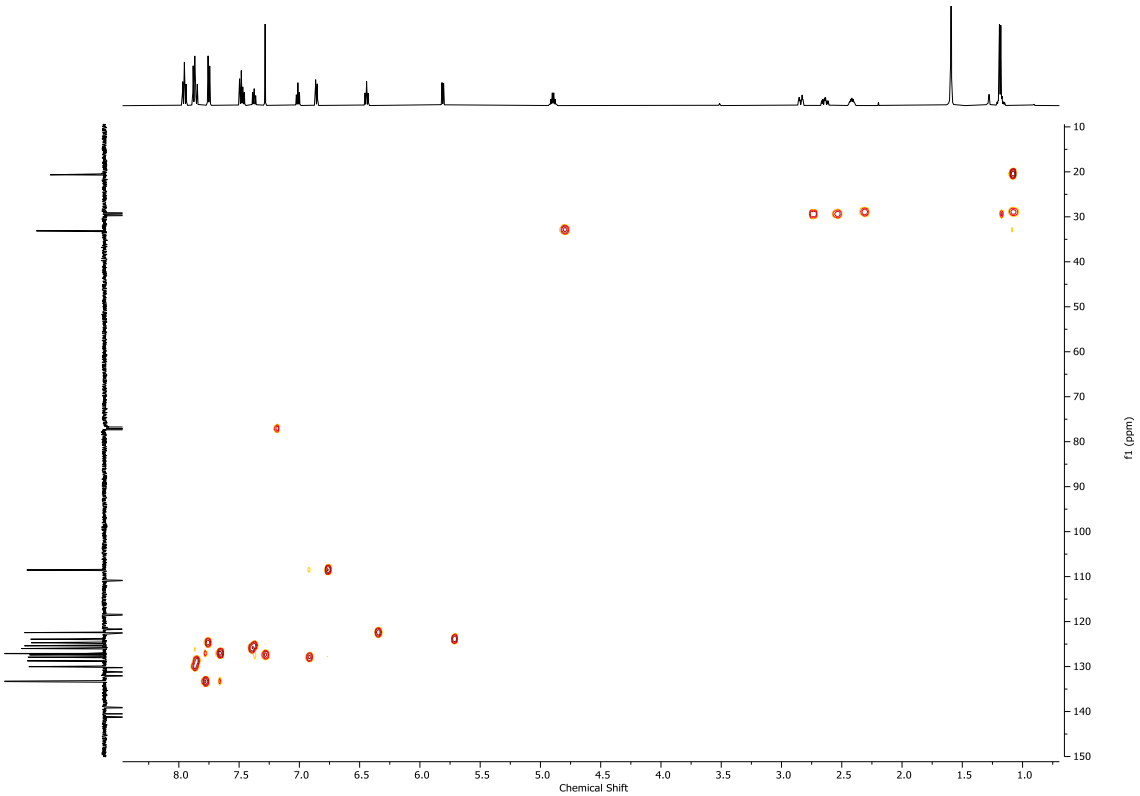

Figure S111: HSQC spectrum of ***E*S-9** in $CDCl_3$.

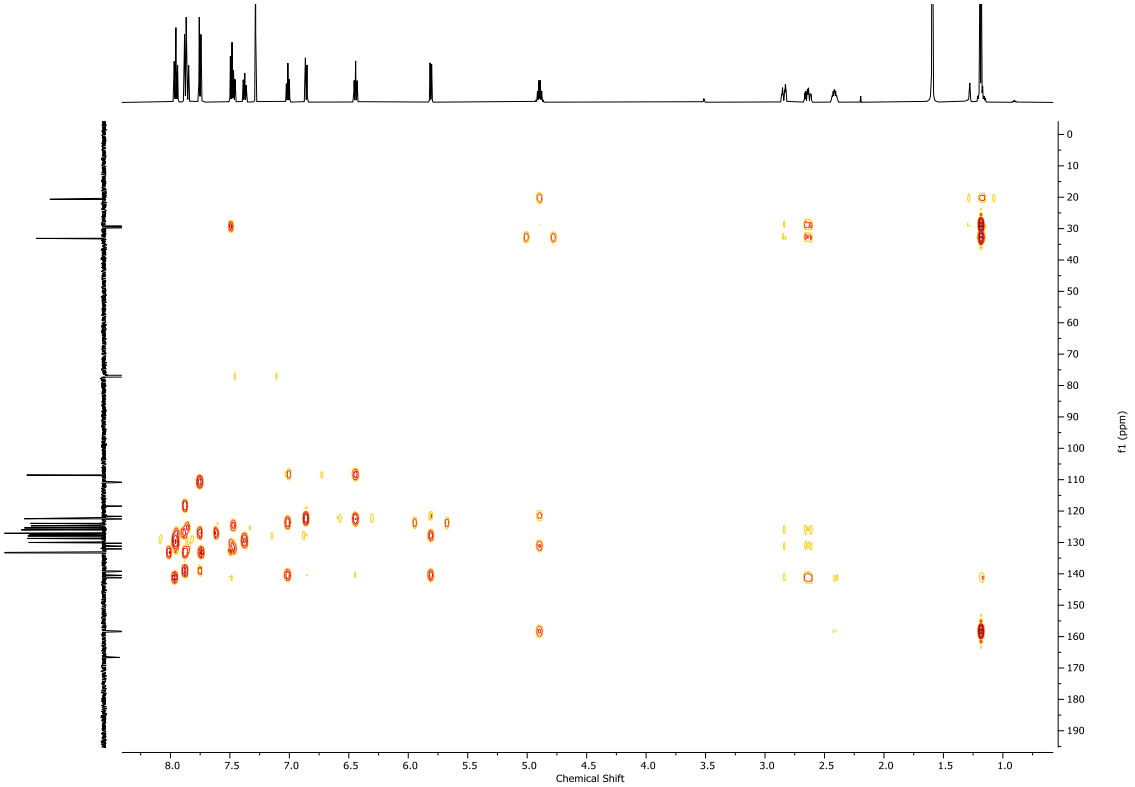

Figure S112: HMBC spectrum of ***E*S-9** in $CDCl_3$.

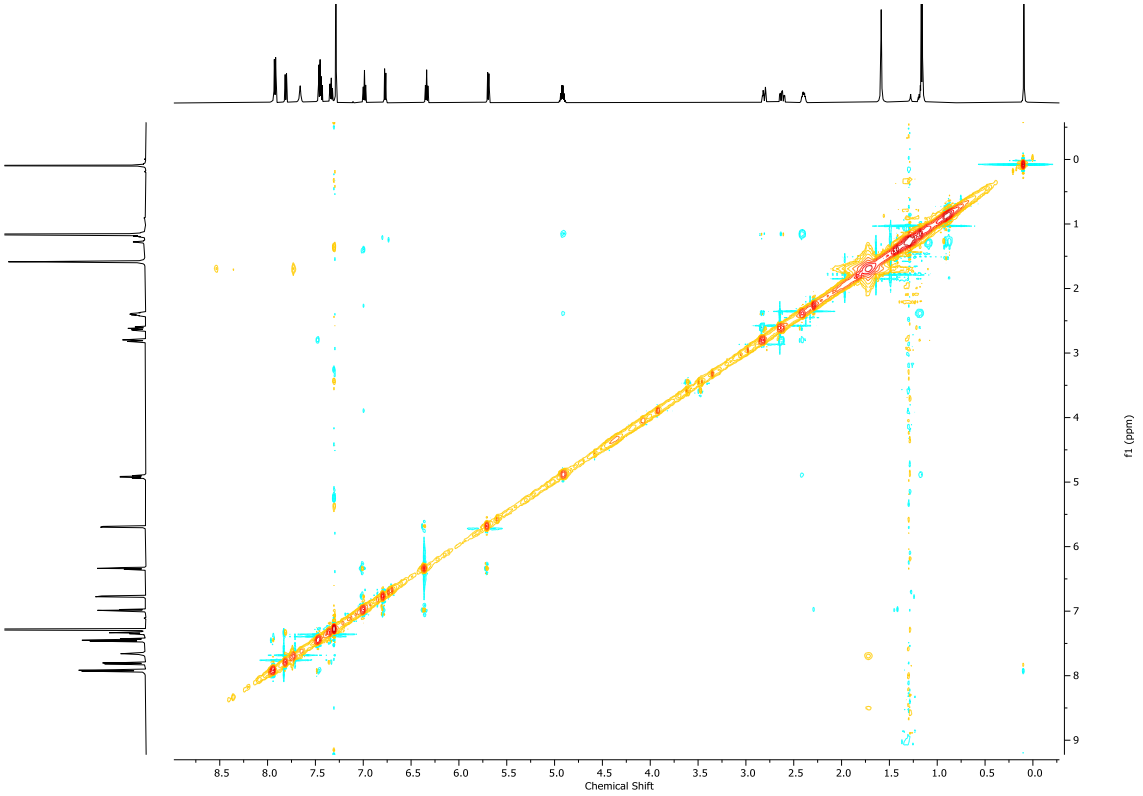

Figure S113: NOESY spectrum of ***E*S-4** in $CDCl_3$.

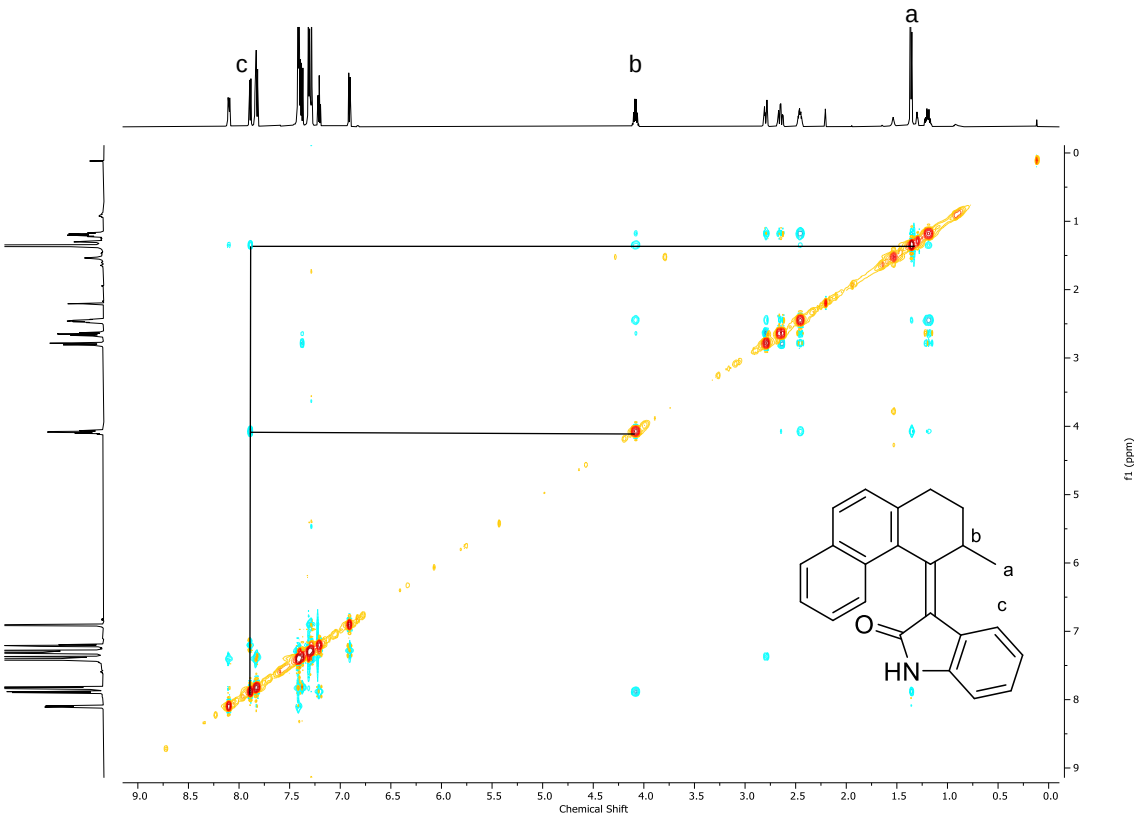

Figure S114: NOESY spectrum of ***Z*S-4** in $CDCl_3$.